

HYDRODYNAMICS AND BROWNIAN MOTION OF SMALL PARTICLES
NEAR A FLUID-FLUID INTERFACE

Thesis by
Seung-Man Yang

In Partial Fulfillment of the Requirements
for the Degree of
Doctor of Philosophy

California Institute of Technology
Pasadena, California

1985

(Submitted January 28, 1985)

Acknowledgments

I wish to express my sincere appreciation to my advisor, Professor L. Gary Leal, for his patient guidance and encouragement throughout the course of this work. I have greatly benefitted from my association with him and his research group. It is a great pleasure to thank many friends with whom my years at Caltech have been immensely enjoyable. The stimulation of discussions with them, the comfort of their friendship, and the encouragement of their generosity have been responsible for the interest and the peace of mind necessary for carrying out this work. My special thanks are due to Kathy Lewis for her excellent typing of this thesis. I would like to express my sincere gratitude to my family for their continuous support and encouragement, especially my wife Eui-Joung for her love and faith in me and her understanding. It is to her and to our daughter Jane that this work is dedicated.

Abstract

The general problems of particle motion in the vicinity of a flat, *non-deforming* fluid interface is studied. The approximate singularity method used by previous workers in this research group has been generalized to consider the motion of a sphere in any linear velocity field compatible with the existence of the undisturbed flat interface, and the motion of slender rod-like particles which undergo an arbitrary translation or rotation in either a quiescent fluid or in a linear flow. The theory yields the hydrodynamic mobility tensors which are necessary to describe Brownian movement near a phase boundary, as well as general trajectory equations for sedimenting particles near a fluid interface with an arbitrary viscosity ratio. These approximate solution results are in good agreement with both exact-solutions where they are available and experimental data for motion of a sphere near a rigid plane wall. Among the most interesting results for motion of slender bodies is the generalization of Jeffery orbit equations for linear simple shear flow.

The Brownian motion of a sphere in the presence of a *deformable* fluid interface is also examined. First, the fluctuation-dissipation theorem is derived for the random distortions of interface shape that are caused by spontaneous thermal impulses from the surrounding fluids. This analysis is carried out using the method of normal modes in conjunction with a Langevin type equation for the Brownian particle, and results in the prediction of autocorrelation functions for the location of the interface, for the random force acting on the particle (evaluated by a generalization of the Faxen's law), and for the particle velocity. The particle velocity correlation, in turn, yields the effective diffusion coefficient due to random fluctuations of the interface shape. Finally, we investigate the effects of interface deformation that are induced by the impulsive motion of a sphere that is undergoing Brownian motion. In this phase of our study, we

consider both the spatially modified hydrodynamic mobility which occurs as a consequence of hydrodynamic interactions, and influence on the mean-square displacement of the Brownian particle of the interface relaxation back towards the flat equilibrium configuration after an initial deformation that is caused by the particle motion.

Table of Contents

<u>Acknowledgment</u>		ii
<u>Abstract</u>		iii
<u>Table of Contents</u>		v
Chapter I.	Particle Motion in Stokes Flow near a Plane Fluid-Fluid Interface. Part 1. Slender Body in a Quiescent Fluid	1
	Abstract	3
	1. Introduction	4
	2. Basic Equations	5
	3. Fundamental Solutions for Translation of a Slender Body near a Flat Fluid Interface	9
	4. Fundamental Solutions for Rotation of a Slender Body near a Flat Fluid Interface	21
	5. Particle Trajectories in Sedimentation	28
	Appendix	36
	References	42
	Figure Captions	44
	Figures	48
Chapter II.	Particle Motion in Stokes Flow near a Plane Fluid-Fluid Interface. Part 2. Linear Shear and Axisymmetric Straining Flows	70
	Abstract	72
	1. Introduction	73
	2. Basic Equations	74
	3. Solutions for a Spherical Particle	79
	4. Solutions for a Slender Body	89

5.	Trajectories near a Flat Interface	100
	Appendix	111
	References	114
	Figure Captions	116
	Figures	119
Chapter III.	Motions of a Sphere in a Time-Dependent Stokes Flow - A Generalization of Faxen's Law	135
	Abstract	136
1.	Introduction	137
2.	Basic Equations and General Solutions	139
3.	Flow Exterior to a Rigid Sphere	148
4.	Discussion	153
	References	160
Chapter IV.	Brownian Motion of Spherical Particles near a Deformable Interface	161
	Abstract	162
1.	Introduction	163
2.	Brownian Motion near a Nondeforming Flat Interface	169
3.	Theory of Nonequilibrium Thermodynamics for Inter- face Fluctuations	175
4.	Brownian Motion near a Spontaneously Fluctuating Interface	195
5.	Brownian Motion near a Deformable Interface	208
	References	218
	Figure Captions	220
	Figures	222

Chapter I.

Particle Motion in Stokes Flow near a Plane Fluid-Fluid Interface

Part 1. Slender Body in a Quiescent Fluid

Particle Motion in Stokes Flow near a Plane Fluid-Fluid Interface

Part 1. Slender Body in a Quiescent Fluid*

by

Seung-Man Yang and L. Gary Leal

Department of Chemical Engineering
California Institute of Technology
Pasadena, California 91125

* The text of Chapter I consists of an article which appeared in the *J. Fluid Mech.* **136**, 393 (1983).

Abstract

The present study examines the motion of a slender body in the presence of a plane fluid-fluid interface with an arbitrary viscosity ratio. The fluids are assumed to be at rest at infinity, and the particle is assumed to have an arbitrary orientation relative to the interface. The method of analysis is slender body theory for Stokes flow using the fundamental solutions for singularities (i.e., Stokeslets and potential doublets) near a flat interface. We consider translation and rotation, each in three mutually orthogonal directions, thus determining the components of the hydrodynamic resistance tensors which relate the total hydrodynamic force and torque on the particle to its translational and angular velocities for a completely arbitrary translational and angular motion. To illustrate the application of these basic results, we calculate trajectories for a freely rotating particle under the action of an applied force either normal or parallel to a flat interface, which are relevant to particle sedimentation near a flat interface or to the processes of particle capture via drop or bubble flotation.

I. INTRODUCTION

When a small particle moves in the vicinity of a boundary, its motion will be affected due to hydrodynamic wall effects. We have previously considered the motion of a spherical particle in creeping motion near a fluid-fluid interface (Lee, Chadwick and Leal, 1979; Lee and Leal, 1980, Berdan and Leal, 1982; Lee and Leal, 1982). The present paper is the first of a series in which we extend this work to consider the creeping motion of slender, rod-like bodies in the the same circumstances. A number of different problems are of potential interest, corresponding to various types of application. For example, the translation and rotation of a fiber-like particle in a quiescent fluid system is relevant to sedimentation phenomena, and to theories of Brownian motion for particles near a fluid-fluid interface. Particle motions in more general flow fields such as pure straining flow or simple shear flow are relevant in suspension mechanics, and to some aspects of the process of particle capture at the surface of a large bubble or drop (cf. Goren and O'Neill, 1971).

In this present work, we use the fundamental solutions of Lee, Chadwick and Leal (1979) in combination with slender-body theory for Stokes' flow (cf. Batchelor 1970; Cox 1970,1971; Johnson and Wu 1979; Keller and Rubinow 1976; Johnson 1980, among others) to study the translation and rotation of an arbitrarily oriented, straight slender body through a quiescent fluid near a *flat* fluid-fluid interface. The resulting solutions are valid, as a zeroth-order approximation, under any conditions where the interface deformation remains small (Lee et al., 1979). On physical grounds, this occurs when either the separation distance between the particle and the interface is much larger than the characteristic length of the particle, or when either the surface tension or the density difference between the two fluids is very large.

Recently, Fulford and Blake (1983) have considered the same general problem considered here, but only for translation with the body oriented either parallel or normal to the interface. Fulford and Blake's analysis yields the hydrodynamic force for these two particular orientations, as well as the induced torque due to the interface, but cannot be used to calculate the instantaneous angular velocity of the particle (as claimed by Fulford and Blake) without solving for particle rotation in a quiescent fluid to determine the relationship between torque and angular velocity in the presence of the interface. Furthermore, the Fulford and Blake solutions cannot describe the motion of an arbitrarily oriented body, and thus cannot, for example, provide trajectories for particle motion under the action of a force if the particle is free to *rotate*.

In the present paper, we consider translation and rotation, each in three mutually orthogonal directions. The solutions of these six fundamental problems, each with an arbitrary orientation of the particle, provide all of the components of the hydrodynamic resistance tensors which relate the hydrodynamic force and torque on the particle to its translational and angular velocities, for arbitrary particle motions in a quiescent fluid. These fundamental solutions are then applied, for illustrative purposes, to calculate particle trajectories for "sedimentation" of a freely rotating particle due to an applied force which acts either normal or parallel to a flat interface.

II. BASIC EQUATIONS

We begin by considering the governing differential equations and boundary conditions for a rigid, non-axisymmetric, straight slender body which moves, with translational velocity \mathbf{U} and angular velocity $\mathbf{\Omega}$ near an interface which separates two immiscible Newtonian fluids. The fluids will be denoted as I and II with the body wholly immersed in the fluid II. It is assumed that the relevant

Reynolds number

$$\text{Re} = \frac{Ul}{\nu_2} \left[\text{or } \frac{\Omega l^2}{\nu_2} \right]$$

is sufficiently small ($\text{Re} \ll 1$) that the quasi-steady, creeping motion approximation is applicable, where ν_2 represents the kinematic viscosity of the fluid II and l is the half-length of the body. As the body moves it induces a disturbance motion in the two fluids, and in slender body theory the associated flow field at low Reynolds number is investigated by examining a nearly equivalent problem in which the body is replaced by a line distribution of Stokeslets along the axis of the body. A slender body with an arbitrary orientation is depicted in Figure 1. We adopt a coordinate system in which the x_1 -axis coincides with the projection of the body centerline onto the interface, which is itself located at $x_3 = 0$. Point forces are distributed over the portion $-l < x < l$ of the body axis, with the magnitude of the point force at any position \mathbf{x}_s on this line denoted as

$$\mathbf{f}_s(\mathbf{x}_s) = 8\pi\mu_2\alpha(\mathbf{x}_s)\delta(\mathbf{x} - \mathbf{x}_s) ,$$

in which $\delta(\mathbf{x})$ is the three-dimensional Dirac delta function. The vector density (or weighting) function, $\alpha(\mathbf{x}_s)$, must be chosen as a function of position along the particle axis so that the no-slip boundary condition

$$\mathbf{u}_2 = \mathbf{U} + \Omega \times \mathbf{x}_s \tag{1}$$

is satisfied on the body surface. In component form, the position vector \mathbf{x}_s is simply represented as:

$$\mathbf{x}_s = (\zeta \cos\theta, 0, \zeta \sin\theta - d) ,$$

in which θ is the angle between the centerline of the body and the plane of the interface, d is the separation distance between the interface and the body center, and ζ is the distance along the centerline measured from the center of

the body.

The fundamental solution of the creeping motion equations for a point force located at an arbitrary point \mathbf{x}_a in fluid II was obtained independently by Aderogba and Blake (1978) and by Lee, Chadwick and Leal (1979). The resulting velocity and pressure fields can be expressed in the form:

$$\mathbf{u}(\mathbf{x}, \mathbf{x}_a; \alpha) = \alpha(\mathbf{x}_a) \cdot \Psi(\mathbf{x}, \mathbf{x}_a) \quad (2a)$$

$$p(\mathbf{x}, \mathbf{x}_a; \alpha) = \alpha(\mathbf{x}_a) \cdot \Pi(\mathbf{x}, \mathbf{x}_a) \quad (2b)$$

where $\Psi(\mathbf{x}, \mathbf{x}_a)$ and $\Pi(\mathbf{x}, \mathbf{x}_a)$ denote Cartesian tensorial Green's functions with components:

$$\Psi_{ij}(\mathbf{x}, \mathbf{x}_a) = \frac{\delta_{ij}}{r} + \frac{r_i r_j}{r^3} + \left[\frac{1-\lambda}{1+\lambda} \cdot \delta_{jl} \cdot \delta_{lk} - \delta_{js} \cdot \delta_{sk} \right] \cdot \left[\frac{\delta_{ik}}{R} + \frac{R_i R_k}{R^3} \right] + \left[\frac{2\lambda}{1+\lambda} \cdot (d - \zeta \sin \theta) \cdot (\delta_{jl} \cdot \delta_{lk} - \delta_{js} \cdot \delta_{sk}) \right] \cdot \frac{\partial}{\partial R_k} \left[\frac{(d - \zeta \sin \theta) R_i}{R^3} + \frac{\delta_{is}}{R} + \frac{R_i R_s}{R^3} \right]$$

and

$$\Pi_j(\mathbf{x}, \mathbf{x}_a) = 2\mu_2 \cdot \left[\frac{r_j}{r^3} + \left(\frac{1-\lambda}{1+\lambda} \cdot \delta_{jl} \cdot \delta_{lk} - \delta_{js} \cdot \delta_{sk} \right) \cdot \frac{R_j}{R^3} + \frac{2\lambda}{1+\lambda} \cdot (d - \zeta \sin \theta) \cdot (\delta_{jl} \cdot \delta_{lk} - \delta_{js} \cdot \delta_{sk}) \cdot \frac{\partial}{\partial R_k} \left(\frac{R_j}{R^3} \right) \right]$$

(summation convention over $l = 1, 2$ and $k = 1, 2, 3$)

where $\mathbf{r} = (\mathbf{x} - \mathbf{x}_a)$, $\mathbf{R} = (\mathbf{x} - \mathbf{x}_a^*)$, $r = |\mathbf{r}|$, $R = |\mathbf{R}|$, $\lambda = \frac{\mu_1}{\mu_2}$, and \mathbf{x}_a^* denotes the reflection point of \mathbf{x}_a in the fluid I. Thus, for a line distribution of Stokeslets with the line density $\alpha(\mathbf{x}_a)$, the resulting fluid velocity $\mathbf{u}(\mathbf{x})$ and pressure $p(\mathbf{x})$ at a point \mathbf{x} in the fluid are given by:

$$\mathbf{u}(\mathbf{x}) = \int_{-l}^l \alpha(\mathbf{x}_a) \cdot \Psi(\mathbf{x}, \mathbf{x}_a) d\zeta$$

(3a)

$$p(\mathbf{x}) = \int_{-l}^l \alpha(\mathbf{x}_s) \cdot \Pi(\mathbf{x}, \mathbf{x}_s) d\zeta. \quad (3b)$$

The velocity and pressure fields defined by these equations automatically satisfy the conditions of zero normal velocity, continuity of tangential velocity and continuity of the shear stress at the fluid-fluid interface, as well as the condition of vanishing velocity in the far field (note that the Green's functions $\Psi(\mathbf{x}, \mathbf{x}_s)$ and $\Pi(\mathbf{x}, \mathbf{x}_s)$ are of $O(1/r)$ and $O(1/r^2)$ for $r \gg 1$). All that remains is to satisfy the no-slip boundary condition (1), according to which the fluid velocity must be $\mathbf{U} + \boldsymbol{\Omega} \times \mathbf{x}_o$ at the body surface. Thus, the unknown function $\alpha(\mathbf{x}_s)$ representing the line density of Stokeslet strengths must be determined so that the disturbance velocity given by (3a) is at least approximately equal to $\mathbf{U} + \boldsymbol{\Omega} \times \mathbf{x}_o$ at all points of the body surface. It should be noted that, in general, a line distribution of Stokeslets alone will not be sufficient to satisfy the no-slip boundary condition at all levels of approximation for all points on a body surface. Higher order singularities (e.g., potential dipoles) are also generally needed, even in the case of an axisymmetric body. However, when the body is slender, the boundary-condition at the body surface can always be satisfied to an order of approximation, $O(\varepsilon)$ where $\varepsilon \equiv \left[\ln \left(\frac{2l}{R_o} \right) \right]^{-1}$, without explicit introduction of the higher order singularities. Furthermore, the total hydrodynamic force or torque acting on the body can be determined from the Stokeslet distribution alone as pointed out previously by Batchelor (1970).

A point on the body surface can be expressed in terms of cylindrical polar coordinates (r, η, x) . It is assumed that the crosssection of the body has an effective radius $r_o(x)$ which is a function of distance x along the body centerline. The maximum value of $r_o(x)$ is denoted as R_o . The cross-sectional shape need not be circular provided only that we choose $r_o(x)$ such that the perimeter is

equal to $2\pi r_o(x)$ (Batchelor 1970). At the body surface,

$$\mathbf{x} = \mathbf{x}_B = (x \cos \theta - r_o \sin \eta \sin \theta, r_o \cos \eta, x \sin \theta - d + r_o \sin \eta \cos \theta).$$

Applying the no-slip boundary condition at the body surface to equation (3a) yields an integral equation for the unknown Stokeslet distribution, $\alpha(\mathbf{x}_B)$, i.e.,

$$\mathbf{U} + \boldsymbol{\Omega} \times \mathbf{x}_o = \int_{-l}^l \alpha(\mathbf{x}_B) \cdot \Psi(\mathbf{x}_B, \mathbf{x}_B) d\zeta. \quad (4)$$

The theoretical analysis which follows will be based on the assumption that both R_o/l and $\frac{R_o}{d - l \sin \theta} \left[> \frac{R_o}{d} \right]$ are small. The first assumption is a slenderness criterion, while the second implies that the slender body is not closer than a few radii from the interface. In view of the linearity of the problem, the translational and rotational components of the particle motion can be considered separately, and we begin with translational motions of an arbitrarily oriented body parallel and perpendicular to the interface.

III. FUNDAMENTAL SOLUTIONS FOR TRANSLATION OF A SLENDER BODY NEAR A FLAT FLUID INTERFACE

A. Motion parallel to the interface along the x_1 -axis

Let us then consider an arbitrarily oriented slender body which is moving with a translational velocity $U_1 \mathbf{e}_1$ in the direction of the x_1 -axis through fluid II. In this case, in order to satisfy the no-slip boundary conditions, it is necessary to employ distributions of Stokeslets oriented in both the \mathbf{e}_1 and \mathbf{e}_3 directions. By substituting

$$\alpha(\mathbf{x}_B) = \left[\alpha_1(\zeta), 0, \alpha_3(\zeta) \right], \quad \mathbf{u}(\mathbf{x}_B) = (U_1, 0, 0)$$

into (4) we obtain three simultaneous integral equations of the form

$$U_i \delta_{i1} = \int_{-l}^l [\alpha_j(\zeta) \cdot \Psi_{ij}(\mathbf{x}_B, \zeta)] d\zeta \quad (5)$$

(i = 1,2,3, summation convention over j = 1,2,3).

These integral equations cannot be solved exactly (except by numerical methods), but can be solved approximately by means of an asymptotic expansion for small R_o/l and R_o/d . After much algebra, expanding equation (5) to

$O\left(\frac{R_o}{l}, \frac{R_o}{d}\right)$, we obtain:

(x_1 - component)

$$\begin{aligned} U_1 = \alpha_1(x) & \left[2 \left[\frac{1}{\varepsilon} + S(x) \right] \cdot (\cos^2\theta + 1) - 2\cos^2\theta + 2\sin^2\eta \cdot \sin^2\theta + P(x;\lambda,\theta,d) \right] \\ & + \alpha_3(x) \left[\sin 2\theta \left[\frac{1}{\varepsilon} + S(x) - 1 \right] - \sin^2\eta \cdot \sin 2\theta + Q(x;\lambda,\theta,d) \right] \\ & + \int_{-l}^l [\alpha_j(\zeta) - \alpha_j(x)] \cdot \Psi_{1j}(\mathbf{x}_B, \zeta) d\zeta + O\left(\frac{R_o}{l}, \frac{R_o}{d}\right) \end{aligned} \quad (6a)$$

(x_2 - component)

$$0 = O\left(\frac{R_o}{l}, \frac{R_o}{d}\right) \quad (6b)$$

(x_3 - component)

$$\begin{aligned} 0 = \alpha_1(x) & \left[\sin 2\theta \left[\frac{1}{\varepsilon} + S(x) - 1 \right] - \sin^2\eta \cdot \sin 2\theta + R(x;\lambda,\theta,d) \right] + \alpha_3(x) \\ & \cdot \left[2 \left[\frac{1}{\varepsilon} + S(x) \right] \cdot (1 + \sin^2\theta) - 2\sin^2\eta \cdot \cos^2\theta - 2\sin^2\theta + W(x;\lambda,\theta,d) \right] \\ & + \int_{-l}^l [\alpha_j(\zeta) - \alpha_j(x)] \cdot \Psi_{3j}(\mathbf{x}_B, \zeta) d\zeta + O\left(\frac{R_o}{l}, \frac{R_o}{d}\right) \end{aligned} \quad (6c)$$

where $\varepsilon = \left[\ln \left(\frac{2l}{R_o} \right) \right]^{-1}$, $S(x) = \ln \left[\frac{\left(1 - \left[\frac{x}{l} \right]^2 \right)^{\frac{1}{2}}}{\frac{r_o(x)}{R_o}} \right]$. [See Appendix for specific for-

mulae for $P(x;\lambda,\theta,d)$, $Q(x;\lambda,\theta,d)$, $R(x;\lambda,\theta,d)$ and $W(x;\lambda,\theta,d)$.] The primary small quantity ε ($\ll 1$) which will be used in the subsequent analysis represents a slenderness parameter, and $S(x)$ is a shape function of the body [specified once $r_0(x)$ is given].

In an analysis of the similar integral equations for the infinite fluid case, Tuck (1964), Tillett (1970) and Batchelor (1970) suggested an expansion of $\alpha(x)$ in powers of ε

$$\alpha_j(x) = \varepsilon\alpha_j^0(x) + \varepsilon^2\alpha_j^1(x) + \varepsilon^3\alpha_j^2(x) + \dots \quad (7)$$

as a straightforward way to obtain an approximate solution of the integral equations (6a-c) for the unknown function $\alpha(x)$. It may be worth pointing out that solving the integral equation (5) using an expansion such as (7) in powers of ε requires retention of an infinite number of terms to insure that the associated error is no larger than the error $O(R_0/l)$ that is inherent in (6a-c). In fact, we determine the first two terms in the expansion (7) satisfying the boundary condition (1) up to $O(\varepsilon^2)$, following in the spirit of Batchelor (1970), Cox (1970) and others who adopted the same level of approximation to calculate such parameters as the hydrodynamic force and torque for slender-body motion in an unbounded fluid.

The $\sin^2\eta$ terms [of $O(\varepsilon^2)$] which appear in (6a) and (6c) are indicative of the fact that higher order singularities are necessary if the boundary conditions are to be satisfied at $O(\varepsilon^2)$. Obviously, with the no-slip condition [cf. Eq. (5)] the fluid velocity at the body surface is required to be independent of η . To remove the η -dependence associated with the Stokeslet distribution, a line distribution of potential dipoles must be superposed on the line distribution of Stokeslets at $O(\varepsilon^2)$. The fundamental solution for a potential dipole located near a plane interface has been obtained by Lee, Chadwick and Leal (1979). The required line dis-

tribution of potential dipoles can be shown to be related to $\alpha(x)$ by the relationship

$$\beta(x) = -\frac{1}{2} [r_0^2(x) \cdot \alpha(x)]. \quad (8)$$

It remains only to determine the distribution function $\alpha(x)$.

After adding the fundamental solution for a line distribution of potential dipoles with line density given by (8) to the Stokeslet solution in the form (7), and utilizing the expansion (7), we find immediately that

$$\alpha_1(x) = \frac{(\sin^2\theta + 1)U_1}{4} \left[\varepsilon - \frac{\varepsilon^2}{2} \left[2S(x) + \frac{3\sin^2\theta - 1}{1 + \sin^2\theta} + A(x;\lambda,\theta,d) \right] \right] + O(\varepsilon^3) \quad (9a)$$

$$\alpha_3(x) = -\frac{\sin 2\theta U_1}{8} \left[\varepsilon - \frac{\varepsilon^2}{2} [2S(x) + 3 + E(x;\lambda,\theta,d)] \right] + O(\varepsilon^3). \quad (9b)$$

Specific formulae for $A(x;\lambda,\theta,d)$ and $E(x;\lambda,\theta,d)$ are given in the Appendix. Russel, Hinch, Leal and Tieffenbruck (1977) have carried out an analysis of the interaction between a cylindrical slender body and a single *rigid* plane wall. The leading-order terms in (9a) and (9b) for $\lambda \rightarrow \infty$ are identical to their asymptotic solutions since the interface (or rigid wall) effects are of order ε^2 .

It may be noted that the shape function $S(x)$ becomes singular at the ends of the body for all but ellipsoidal shapes where $S(x) \equiv 0$, and the solution for the Stokeslet distribution (i.e., Eqs. 9a-b) is not valid at the body ends. However, it can be shown that the singular behavior of $S(x)$ makes no contribution to the total hydrodynamic force and torque exerted on the slender body (since $\lim_{x \rightarrow 0^+} (x^n \ln x) \rightarrow 0$ for any positive integer n), and we make no attempt to improve on the solution near the ends of the body, though methods to do so have been known for some time, Tuck (1964).

The total hydrodynamic force, \mathbf{F} , associated with translation in the \mathbf{e}_1 direc-

tion can be calculated simply by integrating the line density of the Stokeslet distribution, $\alpha(x)$, with respect to x from $-l$ to l .

$$\mathbf{F} = -8\pi\mu_2 \int_{-l}^l \alpha(x) dx \quad (10)$$

The hydrodynamic torque, \mathbf{T} , with respect to the center of the body, can also be obtained from the Stokeslet distribution and is equal to

$$\mathbf{T} = -8\pi\mu_2 \int_{-l}^l \mathbf{x}_0 \wedge \alpha(x) dx . \quad (11)$$

For a circular cylindrical slender body [$r_0(x) = R_0$], the shape function is $S(x) = \frac{1}{2} \ln \left[1 - \left(\frac{x}{l} \right)^2 \right]$, and the total hydrodynamic force and torque can be obtained by direct integration of (10) and (11). The results are

$$\begin{aligned} F_1 = -4\pi\mu_2 U_1 l (\sin^2\theta + 1) \varepsilon \left[1 - \varepsilon \left(\ln 2 - 1 + \frac{3\sin^2\theta - 1}{2(1 + \sin^2\theta)} \right. \right. \\ \left. \left. + \frac{1}{4l} \int_{-l}^l A(x;\lambda,\theta,d) dx \right) \right] + O(\varepsilon^3) \end{aligned} \quad (12a)$$

$$F_3 = 2\pi\mu_2 U_1 l \sin 2\theta \varepsilon \left[1 - \varepsilon \left(\ln 2 + \frac{1}{2} + \frac{1}{4l} \int_{-l}^l E(x;\lambda,\theta,d) dx \right) \right] + O(\varepsilon^3) \quad (12b)$$

$$T_2 = 2\pi\mu_2 U_1 \sin\theta \varepsilon^2 \int_{-l}^l x \cdot H(x;\lambda,\theta,d) dx + O(\varepsilon^3) \quad (13)$$

where $H(x;\lambda,\theta,d)$ is defined by:

$$H(x;\lambda,\theta,d) = \frac{(1 + \sin^2\theta)}{2} A(x;\lambda,\theta,d) + \frac{\cos^2\theta}{2} E(x;\lambda,\theta,d) .$$

For an ellipsoidal body, for which the shape function is $S(x) = 0$, the total hydrodynamic force can also be obtained by substituting $\int_{-l}^l S(x)dx = 0$ in place of $2l(\ln 2 - 1)$ in (12a) and (12b). However, the hydrodynamic torque remains the same since $\int_{-l}^l x \cdot S(x)dx$ vanishes for all even functions of $S(x)$.

When the slender body is oriented perpendicular to the interface ($\theta = 90^\circ$), equations (6a) and (6c) must be modified since $\sec\theta$ is singular. In this case, the resulting expression for the total force and induced torque on a circular cylindrical slender body (i.e., the force and torque corresponding to the translational motion, $U_1 \mathbf{e}_1$) is:

$$F_1 = -8\pi\mu_2 U_1 l \left[\varepsilon - \varepsilon^2 \left[l \ln 2 - \frac{1}{2} + \frac{1}{4l} \int_{-l}^l a(x;\lambda,d) dx \right] \right] + O(\varepsilon^3) \quad (14)$$

$$T_2 = 2\pi\mu_2 U_1 \varepsilon^2 \int_{-l}^l x \cdot a(x;\lambda,d) dx + O(\varepsilon^3) \quad (15)$$

where, again, the function $a(x;\lambda,d)$ is given in the Appendix. The special cases $\theta = 0^\circ$ or 90° were considered by Fulford and Blake (1983), and the present results (12a), (13), (14) and (15) for $\theta = 0^\circ$ and 90° reduce precisely to their results for F_1 and T_2 through terms of $O(\varepsilon^2)$. The instantaneous angular velocities calculated by Fulford and Blake are wrong, however. Although the analysis above yields T_2 as a function of U_1 , the relationship between T_2 and Ω_2 must still be determined, and this was not done by Fulford and Blake (1983) who instead used the relationship for rotation in an *unbounded* fluid.

The effects of hydrodynamic interaction between the particle and the interface are contained in the complicated functions $A(x;\lambda,\theta,d)$, $E(x;\lambda,\theta,d)$, $H(x;\lambda,\theta,d)$ and $a(x;\lambda,d)$ of Eqs. (12)-(15). Thus, in order to illustrate the qualitative nature of these effects, the force components F_1 and F_3 , and the torque T_2 are plotted in Figs. 2, 4 and 5 as a function of the orientation angle θ for $\varepsilon = 0.1887$ (which corresponds to $R_0/l = 0.01$), and two values of particle position, $d/l = 1.01$ and 2. For each value of d/l , we include three values of the viscosity ratio, $\lambda = 0, 1$ and ∞ . Also shown in each case is the corresponding result for motion in an unbounded fluid. The *qualitative* dependence of the drag force, F_1 , on the orientation angle θ is unchanged from the unbounded case by hydrodynamic interac-

tions with the interface. However, due to the presence of the interface, the magnitude of F_1 is either increased or decreased for any arbitrary θ , depending upon the viscosity ratio λ , and this effect is a strong function of the particle position relative to the interface. In particular, the ratio of the drag force, F_1 , to the drag in an infinite fluid for $\theta = 0^\circ$, 45° and 90° , and $\varepsilon = 0.1887$, is seen in Fig. 3 to become a stronger function of λ as d/l decreases *except* for the case of $\theta = 0^\circ$ and $\lambda = 1$. The existence of a critical value of λ separating cases, in which the drag is either increased or decreased due to the presence of the interface, was noted for the special cases $\theta = 0^\circ$ and 90° by Fulford and Blake (1983), and is also similar to the results obtained by Lee, Chadwick and Leal (1979) for translation of a sphere parallel to a flat fluid interface. The magnitude of the effect of the interface on particle drag is, however, considerably larger for a sphere of radius a , with its center at a distance d/a from the interface than for a cylindrical slender body of length $2l$ with its center an equal distance d/l ($\equiv d/a$) away.

The general features of the force component, F_3 , normal to the direction of motion, as a function of θ are again quite similar to those for the case of the same particle moving in an unbounded fluid. The fact that F_3 is nonzero means that a motion in the "1" direction cannot be sustained (say by a force in the "1" direction) without simultaneous application of a force $-F_3$ to the particle by some external means. In the absence of an applied force, $-F_3$, a positive force on the body in the "1" direction will yield a component of motion toward the interface for $0^\circ < \theta < 90^\circ$ (see Figure 1) or away from the interface for $90^\circ < \theta < 180^\circ$. The normal force, F_3 , is increased in magnitude for all λ by the presence of the interface. It may also be noted that the fractional increase in the hydrodynamic force for a given d/l and λ is much larger for F_3 than for F_1 . Thus, the normal force associated with translation at an oblique angle to the symmetry axis is more sensitive to the presence of the interface than the drag.

The induced hydrodynamic torque T_2 , given by Eqs. (13) and (15), is due *solely* to the presence of the interface (i.e., $T_2 \rightarrow 0$ as $d/l \rightarrow \infty$). It is evident, since $T_2 \neq 0$, that a slender body cannot sustain a translational motion, $\mathbf{U} = U_1 \mathbf{e}_1$, without simultaneously rotating unless a torque $-T_2$ is applied to the body by some external means. Thus, a freely suspended slender body (i.e., one with $\mathbf{T} = \mathbf{o}$) will rotate with a sense (i.e., + or -) which depends on λ and on the orientation and position of the body relative to the interface (i.e., θ and d). This rotation can be viewed as a consequence of the gradient in the induced point force strength along the body axis due to the presence of the interface, and is also characteristic of spheres and rigid bodies of other shapes.

The translation of a rigid sphere parallel to a flat interface was analyzed in detail by Lee and Leal (1980). In that case, the sense of rotation was determined, for a given d/a , solely by the viscosity ratio λ . Here, it can be seen from Fig. 5 that the orientation angle plays a critical role, in addition to λ and d/l , in determining the direction of rotation. Indeed, for $\lambda = 1$ and ∞ , rotation in either direction is possible depending on θ . The angle between 90° and 180° (or between -90° and 0°) where $T_2 = 0$ represents a *stable* equilibrium orientation for each particular value of d/l that is illustrated in Figure 5. It should be noted, however, that d/l will increase with time for $90^\circ < \theta < 180^\circ$ unless a force is applied to the particle in the direction normal to the interface. For $\lambda = 0$, on the other hand, a slender body with its center at $d/l = 1.01$ or 2 will rotate in the clockwise direction for all θ so that its leading edge turns away from the interface. In Figure 6, the induced torque is plotted versus the distance between the body center and the interface for $\theta = 0^\circ, 45^\circ$ and 90° , and $\lambda = 0, 1$ and ∞ . It can be noted that the magnitude of the torque increases rapidly as d/l decreases for $\theta = 45^\circ$ and 90° , whereas there exists a critical relative distance, d/l , at which the magnitude of the torque has a maximum value for $\theta = 0^\circ$.

Although it is tempting to conclude from Fig. 6 that the direction of induced rotation is independent of d/l (thus depending only on the viscosity ratio λ and the orientation angle θ), it is dangerous to draw such general conclusions from calculated results for only three values of λ and three values of θ . Indeed, in the case of a rigid sphere near an interface, Lee and Leal (1980) carried out a more detailed examination of the sense of the induced torque and showed, in that case, that there exists a critical distance beyond which the direction of rotation changes for any λ in the range $6 \leq \lambda < \infty$. This change in direction with d would *not* have been evident at all for $\lambda = 0, 1$ or ∞ , the three values considered in Fig. 6.

B. Motion Parallel to the Interface along the x_2 -Axis

Let us now turn to the case of a slender body of arbitrary orientation translating parallel to an infinite plane interface along the x_2 -axis. In this case, the no-slip boundary condition on the body surface is $\mathbf{u}(\mathbf{x}_B) = U_2 \mathbf{e}_2$. By the same approach outlined in the previous sub-section, we have developed a relationship between the velocity $U_2 \mathbf{e}_2$ of the body and the point force density $\alpha_2(x)$.

$$U_2 = \alpha_2(x) \left[\frac{2}{\varepsilon} + 2S(x) + 2\cos^2\eta + B(x; \lambda, \theta, d) \right] + \int_{-l}^l [\alpha_2(\zeta) - \alpha_2(x)] \cdot \Psi_{22}(\mathbf{x}_B, \zeta) d\zeta + O\left(\frac{R_o}{l}, \frac{R_o}{d}\right) \quad (16)$$

In order to remove the η -dependence of the fluid velocity associated with the Stokeslet distribution at $O(\varepsilon^2)$, we again need an additional line distribution of potential dipoles with a density $\beta_2(x) = -\frac{1}{2} r_o^2(x) \alpha_2(x)$. Then, an asymptotic expansion of (16) together with the potential dipole distribution results in the following expression for $\alpha_2(x)$:

$$\alpha_2(x) = \frac{U_2}{2} \left[\varepsilon - \frac{\varepsilon^2}{2} \left(2S(x) + 1 + B(x; \lambda, \theta, d) \right) \right] + O(\varepsilon^3). \quad (17)$$

The hydrodynamic force and torque exerted on a circular cylindrical slender body are thus

$$F_2 = -8\pi\mu_2 U_2 l \varepsilon \left[1 - \varepsilon \left(l \ln 2 - \frac{1}{2} + \frac{1}{4l} \int_{-l}^l B(x; \lambda, \theta, d) dx \right) \right] + O(\varepsilon^3) \quad (18)$$

and

$$T_1 = -2\pi\mu_2 U_2 \sin\theta \varepsilon^2 \int_{-l}^l x \cdot B(x; \lambda, \theta, d) dx + O(\varepsilon^3) \quad (19a)$$

$$T_3 = 2\pi\mu_2 U_2 \cos\theta \varepsilon^2 \int_{-l}^l x \cdot B(x; \lambda, \theta, d) dx + O(\varepsilon^3) \quad (19b)$$

The force and induced torque for the special case of a body oriented perpendicular to the interface must be calculated separately, but it is obvious from symmetry considerations that the results are exactly those already given by equations (14) and (15) [i.e., $F_2 = F_1$ of (14), $T_1 = -T_2$ of (15) and $T_3 = 0$].

The results (18)-(19) are plotted in Figs. 7, 8 and 9 for the same set of parameters as in the previous section. In many respects, the results are similar to those already described for *parallel* motion along the x_1 -axis. There is again a critical viscosity ratio, λ , above or below which the drag in the presence of an interface is either increased or decreased relative to that in an unbounded flow for all d/λ . Furthermore, there is an induced torque due to the interactions between the particle and interface, which will cause the particle to rotate in the absence of externally applied couples, $-T_1$ and $-T_3$. It may be noted that the sensitivity of drag to the orientation angle is very weak. In the particular case of $\lambda = 1$, the drag force is, in fact, nearly constant irrespective of θ . Although the drag force F_2 *must* be independent of θ in an *unbounded fluid*, this would certainly not be expected in the presence of the interface. Figure 8 shows that,

for a given λ , the x_1 component of the angular velocity due to the induced torque T_1 will always have the same sign regardless of θ . On the other hand, the induced torque T_3 always changes sign at the orientation angles $\theta = 0^\circ$ (or 180°) and 90° independent of the viscosity ratio λ and d/l as shown in Fig. 9.

The implication of these somewhat complicated results for the trajectories of a slender particle moving under the action of a force in the x_2 (or x_1) direction will be considered later in the paper.

C. Motion Normal to the Interface along the x_3 -Axis

Finally, let us turn to the problem of a slender body which is translating normal to a plane fluid-fluid interface. The no-slip boundary condition on the body surface is $\mathbf{u}(\mathbf{x}_B) = U_3 \mathbf{e}_3$. As before, this condition cannot be satisfied by a line distribution of Stokeslets alone since the corresponding integral equations contain an η -dependence at $O(\varepsilon^2)$, and a line distribution of potential dipoles is again required with a strength

$$\beta(\mathbf{x}) = -\frac{1}{2} r_0^2(\mathbf{x}) \cdot \alpha(\mathbf{x}) .$$

The corresponding Stokeslet distribution is given by:

$$\alpha_1(\mathbf{x}) = -\frac{\sin 2\theta}{8} U_3 \left[\varepsilon - \frac{\varepsilon^2}{2} \left(2S(\mathbf{x}) + 3 + D(\mathbf{x}; \lambda, \theta, d) \right) \right] + O(\varepsilon^3) \quad (20a)$$

$$\alpha_3 = \frac{(1 + \cos^2 \theta)}{4} U_3 \left[\varepsilon - \frac{\varepsilon^2}{2} \left(2S(\mathbf{x}) + \frac{3\cos^2 \theta - 1}{\cos^2 \theta + 1} + C(\mathbf{x}; \lambda, \theta, d) \right) \right] + O(\varepsilon^3). \quad (20b)$$

For the perpendicular orientation, $\alpha_1(\mathbf{x}) = 0$ and $\alpha_3(\mathbf{x})$ can be obtained simply by substituting $\theta = 90^\circ$ and $b(\mathbf{x}; \lambda, d)$ for $C(\mathbf{x}; \lambda, \theta, d)$ into (20b) [$b(\mathbf{x}; \lambda, d)$, $C(\mathbf{x}; \lambda, \theta, d)$ and $D(\mathbf{x}; \lambda, \theta, d)$ are given in the Appendix].

The total force and hydrodynamic torque acting on a circular cylindrical slender body which translates with velocity $\mathbf{U} = U_3 \mathbf{e}_3$ are

$$F_1 = 2\pi\mu_2 U_3 l \sin 2\theta \varepsilon \left[1 - \varepsilon \left(l \ln 2 + \frac{1}{2} + \frac{1}{4l} \int_{-l}^l D(x; \lambda, \theta, d) dx \right) \right] + O(\varepsilon^3) \quad (21a)$$

$$F_3 = -4\pi\mu_2 U_3 l (\cos^2 \theta + 1) \varepsilon \left[1 - \varepsilon \left(l \ln 2 - 1 + \frac{3\cos^2 \theta - 1}{2(\cos^2 \theta + 1)} + \frac{1}{4l} \int_{-l}^l C(x; \lambda, \theta, d) dx \right) \right] + O(\varepsilon^3) \quad (21b)$$

and

$$T_2 = -2\pi\mu_2 U_3 \cos \theta \varepsilon^2 \int_{-l}^l x J(x; \lambda, \theta, d) dx + O(\varepsilon^3). \quad (22)$$

These results for F_1 , F_3 and T_2 are plotted in Figs. 10-12 as a function of the orientation angle θ for the same set of parameters used in the preceding two cases. The drag force in the direction of motion, F_3 and the force normal to the direction of motion, F_1 , both depend on θ in the same qualitative way as for motion of the same particle in an *unbounded* fluid. The drag force is *increased* relative to the unbounded case, even for $\lambda = 0$, and this effect is enhanced strongly as the body moves closer to the interface. The force normal to the direction of motion is also increased in absolute magnitude with increase of λ or decrease of d/l . It will be noted that F_1 changes sign at $\theta = 0$ and 90° . Thus, for $0^\circ < \theta < 90^\circ$, motion toward the interface will induce translation in the positive "1" direction in the absence of an applied force $-F_1$, while the induced translation will be in the negative "1" direction for $90^\circ < \theta < 180^\circ$. Finally, the hydrodynamic torque, T_2 , induced by the presence of the interface, means that a freely suspended slender body (one with $\mathbf{T} = 0$) cannot translate towards the interface without simultaneously rotating unless the body is oriented parallel or perpendicular to the interface. The former orientation ($\theta = 0^\circ$) is a stable equilibrium point for all λ and d/l while the latter ($\theta = 90^\circ$) is unstable. Thus, a slender body with an arbitrary initial oblique angle ($\theta \neq 90^\circ$) relative to an inter-

face tends to rotate , in the absence of an applied torque, $-T_2$ to a parallel orientation as the body translates towards the interface for all λ .

This completes our detailed study of fundamental solutions of Stokes' equations for translational motion of an arbitrarily oriented slender body in the three mutually orthogonal axis directions specified in Fig. 1. We shall turn shortly to the application of these solutions for trajectory calculations. First, however, in view of the induced hydrodynamic torque which exists due to translational motion near an interface, it is necessary to determine the fundamental solutions for rotation of a slender-body near an interface.

IV. FUNDAMENTAL SOLUTIONS FOR ROTATION OF A SLENDER BODY NEAR A FLAT FLUID INTERFACE

We turn now to the case of a slender body *rotating* with an angular velocity Ω in the presence of a plane fluid-fluid interface. Since the problem is linear, the solution for rotation with an arbitrary angular velocity can be obtained by superposition of the three independent solutions in which the axis of rotation is parallel to one of the three orthogonal x_i ($i = 1,2,3$) axes. As noted earlier, solution of these three fundamental problems will provide all of the components of the hydrodynamic resistance tensors that are *not* obtainable from the results of the preceding section.

First let us consider a rotating slender body when the axis of rotation is parallel to the x_1 -axis (i.e., $\Omega = \Omega_1 \mathbf{e}_1$). In this case, the no-slip boundary condition on the body surface is given by

$$\mathbf{u}(\mathbf{x}_B) = [0, -(x \sin \theta + r_o \sin \eta \cos \theta) \Omega_1, r_o \cos \eta \Omega_1] .$$

We have performed an asymptotic expansion of the integral equation (4) with this boundary condition, using a similar approach to the case of translational

motion, and found the required line distributions of Stokeslets and potential dipoles:

$$\alpha_2(\mathbf{x}) = -\frac{\Omega_1 x \sin\theta}{2} \left[\varepsilon - \frac{\varepsilon^2}{2} \left(2S(\mathbf{x}) - 1 + K(\mathbf{x};\lambda,\theta,d) \right) \right] + O(\varepsilon^3) . \quad (23)$$

The leading term in the line distribution of Stokeslets has a linear dependence on the distance x from the body center, as a consequence of the fact that the magnitude of the velocity near the body surface (i.e., $\frac{|\mathbf{x} - \mathbf{x}_B|}{l} \ll 1$) is also proportional to the distance x for this rotational motion.

Evaluating (10) and (11), we obtain the total torque and force acting on a cylindrical slender body which rotates with angular velocity $\Omega_1 \mathbf{e}_1$:

$$T_1 = -\frac{8}{3} \pi \mu_2 \Omega_1 l^3 \sin^2\theta \varepsilon \left[1 - \varepsilon \left[\ln 2 - \frac{11}{6} + \frac{3}{4l^3} \int_{-l}^l x^2 \cdot K(\mathbf{x};\lambda,\theta,d) dx \right] \right] + O(\varepsilon^3) \quad (24a)$$

$$T_3 = -T_1 \cot\theta \quad (24b)$$

and

$$F_2 = -2\pi\mu_2 \Omega_1 \sin\theta \varepsilon^2 \int_{-l}^l x \cdot B(\mathbf{x};\lambda,\theta,d) dx + O(\varepsilon) . \quad (25)$$

When a particle is oriented perpendicular to the interface, the torque and induced force can be obtained simply by substituting $\theta = 90^\circ$, $c(\mathbf{x};\lambda,d)$ for $K(\mathbf{x};\lambda,\theta,d)$ and $a(\mathbf{x};\lambda,d)$ for $B(\mathbf{x};\lambda,\theta,d)$ into (24a,b) and (25) [$c(\mathbf{x};\lambda,d)$ and $K(\mathbf{x};\lambda,\theta,d)$ are given in the Appendix]. Batchelor (1970) considered the rotation of a straight rigid slender body of an arbitrary crosssection in an *infinite* quiescent fluid, and calculated a hydrodynamic torque which is identical to Eq. (25a) with $\theta = 90^\circ$ up to order of ε .

In Fig. 13, the hydrodynamic torque, T_1 , given by Eq. (24a), is illustrated as a function of the orientation angle, θ , for $d/l = 1.01$, $\varepsilon = 0.1887$ and $\lambda = 0, 1$ and

∞ . Also shown is the corresponding result for rotation in an unbounded infinite fluid. The dependence on the orientation angle, θ , in the presence of an interface is obviously very similar to that obtained for an unbounded fluid. Indeed, the effect of the interface on the required torque becomes very weak when the oblique angle, θ , of the slender body is in the range from $\theta = -45^\circ$ to $\theta = 45^\circ$. In view of the simple relationship between T_1 and T_3 (Eq. 24b), an illustrative figure for T_3 is not necessary. The fact that T_3 is also nonzero (equation 25b) shows that a nonisotropic particle rotating with an angular velocity at an oblique angle θ ($\neq 0$ or 90°) relative to its principal axis will also experience a torque normal to the direction of rotation; a positive torque T_1 (in the absence of an applied torque $-T_3$) will induce a simultaneous rotation in the "3" direction, provided $\theta \neq 0^\circ$ or 90° . The existence of a critical viscosity ratio separating cases of increasing or decreasing torque, evident in Fig. 13, is similar to the results of Lee Chadwick and Leal (1979) for rotation of a sphere with an angular velocity $\Omega = \Omega_1 \mathbf{e}_1$ near a flat interface.

A particle rotating near a flat interface will also experience a hydrodynamic force, F_2 due solely to the presence of the interface, given by Eq. (25). The dimensionless force, $-F_2/\mu_2 \Omega_1 l^2 \varepsilon^2$, required to sustain the specified rotational motion ($\Omega = \Omega_1 \mathbf{e}_1$) without translation is, in fact, identical to the dimensionless torque, $-T_1/\mu_2 U_2 l^2 \varepsilon^2$, required to sustain the translational motion ($\mathbf{U} = U_2 \mathbf{e}_2$) without rotation, which was illustrated previously in Fig. 8. This equality is expected on general theoretical grounds for Stokes' flow with linear boundary conditions. In the absence of a force, $-F_2$, rotation in the "1" direction will induce translation in the "2" direction. The sign of the induced translational velocity depends only on the viscosity ratio, λ .

Now let us consider a rotating slender body whose rotation axis is parallel to the x_2 -axis. With the fluid velocity on the body surface,

$$\mathbf{u}(\mathbf{x}_B) = [(x \sin \theta + r_0 \sin \eta \cos \theta) \Omega_2, 0, -(x \cos \theta - r_0 \sin \eta \sin \theta) \Omega_2],$$

the required line distribution of Stokeslets and potential dipoles is as follows:

$$\alpha_1(x) = \frac{\sin \theta \Omega_2 x}{2} \varepsilon \left[1 - \frac{\varepsilon}{2} \left(2S(x) - 1 + G(x; \lambda, \theta, d) \right) \right] + O(\varepsilon^3) \quad (26a)$$

$$\alpha_3(x) = -\frac{\cos \theta \Omega_2 x}{2} \varepsilon \left[1 - \frac{\varepsilon}{2} \left(2S(x) - 1 + Z(x; \lambda, \theta, d) \right) \right] + O(\varepsilon^3). \quad (26b)$$

The total torque and induced force on the particle can be readily evaluated from the foregoing distribution of Stokeslets:

$$T_2 = -\frac{8}{3} \pi \mu_2 \Omega_2 l^3 \varepsilon \left[1 - \varepsilon \left(l \ln 2 - \frac{11}{6} + \frac{3}{4l^3} \int_{-l}^l x^2 \cdot L(x; \lambda, \theta, d) dx \right) \right] + O(\varepsilon^3) \quad (27)$$

$$F_1 = 2\pi \mu_2 \Omega_2 \sin \theta \varepsilon^2 \int_{-l}^l x \cdot H(x; \lambda, \theta, d) dx + O(\varepsilon^3) \quad (28a)$$

$$F_3 = -2\pi \mu_2 \Omega_2 \cos \theta \varepsilon^2 \int_{-l}^l x \cdot J(x; \lambda, \theta, d) dx + O(\varepsilon^3) \quad (28b)$$

For the perpendicular orientation, $F_3 = 0$,

$$F_1 = 2\pi \mu_2 \Omega_2 \varepsilon^2 \int_{-l}^l x \cdot a(x; \lambda, d) dx + O(\varepsilon^3)$$

and T_2 can be obtained by substituting $c(x; \lambda, d)$ for $L(x; \lambda, \theta, d)$ into (27).

The hydrodynamic torque, T_2 , corresponding to the specified rotational motion, $\Omega_2 \mathbf{e}_2$, is plotted in Fig. 14 for a circular cylindrical slender body as a function of the oblique angle θ for $d/l = 1.01$ and 2, $\varepsilon = 0.1887$ and three values of $\lambda = 0, 1$ and ∞ . Also shown is the corresponding result for rotation in an unbounded fluid. It is evident that the hydrodynamic torque, T_2 , in an unbounded fluid must be independent of the orientation angle θ as shown [indeed, this torque is simply given by equation (27) with $L(x, \lambda, \theta, d) = 0$]. However, the torque in the presence of an interface can be seen to deviate significantly from that in an unbounded fluid with the details depending on the

viscosity ratio and on the orientation and position of the body (i.e., θ and d). Given d/l ($= 2$) and ε ($= 0.1887$), for example, a slender body rotating near a plane solid wall ($\lambda \rightarrow \infty$) experiences a larger hydrodynamic torque than it would be in an unbounded fluid for a certain range of θ (i.e., $-21^\circ < \theta < 21^\circ$ or $75^\circ < \theta < 105^\circ$), but a smaller torque for $21^\circ < \theta < 75^\circ$ or $105^\circ < \theta < 159^\circ$. Further, the torque becomes increasingly sensitive to the orientation angle θ as the viscosity ratio, λ , is increased. For example, in the free surface case (i.e., $\lambda \rightarrow 0$), the torque is still very nearly independent of θ while, in the solid wall case (i.e., $\lambda \rightarrow \infty$), the relative deviation is larger.

As in the case of rotational motion in the "1" direction, there exists an induced hydrodynamic *force* in the present case, which is due to the presence of the interface. The dimensionless induced forces, $F_1/\mu_2\Omega_2 l^2 \varepsilon^2$ and $F_3/\mu_2\Omega_2 l^2 \varepsilon^2$, in this case, are actually identical with the dimensionless induced torques, $T_2/\mu_2 U_1 l^2 \varepsilon^2$ and $T_2/\mu_2 U_3 l^2 \varepsilon^2$, for translation in the "1" and "3" directions, respectively (again, as expected). The direction of the induced force, F_1 , given by equation (28a), depends on the viscosity ratio and on the orientation and position of the body (i.e., θ and d), cf. Fig. 5. However, the direction of action of the induced force, F_3 , obtained from equation (28b), depends only on the orientation angle, θ (see Fig. 12).

Finally, we consider a slender body rotating near a plane interface with an angular velocity $\Omega = \Omega_3 \mathbf{e}_3$. The line distribution of Stokeslets and potential dipoles necessary to satisfy the no-slip boundary condition is

$$\alpha_2(x) = \frac{\cos\theta \Omega_3 x}{2} \varepsilon \left[1 - \frac{\varepsilon}{2} \left(2S(x) - 1 + K(x;\lambda,\theta,d) \right) \right] + O(\varepsilon^3). \quad (29)$$

The total torque and induced force exerted on a cylindrical slender body are then

$$T_1 = \frac{4}{3} \pi \mu_2 \Omega_3 l^3 \sin 2\theta \varepsilon \left[1 - \varepsilon \left(l \ln 2 - \frac{11}{6} + \frac{3}{4l^3} \int_{-l}^l x^2 \cdot K(x; \lambda, \theta, d) dx \right) \right] + O(\varepsilon^3)$$

(30a)

$$T_3 = -\cot \theta \cdot T_1$$

(30b)

and

$$F_2 = 2\pi \mu_2 \Omega_3 \cos \theta \varepsilon^2 \int_{-l}^l x \cdot B(x; \lambda, \theta, d) dx + O(\varepsilon^3)$$

(31)

For the body oriented perpendicular to the interface, the total torque can be shown to be $O(R_0/l, R_0/d)$ and the induced force is obviously zero. This latter result is in agreement with the quiescent infinite-fluid case analyzed by Batchelor (1970).

The hydrodynamic torque, T_3 , given by equation (30b) is plotted in Fig. 15 as a function of the orientation angle θ , including the corresponding result for rotational motion in an unbounded fluid. The effect of the interface is relatively weak and the torque at $d/l = 1.01$ very nearly equals that in an unbounded fluid for all three values of the viscosity ratio, λ . The existence of a "critical" λ separating cases, in which the torque is either increased or decreased is again similar to the results obtained by Lee, Chadwick and Leal (1979) for rotation of a sphere whose rotation axis is normal to an interface. For rotation of a slender body, however, the critical viscosity ratio depends on the particle orientation θ and on the relative distance d/l , and cannot be uniquely determined (as could be done for the sphere).

As in the case of rotation in the "1" direction, a nonspherical axisymmetric body rotating in an unbounded fluid will experience a torque normal to the direction of angular velocity in addition to a torque parallel to that direction unless the axis of rotation is oriented parallel or perpendicular to one of the

principal axes of the particle. The torque T_1 , given by (30a), in the presence of an interface has exactly the same value as the torque T_3 , obtained from (24b), which acts on a slender body with angular velocity, $\Omega = \Omega_1 \mathbf{e}_1$.

The dimensionless induced force $F_2/\mu_2\Omega_3 l^2 \varepsilon^2$, obtained from Eq. (31), in this case, is equal to the dimensionless induced torque $T_3/\mu_2 U_2 l^2 \varepsilon^2$ of Eq. (19b), for translation in the "2" direction. As may be seen from Fig. 9 (the general features of which were discussed in subsection III.B), the direction of induced force F_2 depends on the orientation angle θ and changes sign at $\theta = 0^\circ$ or 90° .

We now have a complete set of fundamental solutions for the translation and rotation of a slender body through a quiescent fluid near a flat interface. These fundamental solutions provide the necessary relationships for calculation of particle trajectories for an arbitrary applied force and/or torque. In general, application of a force parallel to the x_1 -axis produces translation both along the axis, and normal to the interface, as well as rotation, as we shall see shortly. However, in an earlier paper, Fulford and Blake (1983) attempted to calculate the instantaneous angular velocity for a slender-body which they assumed to be translating along the x_1 -axis (only). It is a simple matter to repeat this calculation using (13), (15) and (27). In Fig. 16, the resulting dimensionless angular velocity, $\Omega_2 l / \varepsilon U_1$, is plotted as a function of d/l for $\varepsilon = 0.1887$, and three values of $\theta = 0^\circ, 45^\circ$ and 90° . The corresponding angular velocities calculated by Fulford and Blake (1983) for $\theta = 0^\circ$ and 90° are in error, in some cases by as much as 60%, since they used the relationship $T_2 = -8 \pi/3 \mu_2 l^3 \varepsilon \Omega_2$ instead of (27)[†]

[†] In the final published revision of their paper, Fulford and Blake did not claim to use this expression for T_2 . Instead, they state that the zero torque condition for the freely rotating particle "requires...modification of the force [i.e., Stokeslet] distributions ...". The terms they add to the Stokeslet distributions are just the results precisely equivalent to the expressions, $T_2 = -8/3 \pi \mu_2 l^3 \varepsilon \Omega_2$ for parallel orientation; and $T_2 = 0$ for perpendicular orientation. The hydrodynamic relationship for rotation in the x_2 -direction is, however, $T_2 = -8/3 \pi \mu_2 l^3 \varepsilon \Omega_2$ plus *higher* order terms in the ε -power series which represent the orientation effects (cf. Eq. (27) in the present paper). Furthermore, a careful examination of Eqs. (17) and (18) in Fulford and Blake (1983) shows that *both* of the two equations for angular velocities in

(compare Figs. 3-a and 4-a of Fulford and Blake, 1983, and Fig. 16 in this paper).

V. PARTICLE TRAJECTORIES IN SEDIMENTATION

In the previous sections, we have analyzed separately the individual components of force and torque for a set of mutually perpendicular translational and rotational motions of an arbitrarily oriented slender body. The linearity of Stokes' equations now enables us to solve for arbitrary motions of the body in the presence of a plane interface by superposing the results for these individual translational and rotational motions.

Equations of motion for a rigid body of arbitrary shape in creeping flow can be expressed in general terms, provided the interface remains flat, by defining the so-called translational resistance tensor \mathbf{K}_T , the rotational resistance tensor \mathbf{K}_R , and the coupling tensor \mathbf{K}_C (cf. Happel and Brenner, 1973). Two fundamental relations exist between the translational and angular velocities and the force and torque in terms of these tensors.

$$\mathbf{F} = \mathbf{K}_T \cdot \mathbf{U} + \mathbf{K}_C^t \cdot \Omega \quad (32)$$

$$\mathbf{T} = \mathbf{K}_C \cdot \mathbf{U} + \mathbf{K}_R \cdot \Omega \quad (33)$$

where \mathbf{F} and \mathbf{T} are the total hydrodynamic force and torque, and \mathbf{U} and Ω are the translational and angular velocities, respectively. The tensors, \mathbf{K}_T , \mathbf{K}_R and \mathbf{K}_C can be expressed in the following component form relative to the Cartesian coordinates described in section II:

$$\mathbf{K}_T = \begin{pmatrix} K_T^{11} & 0 & K_T^{13} \\ 0 & K_T^{22} & 0 \\ K_T^{31} & 0 & K_T^{33} \end{pmatrix} \quad (34)$$

each orientation (i.e., perpendicular and parallel) are *still* based on the expression, $T_2 = -8/3 \pi \mu_2 l^3 \varepsilon \Omega_2$ quoted above.

$$\mathbf{K}_R = \begin{pmatrix} K_R^{11} & 0 & K_R^{13} \\ 0 & K_R^{22} & 0 \\ K_R^{31} & 0 & K_R^{33} \end{pmatrix}, \quad K_R^{13} = K_R^{31} \quad (35)$$

and

$$\mathbf{K}_C = \begin{pmatrix} 0 & K_C^{12} & 0 \\ K_C^{21} & 0 & K_C^{23} \\ 0 & K_C^{32} & 0 \end{pmatrix} \quad (36)$$

and the various components of these tensors have already been evaluated in sections III and IV.

Although complete, the equations (32) and (33) are inconvenient for analyzing arbitrary motions of the body because they are based on the coordinate system described in section II. In this coordinate system, we take the x_1 -axis to coincide with the projection of the body center-line onto the interface, and the x_1 - and x_2 -axes must therefore rotate around the x_3 -axis as the body rotates. For trajectory calculations, it is more convenient to use the fixed coordinate system illustrated in Fig. 17. We shall designate the fixed coordinates by the superscript "o". Suppose the angle between the x_1 - and x_1^o -axes becomes φ as the body rotates. Then a simple relationship between the velocity and resistance tensor components in each coordinate system can be established by introducing an orthogonal rotation tensor \mathbf{Q} . For vector quantities, such as the translational velocities, the relationship between vector components is $\mathbf{U} = \mathbf{Q} \cdot \mathbf{U}^o$, where \mathbf{Q} has components of

$$\mathbf{Q} = \begin{pmatrix} \cos\varphi & \sin\varphi & 0 \\ -\sin\varphi & \cos\varphi & 0 \\ 0 & 0 & 1 \end{pmatrix}. \quad (37)$$

Furthermore, the same relationship applies also to the forces, torques and angular velocities in the two coordinate systems. By substituting these relationships into (32) and (33), we have

$$\mathbf{F}^\circ = \mathbf{K}_T^\circ \cdot \mathbf{U}^\circ + \mathbf{K}_C^{1^\circ} \cdot \Omega^\circ \quad (38)$$

$$\mathbf{T}^\circ = \mathbf{K}_C^\circ \cdot \mathbf{U}^\circ + \mathbf{K}_R^\circ \cdot \Omega^\circ \quad (39)$$

where the \mathbf{K}° 's and \mathbf{K} 's are related by

$$\mathbf{K}^\circ = \mathbf{Q}^{-1} \cdot \mathbf{K} \cdot \mathbf{Q} \quad (40)$$

for each of the translation, rotation and coupling tensors.

With the preceding relationships established for the resistance tensors, the velocity vectors and the force and torque vectors all based on a fixed coordinate system, we can readily apply (38) and (39) to general trajectory calculations. For example, let us consider the motion of a slender body near a plane fluid-fluid interface under the action of an external force $\mathbf{F}^{\circ*}$ and torque $\mathbf{T}^{\circ*}$. An instantaneous solution for \mathbf{U}° and Ω° is easily obtained from (38) and (39),

$$\mathbf{U}^\circ = - \left[\mathbf{K}_T^\circ - \mathbf{K}_C^{2^\circ} \cdot \mathbf{K}_R^{\circ-1} \cdot \mathbf{K}_C^\circ \right]^{-1} \cdot \left(\mathbf{F}^{\circ*} - \mathbf{K}_C^{2^\circ} \cdot \mathbf{K}_R^{\circ-1} \cdot \mathbf{T}^{\circ*} \right) \quad (41)$$

$$\Omega^\circ = -\mathbf{K}_R^{\circ-1} \cdot \left(\mathbf{T}^{\circ*} + \mathbf{K}_C^\circ \cdot \mathbf{U}^\circ \right). \quad (42)$$

It is convenient to represent the particle trajectories corresponding to (41) and (42) in terms of the position vector, \mathbf{x}_p , of the body center, and the orientation angles (i.e., Euler's polar angles) θ and φ of the body axis relative to the plane of the interface (for the definitions of θ and φ , see Figs. 1 and 17). The relationships between \mathbf{U}° and Ω° and time rate of changes in \mathbf{x}_p , θ , and φ (simply $\dot{\mathbf{x}}_p$, $\dot{\theta}$ and $\dot{\varphi}$) are as follows:

$$\dot{\mathbf{x}}_p = \frac{d\mathbf{x}_p}{dt} = \mathbf{U}^\circ \quad (43)$$

$$\dot{\theta} = \Omega_1^\circ \sin\varphi - \Omega_2^\circ \cos\varphi \quad (44)$$

$$\dot{\varphi} = -\tan\theta(\Omega_1^\circ \cos\varphi + \Omega_2^\circ \sin\varphi) + \Omega_3^\circ, \text{ for } \theta \neq 90^\circ \quad (45a)$$

and

$$\varphi = \tan^{-1} \left(\frac{\Omega_z^g}{\Omega_I^g} \right) - 90^\circ, \text{ for } \theta = 90^\circ . \quad (45b)$$

These five simultaneous differential equations (43-45) in combination with (41) and (42) are solved below using a fourth-order Runge-Kutta method with appropriate initial conditions. We consider trajectories for the special cases of a torque-free slender body ($\mathbf{T}^\circ \equiv 0$) under the action of non-dimensionalized forces, $\hat{\mathbf{F}}^\circ = \mathbf{F}^\circ / |\mathbf{F}^\circ| = \mathbf{e}_I^g$, parallel to the interface and $\hat{\mathbf{F}}^\circ = \mathbf{e}_3^g$, perpendicular to the interface, respectively. The purpose of these calculations is primarily illustrative. However, these two elementary trajectory problems are relevant to sedimentation phenomena near an interface, as well as being qualitatively related to the processes of particle capture at the surface of a larger bubble or drop which may be viewed as locally planar in the limit where the particle is very much smaller than the collector. First, we begin with the particle motion due to an external force parallel to the interface. This problem for the limit $\lambda = \infty$ was previously considered, both theoretically and experimentally, by Russel, Hinch, Leal and Tiefenbruck (1977). In Fig. 18, the trajectories for a slender body initially located at $\mathbf{x}_p^g = (0, 0, 2)$ with initial orientations $\theta_0 = 0^\circ, 12^\circ, 22^\circ, 50^\circ$ and 79° and $\varphi_0 = 0^\circ$ are plotted in terms of the separation distance d/l and the angle of inclination relative to the interface, θ , for three values of $\lambda = 0, 1$ and ∞ . In this case ($\varphi = 0^\circ$), the axis of the particle is initially in the plane defined by the force and the normal to the interface, and it is only θ and the position of the particle center which change with time. Also shown is the corresponding experimental data for the solid wall case ($\lambda \rightarrow \infty$) obtained by Russel et al. (1977). The present theoretical results are in good agreement with the experimental data of Russel et al. (1977), and show the interesting phenomena of "glancing" and "reversing" turn trajectories that were first identified for $\lambda = \infty$ by the same authors. For a slender body of initial orientation $\theta_0 = 12^\circ$, the force

parallel to the interface not only produces translation of the body parallel to the interface but also translation toward the interface with a simultaneous rotation in the direction of decreasing θ so that the leading edge turns away from the interface. Once the particle becomes parallel to the interface, it begins to move away from the interface as it continues to rotate in the direction of decreasing θ . In this case, the particle does not intersect the wall for any λ . This is an example of a 'glancing turn,' which can be studied in detail in Figs. 18 and 19. For an initial orientation $\theta_0 = 22^\circ$, a slender body near a free surface ($\lambda \rightarrow 0$) still experiences a glancing turn. However, in the cases $\lambda = 1$ and ∞ , the particle reaches the interface before the orientation becomes parallel (actually up to $d/l - |\sin\theta| = 0.01$, which is the separation distance between the tip of the body and the interface). As the initial orientation angle θ_0 is increased further, the direction of rotation changes, and the particle trajectories exhibit so-called 'reversing' turns. In this case, the particle rotates in the direction of increasing θ so that it eventually becomes *perpendicular* to the interface, pivoting about its leading end before moving away from the interface. For example, a slender body with initial orientation $\theta_0 = 79^\circ$ and $\lambda = \infty$ initially approaches the wall while simultaneously rotating with θ increasing until finally the particle is oriented perpendicular to the interface. After this point, the body moves *away* from the interface as it continues to rotate. It may be noted from Figs. 5 and 18 that a slender body near a free surface ($\lambda \rightarrow 0$) never experiences a 'reversing' turn, but instead always rotates in the direction of decreasing θ regardless of the initial orientation, θ_0 , or the relative position of the body, d/l .

In the case $\varphi_0 \neq 0^\circ$, the projection of the particle axis onto the interface is no longer parallel to the external force, $\hat{\mathbf{F}}^0 = \mathbf{e}_1^0$, and the trajectories are different from those in Figs. 18 and 19, in which $\varphi_0 = 0^\circ$. To illustrate the effect of the initial φ -orientation on the particle motion, we have calculated trajectories for a

slender body with initial orientations $\varphi_o = 30^\circ, 60^\circ$ and 90° . The results are shown in Fig. 20.

For small φ_o and θ_o , the qualitative features are similar to those for the case of $\varphi_o = 0^\circ$; however, significantly different features are found for larger φ_o and θ_o . In Fig. 20, the trajectories of a slender body, which is initially located at $\mathbf{x}_p^o = (0,0,2)$ with $\theta_o = 0^\circ, 12^\circ, 22^\circ, 50^\circ$ and 79° and $\varphi_o = 60^\circ$, are plotted in terms of the orientation angle θ and the relative distance d/l from the interface for three values of $\lambda = 0, 1$ and ∞ . It can be seen from Fig. 20 that the trajectories are significantly different from the case of $\varphi_o = 0^\circ$, especially for large values of θ_o and a large viscosity ratio, as the particle not only tumbles end-to-end but also twists relative to the plane defined by the force and the normal to the interface. A rather curious result can be seen for a slender body with $\theta_o = 50^\circ$ or 79° and $\varphi_o = 60^\circ$. Such a particle will, at first, approach a solid wall ($\lambda \rightarrow \infty$) along the trajectory AB shown in Fig. 20, but then moves *away* from the interface along the *reversing* trajectory BAC. In this case, as the particle translates along the \mathbf{x}_1^o -direction it initially moves toward the interface, and rotates in the direction of increasing θ and increasing φ due to the induced torque \mathbf{T}^o of (13), (19) and (22). The increase in φ corresponds to a twisting motion away from the plane defined by the external force and the normal to the interface. Eventually this twisting motion causes the particle axis to become perpendicular to the force (i.e., $\varphi = 90^\circ$ point 'B' in Fig. 20) and further increase in φ then causes the end of the particle furthest from the interface to become the "leading" end insofar as the translational motion is concerned and further translation is accompanied by motion away from the interface exactly along the reversing trajectory BAC in the θ vs. d/l representation due to the symmetry of the system (see Figs. 2, 4, 5 and 7-15).

The other problem considered here is the motion of a torque-free slender body under the action of dimensionless force, $\hat{\mathbf{F}}^o = \mathbf{e}_3^o$, normal to the interface. In Fig. 21, the trajectories for a slender body, which is initially located at $\mathbf{x}_p^o = (0,0,5)$ with orientations $\theta_o = 5^\circ, 30^\circ, 45^\circ, 60^\circ$ and 80° and $\varphi_o = 0^\circ$, are represented in terms of the orientation angle θ and separation distance d/l for three values of $\lambda = 0, 1$ and ∞ . We also include the corresponding results for trajectories in an unbounded fluid. It can be seen from Fig. 12 that the trajectory (θ vs. d/l) for slender body initially oriented parallel or perpendicular to the interface is a vertical straight line. Furthermore, for any initial orientation, θ_o , the particle always rotates towards an orientation *parallel* to the interface. This is perhaps the most interesting and important result of these illustrative calculations. In Fig. 22, the separation distance, d/l , which can be regarded as the "sedimentation distance" is plotted as a function of the "sedimentation time," $|\hat{\mathbf{F}}_o|t/\mu_2 l^2$, for three cases of particle orientation $\theta_o = 5^\circ, 30^\circ$ and 60° . For each orientation, we include three values of $\lambda = 0, 1$ and ∞ . Also shown in each case is the corresponding result for an unbounded fluid. It is evident that the sedimentation time increases due to the presence of interface for any combination of λ and initial orientation. Although the effects of the interface are greatest when the particle is parallel to the interface, the difference from the unbounded fluid case is always relatively small.

This completes our illustrative trajectory calculations using the fundamental solutions that were developed in sections III and IV. It is worth commenting that the scope of the analysis can be readily extended to calculate particle trajectories in any general linear flow field which is consistent with the presence of an interface.

Acknowledgment

This work was supported by a grant from the Fluid Mechanics Program of the National Science Foundation.

APPENDIX

In this appendix, we give detail forms of functions which are defined in sections III and IV that represent the interfacial effects on the motion of slender body near a plane fluid-fluid interface. For convenience, we first define some functions as follows:

$$g(x;\theta,d) = \sinh^{-1} \left| \frac{l - x \cos 2\theta - 2d \sin \theta}{2 \cos \theta (d - x \sin \theta)} \right| + \sinh^{-1} \left| \frac{l + x \cos 2\theta + 2d \sin \theta}{2 \cos \theta (d - x \sin \theta)} \right|$$

$$h(x;\theta,d) = \frac{[l - x \cos 2\theta - 2d \sin \theta]}{\left[(l - x \cos 2\theta - 2d \sin \theta)^2 + \left[2 \cos \theta (d - x \sin \theta) \right]^2 \right]^{1/2}} \\ + \frac{[l + x \cos 2\theta + 2d \sin \theta]}{\left[(l + x \cos 2\theta + 2d \sin \theta)^2 + \left[2 \cos \theta (d - x \sin \theta) \right]^2 \right]^{1/2}}$$

$$k(x;\theta,d) = (d - x \sin \theta) \cdot \left[\frac{1}{\left[(l - x \cos 2\theta - 2d \sin \theta)^2 + \left[2 \cos \theta (d - x \sin \theta) \right]^2 \right]^{1/2}} \right. \\ \left. - \frac{1}{\left[(l + x \cos 2\theta + 2d \sin \theta)^2 + \left[2 \cos \theta (d - x \sin \theta) \right]^2 \right]^{1/2}} \right]$$

$$y(x;\theta,d) = (d - x \sin \theta)^3 \cdot \left[\frac{1}{\left[(l - x \cos 2\theta - 2d \sin \theta)^2 + \left[2 \cos \theta (d - x \sin \theta) \right]^2 \right]^{3/2}} \right. \\ \left. - \frac{1}{\left[(l + x \cos 2\theta + 2d \sin \theta)^2 + \left[2 \cos \theta (d - x \sin \theta) \right]^2 \right]^{3/2}} \right]$$

$$z(x;\theta,d) = \frac{[l - x \cos 2\theta - 2d \sin \theta]^3}{\left[(l - x \cos 2\theta - 2d \sin \theta)^2 + \left[2 \cos \theta (d - x \sin \theta) \right]^2 \right]^{3/2}} \\ + \frac{[l + x \cos 2\theta + 2d \sin \theta]^3}{\left[(l + x \cos 2\theta + 2d \sin \theta)^2 + \left[2 \cos \theta (d - x \sin \theta) \right]^2 \right]^{3/2}}$$

Now the specific formulae for the functions representing the "interfacial effects" can be expressed in terms of $g(x;\theta,d)$, $h(x;\theta,d)$, $k(x;\theta,d)$, $y(x;\theta,d)$, and

$z(x; \theta, d)$.

$$P(x; \lambda, \theta, d) = \frac{1 - \lambda}{1 + \lambda} (1 + \cos^2 \theta) \cdot g(x; \theta, d)$$

$$\begin{aligned} & - \frac{2[2\cos^2 \theta + (1 - 5\cos^2 \theta) \cdot \lambda]}{1 + \lambda} \sin \theta \cdot k(x; \theta, d) + \frac{\cos 2\theta((2 - \cos^2 \theta)\lambda - 2\cos^2 \theta)}{2\cos^2 \theta(1 + \lambda)} h(x; \theta, d) \\ & - \frac{16\lambda \sin \theta \cos 2\theta \cos^2 \theta}{(1 + \lambda)} y(x; \theta, d) + \frac{\lambda \cos 4\theta}{2(1 + \lambda) \cos^2 \theta} z(x; \theta, d) \end{aligned} \quad (A1)$$

$$Q(x; \lambda, \theta, d) = \frac{1 - \lambda}{1 + \lambda} \cos \theta \sin \theta \cdot g(x; \theta, d)$$

$$\begin{aligned} & + \frac{2\cos \theta}{1 + \lambda} (\cos 2\theta + 5\lambda \sin^2 \theta) \cdot k(x; \theta, d) - \frac{\sin \theta (\lambda \cos 2\theta + 4\cos^2 \theta)}{2(1 + \lambda) \cos \theta} h(x; \theta, d) \\ & + \frac{4\lambda \cos \theta \cos 4\theta}{(1 + \lambda)} y(x; \theta, d) + \frac{2\lambda \cos 2\theta \sin \theta}{(1 + \lambda) \cos \theta} z(x; \theta, d) \end{aligned} \quad (A2)$$

$$\begin{aligned} R(x; \lambda, \theta, d) & = -\cos \theta \sin \theta \cdot g(x; \theta, d) - \frac{2\cos \theta}{1 + \lambda} (\cos 2\theta + \lambda \sin^2 \theta) \cdot k(x; \theta, d) \\ & + \frac{\sin \theta (4\cos^2 \theta + 5\lambda \cos 2\theta)}{2(1 + \lambda) \cos \theta} h(x; \theta, d) \\ & - \frac{2\lambda \cos 2\theta \sin \theta}{(1 + \lambda) \cos \theta} z(x; \theta, d) - \frac{4\lambda \cos \theta \cos 4\theta}{1 + \lambda} \cdot y(x; \theta, d) \end{aligned} \quad (A3)$$

$$\begin{aligned} W(x; \lambda, \theta, d) & = -(1 + \sin \theta) \cdot g(x; \theta, d) - \frac{2\sin \theta ((1 + \sin^2 \theta)\lambda - 2\cos^2 \theta)}{1 + \lambda} k(x; \theta, d) \\ & - \frac{\cos 2\theta (2\cos^2 \theta + \lambda(5\cos^2 \theta - 1))}{2(1 + \lambda) \cos^2 \theta} h(x; \theta, d) \\ & - \frac{16\lambda \cos 2\theta \cos^2 \theta \sin \theta}{(1 + \lambda)} y(x; \theta, d) + \frac{\lambda \cos 4\theta}{2(1 + \lambda) \cos^2 \theta} z(x; \theta, d) \\ & - \left[\frac{2\sin \theta \left\{ \cos^2 \theta (3\sin^2 \theta + 1) + \lambda(1 + \sin^2 \theta) \cdot (1 - 3\cos^2 \theta) \right\}}{(1 + \lambda) \cdot (1 + \sin^2 \theta)} \right] k(x; \theta, d) \end{aligned} \quad (A4)$$

$$A(x; \lambda, \theta, d) = \frac{1 - \lambda}{1 + \lambda} \cdot g(x; \theta, d) - \left[\frac{8\lambda \cos 2\theta \cos^2 \theta \sin \theta (1 + 3\sin^2 \theta)}{(1 + \lambda) \cdot (1 + \sin^2 \theta)} \right] y(x; \theta, d)$$

$$\begin{aligned}
 & + \left[\frac{\lambda \cos 4\theta (1 + 3\sin^2\theta)}{4(1 + \lambda) \cos^2\theta (1 + \sin^2\theta)} \right] \cdot z(x; \theta, d) \\
 & - \left[\frac{\cos 2\theta \left(2\cos^2\theta (3\sin^2\theta + 1) - \lambda(12\sin^4\theta - 5\sin^2\theta + 1) \right)}{4(1 + \lambda) \cos^2\theta (1 + \sin^2\theta)} \right] \cdot h(x; \theta, d) \\
 & - \left[\frac{2\sin\theta \left(\cos^2\theta (3\sin^2\theta + 1) + \lambda(1 + \sin^2\theta) \cdot (1 - 3\cos^2\theta) \right)}{(1 + \lambda) \cdot (1 + \sin^2\theta)} \right] \cdot k(x; \theta, d) \tag{A5}
 \end{aligned}$$

$$\begin{aligned}
 B(x; \lambda, \theta, d) &= \frac{1 - \lambda}{1 + \lambda} g(x; \theta, d) - \frac{2\lambda}{1 + \lambda} \sin\theta k(x; \theta, d) \\
 & - \frac{\lambda \cos 2\theta}{2(1 + \lambda) \cos^2\theta} h(x; \theta, d) \tag{A6}
 \end{aligned}$$

$$\begin{aligned}
 C(x; \lambda, \theta, d) &= -g(x; \theta, d) - \left[\frac{2\lambda (1 + 3\cos^2\theta) \sin 4\theta \cos\theta}{(1 + \lambda) \cdot (1 + \cos^2\theta)} \right] \cdot y(x; \theta, d) \\
 & + \left[\frac{\lambda \cos 4\theta (1 + 3\cos^2\theta)}{4(1 + \lambda) \cos^2\theta (1 + \cos^2\theta)} \right] z(x; \theta, d) \\
 & - \left[\frac{2\sin\theta \left(\cos^2\theta (3\cos^2\theta + 1) + \lambda(2\sin^2\theta - 3\sin^4\theta + 2) \right)}{(1 + \lambda) \cdot (1 + \cos^2\theta)} \right] \cdot k(x; \theta, d) \\
 & - \left[\frac{\cos 2\theta \left(2\cos^2\theta (3\cos^2\theta + 1) + \lambda(12\cos^4\theta + 5\cos^2\theta - 1) \right)}{4(1 + \lambda) \cos^2\theta (1 + \cos^2\theta)} \right] \cdot h(x; \theta, d) \tag{A7}
 \end{aligned}$$

$$\begin{aligned}
 D(x; \lambda, \theta, d) &= -g(x; \theta, d) - \left[\frac{\lambda (4\cos 4\theta + 3\sin 2\theta \sin 4\theta)}{(1 + \lambda) \sin\theta} \right] \cdot y(x; \theta, d) \\
 & + \left[\frac{\lambda (3\cos 4\theta - 8\cos 2\theta)}{4(1 + \lambda) \cos^2\theta} \right] \cdot z(x; \theta, d) \\
 & - \left[\frac{(3\sin^2(2\theta) + 4\cos 2\theta) + \lambda 4(4 + 3\sin^2\theta) \sin^2\theta}{2(1 + \lambda) \sin\theta} \right] \cdot k(x; \theta, d) \\
 & + \left[\frac{\cos^2\theta (8 - 6\cos 2\theta) + \lambda \cos 2\theta (7 - 12\cos^2\theta)}{4(1 + \lambda) \cos^2\theta} \right] \cdot h(x; \theta, d) \tag{A8}
 \end{aligned}$$

$$\begin{aligned}
 E(x;\lambda,\theta,d) &= \frac{1-\lambda}{1+\lambda} g(x;\theta,d) - \left[\frac{\lambda(3\sin 4\theta \sin 2\theta - 4\cos 4\theta)}{(1+\lambda)\sin\theta} \right] \cdot y(x;\theta,d) \\
 &\quad + \left[\frac{\lambda(3\cos 4\theta + 8\cos 2\theta)}{4(1+\lambda)\cos^2\theta} \right] \cdot z(x;\theta,d) \\
 &\quad - \left[\frac{2\left[3\cos^2\theta\sin^2\theta - \cos 2\theta + \lambda\sin^2\theta(1-3\cos^2\theta)\right]}{(1+\lambda)\sin\theta} \right] \cdot k(x;\theta,d) \\
 &\quad - \left[\frac{\cos^2\theta(8+6\cos 2\theta) + \lambda\cos 2\theta(12\cos^2\theta-5)}{4(1+\lambda)\cos^2\theta} \right] \cdot h(x;\theta,d)
 \end{aligned} \tag{A9}$$

$$H(x;\lambda,\theta,d) = \frac{(1+\sin^2\theta)}{2} A(x;\lambda,\theta,d) + \frac{\cos^2\theta}{2} E(x;\lambda,\theta,d) \tag{A10}$$

$$J(x;\lambda,\theta,d) = \frac{(1+\cos^2\theta)}{2} C(x;\lambda,\theta,d) + \frac{\sin^2\theta}{2} D(x;\lambda,\theta,d) \tag{A11}$$

$$\begin{aligned}
 K(x;\lambda,\theta,d) &= \frac{1}{x} \cdot \frac{1-\lambda}{1+\lambda} \left[\left[(l - x\cos 2\theta - 2d\sin\theta)^2 + \left[2\cos\theta(d - x\sin\theta) \right]^2 \right]^{1/2} \right. \\
 &\quad \left. - \left[(l + x\cos 2\theta + 2d\sin\theta)^2 + \left[2\cos\theta(d - x\sin\theta) \right]^2 \right]^{1/2} \right] \\
 &\quad + B(x;\lambda,\theta,d) + \frac{1}{x} (d - x\sin\theta) \left[\frac{2}{1+\lambda} \sin\theta g(x;\theta,d) \right. \\
 &\quad \left. - \frac{2\lambda}{1+\lambda} (4\sin^2\theta - 1) k(x;\theta,d) - \frac{\lambda\sin\theta(4\cos^2\theta - 1)}{(1+\lambda)\cos^2\theta} \cdot h(x;\theta,d) \right]
 \end{aligned} \tag{A12}$$

$$\begin{aligned}
 G(x;\lambda,\theta,d) &= \frac{\sin^2\theta - \lambda}{1+\lambda} g(x;\theta,d) + \frac{[2\sin^2\theta \cos^2\theta - \lambda\cos 2\theta(3\cos^2\theta - 4)]}{2(1+\lambda)\cos^2\theta} \cdot h(x;\theta,d) \\
 &\quad - \frac{[(1+2\sin^2\theta)\cos^2\theta + 2\lambda\sin^2\theta]}{(1+\lambda)\sin\theta} \cdot k(x;\theta,d) \\
 &\quad - \frac{2\lambda(\sin 4\theta \sin 2\theta + \cos^2\theta \cos 4\theta)}{(1+\lambda)\sin\theta} \cdot y(x;\theta,d) + \frac{\lambda(\cos 4\theta - 2\cos 2\theta \cos^2\theta)}{2(1+\lambda)\cos^2\theta} \cdot z(x;\theta,d) \\
 &\quad + \frac{\sin^2\theta - \lambda}{(1+\lambda)x} \left[\left[(l - x\cos 2\theta - 2d\sin\theta)^2 + \left[2\cos\theta(d - x\sin\theta) \right]^2 \right]^{1/2} \right. \\
 &\quad \left. - \left[(l + x\cos 2\theta + 2d\sin\theta)^2 + \left[2\cos\theta(d - x\sin\theta) \right]^2 \right]^{1/2} \right]
 \end{aligned}$$

$$\begin{aligned}
 & + \frac{(d - x \sin \theta)}{x} \left[\frac{1 + \sin^2 \theta}{(1 + \lambda) \sin \theta} \cdot g(x; \theta, d) + \right. \\
 & \frac{\cos^2 \theta (4 \cos^4 \theta - 7 \cos^2 \theta + 2) - \lambda \sin^2 \theta (6 \cos^4 \theta - 5 \cos^2 \theta + 2)}{(1 + \lambda) \cos^2 \theta \sin \theta} \cdot h(x; \theta, d) \\
 & + \frac{2 \left[\cos^2 \theta (2 \cos 2\theta - 3) - \lambda (6 \sin^4 \theta + \sin^2 \theta - 4) \right]}{(1 + \lambda)} \cdot k(x; \theta, d) \\
 & + \frac{4 \lambda \cos^2 \theta (16 \sin^4 \theta - 4 \sin^2 \theta - 3)}{(1 + \lambda)} y(x; \theta, d) \\
 & \left. + \frac{\lambda \left[\sin^2 2\theta (4 \cos^2 \theta - 5) + \sin^2 \theta + 1 \right]}{2(1 + \lambda) \cos^2 \theta \sin \theta} \cdot z(x; \theta, d) \right] . \tag{A13}
 \end{aligned}$$

$$\begin{aligned}
 Z(x; \lambda, \theta, d) = & - \frac{\cos^2 \theta + \lambda}{(1 + \lambda)} \cdot g(x; \theta, d) - \frac{2 \cos^4 \theta + \lambda \cos 2\theta (3 \cos^2 \theta + 1)}{2(1 + \lambda) \cos^2 \theta} \cdot h(x; \theta, d) \\
 & + \frac{\sin \theta (2\lambda - 2 \cos^2 \theta - 1)}{(1 + \lambda)} \cdot k(x; \theta, d) + \frac{2\lambda (\sin \theta \cos 4\theta - 2 \cos \theta \sin 4\theta)}{(1 + \lambda)} \cdot y(x; \theta, d) \\
 & + \frac{\lambda (2 \cos 2\theta \sin^2 \theta + \cos 4\theta)}{2(1 + \lambda) \cos^2 \theta} z(x; \theta, d) \\
 & - \frac{\cos^2 \theta + \lambda}{(1 + \lambda)x} \left[\left[(l - x \cos 2\theta - 2d \sin \theta)^2 + \left[2 \cos \theta (d - x \sin \theta) \right]^2 \right]^{1/2} \right. \\
 & \left. - \left[(l + x \cos 2\theta + 2d \sin \theta)^2 + \left[2 \cos \theta (d - x \sin \theta) \right]^2 \right]^{1/2} \right] \\
 & + \frac{(d - x \sin \theta)}{x} \left[\frac{\sin \theta}{1 + \lambda} \cdot g(x; \theta, d) \right. \\
 & - \frac{\sin \theta \left[\cos^2 \theta (4 \cos^2 \theta + 1) + \lambda (6 \cos^4 \theta + \cos^2 \theta - 1) \right]}{(1 + \lambda) \cos^2 \theta} \cdot h(x; \theta, d) \\
 & + \frac{2 \left[(4 \cos^4 \theta - \cos^2 \theta - 1) - \lambda (6 \cos^4 \theta - 7 \cos^2 \theta) \right]}{(1 + \lambda)} \cdot k(x; \theta, d) \\
 & \left. + \frac{4\lambda \left[\sin^2 2\theta (4 \sin^2 \theta - 5) + \cos^2 \theta + 1 \right]}{(1 + \lambda)} \cdot y(x; \theta, d) \right]
 \end{aligned}$$

$$+ \frac{\lambda \sin \theta (16 \sin^4 \theta - 28 \sin^2 \theta + 9)}{2(1 + \lambda) \cos^2 \theta} \cdot z(x; \theta, d) \Big] \quad (\text{A14})$$

$$L(x; \lambda, \theta, d) = \sin^2 \theta G(x; \lambda, \theta, d) + \cos^2 \theta Z(x; \lambda, \theta, d) \quad (\text{A15})$$

For the perpendicular orientation (i.e., $\theta = 90^\circ$),

$$a(x; \lambda, d) = \frac{\lambda - 1}{1 + \lambda} \ln \left[\frac{2d - l - x}{2d + l - x} \right] + \frac{4\lambda l}{1 + \lambda} (d - x) \cdot \frac{[l^2 - d(2d - x)]}{[(2d - x)^2 - l^2]^2} \quad (\text{A16})$$

$$b(x; \lambda, d) = \ln \left[\frac{2d - l - x}{2d + l - x} \right] + \frac{4\lambda l}{1 + \lambda} (d - x) \cdot \frac{[l^2 - d(2d - x)]}{[(2d - x)^2 - l^2]^2} \quad (\text{A17})$$

and

$$c(x; \lambda, d) = a(x; \lambda, d) + 2 \left[\frac{(\lambda - 1)l}{(1 + \lambda)x} + \frac{1}{1 + \lambda} \frac{(x - d)}{x} \cdot \ln \left[\frac{2d - l - x}{2d + l - x} \right] \right] \\ + \frac{4\lambda l}{(1 + \lambda)x} \cdot \left[\frac{3l^2 - (2d - x)(4d - x)}{[(2d - x)^2 - l^2]^2} \right] \cdot (x - d)^2 \quad (\text{A18})$$

References

- Aderogba, K. and Blake, J. R. 1978 Action of a force near the planar surface between two semi-infinite immiscible liquids at very low Reynolds' numbers. *Bull. Aust. Math. Soc.* **18**, 345.
- Batchelor, G. K. 1970 Slender-body theory for particles of arbitrary cross-section in Stokes flow. *J. Fluid Mech.* **44**, 419.
- Berdan II, C. and Leal, L. G. 1982 Motion of a sphere in the presence of a deformable interface. I. Perturbation of the interface from flat: The effect on drag and torque. *J. Colloid Interface Sci.* **87**, 62.
- Cox, R. G. 1970 The motion of long slender bodies in a viscous fluid. Part 1. General theory. *J. Fluid Mech.* **44**, 791.
- Cox, R. G. 1971 The motion of long slender bodies in a viscous fluid. Part 2. Shear flow. *J. Fluid Mech.* **45**, 625.
- Fulford, G. R. and Blake, J. R. 1983 On the motion of a slender body near an interface between two immiscible liquids at very low Reynolds number. *J. Fluid Mech.* **127**, 203.
- Goren, S. L. and O'Neill, M. E. 1971 On the hydrodynamic resistance to a particle of a dilute suspension when in the neighborhood of a large obstacle. *Chem. Eng. Sci.* **26**, 325.
- Happel, J. and Brenner, H. 1973 *Low Reynolds Number Hydrodynamics*. Noordhoff International Publishers.
- Johnson, R. 1980 An improved slender-body theory for Stokes flow. *J. Fluid Mech.* **99**, 441.
- Johnson, R. E. and Wu, T. Y. 1979 Hydrodynamics of low-Reynolds-number flow. Part 5. Motion of a slender torus. *J. Fluid Mech.* **95**, 263.

- Keller, J. B. and Rubinow, S. I. 1976 Slender-body theory for slow visous flow. *J. Fluid. Mech.* **75**, 705.
- Lee, S. H., Chadwick, R. S. and Leal, L.G. 1979 Motion of a sphere in the presence of a plane interface. Part 1. An approximation solution by generalization of the method of Lorentz. *J. Fluid Mech.* **93**, 705.
- Lee, S. H. and Leal, L. G. 1980 Motion of a sphere in the presence of a plane inteface. Part 2. An exact solution in bipolar coordinates. *J. Fluid Mech.* **98**, 193.
- Lee, S. H. and Leal, L. G. 1982 The motion of a sphere in the presence of a deformable interface. II. A numerical study of the translation of a sphere normal to an interface. *J. Colloid Interface Sci.* **87**, 81.
- Russel, W. B., Hinch, E. J., Leal, L. G. and Tieffenbruck, G. 1977 Rods falling near a vertical wall. *J. Fluid Mech.* **83**, 273.
- Tillett, J. P. K. 1970 Axial and transverse Stokes flow past slender axisymmetric bodies. *J. Fluid Mech.* **44**, 401.
- Tuck, E. O. 1964 Some methods for flows past blunt slender bodies. *J. Fluid Mech.* **18**, 619.

Figure Captions

- Figure 1. Description of the coordinate system and orientation of a slender body.
- Figure 2. Dimensionless drag force, $F_1/\mu_2 U_1 l \varepsilon$, as a function of the orientation angle, θ , for translation of a slender body; with $\mathbf{U} = U_1 \mathbf{e}_1$, $\varepsilon = 0.1887$, $S(x) = 1/2 \ln \left[1 - \left(\frac{x}{l} \right)^2 \right]$. — — — for an unbounded fluid case, ----, for $d/l = 1.01$, _____, for $d/l = 2$.
- Figure 3. Ratio of the drag F_1 relative to the drag in an infinite fluid as a function of the dimensionless distance, d/l , between the body center and the interface: $\mathbf{U} = U_1 \mathbf{e}_2$, $\varepsilon = 0.1887$, $S(x) = 1/2 \ln \left[1 - \left(\frac{x}{l} \right)^2 \right]$, — — — for $\theta = 0^\circ$, _____ for $\theta = 45^\circ$, ---- for $\theta = 90^\circ$.
- Figure 4. Dimensionless normal force, $F_3/\mu_2 U_1 l \varepsilon$, as a function of the orientation angle, θ , for translation of a slender body; $\mathbf{U} = U_1 \mathbf{e}_1$, $\varepsilon = 0.1887$, $S(x) = 1/2 \ln \left[1 - \left(\frac{x}{l} \right)^2 \right]$. — — — for an unbounded fluid case, ---- for $d/l = 1.01$, _____ for $d/l = 2$.
- Figure 5. Dimensionless torque, $T_2/\mu_2 U_1 l^2 \varepsilon^2$ (or force, $F_1/\mu_2 \Omega_2 l^2 \varepsilon^2$), as a function of the orientation angle, θ , for translation of a slender body; $\mathbf{U} = U_1 \mathbf{e}_1$ (or $\mathbf{\Omega} = \Omega_2 \mathbf{e}_2$), $\varepsilon = 0.1887$, $S(x) = 1/2 \ln \left[1 - \left(\frac{x}{l} \right)^2 \right]$, ---- for $d/l = 1.01$, _____ $d/l = 2$. — — — for an unbounded fluid.
- Figure 6. Dimensionless torque, $T_2/\mu_2 U_1 l^2 \varepsilon^2$ (or force, $F_1/\mu_2 \Omega_2 l^2 \varepsilon^2$), as a function of the dimensionless distance d/l between the body center and the interface; $\mathbf{U} = U_1 \mathbf{e}_1$ (or $\mathbf{\Omega} = \Omega_2 \mathbf{e}_2$), $\varepsilon = 0.1887$, $S(x) = 1/2 \ln \left[1 - \left(\frac{x}{l} \right)^2 \right]$, — — — for $\theta = 0^\circ$, _____ for $\theta = 45^\circ$, ---- for $\theta = 90^\circ$.

= 90°.

Figure 7. Dimensionless drag force, $F_2/\mu_2 U_2 l \varepsilon$, as a function of the orientation angle, θ , for translation of a slender body; $\mathbf{U} = U_2 \mathbf{e}_2$, $\varepsilon = 0.1887$, $S(x) = 1/2 \ln \left[1 - \left(\frac{x}{l} \right)^2 \right]$, — — — for an unbounded fluid case, ---- for $d/l = 1.01$, _____ for $d/l = 2$.

Figure 8. Dimensionless torque, $T_1/\mu_2 U_2 l^2 \varepsilon^2$ (or force, $F_2/\mu_2 \Omega_1 l^2 \varepsilon^2$), as a function of the orientation angle, θ , for translation (or rotation) of a slender body; $\mathbf{U} = U_2 \mathbf{e}_2$ (or $\mathbf{\Omega} = \Omega_1 \mathbf{e}_1$), $\varepsilon = 0.1887$, $S(x) = 1/2 \ln \left[1 - \left(\frac{x}{l} \right)^2 \right]$. — — — for an unbounded fluid case, ---- for $d/l = 1.01$, _____ for $d/l = 2$.

Figure 9. Dimensionless torque, $T_3/\mu_2 U_2 l^2 \varepsilon^2$ (or force, $F_2/\mu_2 \Omega_3 l^2 \varepsilon^2$), as a function of the orientation angle, θ , for translation (or rotation) of a slender body; $\mathbf{U} = U_2 \mathbf{e}_2$ (or $\mathbf{\Omega} = \Omega_3 \mathbf{e}_3$), $\varepsilon = 0.1887$, $S(x) = 1/2 \ln \left[1 - \left(\frac{x}{l} \right)^2 \right]$. — — — for an unbounded fluid case, ---- for $d/l = 1.01$, _____ for $d/l = 2$.

Figure 10. Dimensionless drag force, $F_3/\mu_2 U_3 l \varepsilon$, as a function of the orientation angle, θ , for translation of a slender body; $\mathbf{U} = U_3 \mathbf{e}_3$, $\varepsilon = 0.1887$, $S(x) = 1/2 \ln \left[1 - \left(\frac{x}{l} \right)^2 \right]$. — — — for an unbounded fluid case. ---- for $d/l = 1.01$, _____ for $d/l = 2$.

Figure 11. Dimensionless normal force, $F_1/\mu_2 U_3 l \varepsilon$, as a function of the orientation angle, θ , for translation of a slender body; $\mathbf{U} = U_3 \mathbf{e}_3$, $\varepsilon = 0.1887$, $S(x) = 1/2 \ln \left[1 - \left(\frac{x}{l} \right)^2 \right]$, — — — for an unbounded fluid case, ---- for $d/l = 1.01$, _____ for $d/l = 2$.

Figure 12. Dimensionless torque, $T_2/\mu_2 U_3 l^2 \varepsilon^2$ (or force, $F_3/\mu_2 \Omega_2 l^2 \varepsilon^2$), as a function of the orientation angle, θ , for translation (or rotation) of a slender body; $\mathbf{U} = U_3 \mathbf{e}_3$ (or $\boldsymbol{\Omega} = \Omega_2 \mathbf{e}_2$), $\varepsilon = 0.1887$, $S(x) = 1/2 \ln \left[1 - \left(\frac{x}{l} \right)^2 \right]$. ---- for $d/l = 1.01$, _____ for $d/l = 2$, _ _ _ for an unbounded fluid case.

Figure 13. Dimensionless torque, $T_1/\mu_2 \Omega_1 l^3 \varepsilon$, as a function of the orientation angle, θ , for rotation of a slender body; $\boldsymbol{\Omega} = \Omega_1 \mathbf{e}_1$, $d/l = 1.01$, $\varepsilon = 0.1887$, $S(x) = 1/2 \ln \left[1 - \left(\frac{x}{l} \right)^2 \right]$, _ _ _ for an unbounded fluid case. The force F_2 induced by this rotation (due to the presence of the interface) is given in Figure 8.

Figure 14. Dimensionless torque, $T_2/\mu_2 \Omega_2 l^3 \varepsilon$, as a function of the orientation angle, θ , for rotation of a slender body; $\boldsymbol{\Omega} = \Omega_2 \mathbf{e}_2$, $d/l = 2$, $\varepsilon = 0.1887$, $S(x) = 1/2 \ln \left[1 - \left(\frac{x}{l} \right)^2 \right]$. _ _ _ for an unbounded fluid case. --- for $d/l = 1.01$, _____ for $d/l = 2$. The force components F_1 and F_3 induced by this rotation are shown, respectively, in Figures 5 and 12.

Figure 15. Dimensionless torque, $T_3/\mu_2 \Omega_3 l^3 \varepsilon$, as a function of the orientation angle, θ , for rotation of a slender body; $\boldsymbol{\Omega} = \Omega_3 \mathbf{e}_3$, $d/l = 1.01$, $\varepsilon = 0.1887$, $S(x) = 1/2 \ln \left[1 - \left(\frac{x}{l} \right)^2 \right]$, - - - -, for an unbounded fluid case. The force components F_2 induced by this rotation is shown in Fig. 9.

Figure 16. Dimensionless angular velocity, $-\Omega_2 l / U_1 \varepsilon$, as a function of the dimensionless distance, d/l , between the body center and the

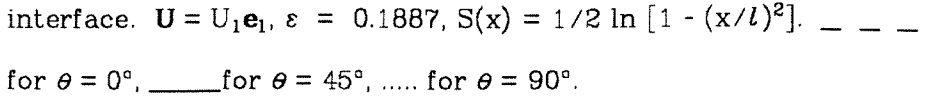
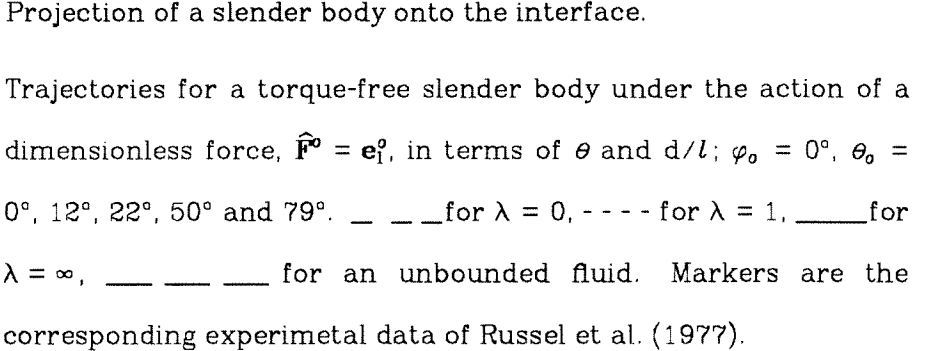
interface. $\mathbf{U} = U_1 \mathbf{e}_1$, $\varepsilon = 0.1887$, $S(x) = 1/2 \ln [1 - (x/l)^2]$. 
for $\theta = 0^\circ$,  for $\theta = 45^\circ$, for $\theta = 90^\circ$.

Figure 17. Projection of a slender body onto the interface.

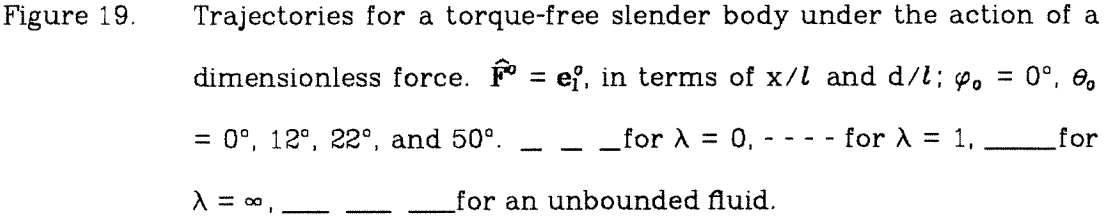
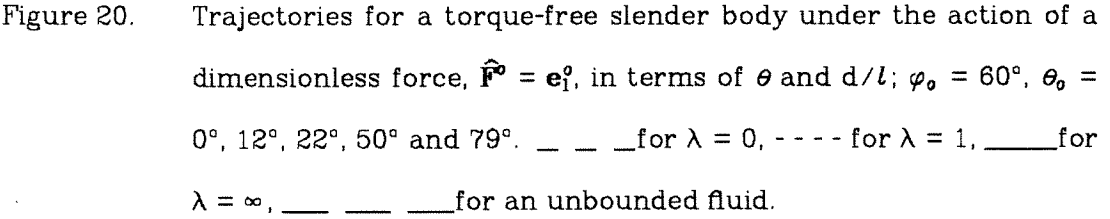
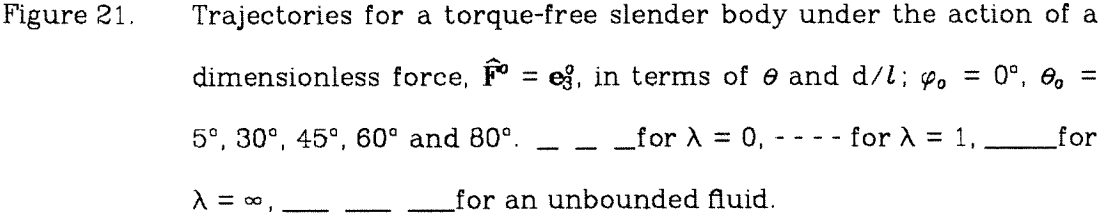
Figure 18. Trajectories for a torque-free slender body under the action of a dimensionless force, $\hat{\mathbf{F}}^o = \mathbf{e}_1^o$, in terms of θ and d/l ; $\varphi_o = 0^\circ$, $\theta_o = 0^\circ, 12^\circ, 22^\circ, 50^\circ$ and 79° .  for $\lambda = 0$, - - - - for $\lambda = 1$,  for $\lambda = \infty$,  for an unbounded fluid. Markers are the corresponding experimental data of Russel et al. (1977).

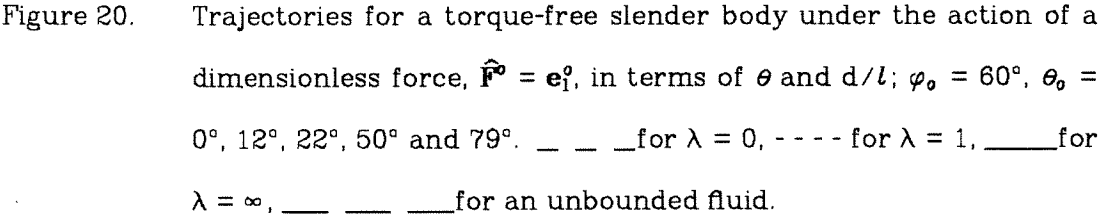
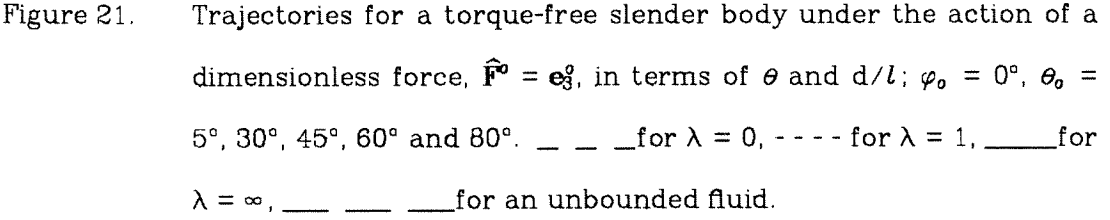
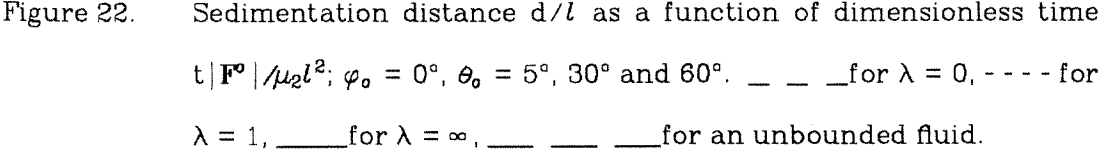
Figure 19. Trajectories for a torque-free slender body under the action of a dimensionless force. $\hat{\mathbf{F}}^o = \mathbf{e}_1^o$, in terms of x/l and d/l ; $\varphi_o = 0^\circ$, $\theta_o = 0^\circ, 12^\circ, 22^\circ$, and 50° .  for $\lambda = 0$, - - - - for $\lambda = 1$,  for $\lambda = \infty$,  for an unbounded fluid.

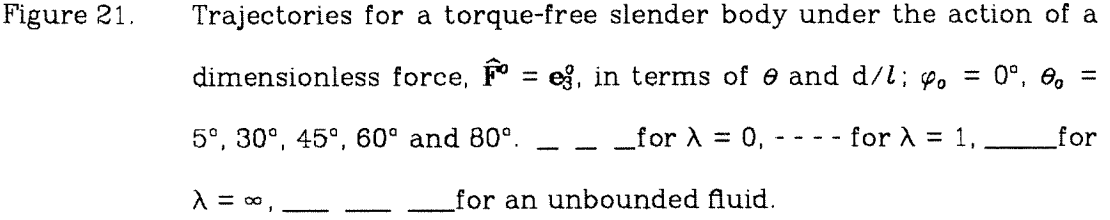
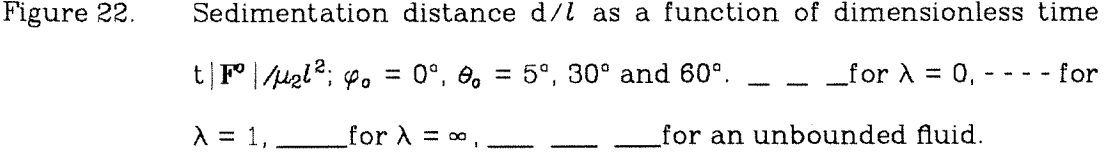
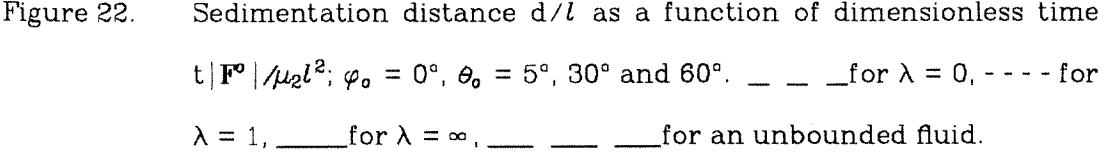
Figure 20. Trajectories for a torque-free slender body under the action of a dimensionless force, $\hat{\mathbf{F}}^o = \mathbf{e}_1^o$, in terms of θ and d/l ; $\varphi_o = 60^\circ$, $\theta_o = 0^\circ, 12^\circ, 22^\circ, 50^\circ$ and 79° .  for $\lambda = 0$, - - - - for $\lambda = 1$,  for $\lambda = \infty$,  for an unbounded fluid.

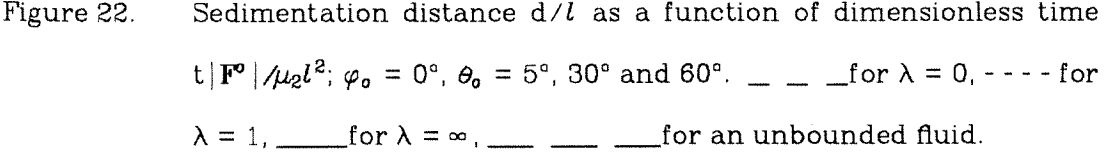
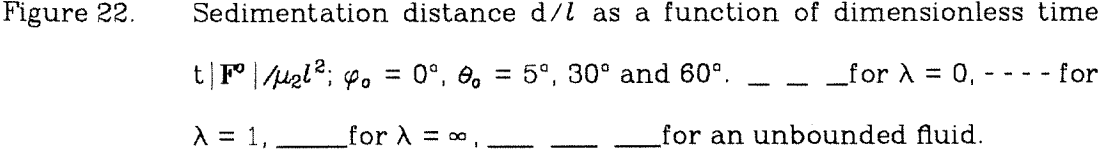
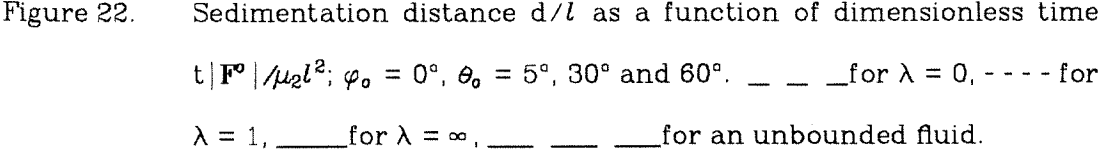
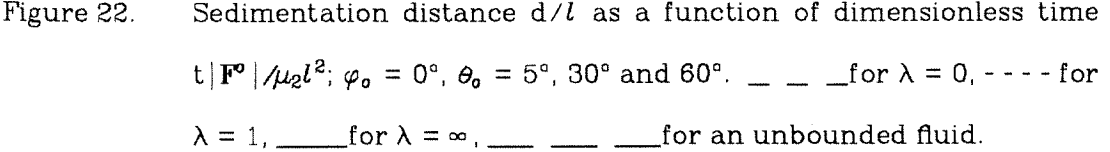
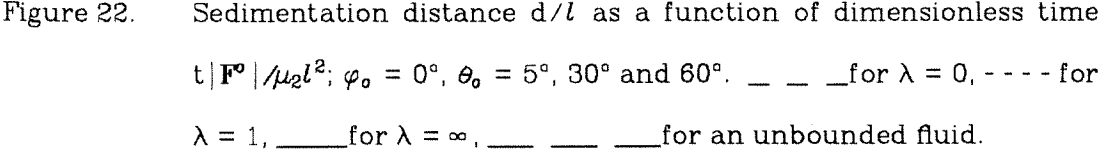
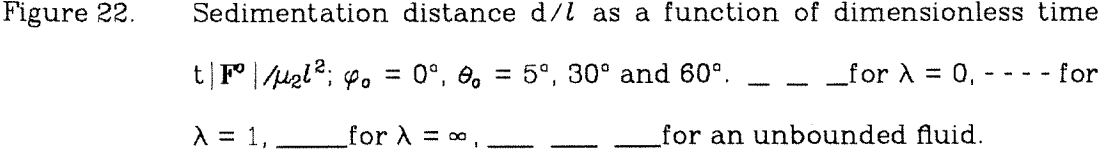
Figure 21. Trajectories for a torque-free slender body under the action of a dimensionless force, $\hat{\mathbf{F}}^o = \mathbf{e}_3^o$, in terms of θ and d/l ; $\varphi_o = 0^\circ$, $\theta_o = 5^\circ, 30^\circ, 45^\circ, 60^\circ$ and 80° .  for $\lambda = 0$, - - - - for $\lambda = 1$,  for $\lambda = \infty$,  for an unbounded fluid.

Figure 22. Sedimentation distance d/l as a function of dimensionless time $t |\mathbf{F}^o| / \mu_2 l^2$; $\varphi_o = 0^\circ$, $\theta_o = 5^\circ, 30^\circ$ and 60° .  for $\lambda = 0$, - - - - for $\lambda = 1$,  for $\lambda = \infty$,  for an unbounded fluid.

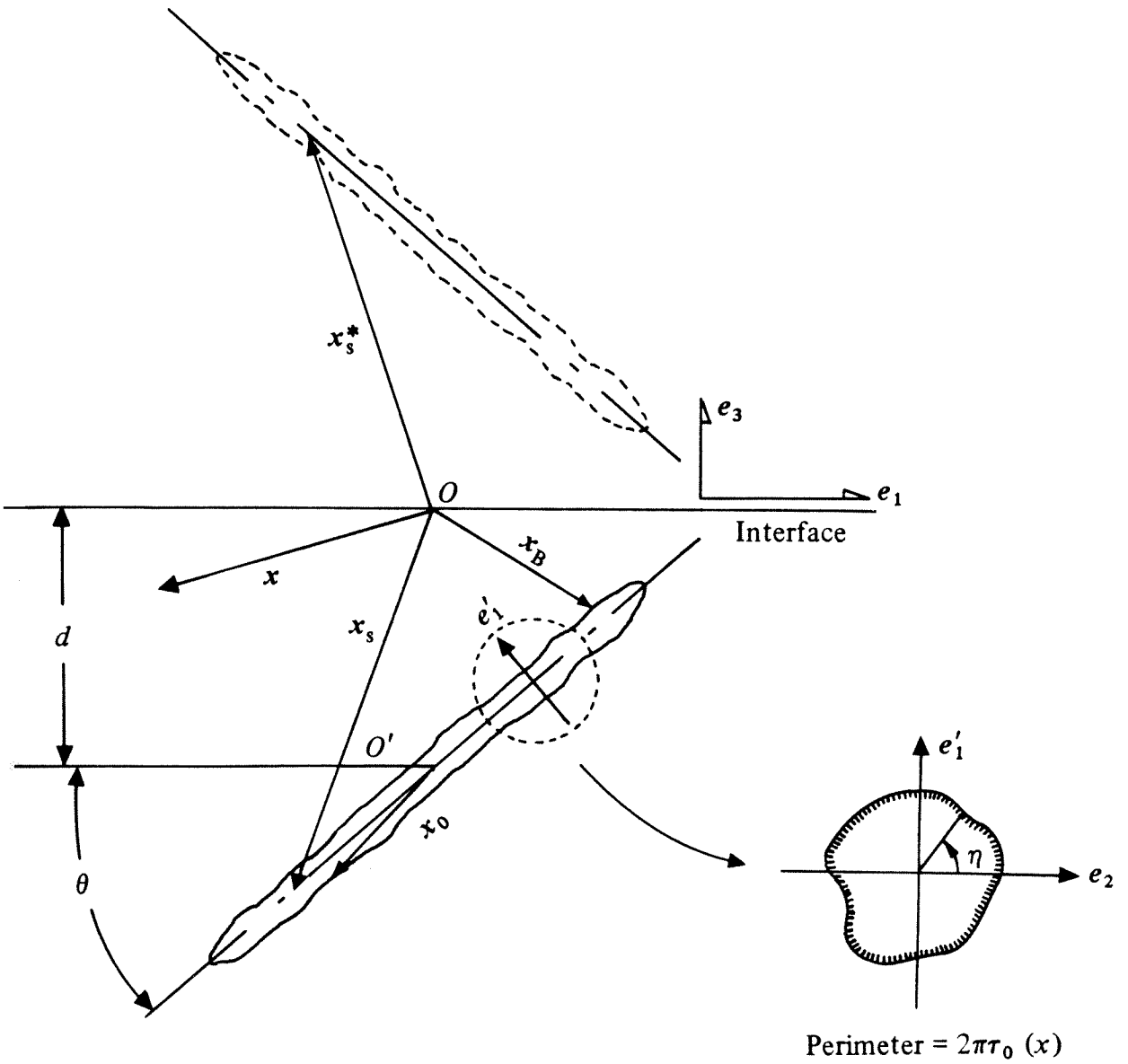


Figure 1

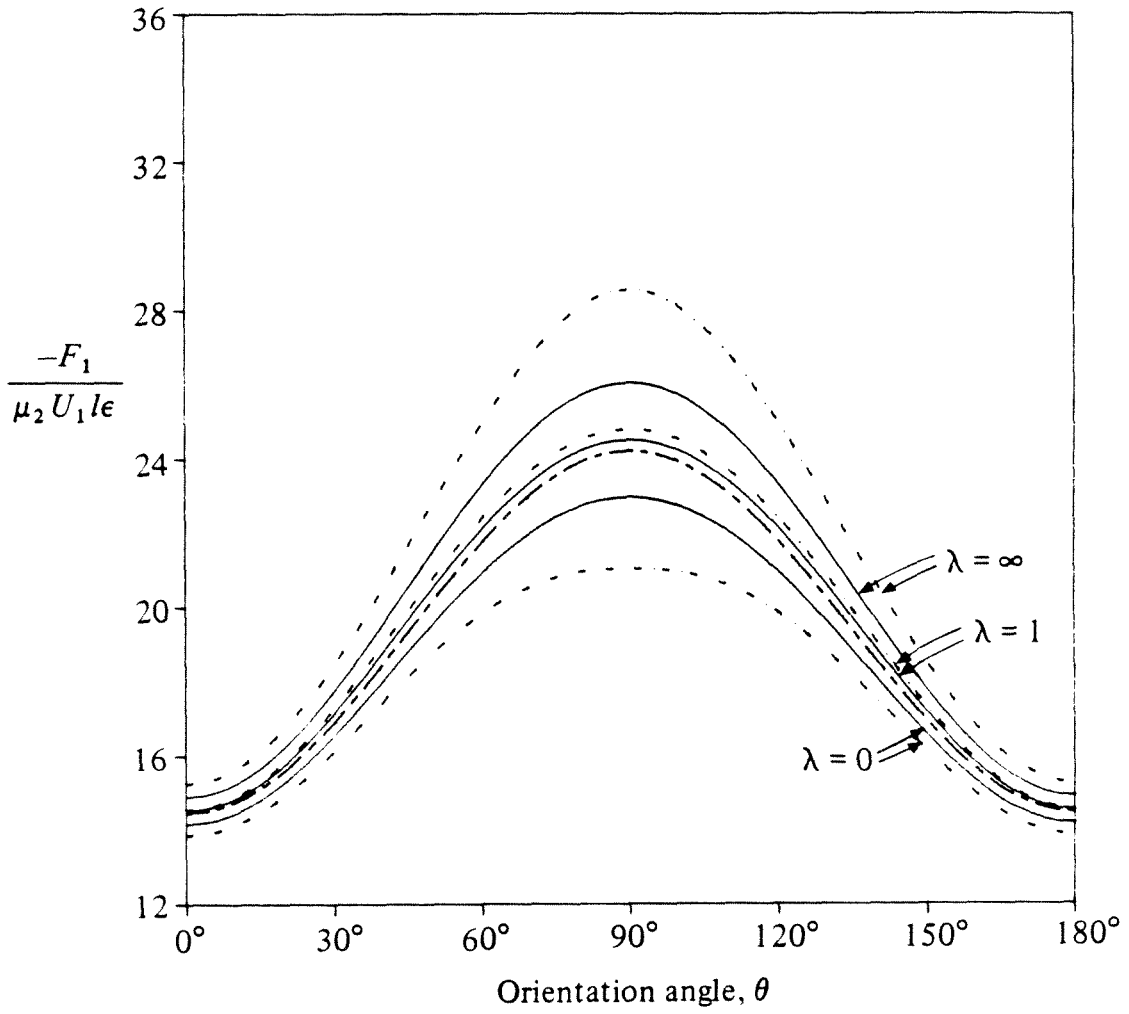


Figure 2

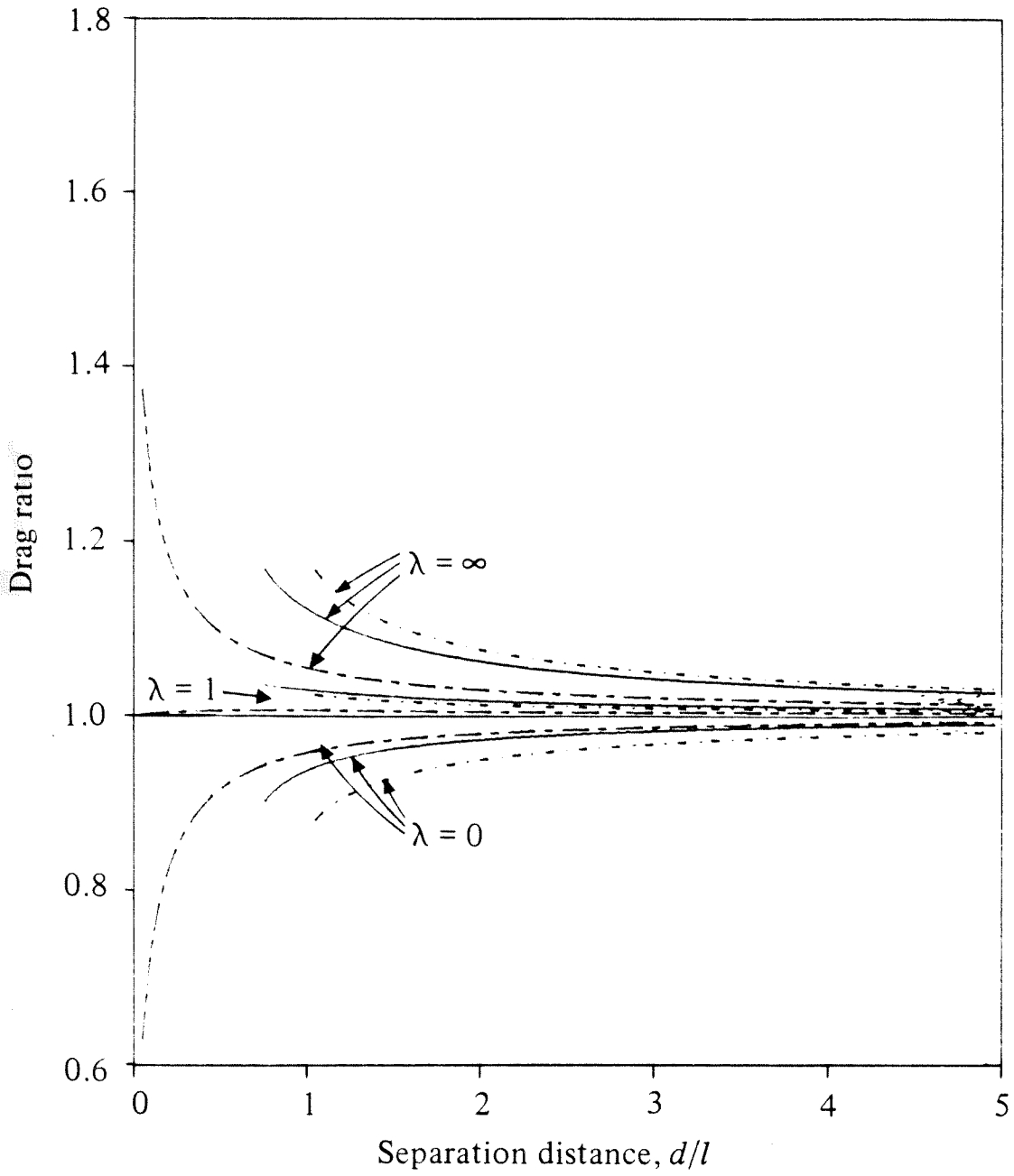


Figure 3

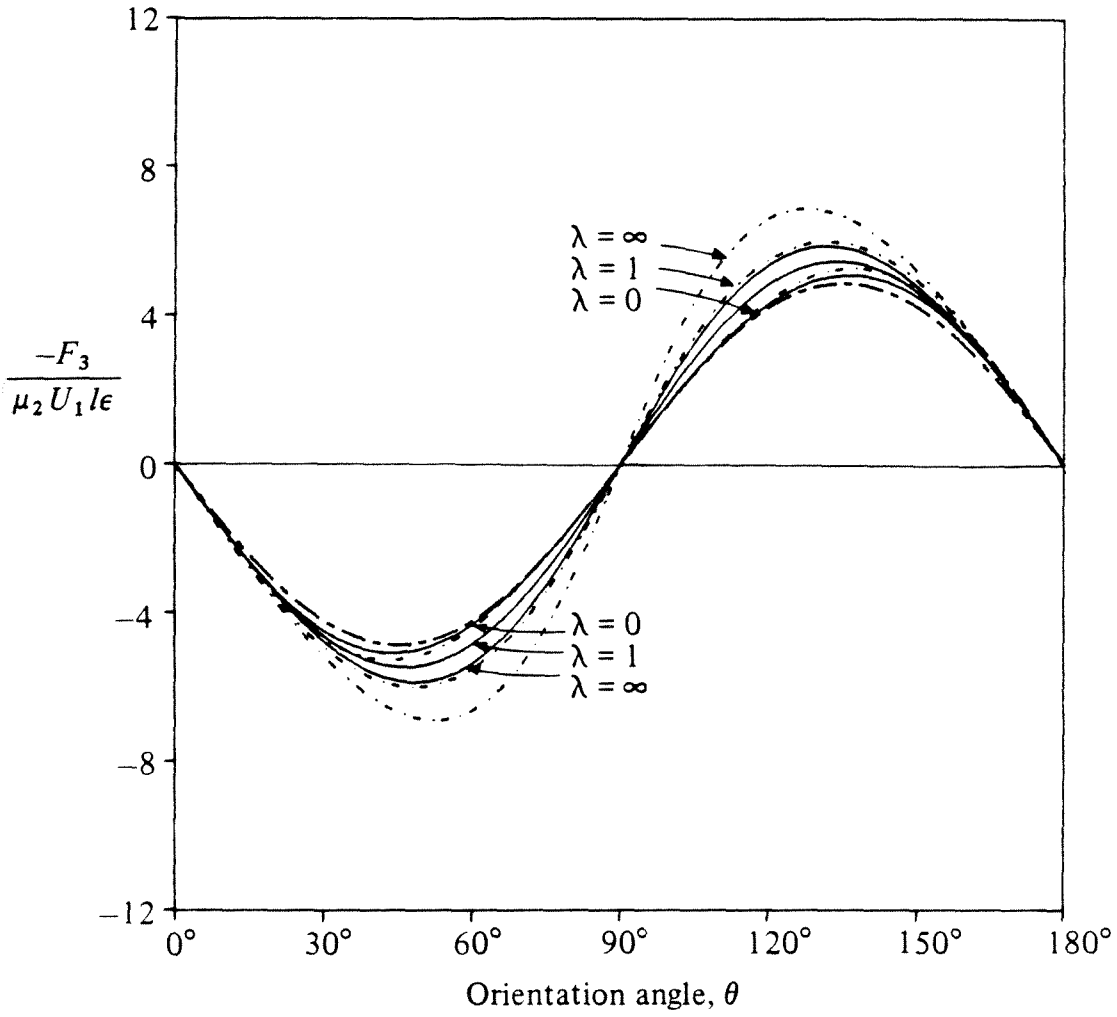


Figure 4

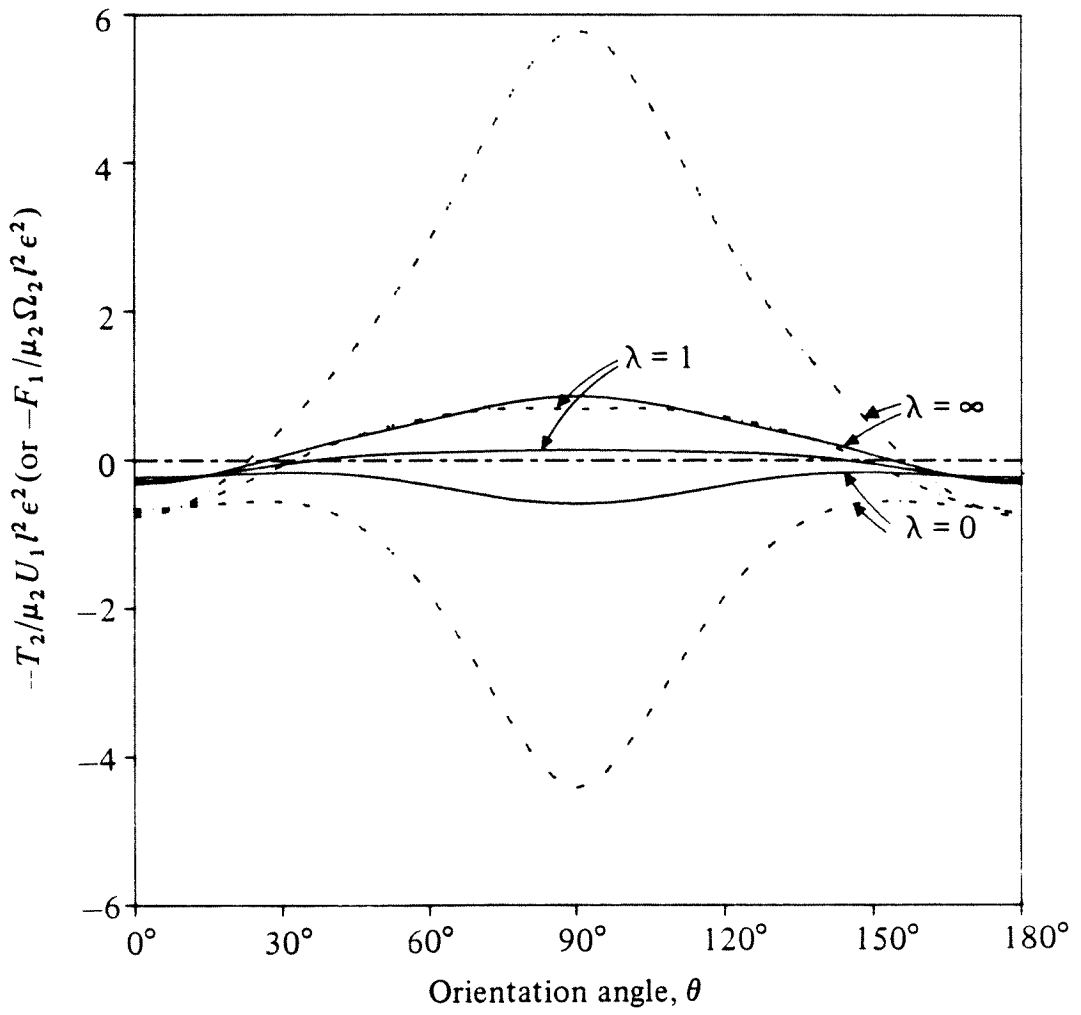


Figure 5

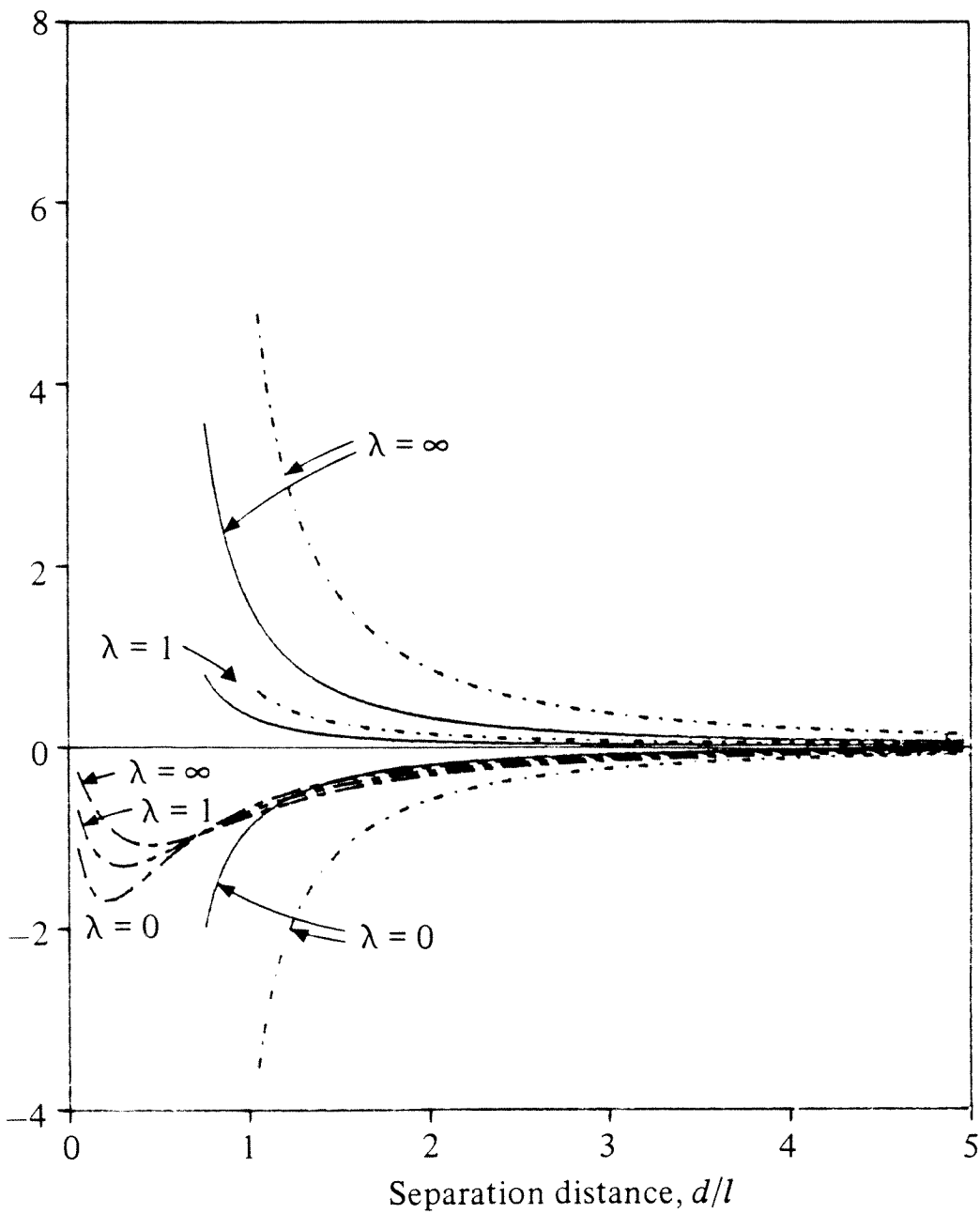


Figure 6

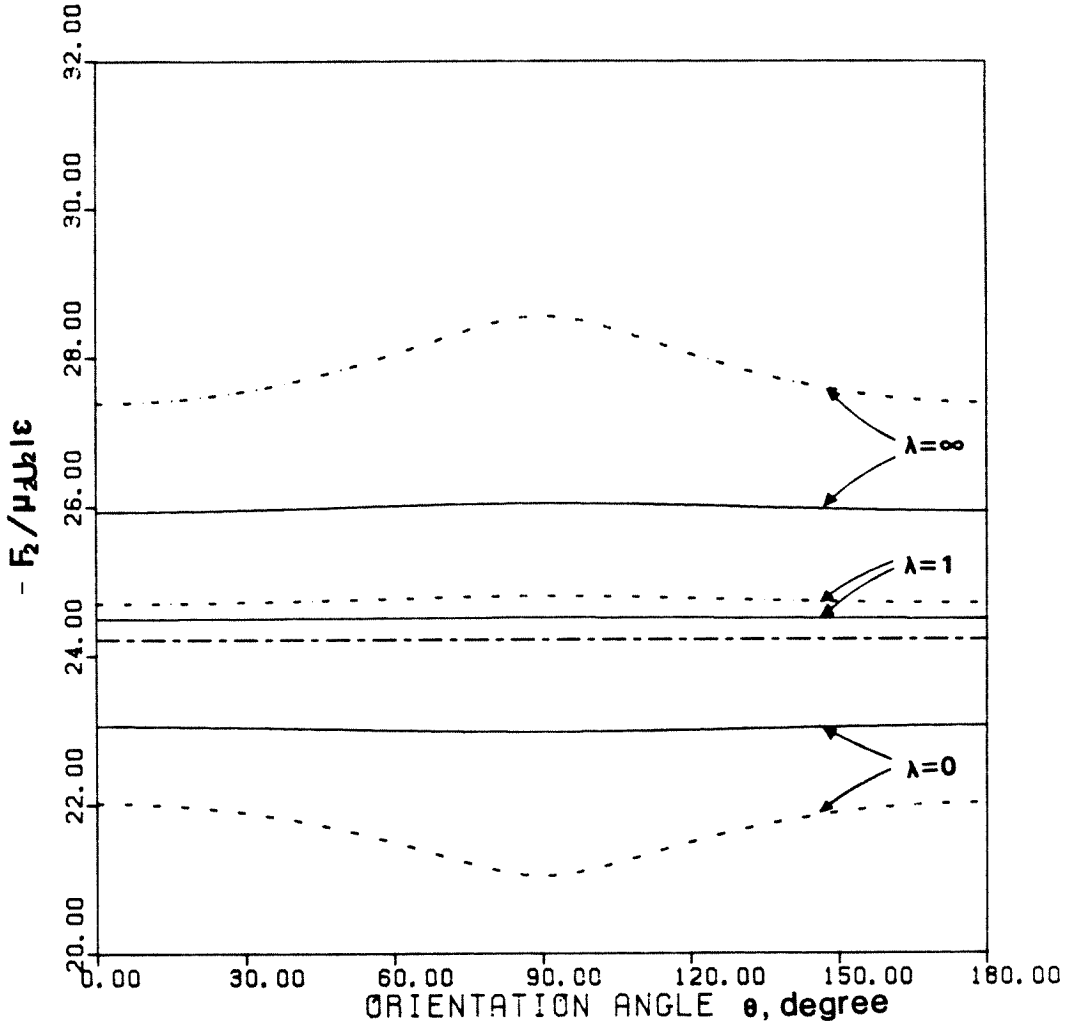


Figure 7

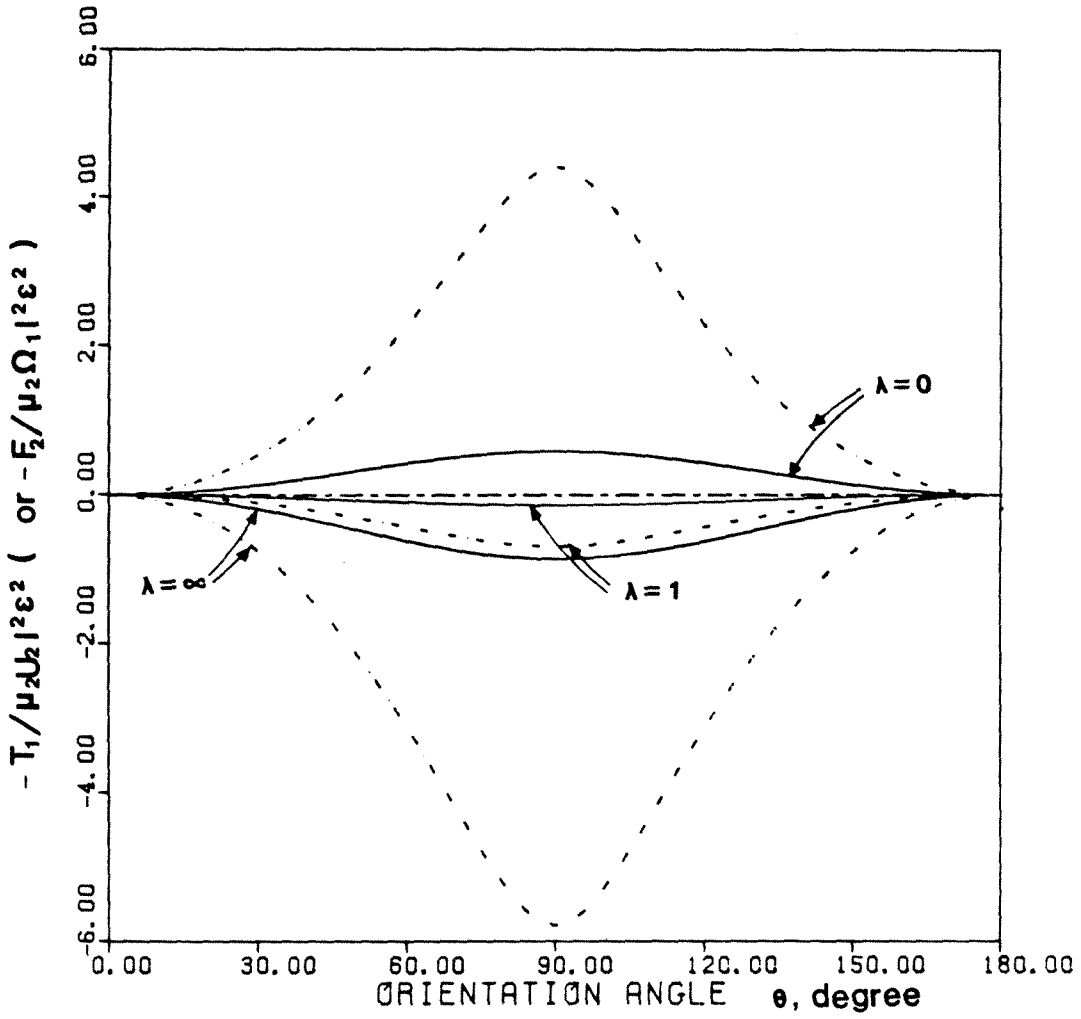


Figure 8

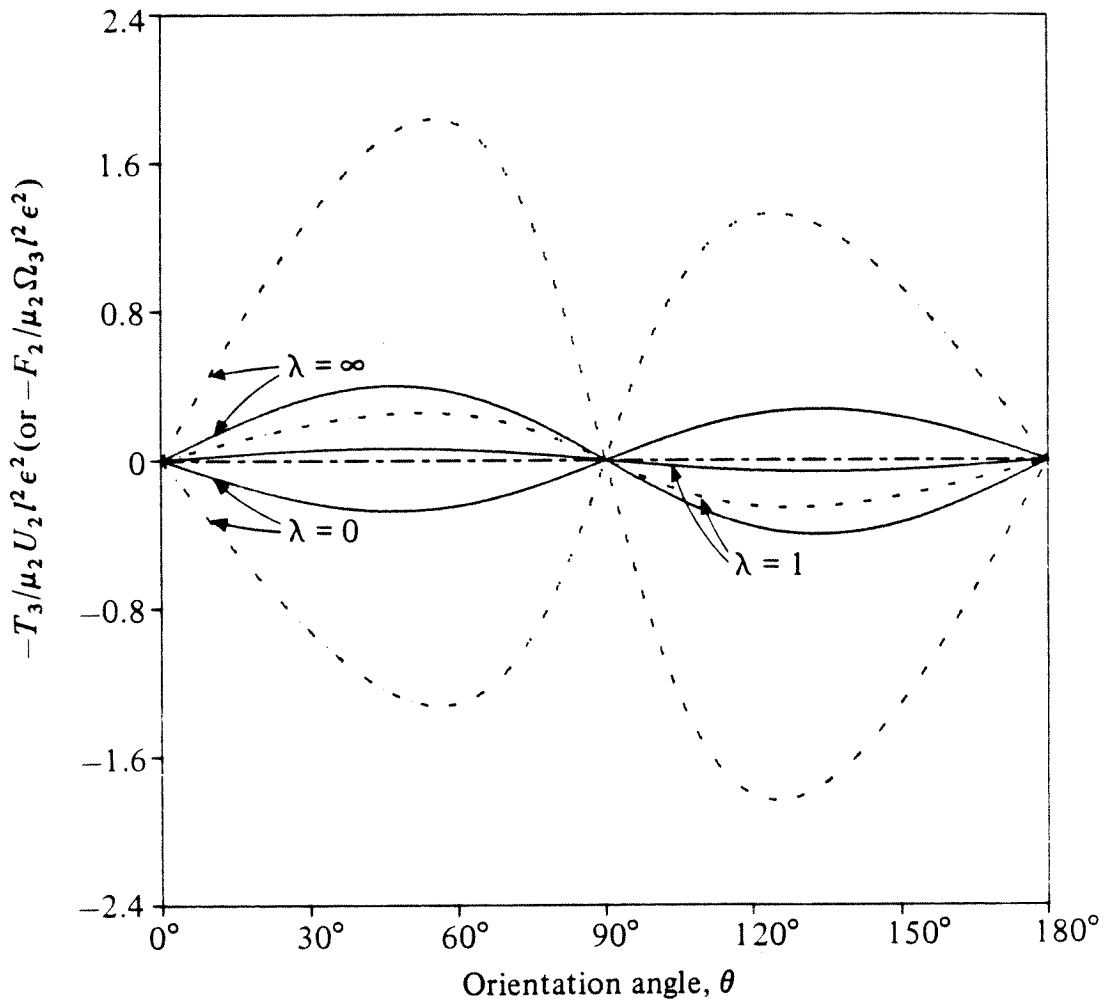


Figure 9

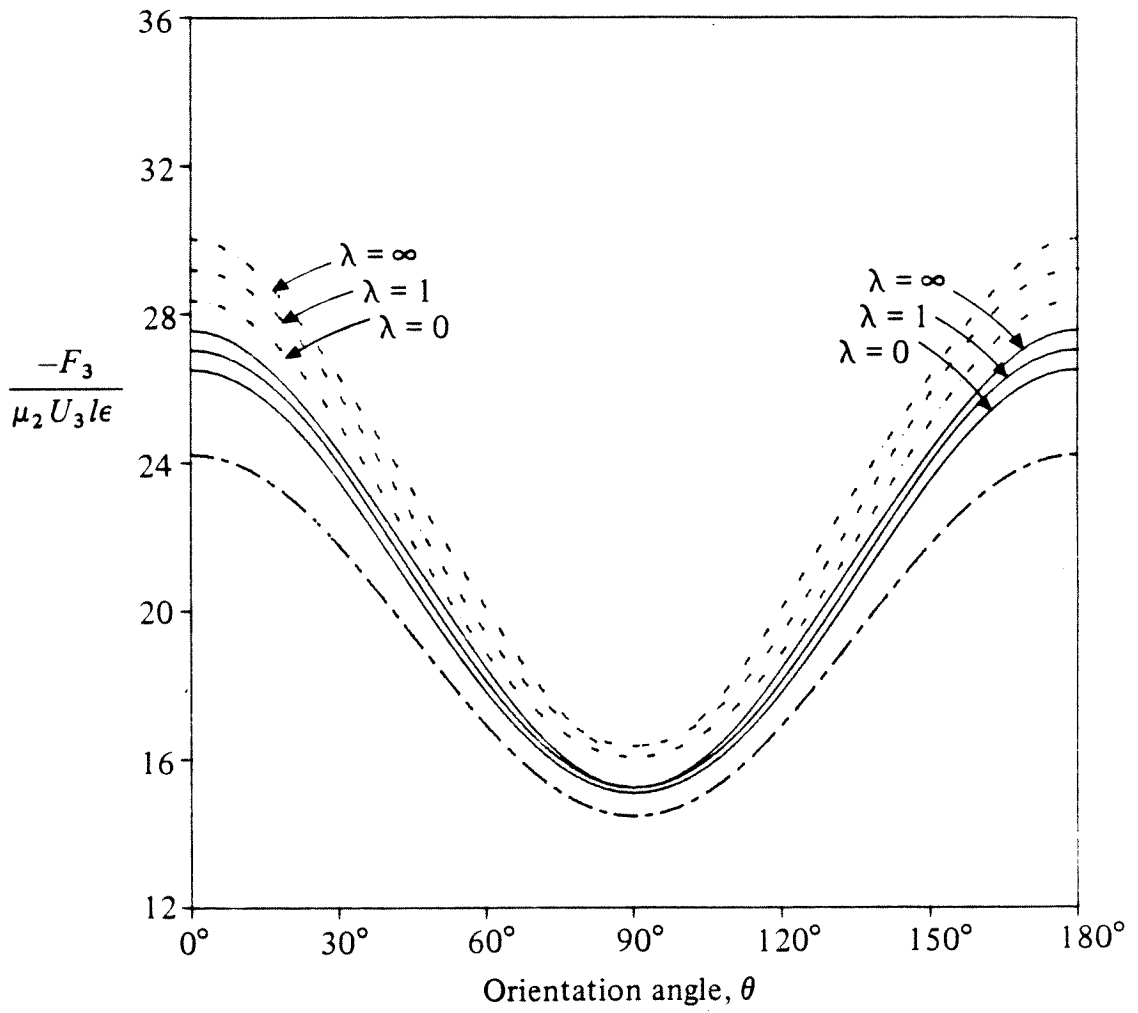


Figure 10

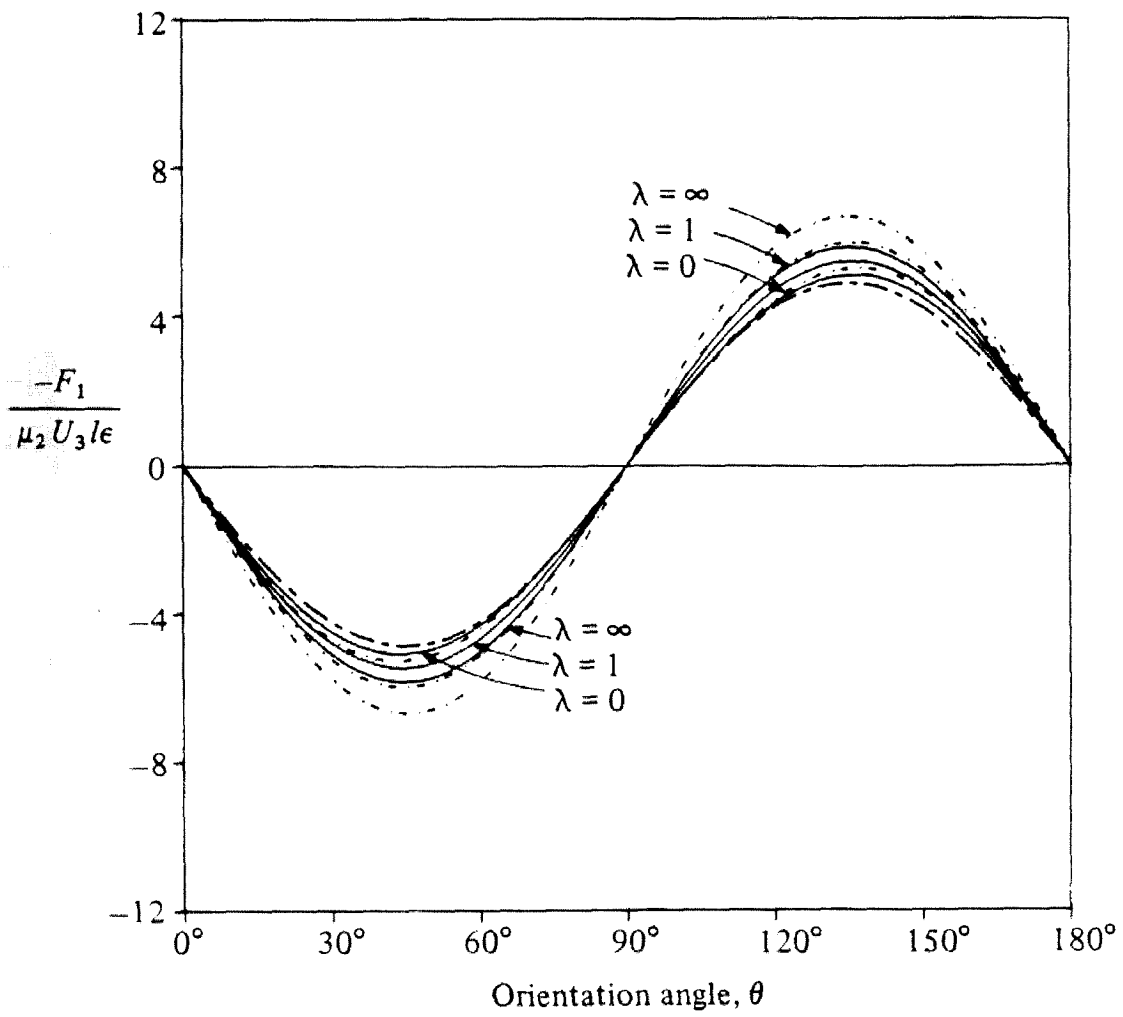


Figure 11

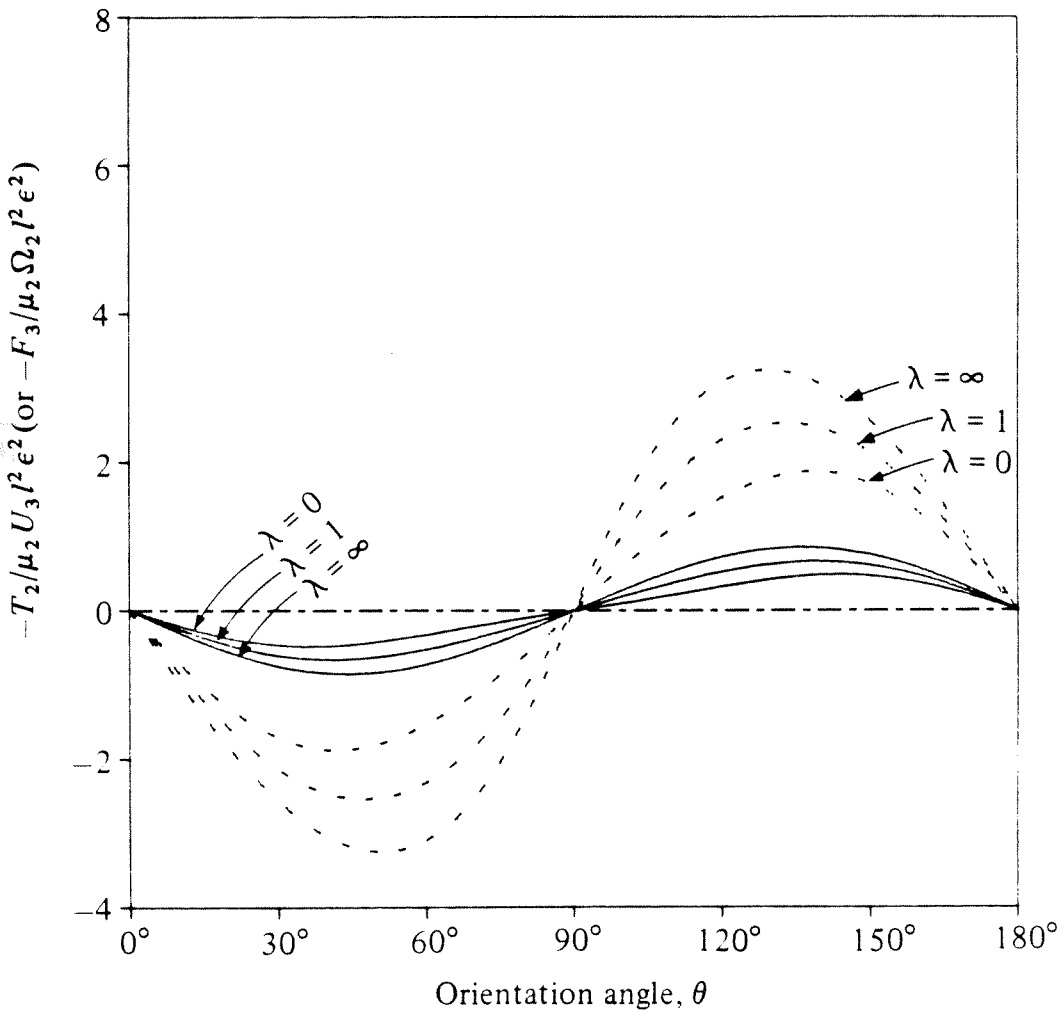


Figure 12

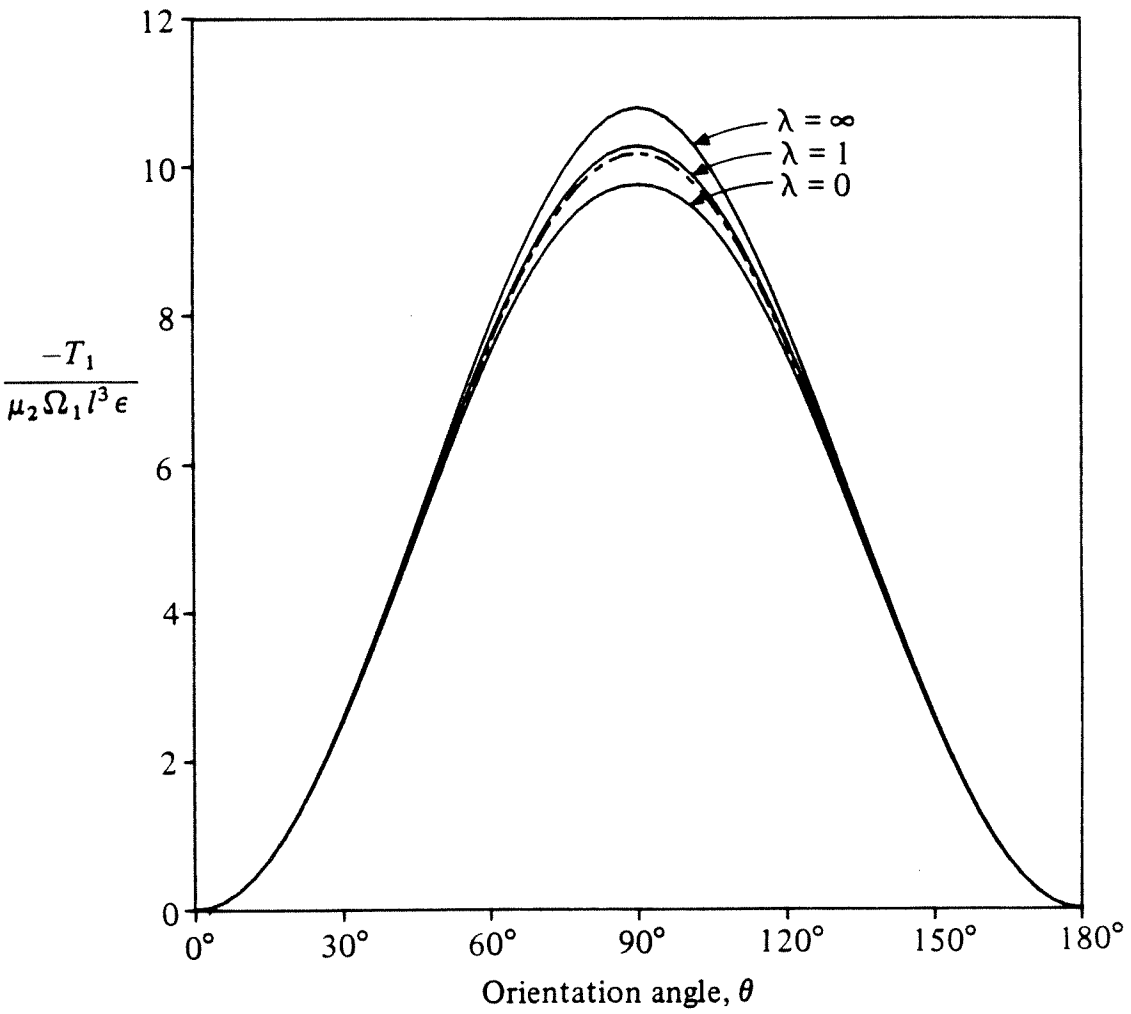


Figure 13

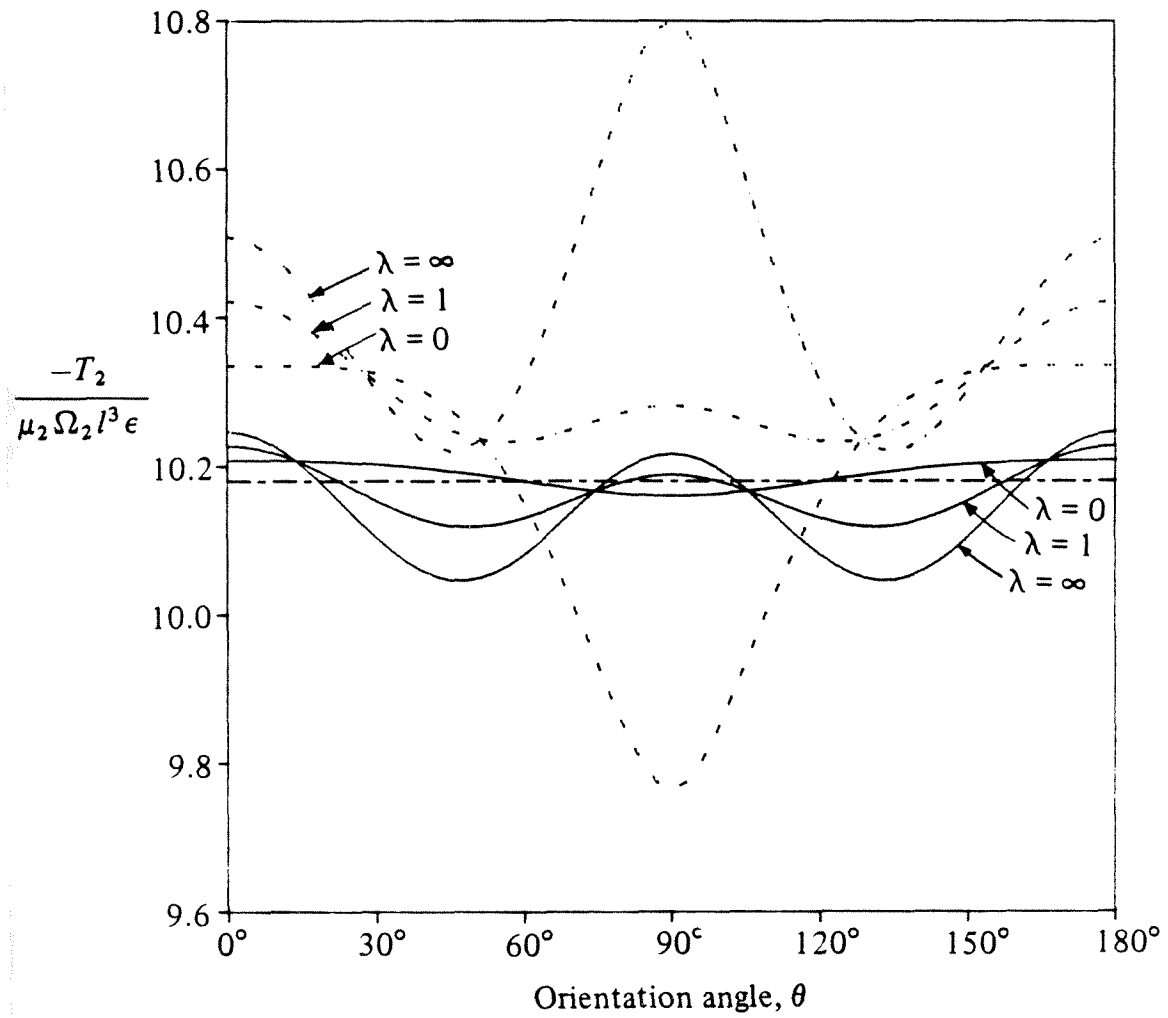


Figure 14

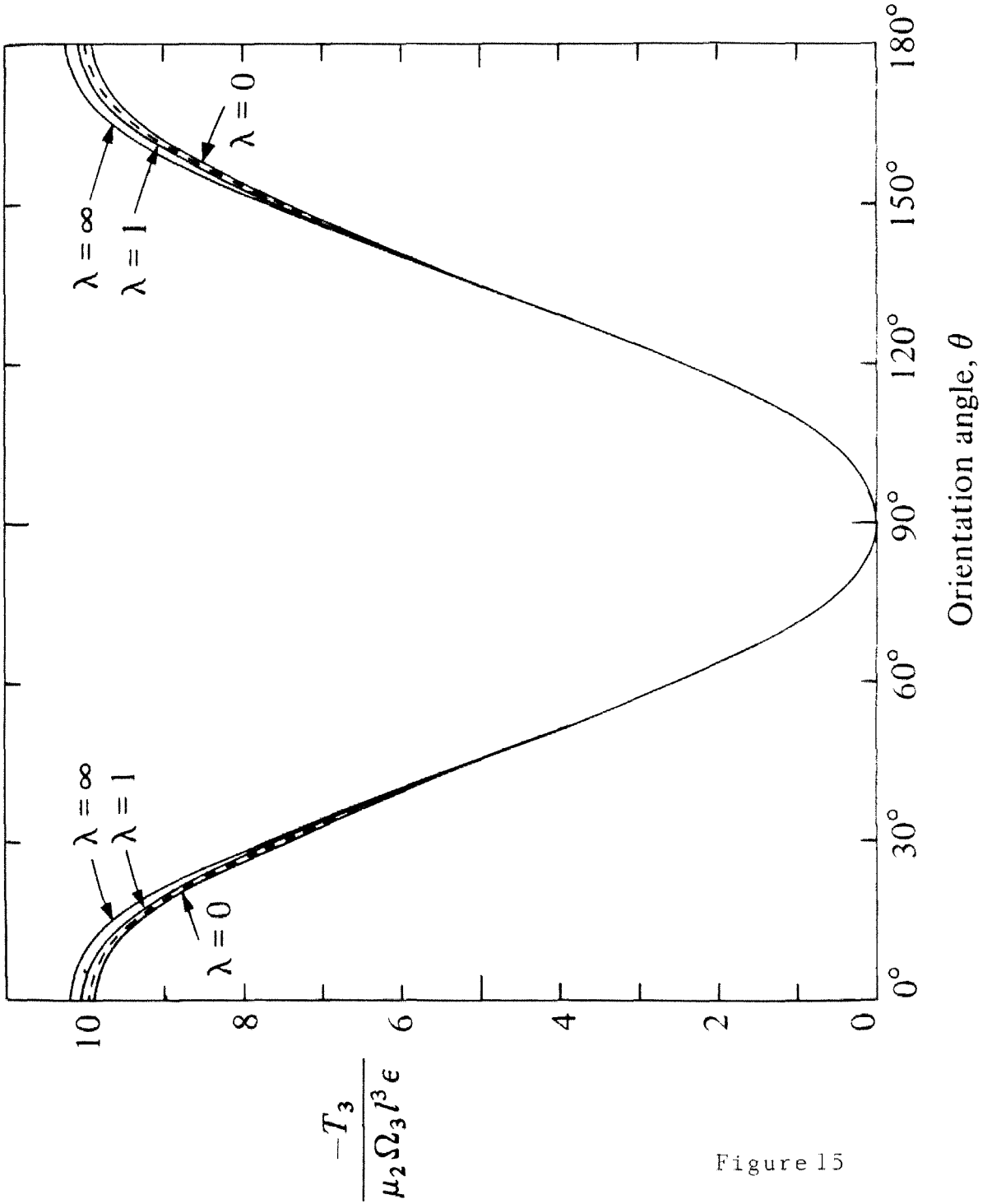


Figure 15

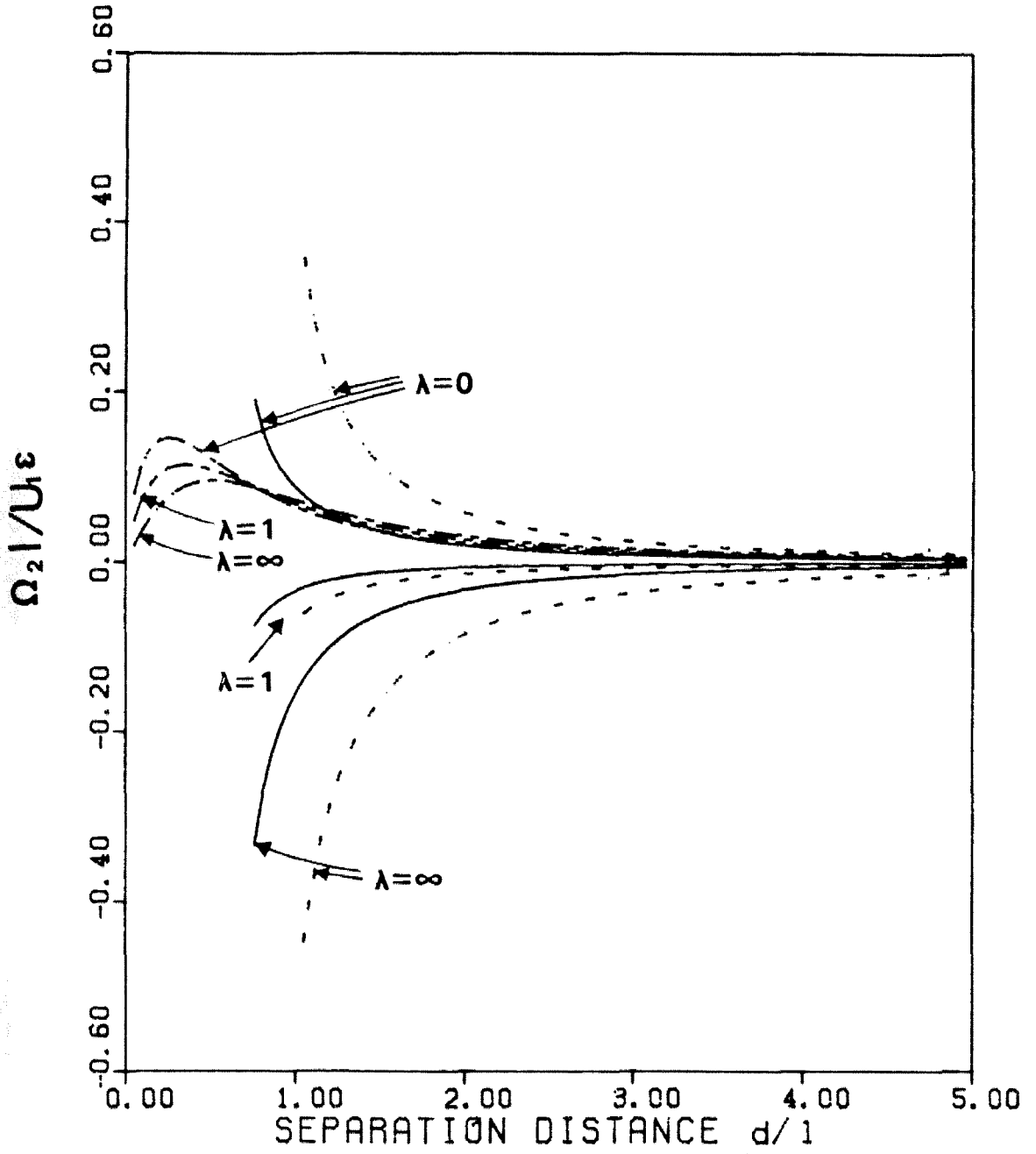


Figure 16

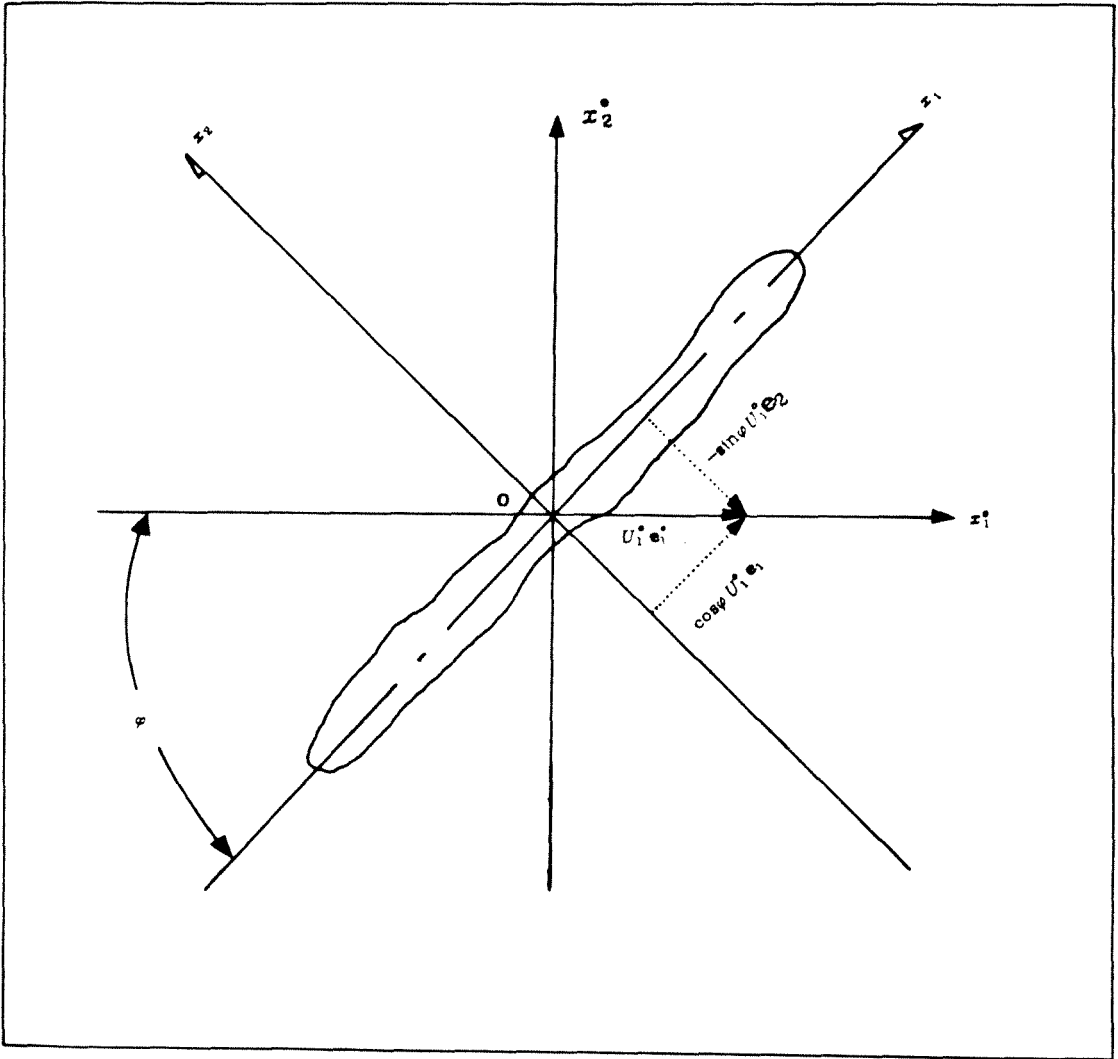


Figure 17

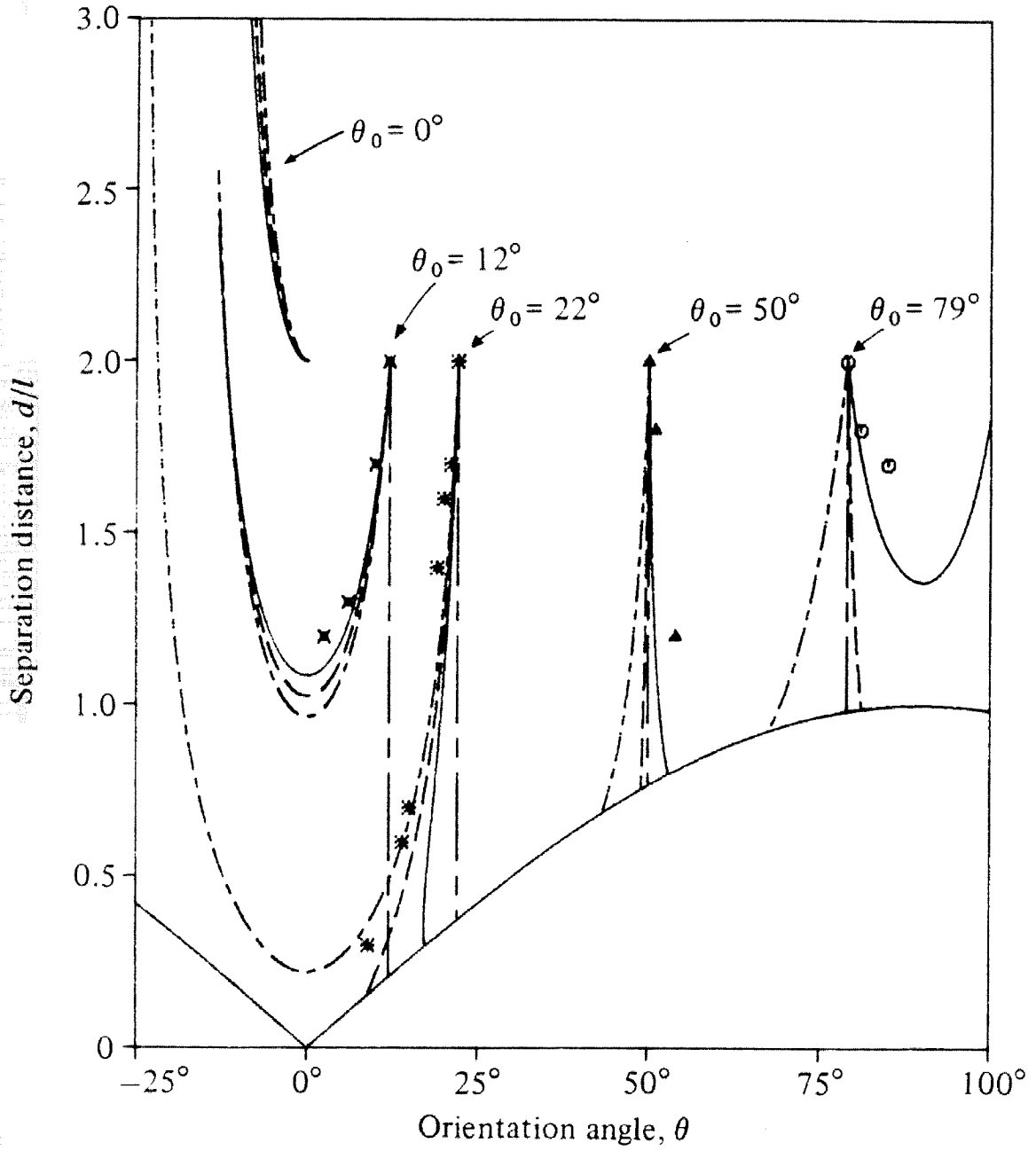


Figure 18

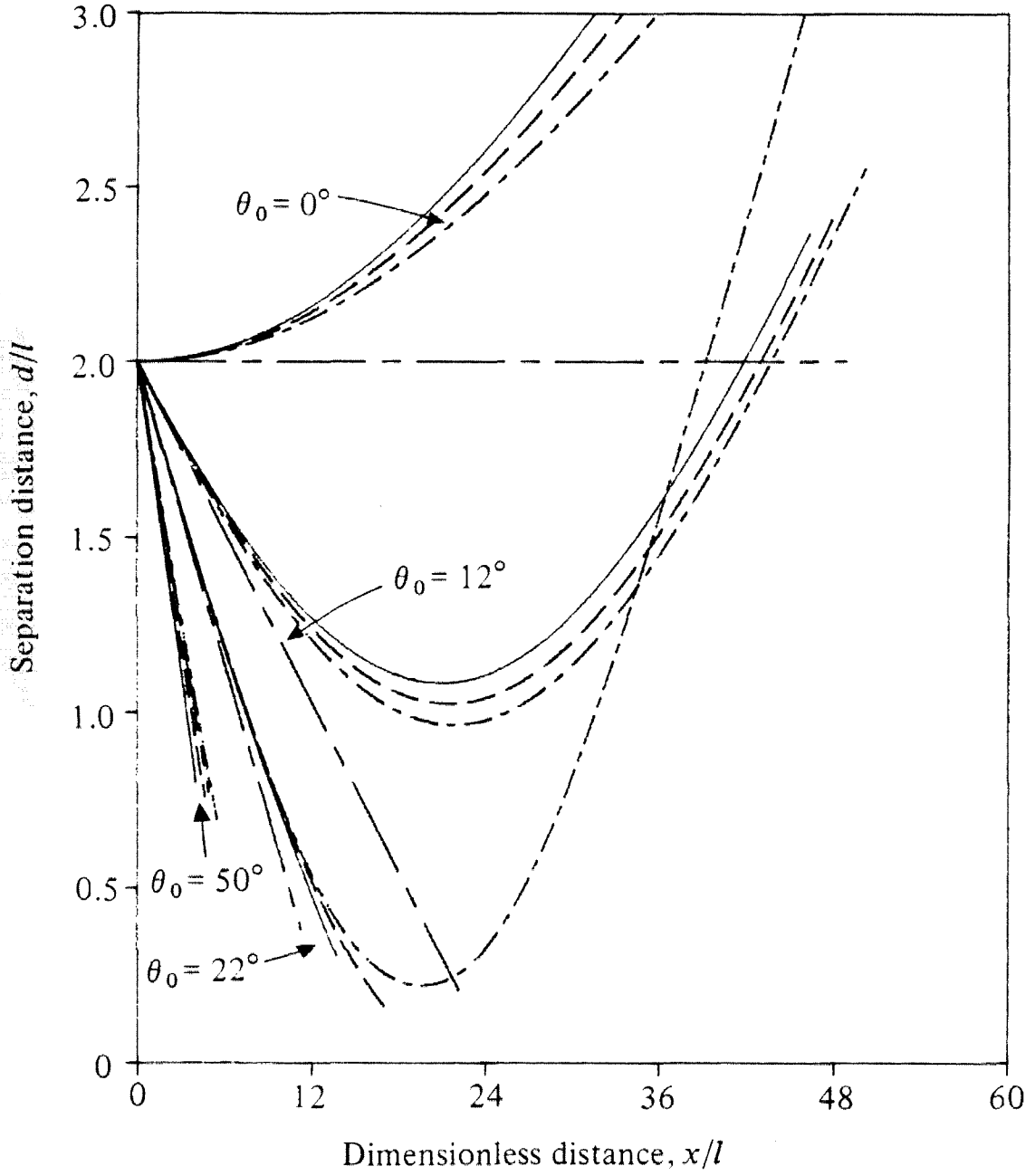


Figure 19

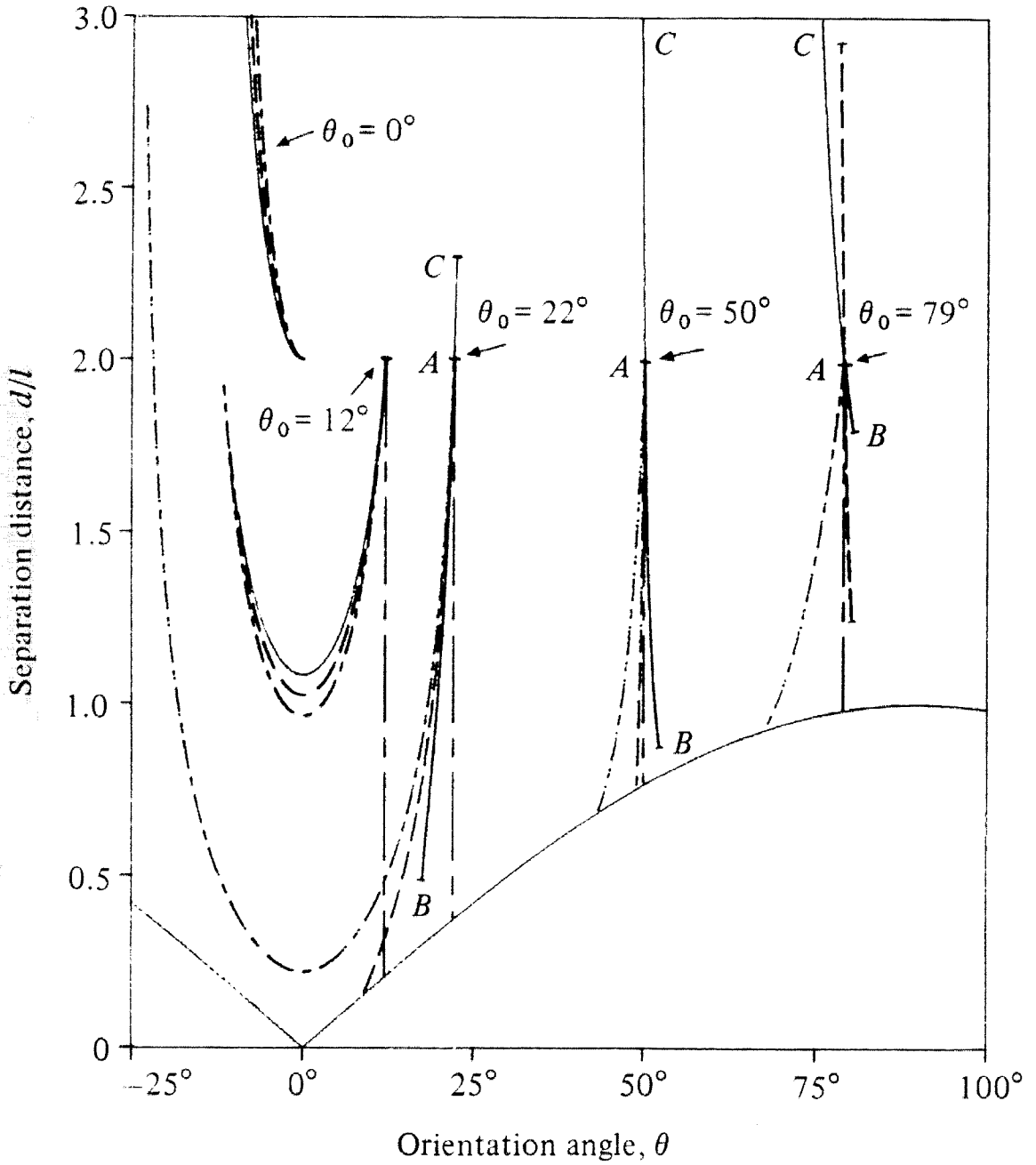


Figure 20

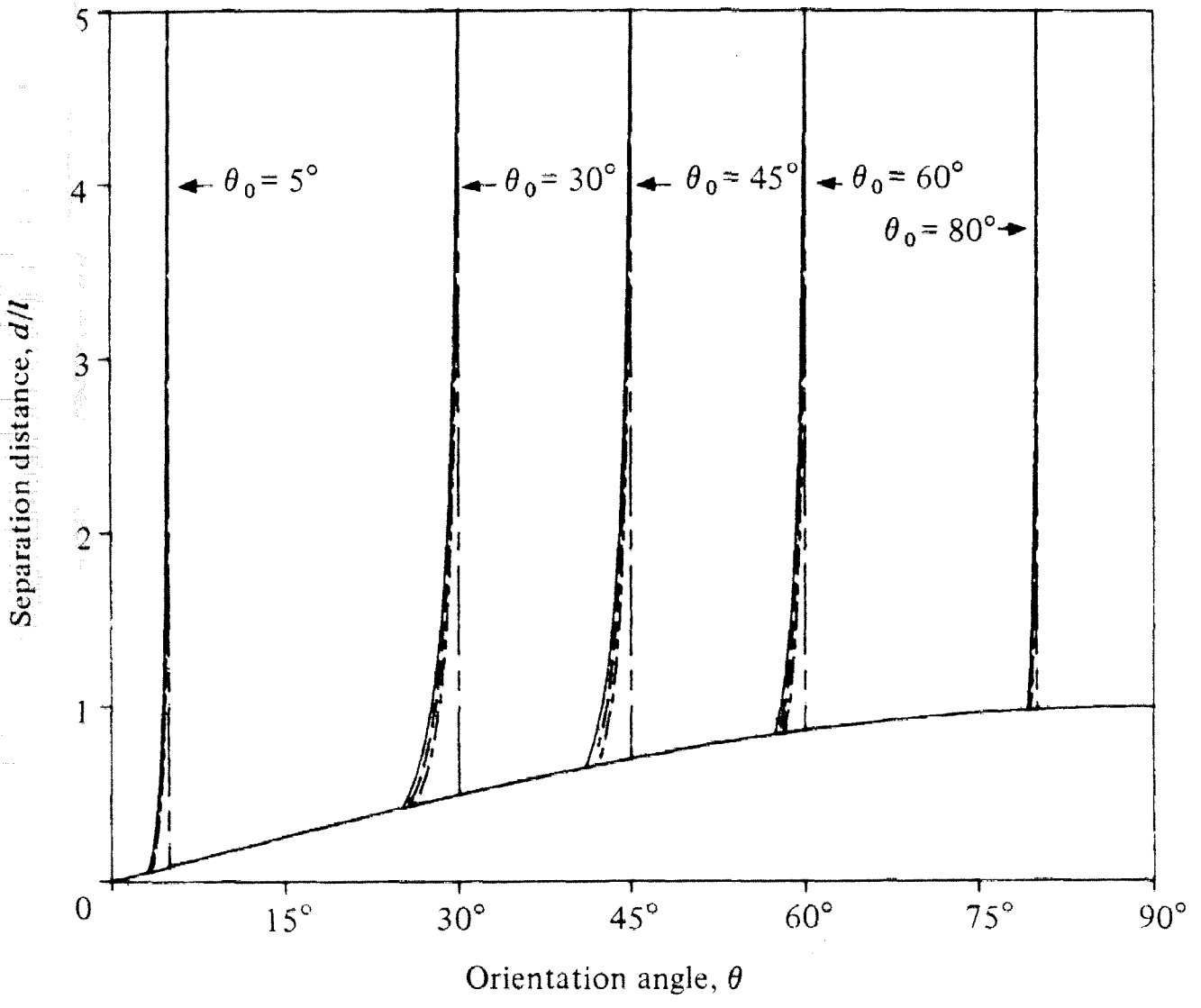


Figure 21

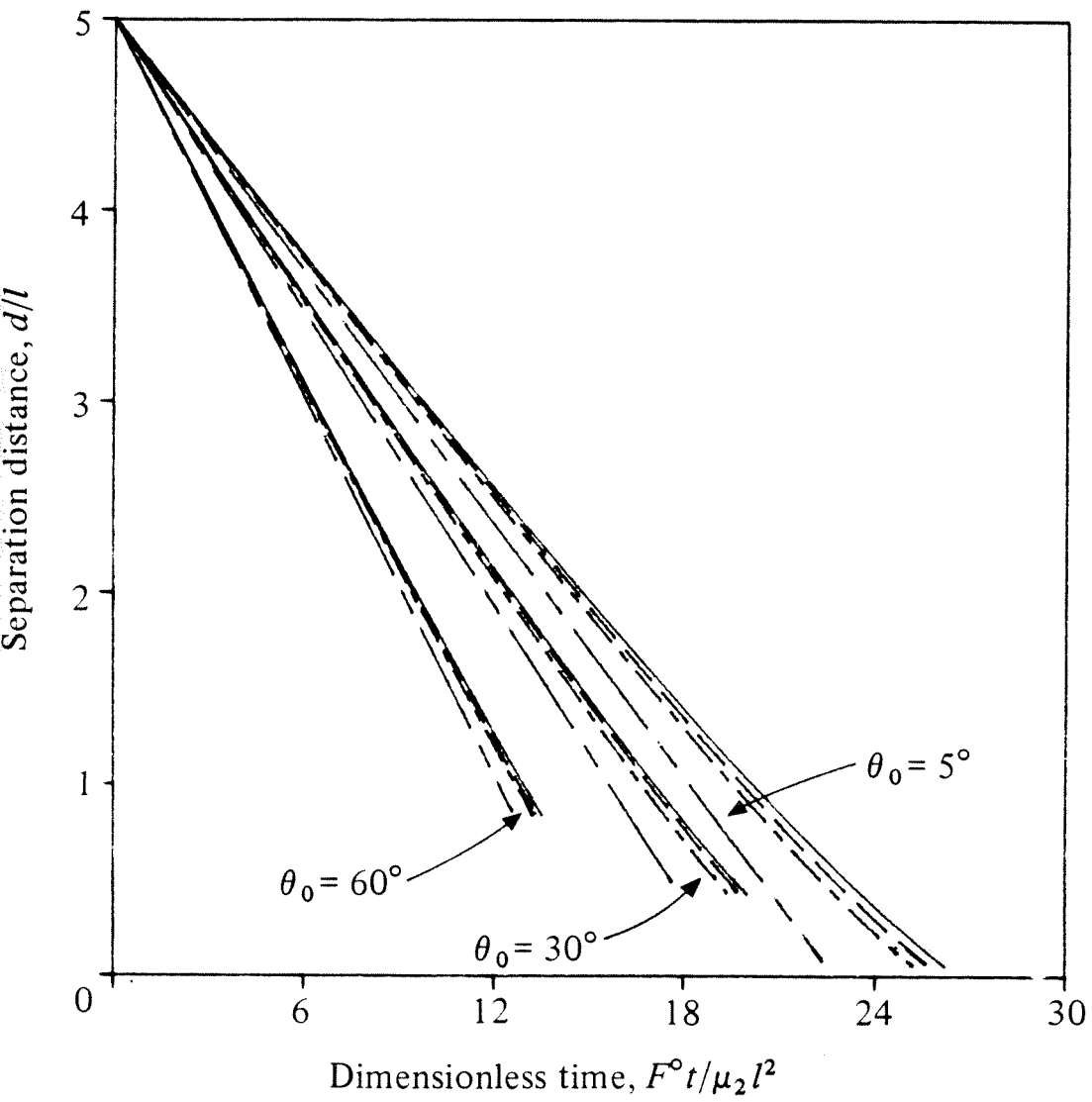


Figure 22

Chapter II.

Particle Motion in Stokes Flow near a Plane Fluid-Fluid Interface

Part 2. Linear Shear and Axisymmetric Straining Flows

**Particle Motion in Stokes Flow near a Plane Fluid-Fluid Interface
Part 2. Linear Shear and Axisymmetric Straining Flows***

by

Seung-Man Yang and L. Gary Leal

Department of Chemical Engineering
California Institute of Technology
Pasadena, California 91125

* The text of Chapter II consists of an article which appeared in the *J. Fluid Mech.* (in press).

Abstract

We consider the motion of a sphere or a slender body in the presence of a plane fluid-fluid interface with an arbitrary viscosity ratio, when the fluids undergo a linear, undisturbed flow. First, the hydrodynamic relationships for the force and torque on the particle at rest in the undisturbed flow field are determined, using the method of reflexions, from the spatial distribution of Stokeslets, rotlets and higher order singularities in Stokes flow. These fundamental relationships are then applied, in combination with the corresponding solutions obtained in earlier publications for the translation and rotation through a quiescent fluid, to determine the motion of a neutrally buoyant particle freely suspended in the flow. The theory yields general trajectory equations for an arbitrary viscosity ratio which are in good agreement with both exact solution results and experimental data for sphere motions near a rigid, plane wall. Among the most interesting results for motion of slender bodies is the generalization of the Jeffrey orbit equations for linear simple shear flow.

1. Introduction

In this paper we consider the creeping motion of a sphere or a slender body in linear shear and axisymmetric straining flows near a plane fluid-fluid interface. Previously, we considered translation and rotation of a sphere when the fluids are at rest at infinity (Lee, Chadwick and Leal, 1979; Lee and Leal, 1980), and, in Part I of the present pair of papers, the same problem was solved for a rigid, straight slender body (Yang and Leal, 1983). Although the quiescent fluid problem is of some intrinsic interest, and is a logical starting point for investigation of particle motions near a fluid interface, many problems of practical significance involve particle motions in a mean flow at infinity (cf. Goldman, Cox and Brenner, 1967a,b; Goren and O'Neill, 1971; Spielman, 1977, and references therein). This is true of boundary effects in the rheology of dilute suspensions, theories of Brownian motion near a phase boundary and the development of trajectory equations to model the "collection" of very small particles at the surface of larger bubbles or drops in flotation processes (cf. Dukhin and Rudev, 1977).

The majority of previous analyses of creeping particle motion near a flat wall or interface were restricted to spherical particles, and utilized separation of variables in bipolar coordinates, cf. Jeffery (1912), Brenner (1961) and Lee and Leal (1980) for motion in a quiescent flow. Goren and O'Neill (1971) used the same approach to consider the motion of a sphere in simple shear flow near a solid, plane wall, and, more recently, Dukhin and Rudev (1977) considered a sphere on the axis of symmetry of a pure straining flow near a gas-liquid interface. An alternative approach, which is essential if the particles are not spherical, is to construct solutions using spatial distributions of fundamental singularities. This approach has been known since the pioneering work of Lorentz (1907). Recently, fundamental solutions were developed for a point force and higher order singularities near a fluid-fluid interface by a generalization of the

Lorentz analysis, and used to solve for the creeping motion of a spherical particle when the fluids are at rest at infinity (Lee, Chadwick and Leal, 1979). The same basic method has also been applied, in a slender-body approximation, to investigate the translation and rotation of a straight, rigid slender body through a quiescent fluid (Fulford and Blake, 1983, for translation with the particle axis either perpendicular or parallel to the interface; Yang and Leal, 1983, for translation and rotation with an arbitrary orientation).

In this present work, we use the singularity method to study the hydrodynamic interactions between either a sphere or a straight, rigid slender body and a flat fluid-fluid interface in linear flows which are compatible with the presence of a plane interface. The solutions we obtain provide the hydrodynamic "resistance" tensors that define the relationships between the force and torque on the particle at rest in the flow field, the undisturbed flow parameters such as strain rate or shear rate, and the translational and angular velocities of the particle. These fundamental relationships are then used to calculate the particle trajectories in simple shear and axisymmetric straining flows.

2. Basic Equations

We begin by considering the governing equations and boundary conditions for a rigid particle (i.e., sphere or slender body) at rest near a flat fluid-fluid interface of two immiscible fluids 1 and 2. The particle is assumed to be located in fluid 2, and the undisturbed velocity field is given in the form:

$$\hat{\mathbf{U}}_1 = \mathbf{E} \cdot \mathbf{x} \quad \text{for pure straining flow} \tag{1a}$$

or

$$\begin{aligned} \hat{\mathbf{U}}_1 &= \frac{1}{\lambda} \Gamma \cdot \mathbf{x} \\ \hat{\mathbf{U}}_2 &= \Gamma \cdot \mathbf{x} \end{aligned} \quad \text{for simple shear flow}$$

(1b)

in which $\lambda (= \mu_1/\mu_2)$ is the viscosity ratio of the two fluids, $\hat{\mathbf{U}}_i$ is the undisturbed velocity field in fluid i ($= 1,2$), and \mathbf{x} denotes a position vector measured from an origin that is placed at the interface. These undisturbed flow fields are depicted in Figs. 1A and D, and are consistent with the existence of a flat interface at which the normal components of velocities are identically zero (i.e., $\hat{\mathbf{U}}_i \cdot \mathbf{n} = 0$).

The linear operator \mathbf{E} for an axisymmetric extensional flow takes the form

$$\mathbf{E} = \begin{bmatrix} \mathbf{E} & 0 & 0 \\ 0 & \mathbf{E} & 0 \\ 0 & 0 & -2\mathbf{E} \end{bmatrix}$$

while that for a linear simple shear flow parallel to the interface is

$$\mathbf{\Gamma} = \begin{bmatrix} 0 & 0 & \Gamma_{13} \\ 0 & 0 & \Gamma_{23} \\ 0 & 0 & 0 \end{bmatrix}.$$

Here, \mathbf{E} and Γ_{j3} ($j = 1,2$) are usually denoted as the strain rate and shear rate, respectively.

In the present problem, the Reynolds number is defined by

$$\text{Re} = \frac{\mathbf{E}l_c^2}{\nu_2} \left(\text{or } \frac{\Gamma_{j3}l_c^2}{\nu_2} \right)$$

where l_c is a characteristic length scale of the particle (i.e., either the sphere radius, a , or the half-length of the slender body, l), and ν_2 represents the kinematic viscosity of fluid 2. We assume that the Reynolds number is sufficiently small (i.e., $\text{Re} \ll 1$) that the motion is quasi-steady and the creeping motion approximation applicable. The equations of motion therefore reduce to steady Stokes' equations in both fluids. Further, the linearity of the Stokes' equation enables us to decompose the undisturbed flow field $\hat{\mathbf{U}}_i = \mathbf{L}_i \cdot \mathbf{x}$ into a constant vector (i.e., a uniform streaming flow, Figs. 1B and E)

$$\hat{\mathbf{U}}_1 = \mathbf{L}_2 \cdot \mathbf{x}_p \quad (2a)$$

and a linear part with vanishing velocity at the body center (i.e., Figs. 1C and F),

$$\hat{\mathbf{U}}_1 = \mathbf{L}_1 \cdot \mathbf{x} - \mathbf{L}_2 \cdot \mathbf{x}_p \quad (2b)$$

Here, \mathbf{L}_i denotes either the strain rate tensor \mathbf{E} in each fluid, or shear rate tensors $\mu_1/\mu_2 \Gamma$ for $i = 1$ and 2 . The Stokes' problem for $\hat{\mathbf{U}}_1 = \mathbf{L}_2 \cdot \mathbf{x}_p$ of Eq. (2a), which is simply a translation of the fluid system including the interface past a stationary particle is precisely equivalent to the problem of particle translation with velocity $-\mathbf{L}_2 \cdot \mathbf{x}_p$ through a quiescent fluid with stationary interface (cf. Figs. 1B and E). A complete detailed solution is available for this problem for both a sphere and a slender body from Lee, Chadwick and Leal (1979) and Yang and Leal (1983) who determined the relationship between the hydrodynamic force \mathbf{F} and torque \mathbf{T} on the body and the translational velocity

$$\mathbf{F} = -\mathbf{K}_T \cdot \mathbf{L}_2 \cdot \mathbf{x}_p \quad (3a)$$

$$\mathbf{T} = -\mathbf{K}_C \cdot \mathbf{L}_2 \cdot \mathbf{x}_p \quad (3b)$$

where \mathbf{K}_T and \mathbf{K}_C denote the translational and coupling tensors, respectively.

It thus remains only to solve the problem for the linear undisturbed flow $\hat{\mathbf{U}}_1 = \mathbf{L}_1 \cdot \mathbf{x} - \mathbf{L}_2 \cdot \mathbf{x}_p$ with $\hat{\mathbf{U}}_2 = \mathbf{0}$ at the body center (cf. Figs. 1C and F). We define, for convenience, a disturbance velocity field \mathbf{u} , as the difference between the actual velocity $\hat{\mathbf{u}}$ in the presence of the particle and the undisturbed flow, i.e.,

$$\mathbf{u}_i = \hat{\mathbf{u}}_i - \{\mathbf{L}_i \cdot \mathbf{x} - \mathbf{L}_2 \cdot \mathbf{x}_p\} \quad (i = 1, 2).$$

The equations of motion for the disturbance velocity field are

$$\nabla p_i = \frac{\mu_1}{\mu_2} \nabla^2 \mathbf{u}_i \quad (4a)$$

$$\nabla \cdot \mathbf{u}_i = 0 \quad (i = 1, 2) \quad (4b)$$

in which the variables may be considered to be non-dimensionalized with

respect to the characteristic variables: $l_c = a$ (or l), $t_c = 1/E$ (or $1/\Gamma_{j3}$) and $p_c = \mu_2 E$ (or $\mu_2 \Gamma_{j3}$). Thus, for the following analysis, the non-dimensionalized variables such as the hydrodynamic force and torque, \mathbf{F} and \mathbf{T} , and the translational and angular velocities of the body, \mathbf{U} and $\mathbf{\Omega}$, are based on the corresponding characteristic variables, i.e., $F_c = \mu_2 E l_c^2$ (or $\mu_2 \Gamma_{j3} l_c^2$), $T_c = \mu_2 E l_c^3$ (or $\mu_2 \Gamma_{j3} l_c^3$), $U_c = E l_c$ (or $\Gamma_{j3} l_c$) and $\Omega_c = E$ (or Γ_{j3}), respectively. The boundary conditions for \mathbf{u}_1 and \mathbf{u}_2 in this disturbance flow problem are:

$$\mathbf{u}_1, \mathbf{u}_2 \rightarrow \mathbf{0} \text{ as } |\mathbf{x}| \rightarrow \infty \quad (5a)$$

$$\mathbf{u}_2 = -\mathbf{L}_2 \cdot (\mathbf{x}_B - \mathbf{x}_p) \text{ on } \mathbf{x}_B \in S_p \quad (5b)$$

plus the interface conditions (i.e., continuity of velocity and tangential stress and zero normal velocity). In Eq. (5b), \mathbf{x}_B denotes a point on the body surface S_p . From the point of view of (4) and (5), the problem is seen to be exactly the same as if a velocity field $\mathbf{u}_2(\mathbf{x}_B) = -\mathbf{L}_2 \cdot (\mathbf{x}_B - \mathbf{x}_p)$ is generated at the surface of a body which is near a flat fluid-fluid interface in a fluid at rest at infinity.

For a spherical particle, we consider the asymptotic limit

$$\delta = \frac{a}{d} \ll 1$$

in which d is a separation distance between the sphere center and the interface. In this case, the singularity method can be reduced to the superposition of fundamental solutions for a point force α (i.e., Stokeslet), a potential dipole β and higher order singularities (e.g., a stresslet, a rotlet, a potential quadrupole, etc.) at the sphere center. Fundamental solutions of the creeping motion equation for a point force (and higher order singularities) can be obtained easily from the corresponding solutions in an unbounded fluid by following the prescription of Lee, Chadwick and Leal (1979). The fundamental solutions automatically satisfy the conditions of velocity and stress continuity as well as zero normal velocity at

a flat fluid interface, plus the boundary condition (5a) of vanishing velocity in the far field (cf. Lee, Chadwick and Leal, 1979). All that remains is to determine the combination of these singularities at the sphere center, \mathbf{x}_p , which satisfies the boundary condition (5b). In particular, we must determine the densities and orientations of these singularities so that the disturbance velocity $\mathbf{u}_2(\mathbf{x})$ is at least approximately equal to $-\mathbf{L}_2 \cdot (\mathbf{x}_p - \mathbf{x}_p)$ at all points of the sphere surface.

For a slender body, the problem of particle motion near an interface (i.e., the disturbance flow problem, Eqs. (4) and (5) can be solved using the slender body theory of low Reynolds number flow (Batchelor, 1970; Fulford and Blake, 1983; Yang and Leal, 1983; and others). In this approach, the disturbance flow produced by the body is approximated by a line distribution of Stokeslets and potential dipoles along the body center line (rather than a superposition of higher order singularities at one point \mathbf{x}_p or a surface distribution of point forces), and the orientation and strength of these singularities are determined in order to satisfy the boundary condition (5b) to an order of approximation $O(\varepsilon^2)$, where $\varepsilon = [\ln 2\kappa]^{-1}$ and κ is the axis ratio of the slender body.

The complete solution for a particle located at arbitrary point \mathbf{x}_p in a linear flow field $\hat{\mathbf{U}}_1 = \mathbf{L}_1 \cdot \mathbf{x}$ near a flat interface is obtained by superposition of the corresponding solution for the linear flow $\hat{\mathbf{U}}_1 = \mathbf{L}_1 \cdot \mathbf{x} - \mathbf{L}_2 \cdot \mathbf{x}_p$ with $\hat{\mathbf{U}}_2 = \mathbf{0}$ at the body center and the solution [i.e., Eqs. (3a) and (3b)] for the uniform streaming flow $\hat{\mathbf{U}}_1 = \mathbf{L}_2 \cdot \mathbf{x}_p$. In the theoretical analysis which follows, we consider the hydrodynamic force and torque acting on a stationary particle (sphere or slender body) in the presence of both an axisymmetric uniaxial extensional flow and a linear shear flow. These results are then used in Section 5 to calculate the trajectories of a freely suspended sphere or slender body in the same flows near a fluid-fluid interface.

3. Solutions for a Spherical Particle

3.A. Pure Straining Flow

We begin with the creeping motion of a fluid in the vicinity of a stationary spherical particle that is located at an arbitrary point $\mathbf{x}_p = (x_{p1}, x_{p2}, -d)$ in fluid 2 when the undisturbed motion is an axisymmetric uniaxial straining flow, Eq. (1a), with origin at the particle center. Here we utilize the disturbance flow formulation defined by Eqs. (4) and (5), and consider only the limit $\delta \equiv a/d \ll 1$.

Since $\delta \ll 1$, the most convenient solution technique is the method of reflections, as was also used and explained in some detail by Lee, Chadwick and Leal (1979) for the uniform streaming problem. The zeroth-order approximation in this procedure $(\mathbf{u}_2^{(0)}, p_2^{(0)})$, is the single fluid, unbounded domain solution which satisfies boundary conditions exactly at the sphere surface. The problem of a sphere in an axisymmetric straining flow, $\hat{\mathbf{U}} = \mathbf{E} \cdot (\mathbf{x} - \mathbf{x}_p)$, for an *unbounded* single fluid was solved by Chwang and Wu (1975), who showed that a potential quadrupole (σ, ν) and a stresslet (ρ, μ) , of the form

$$\text{stresslet: } (\rho, \mu) = \left(\frac{5}{2} \mathbf{e}_3, \mathbf{e}_3 \right)$$

$$\text{potential quadrupole: } (\sigma, \nu) = \left(\frac{1}{2} \mathbf{e}_3, \mathbf{e}_3 \right)$$

were required at the sphere center to satisfy the boundary condition (5b) at the sphere surface. Thus, the zeroth order (i.e., unbounded single fluid) solution in the method of reflections expansion can be written as

$$\mathbf{u}_2^{(0)}(\mathbf{x}) = \frac{1}{2} \left[\frac{\partial}{\partial x_3} \mathbf{u}_D(\mathbf{x}, \mathbf{x}_p; \mathbf{e}_3) + 5 \mathbf{u}_{SS}(\mathbf{x}, \mathbf{x}_p; \mathbf{e}_3, \mathbf{e}_3) \right] \quad (6a)$$

$$p_2^{(0)}(\mathbf{x}) = \frac{5}{2} p_{SS}(\mathbf{x}, \mathbf{x}_p; \mathbf{e}_3, \mathbf{e}_3) . \quad (6b)$$

Here, $\mathbf{u}_D(\mathbf{x}, \mathbf{x}_p; \beta)$, $\mathbf{u}_{SS}(\mathbf{x}, \mathbf{x}_p; \rho, \mu)$ and $p_{SS}(\mathbf{x}, \mathbf{x}_p; \rho, \mu)$ denotes the fundamental

solutions for a potential dipole β and a stresslet (ρ, μ) located at \mathbf{x}_p in an *unbounded* fluid, cf. Chwang and Wu (1975).

Though $\mathbf{u}_2^{(0)}(\mathbf{x})$ of Eq. (6a) exactly satisfies the boundary condition $\mathbf{u}_2(\mathbf{x}_B) = -\mathbf{E}(\mathbf{x}_B - \mathbf{x}_p)$ at all points on the sphere surface, it does not satisfy the conditions at the flat interface. However, Lee et al. (1979) have already shown that the first correction in the reflections method, $(\mathbf{u}_2^{(1)}, p_2^{(1)})$, for the presence of the interface can always be obtained by simply utilizing the same form, Eqns. (6a,b) as in the zeroth-order solution but with the fundamental solutions \mathbf{u}_D , \mathbf{u}_{SS} and p_{SS} (for an unbounded fluid) replaced by the corresponding fundamental solutions in the presence of the flat interface, obtained by the simple transformation rule of Lee et al. This yields $(\mathbf{u}_2^{(0)} + \mathbf{u}_2^{(1)}, p_2^{(0)} + p_2^{(1)})$. The first "wall correction" can then be obtained by subtracting the zeroth order-solution $(\mathbf{u}_2^{(0)}, p_2^{(0)})$:

$$\mathbf{u}_2^{(1)}(\mathbf{x}) = \frac{1}{2} \left[\frac{\partial}{\partial x_3} \{ \mathbf{u}_{2,D}(\mathbf{x}, \mathbf{x}_p; \mathbf{e}_3) - \mathbf{u}_D(\mathbf{x}, \mathbf{x}_p; \mathbf{e}_3) \} + 5 \{ \mathbf{u}_{2,SS}(\mathbf{x}, \mathbf{x}_p; \mathbf{e}_3, \mathbf{e}_3) - \mathbf{u}_{SS}(\mathbf{x}, \mathbf{x}_p; \mathbf{e}_3, \mathbf{e}_3) \} \right] \quad (7a)$$

$$p_2^{(1)}(\mathbf{x}) = \frac{1}{2} \left[\frac{\partial}{\partial x_3} p_{2,D}(\mathbf{x}, \mathbf{x}_p; \mathbf{e}_3) + 5 \{ p_{2,SS}(\mathbf{x}, \mathbf{x}_p; \mathbf{e}_3, \mathbf{e}_3) - p_{SS}(\mathbf{x}, \mathbf{x}_p; \mathbf{e}_3, \mathbf{e}_3) \} \right] \quad (7b)$$

where we have denoted the resulting fundamental solutions in the presence of the interface as $\mathbf{u}_{2,D}$ and $\mathbf{u}_{2,SS}$, respectively. Although the combined solution $(\mathbf{u}_2^{(0)} + \mathbf{u}_2^{(1)}, p_2^{(0)} + p_2^{(1)})$ satisfies the interface boundary conditions, it now does not satisfy the condition $\mathbf{u}_2(\mathbf{x}_B) = -\mathbf{E}(\mathbf{x}_B - \mathbf{x}_p)$ and additional singularities are needed at the center of the sphere that cancel the velocity field correction $\mathbf{u}_2^{(1)}(\mathbf{x})$ at the sphere surface \mathbf{x}_B ; namely, the interface 'reflection' of the potential quadrupole $(\sigma, \nu) = (1/2 \mathbf{e}_3, \mathbf{e}_3)$ and the stresslet $(\rho, \mu) = (5/2 \mathbf{e}_3, \mathbf{e}_3)$ which is nonzero at the sphere surface.

Since the detailed form of $\mathbf{u}_2^{(1)}(\mathbf{x}_B)$ is highly complicated, it is not possible to determine singularities at the sphere center which precisely satisfy the boundary condition (5b) at all points on the sphere surface. Instead, we choose singularities to cancel only the first few terms of $\mathbf{u}_2^{(1)}(\mathbf{x}_B)$ at the sphere surface, with $\mathbf{u}_2^{(1)}(\mathbf{x}_B)$ expanded in powers of δ for $\delta = a/d \ll 1$. The leading terms of $\mathbf{u}_2^{(1)}$ near the sphere, for small δ , are in component form:

$$u_2^{(1)} = \delta^3 \frac{5x_1}{16} \frac{1+2\lambda}{1+\lambda} + O(\delta^4) \quad (8a)$$

$$v_2^{(1)} = \delta^3 \frac{5x_2}{16} \frac{1+2\lambda}{1+\lambda} + O(\delta^4) \quad (8b)$$

$$w_2^{(1)} = -\delta^2 \frac{5}{16} \frac{2+3\lambda}{1+\lambda} - \delta^3 \frac{5}{8} \frac{1+2\lambda}{1+\lambda} (x_3 + d) + O(\delta^4) \quad (8c)$$

where the subscript 2 denotes the velocity components in fluid 2. It can be seen from Eqs. (8a,b,c) that the presence of the interface will induce a steady streaming flow at $O(\delta^2)$ normal to the interface and an axisymmetric uniaxial extensional flow at $O(\delta^3)$ with a stagnation point at the sphere center. The singularities required to cancel this additional velocity field at the sphere surface can be readily evaluated and the resulting solution for a stationary sphere near a flat interface in the pure straining flow, $\hat{\mathbf{U}}_2 = \mathbf{E} \cdot (\mathbf{x} - \mathbf{x}_p)$, is as follows:

$$\begin{aligned} \mathbf{u}_2(\mathbf{x}, \mathbf{x}_p) = & \frac{5}{8} \left[\frac{3}{8} \frac{2+3\lambda}{1+\lambda} \delta^2 + \left(\frac{3}{8} \frac{2+3\lambda}{1+\lambda} \right)^2 \delta^3 + O(\delta^4) \right] \mathbf{u}_{2,S}(\mathbf{x}, \mathbf{x}_p; \mathbf{e}_3) \quad (\text{Stokeslet}) \\ & + \frac{5}{8} \left[\frac{3}{8} \frac{2+3\lambda}{1+\lambda} \delta^2 + \left(\frac{3}{8} \frac{2+3\lambda}{1+\lambda} \right)^2 \delta^3 + O(\delta^4) \right] \mathbf{u}_{2,D}(\mathbf{x}, \mathbf{x}_p; -\frac{1}{3} \mathbf{e}_3) \quad (\text{Potential Dipole}) \\ & + \frac{5}{2} \left[1 + \frac{5}{16} \frac{1+2\lambda}{1+\lambda} \delta^3 + O(\delta^4) \right] \mathbf{u}_{2,SS}(\mathbf{x}, \mathbf{x}_p; \mathbf{e}_3, \mathbf{e}_3) \quad (\text{Stresslet}) \\ & + \frac{1}{2} \left[1 + \frac{5}{16} \frac{1+2\lambda}{1+\lambda} \delta^3 + O(\delta^4) \right] \frac{\partial}{\partial x_3} \mathbf{u}_{2,D}(\mathbf{x}, \mathbf{x}_p; \mathbf{e}_3) \quad (\text{Potential Quadrupole}). \end{aligned} \quad (9)$$

Now, let us turn to the original problem of calculating the force and torque acting on a stationary sphere that is located at arbitrary point \mathbf{x}_p in fluid 2 which is undergoing the axisymmetric uniaxial extension flow $\hat{\mathbf{U}}_2 = \mathbf{E} \cdot \mathbf{x}$ with origin at the interface (i.e., Fig. 1A). As we showed in Section 2, the hydrodynamic force and torque exerted in this case can be determined by a superposition of the force and torque for a uniform streaming flow with translational velocity $\hat{\mathbf{U}}_1 = \mathbf{E} \cdot \mathbf{x}_p$ and for a uniaxial straining flow $\hat{\mathbf{U}}_1 = \mathbf{E} \cdot (\mathbf{x} - \mathbf{x}_p)$ with stagnation point at the sphere center. The force and torque in the latter case can be evaluated directly from the strength of the singularities in the solution, Eq. (9). The result is

$$\mathbf{F} = -\mathbf{K}_T \cdot \mathbf{E} \cdot \mathbf{x}_p - 5\pi \left[\frac{3}{8} \delta^2 \frac{2+3\lambda}{1+\lambda} + \left(\frac{3}{8} \delta \frac{2+3\lambda}{1+\lambda} \right)^2 \delta \right] \mathbf{e}_3 + O(\delta^4) \quad (10a)$$

$$\mathbf{T} = -\mathbf{K}_C \cdot \mathbf{E} \cdot \mathbf{x}_p + O(\delta^4). \quad (10b)$$

The components of the translation and coupling tensors, \mathbf{K}_T and \mathbf{K}_C , were determined up to $O(\delta^2)$ by Lee et al. (1979) for motion of a sphere near a plane fluid-fluid interface. The $O(\delta^3)$ terms in the components of the hydrodynamic tensors, \mathbf{K}_T and \mathbf{K}_C , which are necessary to be compatible with the inclusion of $O(\delta^3)$ terms in (9), can be evaluated by expanding the corresponding wall correction $\mathbf{u}_2^{(1)}(\mathbf{x})$ up to $O(\delta^3)$ and superimposing the fundamental solutions for singularities in order to cancel the interface reflection at the sphere surface at the same level of approximation, $O(\delta^3)$. The resulting nonzero components of the hydrodynamic tensors \mathbf{K}_T , \mathbf{K}_C are given by

$$K_T^{11} = 6\pi \left[1 + \sum_{n=1}^3 \left(\frac{3}{16} \delta \frac{3\lambda-2}{1+\lambda} \right)^n - \frac{1+2\lambda}{16(1+\lambda)} \delta^3 \right] + O(\delta^4) \quad (11a)$$

$$K_T^{22} = K_T^{11} \quad (11b)$$

$$K_T^{33} = 6\pi \left[1 + \sum_{n=1}^3 \left(\frac{3}{8} \delta \frac{2+3\lambda}{1+\lambda} \right)^n - \frac{1+4\lambda}{8(1+\lambda)} \delta^3 \right] + O(\delta^4) \quad (11c)$$

$$K_C^{12} = \frac{3\pi}{2} \delta^2 \frac{1}{1+\lambda} \left[1 + \frac{3}{16} \delta \frac{3\lambda-2}{1+\lambda} \right] + O(\delta^4) \quad (11d)$$

and

$$K_C^{21} = -K_C^{12} \quad (11e)$$

Here, the terms in the summed series, $\left[\frac{3}{16} \delta (3\lambda - 2) / (1 + \lambda) \right]^n$ in K_T^{11} and $\left[\frac{3}{8} \delta (2 + 3\lambda) / (1 + \lambda) \right]^n$ in K_T^{33} , are the corresponding n-th reflexions to the terms of $O(\delta)$ in the first wall corrections, $\mathbf{u}_2^{(1)}(\mathbf{x})$, and the summed series continue beyond $O(\delta^3)$. The terms of $O(\delta^3)$, $(-1 + 2\lambda) / 16(1 + \lambda) \delta^3$ in K_T^{11} and $(-1 + 4\lambda) / 8(1 + \lambda) \delta^3$ in K_T^{33} , result from the correction terms of $O(\delta^3)$ in $\mathbf{u}_2^{(1)}(\mathbf{x})$ which represent a paraboloidal velocity field with origin at the sphere center and a steady streaming flow, both either parallel or normal to the interface. The term of $O(\delta^3)$ in K_C^{12} or K_C^{21} is associated with the reflected simple shearing flow of either the $O(\delta)$ term in $\mathbf{u}_2^{(1)}(\mathbf{x})$ for translation parallel to the interface or the $O(\delta^2)$ term in $\mathbf{u}_2^{(1)}(\mathbf{x})$ for rotation with axis of rotation parallel to the interface.

Dukhin and Rulev (1977) determined the drag force on a small solid sphere which was located at the axis of symmetry in an axisymmetric uniaxial extensional flow, $\hat{\mathbf{U}}_1 = \mathbf{E} \cdot \mathbf{x}$, near a gas-liquid interface (i.e., $\lambda \rightarrow 0$), using the eigensolutions of Laplace's equation in bipolar coordinates. It is a simple matter to calculate the drag force, F_3 , on the sphere from the present asymptotic solution, Eq. (10a) with $\mathbf{x}_p = (0,0,-d)$. The drag ratio (the drag F_3 divided by Stokes' drag, $12\pi\mu_2 adE$) is simply given as

Drag Ratio =

$$1 + \sum_{n=1}^3 \left(\frac{3}{8} \delta \frac{2+3\lambda}{1+\lambda} \right)^n - \frac{1+4\lambda}{8(1+\lambda)} \delta^3 - \frac{5}{12d} \sum_{n=1}^2 \delta \left(\frac{3}{8} \delta \frac{2+3\lambda}{1+\lambda} \right)^n + O(\delta^4). \quad (12)$$

In Fig. 2, the drag ratio, Eq. (12), is plotted as a function of d , the distance between the sphere and the stagnation point, for three values of $\lambda = 0, 1$ and ∞ . Also shown for comparison is the corresponding exact solution of Dukhin and Rudev (1977). There is very good agreement between the two solutions except in the region near $d = 1$. As expected, the difference between the two results becomes larger as the sphere approaches the interface due to the poor convergence of the asymptotic solution in powers of δ , Eq. (12). However, a detailed comparison shows that the maximum error in the asymptotic solution, Eq. (12), compared to the exact solution of Dukhin and Rudev (1977), is only 2.72% for $d = 1.001$ which is the smallest value considered by Dukhin and Rudev (1977), while the error for $d > 1.5$ becomes less than 0.98%.

3.B Simple Shear Flow

Let us turn now to the case of a sphere located at an arbitrary point \mathbf{x}_p in a simple shear flow, $\hat{\mathbf{U}}_1 = \mu_1/\mu_2 \Gamma \cdot \mathbf{x}$, parallel to the interface as shown in Fig. 1D (the case in which $\hat{\mathbf{U}}_1 = \mathbf{C} \neq \mathbf{0}$ at the interface can be treated by superimposing a uniform streaming flow past a sphere, $\hat{\mathbf{U}}_1 = \mathbf{C}$, with the simple shear flow $\hat{\mathbf{U}}_1 = \mu_1/\mu_2 \Gamma \cdot \mathbf{x}$). Again, the problem can be decomposed into a simple translation of the fluid system including the interface with velocity $\hat{\mathbf{U}}_1 = \Gamma \cdot \mathbf{x}_p$ past the stationary sphere (i.e., Fig. 1E) and a linear shear flow, $\hat{\mathbf{U}}_1 = \mu_1/\mu_2 \Gamma \cdot \mathbf{x} - \Gamma \cdot \mathbf{x}_p$, with the velocity $\hat{\mathbf{U}}_2 = \mathbf{0}$ at the sphere center (i.e., Fig. 1F). In view of the linearity of the problem and the symmetry of the sphere-interface geometry, we need only solve the case of $\hat{\mathbf{U}}_1 = \mu_1/\mu_2 \Gamma_{13} \cdot x_3 \mathbf{e}_1$, corresponding to

$$\mathbf{L} = \Gamma = \begin{bmatrix} 0 & 0 & \Gamma_{13} \\ 0 & 0 & 0 \\ 0 & 0 & 0 \end{bmatrix} \quad : \text{ shear rate tensor .}$$

In order to analyze the velocity field for a sphere in the undisturbed flow $\hat{\mathbf{U}}_i = \Gamma_{13}[\mu_1/\mu_2 x_3 + d] \mathbf{e}_1$ which vanishes at the sphere center, we follow the procedure of the preceding section and solve the equivalent problem in which a velocity field $\mathbf{u}_2(\mathbf{x})$ is viewed as being generated in a quiescent fluid by a nonzero velocity distribution

$$\mathbf{u}_2(\mathbf{x}_B) = -\Gamma_{13}((\mathbf{x}_B)_3 + d)\mathbf{e}_1 \quad (13)$$

at the surface of the sphere. As in the preceding analysis, we use the method of reflections, with the solution in an unbounded fluid taken from the work of Chwang and Wu (1975) who showed that the condition (13) was satisfied by superposition of a stresslet, a rotlet and a potential quadrupole at the center of the sphere, i.e.,

$$\text{stresslet: } (\rho, \mu) = \left(-\frac{5}{6} \Gamma_{13} \mathbf{e}_1, \mathbf{e}_3\right)$$

$$\text{rotlet: } \gamma = -\frac{1}{2} \Gamma_{13} \mathbf{e}_2$$

$$\text{potential quadrupole: } (\sigma, \nu) = \left(-\frac{1}{6} \Gamma_{13} \mathbf{e}_3, \mathbf{e}_1\right).$$

As in the preceding example, the first correction for the presence of the interface in the reflections expansion, can now be obtained easily from Chwang and Wu's solution by simply replacing the fundamental solutions \mathbf{u}_R , \mathbf{u}_D and \mathbf{u}_{SS} (which pertain to an unbounded fluid) with the corresponding fundamental solutions $\mathbf{u}_{2,R}$, $\mathbf{u}_{2,D}$ and $\mathbf{u}_{2,SS}$ that satisfy boundary conditions on the flat interface (and are generated using the procedure of Lee et al., 1979). The result is the first two terms in the reflections expansion, i.e., $(\mathbf{u}_2^{(0)} + \mathbf{u}_2^{(1)}, p_2^{(0)} + p_2^{(1)})$. Subtracting the zeroth-order (Chwang and Wu, 1975) solution, we get

$$\mathbf{u}_2^{(1)}(\mathbf{x}) = -\Gamma_{13} \left[\frac{5}{6} \mathbf{u}_{2,SS}(\mathbf{x}, \mathbf{x}_p; \mathbf{e}_1, \mathbf{e}_3) + \frac{1}{2} \mathbf{u}_{2,R}(\mathbf{x}, \mathbf{x}_p; \mathbf{e}_2) + \frac{1}{6} \frac{\partial}{\partial x_3} \mathbf{u}_{2,D}(\mathbf{x}, \mathbf{x}_p; \mathbf{e}_1) \right] - \mathbf{u}_2^{(0)}(\mathbf{x}).$$

(14)

Although the combined solution ($\mathbf{u}_2^{(0)} + \mathbf{u}_2^{(1)}$, $p_2^{(0)} + p_2^{(1)}$) satisfies the boundary conditions at the interface, the boundary condition (13) on the sphere is not satisfied because the "reflected flow field" $\mathbf{u}_2^{(1)}$ is nonzero at the sphere surface. Following the previous section, we examine the leading terms of this reflected field at the sphere surface as a power series in δ .

$$\mathbf{u}_2^{(1)} = \delta^2 \frac{5\lambda - 2}{16(1 + \lambda)} \Gamma_{13} + \delta^3 \frac{1}{8} \frac{3\lambda - 1}{(1 + \lambda)} \Gamma_{13}(x_3 + d) + O(\delta^4) \quad (15a)$$

$$v_2^{(1)} = O(\delta^4) \quad (15b)$$

and

$$w_2^{(1)} = \delta^3 \frac{1}{8} \frac{2 + 3\lambda}{(1 + \lambda)} \Gamma_{13} x_1 + O(\delta^4). \quad (15c)$$

Thus, insofar as (15a)-(15c) are concerned, the presence of the interface is equivalent to an induced steady simple shear flow at $O(\delta^3)$ either normal or parallel to the interface and a steady streaming motion at $O(\delta^2)$ parallel to the flow field (i.e., \mathbf{e}_1 direction).

In order to satisfy the condition (13), additional singularities are required at the sphere center. These can be determined following the procedures of Lee et al. (1979), as well as the previous section of this paper. The resulting solution, expressed in terms of the fundamental solutions for a Stokeslet, potential dipole and higher order singularities near an interface (Lee et al., 1979) is

$$\mathbf{u}_2(\mathbf{x}, \mathbf{x}_p) = \mathbf{u}_{2,S}(\mathbf{x}, \mathbf{x}_p; \mathbf{e}_1) \left[\frac{-3}{64} \Gamma_{13} \frac{5\lambda - 2}{\lambda + 1} \delta^2 \left(1 - \frac{3}{16} \frac{2 - 3\lambda}{1 + \lambda} \delta \right) + O(\delta^4) \right] \quad (\text{Stokeslet})$$

$$+ \mathbf{u}_{2,D}(\mathbf{x}, \mathbf{x}_p; -\frac{1}{3} \mathbf{e}_1) \left[\frac{-3\Gamma_{13}}{64} \frac{5\lambda - 2}{1 + \lambda} \delta^2 \left(1 - \frac{3}{16} \frac{2 - 3\lambda}{1 + \lambda} \delta \right) + O(\delta^4) \right] \quad (\text{Potential Dipole})$$

$$+ \mathbf{u}_{2,SS}(\mathbf{x}, \mathbf{x}_p; \mathbf{e}_1, \mathbf{e}_3) \frac{5\Gamma_{13}}{6} \left[-1 - \frac{1}{8} \frac{1+6\lambda}{1+\lambda} \delta^3 + 0(\delta^4) \right] \quad (\text{Stresslet})$$

$$+ \mathbf{u}_{2,R}(\mathbf{x}, \mathbf{x}_p; \mathbf{e}_2) \frac{\Gamma_{13}}{2} \left[-1 + \frac{3}{8} \frac{1}{1+\lambda} \delta^3 + 0(\delta^4) \right] \quad (\text{Rotlet})$$

$$+ \frac{\partial}{\partial x_3} \mathbf{u}_{2,D}(\mathbf{x}, \mathbf{x}_p; \mathbf{e}_1) \frac{\Gamma_{13}}{6} \left[-1 - \frac{1}{8} \frac{3\lambda-1}{1+\lambda} \delta^3 \right] - \frac{\partial}{\partial x_1} \mathbf{u}_{2,D}(\mathbf{x}, \mathbf{x}_p; \mathbf{e}_3) \frac{\Gamma_{13}}{48} \frac{2+3\lambda}{1+\lambda} \delta^3 + 0(\delta^4) \quad (16)$$

(Potential Quadrupole).

From this solution and Eqs. (3a) and (3b), we can easily determine the hydrodynamic force and torque exerted on a sphere located at an arbitrary point \mathbf{x}_p , in the simple shear flow, $\hat{\mathbf{U}}_i = \mu_1/\mu_2 \Gamma \cdot \mathbf{x}$, with $\hat{\mathbf{U}}_i = \mathbf{0}$ at the interface. This result is

$$\mathbf{F} = -\mathbf{K}_\Gamma \cdot \Gamma \cdot \mathbf{x}_p + \mathbf{K}_{SF} \cdot \boldsymbol{\xi}_s \quad (17a)$$

$$\mathbf{T} = -\mathbf{K}_C \cdot \Gamma \cdot \mathbf{x}_p + \mathbf{K}_{ST} \cdot \boldsymbol{\xi}_s \quad (17b)$$

in which $\boldsymbol{\xi}_s$ is defined by $\boldsymbol{\xi}_s = (\Gamma_{13}, \Gamma_{23}, 0)$ and the nonzero components of the hydrodynamic tensors \mathbf{K}_{SF} and \mathbf{K}_{ST} are given by

$$K_{SF}^{11} = \frac{3\pi}{8} \frac{5\lambda-2}{1+\lambda} \delta^2 \left[1 - \frac{3}{16} \frac{2-3\lambda}{1+\lambda} \delta \right] + 0(\delta^4) \quad (18a)$$

$$K_{SF}^{22} = K_{SF}^{11} \quad (18b)$$

$$K_{SF}^{12} = -4\pi \left[1 - \frac{1}{8} \frac{3}{1+\lambda} \delta^3 \right] + 0(\delta^4) \quad (18c)$$

$$K_{ST}^{21} = -K_{ST}^{12} \quad (18d)$$

The drag ratio (the drag divided by Stokes' drag, $-6\pi\mu_2\Gamma_{13}da$) is simply given as

Drag Ratio =

$$1 + \sum_{n=1}^3 (-1)^n \left[\frac{3}{16} \delta \frac{2-3\lambda}{1+\lambda} \right]^n - \frac{1+2\lambda}{16(1+\lambda)} \delta^3$$

$$+ \frac{1}{16d} \delta^2 \frac{2-5\lambda}{1+\lambda} \left[1 - \frac{3}{16} \delta \frac{2-3\lambda}{1+\lambda} \right] + O(\delta^4) \quad (19)$$

where we have again adopted $\xi_s = (\Gamma_{13}, 0, 0)$ with no loss of generality.

For a simple shear flow parallel to a rigid plane boundary, Goren and O'Neill (1971) calculated the hydrodynamic force and torque on a sphere, using the eigensolutions of Laplace's equation in bipolar coordinates developed by Jeffery (1912). In Fig. 3, the drag ratio, Eq. (19), is plotted as a function of d , the distance between the sphere and the interface for three values of $\lambda = 0, 1$ and ∞ . Also shown for comparison are the corresponding drag ratios determined by Goren and O'Neill. As mentioned previously, we presume $\delta \ll 1$ in the derivation of (19). Thus for $\delta \ll 1$ (i.e., $d \gg 1$) the asymptotic solution, Eq. (19), coincides almost exactly with Goren and O'Neill's result which is the exact solution for the simple shear flow parallel to a solid wall. Even for $d \approx 1.5$, the approximate solution shows reasonably good agreement with the exact solution. Indeed, the relative error is within 2.6% for $d > 1.5$. Wakiya (1957) considered the case of a sphere in a linear shear flow between two rigid parallel flat planes (i.e., $\lambda \rightarrow \infty$), in which one plane is held stationary and the other is moved parallel to itself under the assumption that the motion of the sphere is parallel to the walls. Wakiya determined the drag and torque on the sphere located at a distance ' d ' from the stationary plate and ' $3d$ ' away from the moving plate, using the general method developed by Faxen (1921). The drag ratios asymptotically calculated by Wakiya for the limit $\delta \ll 1$ are also shown in Fig. 3. As might be expected, Wakiya's results converge to the asymptotic solution, Eq. (19) with $\lambda \rightarrow \infty$, as the distance d is increased, since the effect of the moving plate becomes negligible compared to the effect of the stationary plate with increase in the distance.

The hydrodynamic torque on a sphere in the flow $\hat{U}_i = \mu_1/\mu_2 \Gamma \cdot \mathbf{x}$ can be evaluated from (17b) and is equal to

$$\mathbf{T} = 4\pi\Gamma_{13} \left[1 + \frac{3}{8} \delta \cdot \frac{1}{1+\lambda} \left[1 - \frac{3}{16} \delta \frac{2-3\lambda}{1+\lambda} - \delta^2 \right] \right] \mathbf{e}_2 + O(\delta^4). \quad (20)$$

This is the negative of the torque which is required to keep the sphere from rotating. It can be compared directly with the corresponding results from Goren and O'Neill's exact solution for a single rigid wall and from Wakiya's asymptotic solution for two parallel plates with the same sphere location (i.e., d away from one plate and $3d$ away from the other). There is good agreement between the asymptotic solution, Eq. (20), and the exact solution of Goren and O'Neill (1971) in the region of $\delta \ll 1$, though it can be noted from (20) that, when $\lambda \rightarrow \infty$, the interface contribution to the torque \mathbf{T} is zero through $O(\delta^4)$. Although the discrepancy between the two solutions becomes larger as $\delta \rightarrow 1$, it still remains relatively small (e.g., the relative error at $d = 1.01$ is only 5.84% and the error is within 3% for $d > 1.5$). As expected, Wakiya's solution also approaches the asymptotic solution for $\lambda \rightarrow \infty$ as the distance d is increased. However, for the two-parallel-plate case the torque is increased in magnitude by the presence of plane boundaries in contradiction to the single wall case.

In this section, we have determined the solutions of Stokes' equations for a sphere at rest at an arbitrary point either in a pure straining flow or in a simple shear flow near a fluid-fluid interface with an arbitrary viscosity ratio. We shall turn shortly to the application of these solutions for trajectory calculations. First, however, we consider corresponding solutions for a rod-like slender body.

4. Solutions for a Slender Body

Let us turn now to the case of a rod-like slender body whose center is located at an arbitrary point, \mathbf{x}_p , near an interface in the presence of a linear

undisturbed flow field (pure straining or simple shear), $\hat{\mathbf{U}}_1 = \mathbf{L}_1 \cdot \mathbf{x}$ with origin at the interface. The slender body is assumed to be at rest and completely immersed in fluid 2 with an arbitrary orientation which can be expressed in terms of Euler angles θ and φ relative to the interface. For present purposes, we define θ as the oblique angle between the body-axis and the interface, while φ is a subtended angle between the x_1 - x_3 plane and the plane defined by the body-axis and normal vector \mathbf{e}_3 to the interface (cf. Fig. 4). At the outset, we assume that the body is oriented with arbitrary oblique angle θ , but that $\varphi = 0^\circ$. Thus, the projection of the body-axis onto the interface exactly coincides with the x_1 -axis. The solution for an arbitrary φ -orientation can be simply obtained from the case of $\varphi = 0^\circ$, by use of an orthogonal rotation tensor, \mathbf{Q} defined by

$$\mathbf{Q} = \begin{bmatrix} \cos\varphi & \sin\varphi & 0 \\ -\sin\varphi & \cos\varphi & 0 \\ 0 & 0 & 1 \end{bmatrix}.$$

4.A Pure Straining Flows

Now, let us turn to the case of a slender body held with its center fixed at an arbitrary point \mathbf{x}_p in a uniaxial axisymmetric extension flow, $\hat{\mathbf{U}}_1 = \mathbf{E} \cdot \mathbf{x}$ with stagnation point at the interface. The problem can be treated, as in the case of a sphere, by decomposing the undisturbed flow into a simple translation $\hat{\mathbf{U}}_1 = \mathbf{E} \cdot \mathbf{x}_p$ past the slender body and a linear flow $\hat{\mathbf{U}}_1 = \mathbf{E} \cdot (\mathbf{x} - \mathbf{x}_p)$ with stagnation point at \mathbf{x}_p . The simple translation problem was treated in part I of this series. Here, we solve the problem with undisturbed flow $\hat{\mathbf{U}}_1 = \mathbf{E} \cdot (\mathbf{x} - \mathbf{x}_p)$. For this purpose, it is convenient to consider the equivalent problem in which the body generates a velocity field $\mathbf{u}_2(\mathbf{x}_B) = -\mathbf{E} \cdot (\mathbf{x}_B - \mathbf{x}_p)$ at the body surface; i.e., we solve

$$-\mathbf{E} \cdot (\mathbf{x}_B - \mathbf{x}_p) = \int_{-1}^1 \left[\alpha(\mathbf{x}_s) - \frac{1}{2} \beta(\mathbf{x}_s) \nabla^2 \right] \cdot \psi(\mathbf{x}_B, \mathbf{x}_s) d\zeta \quad (21)$$

in which $\psi(\mathbf{x}_B, \mathbf{x}_s)$ denotes the Cartesian tensorial Green function for a unit point force located at \mathbf{x}_s (cf. Yang and Leal, 1983).

The integral Eq. (21) cannot be solved exactly (except in a numerical sense), but can be solved approximately by means of an asymptotic expansion for small $1/\kappa$ and R_0/d , where R_0 is the maximum radius of the body cross section. By expanding Eq. (21) to $O(1/\kappa, R_0/d)$ with $\alpha(\zeta) = (\alpha_1(\zeta), 0, \alpha_3(\zeta))$ and $\beta(\zeta) = (\beta_1(\zeta), 0, \beta_3(\zeta))$, it can be shown that the potential dipole strength, $\beta(x)$, and the Stokeslet strength, $\alpha(x)$, must be related according to

$$\beta(x) = -\frac{1}{2} r_0^2(x) \cdot \alpha(x) \quad (22)$$

in order to satisfy the no-slip condition (5b) at the body surface to $O(\varepsilon^2)$.

The simultaneous equations, which are obtained from (21) by substituting for $\beta(x)$ according to (22), can be solved by expansion of $\alpha(x)$ in powers of ε for $\varepsilon \ll 1$. The use of an expansion in ε to obtain an approximate solution of this type has been widely reported (cf. Batchelor, 1970) for motion of a slender body in a single unbounded fluid, and was used by us in part I for simple translation and rotation near an interface. The resulting line distribution of Stokeslets, in component form, is

$$\alpha_1(x) = -\frac{(1 + \sin^2\theta) \cdot \cos\theta}{4} x \left[\varepsilon - \frac{\varepsilon^2}{2} \left(2S(x) + \frac{\sin^2\theta - 3}{1 + \sin^2\theta} + U(x; \lambda, \theta, d) \right) \right] \\ - \frac{\sin^2\theta \cos\theta}{2} x \left[\varepsilon - \frac{\varepsilon^2}{2} \left(2S(x) + 1 + X(x; \lambda, \theta, d) \right) \right] \quad (23a)$$

and

$$\alpha_3(x) = \frac{\sin\theta \cos^2\theta}{4} x \left[\varepsilon - \frac{\varepsilon^2}{2} \left(2S(x) + 1 + V(x; \lambda, \theta, d) \right) \right] \\ + \frac{(1 + \cos^2\theta) \cdot \sin\theta}{2} x \left[\varepsilon - \frac{\varepsilon^2}{2} \left(2S(x) + \frac{\cos^2\theta - 3}{1 + \cos^2\theta} + Y(x; \lambda, \theta, d) \right) \right] \quad (23b)$$

where $S(x) = \ln \left[\frac{\left(1 - \left[\frac{x}{l} \right]^2 \right)^{1/2}}{r_0(x)/R_0} \right]$ and $r_0(x)$ is the radius of the body cross sec-

tion which is a function of distance x along the body center line and has a maximum value of R_0 . Here, $U(x;\lambda,\theta,d)$, $X(x;\lambda,\theta,d)$, $V(x;\lambda,\theta,d)$ and $Y(x;\lambda,\theta,d)$ represent the effects of the interface on the slender body and vanish as $d \rightarrow \infty$ (see Appendix for specific formulae of these functions).

The net force and torque exerted on a slender body located at the stagnation point in the undisturbed flow field, $\hat{U}_i = \mathbf{E} \cdot (\mathbf{x} - \mathbf{x}_p)$, can be evaluated simply from the Stokeslet distribution and expressed in the following form:

$$\mathbf{F} = -\mathbf{K}_{PF} \cdot \xi_p \quad (24a)$$

$$\mathbf{T} = -\mathbf{K}_{PT} \cdot \xi_p \quad (24b)$$

where the vector $\xi_p = (1,1,-2)$, and the nonzero components of the hydrodynamic resistance tensor \mathbf{K}_{PF} are

$$K_{PF}^{11} = -\pi(1 + \sin^2\theta)\cos\theta \cdot \varepsilon^2 \int_{-1}^1 x \cdot U(x;\lambda,\theta,d) dx + O(\varepsilon^3) \quad (25a)$$

$$K_{PF}^{31} = \pi \sin\theta \cos^2\theta \cdot \varepsilon^2 \int_{-1}^1 x \cdot V(x;\lambda,\theta,d) dx + O(\varepsilon^3) \quad (25b)$$

$$K_{PF}^{13} = \pi \cos\theta \sin^2\theta \cdot \varepsilon^2 \int_{-1}^1 x \cdot X(x;\lambda,\theta,d) dx + O(\varepsilon^3) \quad (25c)$$

$$K_{PF}^{33} = -\pi(1 + \cos^2\theta)\sin\theta \cdot \varepsilon^2 \int_{-1}^1 x \cdot Y(x;\lambda,\theta,d) dx + O(\varepsilon^3) \quad (25d)$$

The tensor \mathbf{K}_{PT} has the following nonzero components:

$$K_{PT}^{21} = \frac{8\pi}{3} \sin\theta \cos\theta \cdot \varepsilon \left[1 - \varepsilon \left[\ln 2 - \frac{11}{6} + \frac{3}{8} \int_{-1}^1 \left[(1 + \sin^2\theta) \cdot U(x;\lambda,\theta,d) + \cos^2\theta \cdot V(x;\lambda,\theta,d) \right] \cdot x^2 dx \right] \right] + O(\varepsilon^3) \quad (25e)$$

$$K_{PT}^{23} = -\frac{8\pi}{3} \sin\theta \cos\theta \cdot \varepsilon \left[1 - \varepsilon \left[\ln 2 - \frac{11}{6} + \frac{3}{8} \int_{-1}^1 \left[(1 + \cos^2\theta) \cdot Y(x;\lambda,\theta,d) + \sin^2\theta \cdot X(x;\lambda,\theta,d) \right] \cdot x^2 dx \right] \right] + O(\varepsilon^3) .$$

(25f)

In Figs. 5 and 6 the force components, F_1 and F_3 of (24a), are plotted as a function of the orientation angle θ for $\varepsilon = 0.1883$ which corresponds to $\kappa = 100$, and $d = 1.01$ and 2.0 . In each case we consider three values of $\lambda = 0, 1$ and ∞ . In an unbounded, single fluid, the net force on a particle located at the stagnation point of a linear straining flow would be zero. Obviously, in the case of a sphere, this parallel force component is zero due to the symmetry of the sphere. The existence of a nonzero force component, F_3 , as shown in Fig. 6, was also found for the sphere. The force component F_3 is always oriented away from the interface and the magnitude is increased as the viscosity ratio λ becomes larger, which is exactly the same as for the sphere (compare Eq. (10a) and Fig. 6). Thus, a positive external force, $-F_3$, would have to be applied to the body to keep it from translating away from the stagnation point \mathbf{x}_p of the flow regardless of the particle orientation and position, or the viscosity ratio of the two fluids. It should be understood that, in this flow field $\hat{\mathbf{U}}_i = \mathbf{E}(\mathbf{x} - \mathbf{x}_p)$ of Fig. 1C, the interface translates with velocity $-2d\mathbf{e}_3$ toward the stagnation point \mathbf{x}_p at which the body-center is held fixed. This "interface motion" can be viewed as the source of both F_1 and F_3 .

The hydrodynamic torque, T_2 of (24b), is nonzero even in an unbounded single fluid, but is significantly modified in the presence of an interface. The torque T_2 is plotted in Fig. 7 as a function of the orientation angle θ , for $d = 1.01$ and three values of $\lambda = 0, 1$ and ∞ . The corresponding result in an unbounded single fluid is almost identical to the case, $\lambda = 0$. It is evident, since $T_2 \neq 0$, that a freely suspended slender body (i.e., one with $\mathbf{T} = \mathbf{0}$) would rotate in a direction which depends on λ , and on the orientation and position of the body relative to the interface (i.e., θ and d). For $\lambda = 0$ and 1 , there exist two possible equilibrium orientations, at which $T_2 = 0$ and this is also true in a single unbounded fluid.

However, only one of these, $\theta = 0^\circ$, is stable, while the other, $\theta = 90^\circ$, is unstable. When $\theta = 0^\circ$, the particle axis is parallel to the interface. On the other hand, for $\lambda = \infty$, there exist two unstable equilibrium orientations corresponding to points A and B in Fig. 7, and two stable equilibrium orientations with the particle axis either parallel or perpendicular to the solid wall. The equilibrium orientation which would ultimately be attained in this case by a freely suspended body depends on its initial orientation. It should be noted that the qualitative features evident in Fig. 7 for $\lambda = \infty$ (i.e., the existence of two stable and two unstable equilibrium orientations) will occur whenever the viscosity ratio λ is larger than a critical value (e.g., $\lambda_{cr} = 3.273$ for $d = 1.01$), for which the two unstable equilibrium orientations overlap exactly at the perpendicular orientation (i.e., the unique unstable equilibrium $\theta = 90^\circ$). A detailed examination of (24b) shows that the two unstable equilibrium angles, for a given viscosity ratio, are also shifted to $\theta = 90^\circ$ as the separation distance d is increased. For example, for $\lambda \rightarrow \infty$, the two equilibrium angles (θ_e) are $90^\circ \pm 13.28^\circ$ for $d = 1.01$ (which is the case illustrated in Fig. 7), but become equal to $90^\circ \pm 10^\circ$ for $d = 1.216$, and eventually become coincident at $\theta = 90^\circ$ for a critical distance $d_{cr} = 1.409$, beyond which there exist the only two distinct equilibrium orientations, $\theta = 0^\circ$ (stable) and $\theta = 90^\circ$ (unstable), independent of the viscosity ratio λ of the two fluids for a given $\varepsilon = 0.1887$.

In Fig. 8, the critical viscosity ratio λ_{cr} is plotted as a function of the separation distance for three values of the aspect ratio $\kappa = 20, 50$ and 100 which correspond to $\varepsilon = 0.2711, 0.2171$ and 0.1887 , respectively. It can be seen that the critical viscosity ratio is increased, for any given distance d ($< d_{cr}$), as the body becomes more slender, while the critical distance d_{cr} is decreased (i.e., $d_{cr} = 1.876$ for $\kappa = 20$, 1.580 for $\kappa = 50$, and 1.409 for $\kappa = 100$). Thus, for a given aspect ratio (or ε), the condition for existence of the two stable ($\theta = 0^\circ$ and 90°)

and two unstable equilibrium orientations is $\lambda > \lambda_{cr}$ for a distance $d < d_{cr}$. The implication of these somewhat complicated results for trajectories of a slender body in an extensional flow will be considered later.

The undisturbed straining flow, $\hat{\mathbf{U}}_1 = \mathbf{E} \cdot (\mathbf{x} - \mathbf{x}_p)$, is axisymmetric around the x_3 -axis with origin at the body center, \mathbf{x}_p , and the magnitudes and directions of the total force and torque therefore remain unchanged by rotation of the body around the x_3 -axis (i.e., they are independent of φ -orientation). Indeed, the vector components of the total force and torque for arbitrary φ can be obtained by simply using $\mathbf{Q}^{-1} \cdot \mathbf{K}$ for each tensor quantity \mathbf{K} in (24a,b), which is the result for $\varphi = 0^\circ$ (i.e., the x_1 -axis coincides with the projection of the body axis onto the interface).

All of the preceding discussion is concerned with the force and torque on a body in the flow $\hat{\mathbf{U}}_1 = \mathbf{E} \cdot (\mathbf{x} - \mathbf{x}_p)$ with stagnation point at the body center. In order to determine the force and torque when the body is located at an arbitrary point \mathbf{x}_p in the undisturbed flow $\hat{\mathbf{U}}_1 = \mathbf{E} \cdot \mathbf{x}$, which is zero at the interface, the results of (24a,b) must be combined with the corresponding results from part I for translation with velocity $-\mathbf{E} \cdot \mathbf{x}_p$; i.e.,

$$\mathbf{F} = -\mathbf{K}_T \cdot \mathbf{E} \cdot \mathbf{x}_p + \mathbf{Q}^{-1} \cdot \mathbf{K}_{PF} \cdot \xi_p \quad (26a)$$

and

$$\mathbf{T} = -\mathbf{K}_C \cdot \mathbf{E} \cdot \mathbf{x}_p + \mathbf{Q}^{-1} \cdot \mathbf{K}_{PT} \cdot \xi_p \quad (26b)$$

The resistance matrices \mathbf{K}_T and \mathbf{K}_C , were determined in part I of this work (Yang and Leal, 1983). The hydrodynamic force and torque, (26a,b), will be used to calculate complete particle trajectories for the general flow, $\hat{\mathbf{U}}_2 = \mathbf{E} \cdot \mathbf{x}$, in section 5.

4.B Simple Shear Flow

Finally, we turn to the case of a slender body in the simple shear flow, $\hat{\mathbf{U}}_i = \mu_1/\mu_2 \Gamma \cdot \mathbf{x}$. A general solution for this problem can be obtained by superimposing the results for a uniform translation with velocity $\hat{\mathbf{U}}_i = \Gamma \cdot \mathbf{x}_p$ and a linear shear flow with origin at the body center, $\hat{\mathbf{U}}_i = \Gamma \cdot (\mu_1/\mu_2 \mathbf{x} - \mathbf{x}_p)$. Without loss of generality, we assume that the particle is oriented either parallel to the plane of the flow [i.e., $\varphi = 0^\circ$, $\hat{\mathbf{U}}_i = \Gamma_{13} (\mu_1/\mu_2 x_3 + d)\mathbf{e}_1$] or perpendicular to the plane [i.e., $\varphi = 90^\circ$, $\hat{\mathbf{U}}_i = \Gamma_{23} (\mu_1/\mu_2 x_3 + d)\mathbf{e}_2$]. The solution for an arbitrary φ -orientation can then be determined from the solutions for these two cases using the orthogonal rotation tensor \mathbf{Q} which transforms any arbitrary velocity components of $\hat{\mathbf{U}}_i$ parallel to the interface to components parallel and perpendicular to the plane in which the particle is placed (see Fig. 4).

First, we consider the case of a slender body with arbitrary θ -orientation, but $\varphi = 0^\circ$, in the simple shear flow $\hat{\mathbf{U}}_i = \Gamma_{13} (\mu_1/\mu_2 x_3 + d)\mathbf{e}_1$ which vanishes at the body center. The required Stokeslet and potential dipole distributions along the body center-line to satisfy the boundary condition (5b) can be determined using the approach outlined in the previous section. The result is

$$\alpha_1(\mathbf{x}) = -(1 + \sin^2\theta)\sin\theta \frac{\Gamma_{13}\mathbf{x}}{4} \left[\varepsilon - \frac{\varepsilon^2}{2} \left[2S(\mathbf{x}) + \frac{\sin^2\theta - 3}{1 + \sin^2\theta} + U(\mathbf{x};\lambda,\theta,d) \right] \right] + 0(\varepsilon^3) \quad (27a)$$

and

$$\alpha_3(\mathbf{x}) = \sin^2\theta\cos\theta \frac{\Gamma_{13}\mathbf{x}}{4} \left[\varepsilon - \frac{\varepsilon^2}{2} \left[2S(\mathbf{x}) + 1 + V(\mathbf{x};\lambda,\theta,d) \right] \right] + 0(\varepsilon^3). \quad (27b)$$

From the Stokeslet distribution we can evaluate the hydrodynamic force and torque on the body (i.e., Fig. 1F).

$$\mathbf{F}_1 = -\pi\sin\theta(1 + \sin^2\theta) \Gamma_{13} \varepsilon^2 \int_{-1}^1 \mathbf{x} \cdot U(\mathbf{x};\lambda,\theta,d) d\mathbf{x} + 0(\varepsilon^3) \quad (28a)$$

$$F_3 = \pi \sin^2 \theta \cos \theta \Gamma_{13} \varepsilon^2 \int_{-1}^1 x \cdot V(x; \lambda, \theta, d) dx + O(\varepsilon^3) \quad (28b)$$

and

$$T_2 = \frac{8}{3} \pi \sin^2 \theta \Gamma_{13} \varepsilon \cdot \left[1 - \varepsilon \left[\ln 2 - \frac{11}{6} + \frac{3}{8} \int_{-1}^1 [(1 + \sin^2 \theta) U(x; \lambda, \theta, d) + \cos^2 \theta \cdot V(x; \lambda, \theta, d)] x^2 dx \right] \right] + O(\varepsilon^3). \quad (28c)$$

In Figs. 9 and 10 the force components F_1 and F_3 of Eqs. (28a,b) are plotted as a function of the orientation angle θ for $d = 1.01$ and 2 . It can be noted from Fig. 9 that in the flow $\hat{U}_2 = \Gamma_{13}(x_3 + d)\mathbf{e}_1$, with origin at the center of the body axis, the direction of the induced force F_1 , which is obviously zero in an unbounded single fluid, depends on the viscosity ratio λ with a degree of sensitivity that is a strong function of the particle position and orientation relative to the interface.

The force component F_3 , which is very small compared to the parallel force F_1 , is a consequence of the the asymmetry of particle-interface geometry for $\theta \neq 0, 90^\circ$ (indeed, the force F_3 is zero for a sphere). The qualitative features of F_3 as a function of the orientation angle θ are, in fact, quite similar for all viscosity ratios λ and particle positions relative to the interface. Thus, for $0^\circ < \theta < 90^\circ$, the interface will induce a translation away from the interface in the absence of an applied force, $-F_3$, while the induced translation would be toward the interface for $90^\circ < \theta < 180^\circ$.

Detailed calculation of the hydrodynamic torque, T_2 given by Eq. (28c) shows that the qualitative dependence of T_2 on the orientation angle θ is unchanged by the interface. In fact, the effect of the interface becomes very weak when the orientation angle θ of the body axis is in the range from $\theta = -30^\circ$ to 30° (i.e., the effect of the interface on the torque is significant only when one end of the body

passes close to the interface).

We have already noted that the existence of the normal force F_3 , Eq. (28b), implies that a freely suspended slender body, in a simple shear flow $\hat{\mathbf{U}}_2 = \Gamma_{13}(x_3 + d)\mathbf{e}_1$ with origin at the body center, would move in and out relative to the interface as it rotates around the x_2 -axis due to the hydrodynamic torque T_2 given by (28c). However, the trajectory is *not* periodic since the torque vanishes in the slender-body approximation at $\theta = n\pi$, and the body is predicted to experience a net outward displacement relative to the interface from its initial position. Comparison with existing theoretical results for a slender body in simple shear flow of a single, unbounded fluid suggests strongly that this non-periodicity in the particle motion is a consequence of the slender-body approximation. In particular, Cox (1971) showed that the force and torque on an axisymmetric slender body which is at rest and oriented parallel to a simple shear flow ($\theta = n\pi$) is $O((1/\kappa)^2 \varepsilon)$, which is very small compared to the $O(\varepsilon^2)$ terms retained in (28a-c), but is definitely nonzero. According to Cox's analysis, a slender body will rotate very slowly through the aligned, or nearly aligned state, but will experience a periodic rotation for any large (but finite) κ . Similar behavior in the present problem of particle motion near an interface would imply that any real particle (with finite κ) would both rotate and move in and out continuously. We shall return shortly to the details of this motion, which is a generalization of the famous Jeffery's (1922) orbit for rotation in simple shear flow of a single, unbounded fluid.

Now, let us turn to the hydrodynamic interface effects on a slender body in the simple shear flow, $\hat{\mathbf{U}}_1 = \Gamma_{23}(\mu_1/\mu_2 x_3 + d)\mathbf{e}_2$, which is perpendicular to the plane defined by the body-axis and normal vector \mathbf{e}_3 to the interface. In this case, the boundary condition at the body surface (5b) is

$$\mathbf{u}_2(\mathbf{x}_B) = -\Gamma_{23} \mathbf{x} \sin\theta \mathbf{e}_2 + O\left(\frac{1}{\kappa}\right), \quad \mathbf{x}_B \in S_p. \quad (29)$$

It may be noted, however, that this boundary condition is exactly the same as for particle rotation near a flat interface with angular velocity $\Omega = \Omega_1 \mathbf{e}_1$ through a fluid at rest at infinity, with $\Omega_1 = \Gamma_{23}$. Equations for the hydrodynamic force and torque in this latter case have already been derived by Yang and Leal (1983).

We now have a complete solution for a slender body in a simple shear flow, $\hat{\mathbf{U}}_i = \Gamma \cdot (\mu_1/\mu_2 \mathbf{x} - \mathbf{x}_p)$ with origin at the body center, and the undisturbed velocity either parallel or perpendicular to the plane defined by the body centerline and normal vector \mathbf{e}_3 to the interface. From these results we can also evaluate the force and torque on a slender body with an arbitrary orientation (θ, φ) located at an arbitrary position \mathbf{x}_p in a simple shear flow $\hat{\mathbf{U}}_i = \mu_1/\mu_2 \cdot \Gamma \cdot \mathbf{x}$, with origin at the interface. Combining the results of the present section with those for uniform streaming flow, we obtain

$$\mathbf{F} = -\mathbf{K}_T \cdot \Gamma \cdot \mathbf{x}_p + \mathbf{Q}^{-1} \cdot \mathbf{K}_{SF} \cdot \mathbf{Q} \cdot \xi_s \quad (30a)$$

and

$$\mathbf{T} = -\mathbf{K}_C \cdot \Gamma \cdot \mathbf{x}_p + \mathbf{Q}^{-1} \cdot \mathbf{K}_{ST} \cdot \mathbf{Q} \cdot \xi_s. \quad (30b)$$

Here, the nonzero components of hydrodynamic tensors \mathbf{K}_{SF} and \mathbf{K}_{ST} are given by

$$K_{SF}^{11} = -\pi(1 + \sin^2\theta) \sin\theta \cdot \varepsilon^2 \int_{-1}^1 x \cdot U(x; \lambda, \theta, d) dx + O(\varepsilon^3) \quad (31a)$$

$$K_{SF}^{22} = -2\pi \sin\theta \cdot \varepsilon^2 \int_{-1}^1 x \cdot B(x; \lambda, \theta, d) dx + O(\varepsilon^3) \quad (31b)$$

$$K_{SF}^{31} = \pi \sin^2\theta \cos\theta \cdot \varepsilon^2 \int_{-1}^1 x \cdot V(x; \lambda, \theta, d) dx + O(\varepsilon^3) \quad (31c)$$

$$K_{ST}^{12} = -\frac{8}{3} \pi \sin^2\theta \cdot \varepsilon \cdot \left[1 - \varepsilon \left(\ln 2 - \frac{11}{6} + \frac{3}{4} \int_{-1}^1 x^2 K(x; \lambda, \theta, d) dx \right) \right] + O(\varepsilon^3)$$

(31d)

$$K_{Sf}^{21} = \frac{8}{3} \pi \sin^2 \theta \cdot \varepsilon \cdot \left[1 - \varepsilon \left(\ln 2 - \frac{11}{6} + \frac{3}{8} \int_{-1}^1 \left[(1 + \sin^2 \theta) U(x; \lambda, \theta, d) + \cos^2 \theta V(x; \lambda, \theta, d) \right] x^2 dx \right) \right] + O(\varepsilon^3)$$

(31e)

and

$$K_{Sf}^{32} = -K_{Sf}^{12} \cot \theta .$$

(31f)

Specific formulae for $U(x; \lambda, \theta, d)$, $V(x; \lambda, \theta, d)$, $K(x; \lambda, \theta, d)$ and $B(x; \lambda, \theta, d)$ are given in the Appendix.

We now have a complete set of solutions either for a stationary sphere or slender body located at an arbitrary point \mathbf{x}_p with an arbitrary orientation relative to the interface in either an axisymmetric pure extensional flow, or in a simple shearing flow field. These solutions provide the necessary relationships between the flow parameters (e.g., strain rate or shear rate) and the hydrodynamic force and torque for calculation of particle trajectories, which we shall consider in the next section.

5. Trajectories near a Flat Interface

Whenever the creeping motion approximation is applicable, general relationships can be written between the force and torque acting on a particle in a *quiescent* fluid near a flat interface, and its translational and angular velocities in terms of

$$\mathbf{F}_{ex} = \mathbf{K}_T \cdot \mathbf{U} + \mathbf{K}_C \cdot \boldsymbol{\Omega}$$

(32a)

$$\mathbf{T}_{ex} = \mathbf{K}_C \cdot \mathbf{U} + \mathbf{K}_R \cdot \boldsymbol{\Omega}$$

(32b)

the so-called hydrodynamic resistance tensors, \mathbf{K}_T , \mathbf{K}_R and \mathbf{K}_C . The components of these tensors for a spherical particle were evaluated through terms of $O(\delta^2)$

by Lee, Chadwick and Leal (1979), and through terms of $O(\delta^3)$ in the present study, Eqs. (11a-e). For a slender body, Yang and Leal (1983) obtained the various components of these tensors up to $O(\varepsilon^2)$.

In the present paper we consider only the simplest case of a neutrally buoyant freely suspended body. In this case, the translational and angular velocities of the particle are given by

$$\mathbf{U} = \frac{d\mathbf{x}_p}{dt} = (\mathbf{K}_T - \mathbf{K}_C^t \cdot \mathbf{K}_R^{-1} \cdot \mathbf{K}_C)^{-1} \cdot (\mathbf{F} - \mathbf{K}_C^t \cdot \mathbf{K}_R^{-1} \cdot \mathbf{T}) \quad (33a)$$

$$\boldsymbol{\Omega} = (\mathbf{K}_R - \mathbf{K}_C \cdot \mathbf{K}_T^{-1} \cdot \mathbf{K}_C^t)^{-1} \cdot (\mathbf{T} - \mathbf{K}_C \cdot \mathbf{K}_T^{-1} \cdot \mathbf{F}) . \quad (33b)$$

Here, \mathbf{F} and \mathbf{T} are the hydrodynamic force and torque acting on a stationary particle due to the existence of a pure straining or simple shearing flow at large distance from the particle. Thus, given the initial position and orientation of the particle, these equations provide its complete trajectory (i.e., its position and orientation as a function of time). In the present work, we use a simple Runge-Kutta scheme described by Yang and Leal (1983) to integrate Eqs. (33a,b).

5.A Trajectories of a Sphere

First, we begin with the case of a neutrally buoyant sphere freely suspended in the pure straining flow $\hat{\mathbf{U}}_i = \mathbf{E} \cdot \mathbf{x}$ with stagnation point at the interface. The results for the torque and force, \mathbf{F} and \mathbf{T} , in this case are given in Eqs. (10a,b). Substituting for \mathbf{F} and \mathbf{T} in Eq. (33), it is a simple matter to show that the translational and angular velocities of the particle are

$$\mathbf{U} = \mathbf{E} \cdot \mathbf{x}_p - \frac{\frac{5}{16} \delta^2 \frac{2+3\lambda}{1+\lambda} \left[1 + \frac{3}{8} \delta \frac{2+3\lambda}{1+\lambda} \right]}{\left[1 + \sum_{n=1}^3 \left(\frac{3}{8} \delta \frac{2+3\lambda}{1+\lambda} \right)^n - \frac{1+4\lambda}{8(1+\lambda)} \delta^3 \right]} \mathbf{e}_3 \quad (34a)$$

and

$$\boldsymbol{\Omega} = \mathbf{0}. \quad (34b)$$

Thus, the particle does not rotate at all, at the level of approximation represented by (34a,b), and it is only the U_3 component of the translational velocity that is altered from the undisturbed velocity of the fluid by the presence of an interface.

It can be noted from Eq. (34a), that the particle velocity U_3 is always decreased in magnitude by the presence of an interface, independently of the viscosity ratio λ . Furthermore, the difference between U_3 and the undisturbed velocity of the fluid $\mathbf{E} \cdot \mathbf{x}_p \cdot \mathbf{e}_3$ is monotonically increased as the separation between the interface and sphere is decreased, but is independent of the distance from the axis of symmetry of the undisturbed flow.

The motion of a sphere in a linear shear flow, $\hat{\mathbf{U}}_1 = -\mu_1/\mu_2 x_3 \mathbf{e}_1$, parallel to the interface can be resolved in a similar manner. Since the hydrodynamic force on the sphere is oriented parallel to the undisturbed flow, i.e., $\mathbf{F} = F_1 \mathbf{e}_1$ [cf. Eq. (17a)], the path followed by the sphere in the $x_1 - x_3$ plane is exactly coincident with a streamline of the undisturbed flow. However, the translational velocity of the sphere is altered considerably from the undisturbed velocity of the fluid by interaction with the interface. This is illustrated in Fig. 11, where the difference between the velocity of the sphere and the undisturbed velocity of the fluid, $U_1 - d$, is given as a function of the separation distance between the sphere and the interface, d , for three values of $\lambda = 0, 1$ and ∞ . Also included for comparison are the corresponding results of Goldman, Cox and Brenner (1976b) who obtained an exact solution of Stokes' equations, using bipolar coordinates, for the translational and angular velocities of a neutrally buoyant sphere moving in a linear shear flow in proximity to a single plane wall (i.e., $\lambda \rightarrow \infty$). It can be seen from Fig. 11 that the present asymptotic result for the translational velocity is in

reasonable agreement with the exact solution in the entire region of $d > 1$. Indeed, the relative error associated with the asymptotic solution is less than 2.0% for $d > 1.54$.

The angular velocity, $-\Omega_2$ [Eq. (33b)], for motion of a freely suspended sphere in the simple shearing flow is plotted in Fig. 12 as a function of d for three values of $\lambda = 0, 1$ and ∞ . Darabaner and Mason (1967) experimentally measured the angular velocity of a neutrally buoyant sphere in a Couette viscometer as a function of the separation distance between the sphere and the wall of the viscometer. Their results are included in the figure. In addition, the exact solution of Goldman, Cox and Brenner (1967b) for $\lambda = \infty$ is also compared with our approximate solution in this figure. The present asymptotic solution is qualitatively consistent both with the experimental data and the exact solution over the whole range of d , and is quantitatively accurate except in the region of $d \sim 1$. Considering that the experimental data have not been corrected for wall curvature nor for the presence of a second wall at a larger distance, and in view of the difficulties of maintaining and measuring the separation distance from the wall, the agreement is quite good.

5.B Trajectories of a Slender Body

Let us turn now to the case of a slender body suspended freely in a linear flow field. Since each hydrodynamic resistance tensor in Eqs. (33a,b) is a function of the orientation of the body axis (θ, φ) , in addition to the position of the body relative to the interface (i.e., d), it is convenient to relate the angular velocity Ω in (33b) to $\dot{\theta}$ and $\dot{\varphi}$, the time rate of changes in θ and φ (cf. Yang and Leal, 1983).

We begin with the trajectory of a slender body in the pure straining flow $\hat{U}_1 = \mathbf{E} \cdot \mathbf{x}$. As we noted in section 4.A, the hydrodynamic torque on the body in this flow is due primarily to the basic flow rather than the interaction between

the particle and the interface. Only for $\lambda \geq 0(1)$ with $d - 1 \ll 0(1)$ and θ in the range $45^\circ \sim 135^\circ$ so that one end of the particle is relatively close to the interface is there a significant contribution to the torque from the particle-interface interaction (cf. Figs. 7 and 8). We now thus consider a slender body initially located at $\mathbf{x}_p^0 = (0,0,-2)$, which is relatively close to the interface, with initial oblique angles $\theta_0 = 0^\circ, 30^\circ, 60^\circ, 70^\circ, 75^\circ, 85^\circ$ and 90° relative to the interface and $\varphi_0 = 0^\circ$. In this case ($\varphi_0 = 0^\circ$), the axis of the particle is initially in the $x_1 - x_3$ plane and remains so as it travels along the flow field. In Fig. 13, the trajectories for a slender body with prescribed initial position and orientations are represented in terms of the orientation angle, θ , and the separation distance, d , for three values of $\lambda = 0, 1$ and ∞ . We also include the corresponding results for trajectories in an unbounded fluid, which nearly coincide with those for the $\lambda = 0$ case. A slender body initially oriented parallel or perpendicular to the interface will travel along the flow without rotation, and thus the trajectory (d vs. θ) in each case is a vertical straight line. Furthermore, for any initial orientation θ_0 , except the case of $\lambda = \infty$ and $\theta_0 = 85^\circ$, the particle always rotates toward an orientation parallel to the interface independently of λ . For the case of $\lambda = \infty$ and $\theta_0 = 85^\circ$, on the other hand, the particle rotates towards the perpendicular orientation which, as we have noted earlier, is a second stable equilibrium orientation for this case. The final orientation for $\lambda = \infty$ is determined by the initial position and orientation of the particle. This rather curious result for $\lambda = \infty$ will actually occur for any value of $\lambda > \lambda_{cr}$, which is determined from Fig. 8. It may be noted that a slender body with initial orientation $\theta_0 \leq 70^\circ$ achieves an orientation parallel to the interface before the particle reaches the interface [actually up to $d/1 - |\sin\theta| = 0.01$, which is the separation distance between the tip of the body and the interface]. On the other hand, a particle with $\theta_0 \geq 75^\circ$, except the case of $\lambda = 0$ and $\theta_0 = 75^\circ$, touches the interface before it arrives at the

equilibrium orientation either parallel or perpendicular to the interface, depending on the viscosity ratio. The critical value of the initial orientation θ_0 , determining the final orientation, depends on the viscosity ratio λ and the initial separation from the interface. However, a particle initially located at sufficiently large distance (i.e., $d \rightarrow \infty$) with arbitrary orientation ($\theta \neq 90^\circ$) will always rotate parallel to the interface before it reaches the interface.

The trajectories for other initial positions $\mathbf{x}_p^0 = (0.5, 0, -2)$, $(1, 0, -2)$, $(3, 0, -2)$ and $(5, 0, -2)$, which are displaced from the axis of symmetry, were also examined. The trajectories in the $x_1 - x_3$ plane (i.e., d vs. x) do not deviate significantly from the corresponding streamlines of the undisturbed flow field. Furthermore, the hydrodynamic torque on the particle in the flow, i.e., $\mathbf{T} - \mathbf{K}_C \cdot \mathbf{K}_T^{-1} \cdot \mathbf{F}$ from Eq. (33b) in combination with Eqs. (26a,b), equals $\mathbf{Q}^{-1} \cdot \mathbf{K}_{PT} \cdot \xi_p - \mathbf{K}_C \cdot \mathbf{K}_T^{-1} \cdot \mathbf{Q}^{-1} \cdot \mathbf{K}_{PF} \cdot \xi_p$, which depends on the separation distance d from the interface and the particle orientation (θ, φ) , but is *independent* of the particle position relative to the axis of symmetry. The terms, $\mathbf{Q}^{-1} \cdot \mathbf{K}_{PT} \cdot \xi_p$ and $\mathbf{Q}^{-1} \cdot \mathbf{K}_{PF} \cdot \xi_p$, are the hydrodynamic torque and force on a particle in the pure straining flow which has its origin coincident with position of the particle center, while $\mathbf{K}_C \cdot \mathbf{K}_T^{-1} \cdot \mathbf{Q}^{-1} \cdot \mathbf{K}_{PF} \cdot \xi_p$ is the torque acting on the same particle as a consequence of force $\mathbf{Q}^{-1} \cdot \mathbf{K}_{PF} \cdot \xi_p$ and the reciprocity of Stokes flow with linear boundary conditions. Thus, the angular velocity, Eq. (33b), of a slender body located at arbitrary point \mathbf{x}_p^0 is determined by the separation d from the interface, for a given orientation (θ, φ) , and is independent of the particle position relative to the axis of symmetry. The general features of the particle trajectories in terms of the orientation θ vs. the separation distance d , which were described for $\mathbf{x}_p^0 = (0, 0, -2)$, are therefore preserved whether or not the initial location is on the axis of symmetry, at least for the special initial separation distance, i.e., $d = 2$, considered here.

The other problem which we examine in this section is an undisturbed simple shearing flow, $\hat{\mathbf{U}}_2 = -x_3 \mathbf{e}_1$, parallel to the interface into which a slender ellipsoid of revolution (i.e., $S(\mathbf{x}) = 0$) is placed with an arbitrary orientation being determined by spherical polar angles θ and φ based upon the plane of the interface (cf. Fig. 4). If the axis ratio for the ellipsoid is arbitrarily small, but *nonzero*, and the ellipsoid is suspended freely in simple shear flow of an *unbounded* single fluid, Jeffery (1922) showed that the motion of the axis of revolution of the particle is described, apart from a simple translation parallel to the flow, by periodic (Jeffery) orbit equations, relating $\dot{\theta}$ and $\dot{\varphi}$ to κ , θ and φ . The corresponding equations for slender-body rotation in an unbounded single fluid can be calculated readily from the present slender-body solution of $O(\varepsilon^2)$ by using Eqs. (30) and (33),

$$\dot{\theta} = \cos\varphi \sin^2\theta (1 - 0.5\varepsilon) + O(\varepsilon^2) \tag{35a}$$

$$\dot{\varphi} = \sin\varphi \tan\theta (1 - 0.5\varepsilon) + O(\varepsilon^2). \tag{35b}$$

In the limit $\kappa \rightarrow \infty$ (or $\varepsilon \rightarrow 0$), the exact and slender body results are identical except for $\theta \approx n\pi$ (where n is any non-negative integer), when the exact equations yield

$$\dot{\theta} \approx \cos\varphi \kappa^{-2} \tag{36}$$

while the slender-body approximation reduces to $\dot{\theta} = \dot{\varphi} = 0$.

In an unbounded fluid, particles with an arbitrarily large but finite aspect ratio κ thus rotate periodically through the aligned (or nearly aligned) orientation, $\theta = n\pi$, due to the small $O(\kappa^{-2})$ term of (36), while the slender body theory predicts that the particles asymptotically approach the aligned position, but do not continue to rotate. Thus, although successful in giving the hydrodynamic resistance for nonaligned orientations (i.e., $\theta \neq n\pi$), the classical slender body theory fails to give any results for the fully aligned state and this is a critical

failure for adequate description of the periodic orbital motion in simple shear flow. This problem was considered in detail for a slender body in a single, unbounded fluid by Cox (1971). Cox (1971) determined the hydrodynamic torque acting on the slender body with aligned orientation, $\theta = n\pi$, in a linear shearing flow of a single, unbounded fluid as an asymptotic expansion in terms of $1/\kappa$, i.e.,

$$T = \frac{8\pi}{3} \frac{\cos\varphi \kappa^{-2} \varepsilon}{[1 - 0.5\varepsilon]} + O(\kappa^{-3}) . \quad (37)$$

which is responsible for the slow rotation of a real particle through the aligned orientations $\theta \sim n\pi$. From (37) and the hydrodynamic relationship between the torque and the angular velocity, we can readily evaluate the angular velocity $\dot{\theta}$ through the aligned orientation ($\theta = n\pi$).

$$\dot{\theta} = \cos\varphi \kappa^{-2} (1 + 0.25\varepsilon^2) + O(\kappa^{-2}\varepsilon^3) \quad (38)$$

which is consistent with the exact Jeffery orbit equation with $\theta = n\pi$, i.e., Eq. (36). Leal (1975) has shown that a useful and uniformly valid first approximation to the orbit equation in an unbounded single fluid case can be obtained simply by combining the first-order slender body solutions of $O(\varepsilon)$ with the expression (36) in the form

$$\dot{\theta} \sim \cos\varphi (\sin^2\theta + \kappa^{-2}) \quad (39a)$$

and

$$\dot{\varphi} \sim \sin\varphi \tan\theta , \quad (39b)$$

and that the detailed orbit shapes corresponding to (39a,b) are nearly identical to the famous (and exact) Jeffery orbits. We now examine the trajectories of a slender body in simple shearing flow near a plane interface using the same approximation (38) to describe rotation $\dot{\theta}$ of the body axis through the aligned orientations near $\theta \sim n\pi$.

First, we begin with the motion of a particle from an initial φ -orientation, $\varphi_0 = 0^\circ$, in which the axis of the particle is in the $x_1 - x_3$ plane defined by the flow direction and the normal to the interface. Thus, the slender body remains always in the plane, $\varphi = 0^\circ$, and it is only θ and the position of the particle center that change with time. In Fig. 14, the trajectories for a slender body located initially at $\mathbf{x}_p^0 = (0,0,-1.2)$ with initial θ -orientations $\theta_0 = -30^\circ, 0^\circ, 10^\circ$ and 50° are represented in terms of the *increment* of the orientation angle, $\theta - \theta_0$, and the separation distance between the body center and the interface, d , for three values of $\lambda = 0, 1$ and ∞ . For an unbounded fluid, the \mathbf{e}_3 component of the hydrodynamic force $\mathbf{F} - \mathbf{K}_C \cdot \mathbf{K}_R^{-1} \cdot \mathbf{T}$ in (33a) is obviously zero (cf. Fig. 10) and thus the trajectory, d vs. θ , in that case is a horizontal line regardless of the initial θ -orientation. Here, \mathbf{F} denotes the hydrodynamic force acting on the slender body in the simple shearing flow without rotation, Eq. (30a), and \mathbf{T} is the hydrodynamic torque on the same particle without translation, Eq. (30b). The trajectories (d vs. θ) represented in Fig. 14 show, however, somewhat complicated features in the presence of an interface. The present theoretical results show that the hydrodynamic force, $\mathbf{F} - \mathbf{K}_C \cdot \mathbf{K}_R^{-1} \cdot \mathbf{T}$ in (33a), induced by the flow field yields not only translation of the body parallel to the interface but also translation towards or away from the interface with a simultaneous rotation in the direction of increasing θ so that the leading edge turns towards the interface. Although the hydrodynamic force is at equilibrium in the x_3 -direction at each extremum point in Fig. 14, the particle orientation changes (i.e., θ is increased) due to the nonzero torque, $\mathbf{T} - \mathbf{K}_C \cdot \mathbf{K}_R^{-1} \cdot \mathbf{F}$ in (33b). Thus, the equilibrium cannot be maintained, and the body continues to move in and out relative to the interface as it translates continuously parallel to the interface with a simultaneous rotation. When the particle becomes parallel ($\theta = 0^\circ$ or 180°) to the interface (which corresponds to the steepest peak point in the trajectory for each initial

θ_0 -orientation considered here), it begins to travel along the symmetrical trajectory with respect to $\theta = 0^\circ$ (or 180°), as it rotates very slowly through alignment. It is worth pointing out that, due to the symmetry of the system, the trajectories are exactly symmetrical with respect to $\theta = 0^\circ$ (or 180°), as the particle rotates very slowly through the aligned state. The trajectories are also exactly symmetrical with respect to $\theta = n\pi/2$ (n : integer), and thus the particle eventually reaches the initial separation distance from the interface (i.e., in this case $d = 1.2$) at the orientation angle $\theta = \pi + \theta_0$, beyond which the body passes along the same periodic trajectories as those shown in Fig. 14.

Finally, we consider the case of a slender body initially oriented with $\varphi_0 \neq 0^\circ$ and the same θ_0 's considered in the foregoing case. In the case $\varphi_0 \neq 0^\circ$, the body axis is no longer in the plane of the flow defined by the flow direction \mathbf{e}_1 and the normal to the interface \mathbf{e}_3 , and the trajectories are different from those in Fig. 14, in which $\varphi_0 = 0^\circ$. In Fig. 15, we compare the detailed particle rotation for $\varphi_0 = 0^\circ, \pi/48, \pi/36, \pi/24$ and $\pi/12$, as indicated by the projection of the end of the particle onto the plane of the shear flow in a frame of reference fixed to the body center. The various orbital trajectories for different values of φ_0 indicate that the precise projection is quite sensitive to the initial orientation (θ_0, φ_0). Most clearly evident, on comparing the calculated orbits, is the fact that the general features of trajectories in Fig. 15 are preserved whether or not the interface is introduced, and the orbital motion is periodic independently of the viscosity ratio λ and the initial orientation of the body axis. Indeed, the orbital trajectories for $\lambda = 1$ in Fig. 15 are almost identical to those in an unbounded single fluid. However, the origin of Fig. 15 (i.e., the body center) in the presence of an interface periodically oscillates relative to the interface. Thus, the trajectories in terms of the separation distance, d , from the interface and the orientation angle, θ , are significantly different from the case of $\varphi_0 = 0^\circ$, in which the

angle θ is continuously increased as the body rotates. In Fig. 16, the orbital trajectories for one period in the plane of d vs. θ are plotted for $\varphi_0 = 30^\circ$ and $\theta_0 = -30^\circ, 0^\circ, 10^\circ, 50^\circ$ and for three values of $\lambda = 0, 1$ and ∞ to illustrate the effect of the initial φ -orientation on the particle motion. Also shown for comparison are the results for an unbounded infinite fluid, in which the trajectory (d vs. θ) is the *horizontal* line. In this case of $\varphi_0 \neq 0^\circ$, the body not only tumbles end-to-end but also twists relative to the plane of the flow (i.e., $x_1 - x_3$ plane) due to the hydrodynamic force and torque, $\mathbf{F} = \mathbf{K}_C \cdot \mathbf{K}_R^{-1} \cdot \mathbf{T}$ and $\mathbf{T} = \mathbf{K}_C \cdot \mathbf{K}_T^{-1} \cdot \mathbf{F}$ in Eqs. (33a,b). A detailed calculation shows that the twisting motion (i.e., rotation with $\dot{\varphi}$) is enhanced by the presence of an interface, which tends to reduce the parallel translation of the nearest end to the interface and yields additional hydrodynamic torque on the body to increase $\dot{\varphi}$.

We have also examined the trajectories of a slender body with $\varphi_0 = 60^\circ$ and 90° . However, the qualitative features of the trajectories (d vs. θ) for these cases are quite similar to the case of $\varphi_0 = 30^\circ$ and illustrative figures are not necessary.

This completes our illustrative trajectory calculations for a neutrally buoyant particle (i.e., sphere or slender body) freely suspended in a pure straining or in a simple shearing flow, using the basic solutions that were developed in sections 3 and 4. In future research, we plan to consider the application of the results of this paper to particle capture at the surface of a large bubble or drop (i.e., capture rates in flotation processes), and to the rheology of dilute suspensions.

Acknowledgment: This work was supported by a grant from the National Science Foundation, Fluid Mechanics Program of the Engineering Directorate. The authors are grateful for this support.

APPENDIX

In this appendix, we give detailed forms of the functions defined in Section 4 in terms of $g(x;\theta,d)$, $h(x;\theta,d)$, $k(x;\theta,d)$, $y(x;\theta,d)$, $z(x;\theta,d)$, $A(x;\lambda,\theta,d)$, $C(x;\lambda,\theta,d)$, $D(x;\lambda,\theta,d)$ and $E(x;\lambda,\theta,d)$ for which definitions are given in the appendix of Part 1 of this series.

$$\begin{aligned}
 U(x;\lambda,\theta,d) &= A(x;\lambda,\theta,d) + \frac{1-\lambda}{1+\lambda} \frac{1}{x} \left[\{(1-x\cos 2\theta - 2d\sin\theta)^2 \right. \\
 &+ (2\cos\theta(d-x\sin\theta))^2\}^{1/2} - \{(1+x\cos 2\theta + 2d\sin\theta)^2 + (2\cos\theta(d+x\sin\theta))^2\}^{1/2} \\
 &+ \frac{1}{x} (d-x\sin\theta) \left[\frac{\sin\theta(3\sin^2 2\theta + 8 - 3\lambda(\sin^2 2\theta + 4\cos^2 \theta))}{2(1+\lambda)(1+\sin^2 \theta)} g(x;\theta,d) \right. \\
 &+ \frac{2\cos^2 \theta((4\cos^2 \theta - 3)(1+3\sin^2 \theta) + 3\lambda\sin^2 \theta(3\cos^2 \theta - 2))}{(1+\lambda)(1+\sin^2 \theta)} k(x;\theta,d) \\
 &\quad \left. - \frac{\lambda(21\sin^2 2\theta - 4\sin^2 \theta - 8)}{2(1+\lambda)} k(x;\theta,d) \right. \\
 &- \sin\theta \left[\frac{2(4\cos^2 \theta - 1)(1+3\sin^2 \theta) + 9\lambda\sin^2 \theta \cos 2\theta}{2(1+\lambda)(1+\sin^2 \theta)} - \frac{\lambda(6\cos^4 \theta + 7\cos^2 \theta - 4)}{2(1+\lambda)\cos^2 \theta} \right] h(x;\theta,d) \\
 &\quad + \frac{4\lambda\cos^2 \theta(1+3\sin^2 \theta)(16\sin^4 \theta - 12\sin^2 \theta + 1)}{(1+\lambda)(1+\sin^2 \theta)} y(x;\theta,d) \\
 &\quad \left. + \frac{\lambda\sin\theta(1+3\sin^2 \theta)(16\cos^4 \theta - 12\cos^2 \theta + 1)}{2(1+\lambda)\cos^2 \theta(1+\sin^2 \theta)} z(x;\theta,d) \right] \\
 V(x;\lambda,\theta,d) &= E(x;\lambda,\theta,d) + \frac{1-\lambda}{1+\lambda} \frac{1}{x} \left[\{(1-x\cos 2\theta - 2d\sin\theta)^2 \right. \\
 &+ (2\cos\theta(d-x\sin\theta))^2\}^{1/2} - \{(1+x\cos 2\theta + 2d\sin\theta)^2 + (2\cos\theta(d+x\sin\theta))^2\}^{1/2} \\
 &\quad + \frac{(d-x\sin\theta)}{x} \left[-\frac{4(3\cos^4 \theta - 2) + 3\lambda\sin^2 2\theta}{2(1+\lambda)\sin\theta} g(x;\theta,d) \right. \\
 &\quad \left. + \frac{2\sin\theta((12\cos^4 \theta - \cos^2 \theta - 2) - \lambda(30\cos^4 \theta - 19\cos^2 \theta - 3))}{(1+\lambda)} k(x;\theta,d) \right.
 \end{aligned}$$

$$\begin{aligned}
 & - \left\{ \frac{3\sin^2 2\theta - 5\cos^2 \theta + 3}{(1 + \lambda)\sin \theta} + \frac{\lambda \sin \theta (12\cos^4 \theta + 2\cos^2 \theta - 5)}{2(1 + \lambda)\cos^2 \theta} \right\} h(x; \theta, d) \\
 & + \frac{8\lambda(16\cos^6 \theta - 4\cos^4 \theta - 7\cos^2 \theta + 1)}{(1 + \lambda)} y(x; \theta, d) \\
 & + \frac{\lambda(16\sin^6 \theta - 36\sin^4 \theta + 17\sin^2 \theta - 1)}{(1 + \lambda)\sin \theta \cdot \cos^2 \theta} z(x; \theta, d) \Big]
 \end{aligned}$$

$$X(x; \lambda, \theta, d) = D(x; \lambda, \theta, d) - \frac{1}{x} \left[\{(1 - x\cos 2\theta - 2d\sin \theta)^2
 \right.$$

$$\left. + (2\cos \theta (d - x\sin \theta))^2 \}^{1/2} - \{(1 + x\cos 2\theta + 2d\sin \theta)^2 + (2\cos \theta (d + x\sin \theta))^2 \}^{1/2}$$

$$+ \frac{(d - x\sin \theta)}{x} \left[\frac{3\sin^2 2\theta - 6\cos 2\theta - 2 + 12\lambda \sin^2 \theta (1 + \sin^2 \theta)}{2(1 + \lambda)\sin \theta} g(x; \theta, d)
 \right.$$

$$\left. + \frac{2(8\cos^4 \theta - 14\cos^2 \theta + 2 - \lambda(30\cos^4 \theta - 67\cos^2 \theta + 27))}{1 + \lambda} k(x; \theta, d)
 \right.$$

$$\left. + \left\{ \frac{2(4\cos^4 \theta - 9\cos^2 \theta + 4)}{(1 + \lambda)\sin \theta} - \frac{\lambda \sin \theta (12\cos^4 \theta + 2\cos^2 \theta + 7)}{2(1 + \lambda)\cos^2 \theta} \right\} h(x; \theta, d)
 \right.$$

$$\left. + \frac{8\lambda(16\cos^6 \theta - 36\cos^4 \theta + 17\cos^2 \theta - 1)}{(1 + \lambda)} y(x; \theta, d)
 \right.$$

$$\left. + \frac{\lambda(16\sin^6 \theta - 4\sin^4 \theta - 7\sin^2 \theta + 1)}{(1 + \lambda)\sin \theta \cdot \cos^2 \theta} z(x; \theta, d) \right]$$

$$Y(x; \lambda, \theta, d) = C(x; \lambda, \theta, d) - \frac{1}{x} \left[\{(1 - x\cos 2\theta - 2d\sin \theta)^2
 \right.$$

$$\left. + (2\cos \theta (d - x\sin \theta))^2 \}^{1/2} - \{(1 + x\cos 2\theta + 2d\sin \theta)^2 + (2\cos \theta (d + x\sin \theta))^2 \}^{1/2}$$

$$+ \frac{(d - x\sin \theta)}{x} \left[\frac{\sin \theta (4(3\cos^4 \theta - 1) + 3\lambda \sin^2 2\theta)}{(1 + \lambda)(1 + \cos^2 \theta)} g(x; \theta, d)
 \right.$$

$$\left. + \frac{2\cos^2 \theta ((4\cos^2 \theta - 3)(1 + 3\cos^2 \theta) + 3\lambda \sin^2 \theta (7\cos^2 \theta - 4))}{(1 + \lambda)(1 + \cos^2 \theta)} k(x; \theta, d)
 \right.$$

$$\left. - \frac{2\lambda(9\cos^4 \theta - 13\cos^2 \theta + 3)}{(1 + \lambda)} k(x; \theta, d)
 \right]$$

$$\begin{aligned}
 & - \sin\theta \left[\frac{2(4\cos^2\theta - 1)(3\cos^2\theta + 1) - 3\lambda\sin^2\theta(2\cos^2\theta + 1)}{2(1 + \lambda)(1 + \cos^2\theta)} \right. \\
 & \quad \left. + \frac{\lambda(18\cos^4\theta - 7\cos^2\theta + 1)}{2(1 + \lambda)\cos^2\theta} \right] h(x;\theta,d) \\
 & + \frac{4\lambda\cos^2\theta(1 + 3\cos^2\theta)(16\sin^4\theta - 12\sin^2\theta + 1)}{(1 + \lambda)(1 + \cos^2\theta)} y(x;\theta,d) \\
 & + \left. \frac{\lambda\sin\theta(16\cos^4\theta - 12\cos^2\theta + 1)(1 + 3\cos^2\theta)}{2(1 + \lambda)\cos^2\theta(1 + \cos^2\theta)} z(x;\theta,d) \right]
 \end{aligned}$$

For specific formulae of the functions $B(x;\lambda,\theta,d)$ and $K(x;\lambda,\theta,d)$ in Eqns. (31b)

and (31d), refer to the Appendix in Yang and Leal (1983), Part 1 of this series.

References

1. Batchelor, G.K. 1970 Slender-body theory for particles of arbitrary cross section in Stokes flow. *J. Fluid Mech.* **44**, 419.
2. Brenner, H. 1961 The slow motion of a sphere through a viscous fluid towards a plane surface. *Chem. Eng. Sci.* **16**, 242.
3. Chwang, A.T. and Wu, T.Y-T. 1975 Hydrodynamics of low-Reynolds-number flow. Part 2. Singularity method for Stokes flows. *J. Fluid Mech.* **67**, 787.
4. Cox, R.G. 1971 The motion of long slender bodies in a viscous fluid. Part 2. Shear Flow. *J. Fluid Mech.* **45**, 625.
5. Darabaner, C.L. and Mason, S.G. 1967 Particle motions in sheared suspensions. XXII: Interactions of rigid sphere. *Rheol. Acta* **6**, 273.
6. Dukhin, S.S. and Rulev, N.N. 1977 Hydrodynamic interaction between a solid spherical particle and a bubble in the elementary act of flotation. *Colloid J. USSR* **39**, 270.
7. Faxen, H. 1921 Dissertation, Uppsala University.
8. Fulford, G.R. and Blake, J.R. 1983 On the motion of a slender body near an interface between two immiscible liquids at very low Reynolds number. *J. Fluid Mech.* **127**, 203.
9. Goldman, A.J., Cox, R.G. and Brenner, H. 1967a Slow viscous motion of a sphere parallel to a plane wall. I. Motion through a quiescent fluid. *Chem. Eng. Sci.* **22**, 637.
10. Goldman, A.J., Cox, R.G. and Brenner, H. 1967b Slow viscous motion of a sphere parallel to a plane wall. II. Couette flow. *Chem. Eng. Sci.* **22**, 653.

11. Goren, S.L. and O'Neill, M.E. 1971 On the hydrodynamic resistance to a particle of a dilute suspension when in the neighborhood of a large obstacle. *Chem. Eng. Sci.* **26**, 325.
12. Jeffery, G.B. 1912 On a form of the solution of Laplace's equation suitable for problems relating to two spheres. *Proc. Roy. Soc. A* **87**, 109.
13. Jeffery, G.B. 1922 The motion of ellipsoidal particles immersed in a viscous fluid. *Proc. Roy. Soc. A* **102**, 161.
14. Leal, L.G. 1975 The slow motion of slender rod-like particles in a second-order fluid. *J. Fluid Mech.* **69**, 305.
15. Lee, S.H., Chadwick, R.S. and Leal, L.G. 1979 Motion of a sphere in the presence of a plane interface. Part 1. An approximate solution by generalization of the method of Lorentz. *J. Fluid Mech.* **93**, 705.
16. Lee, S.H. and Leal, L.G. 1980 Motion of a sphere in the presence of a plane interface. Part 2. An exact solution in bipolar coordinates. *J. Fluid Mech.* **98**, 193.
17. Lorentz, H.A. 1907 A general theory concerning the motion of a viscous fluid. *Abhandl. Theoret. Phys.* **1**, 23.
18. Spielman, L.A. 1977 Particle capture from low-speed laminar flows. *Ann. Rev. Fluid Mech.* **9**, 297.
19. Wakiya, S. 1957 Viscous flows past a spheroid. *J. Phys. Soc. Japan* **12**, 1130.
20. Yang, S.-M. and Leal, L.G. 1983 Particle motion in Stokes flow near a plane fluid-fluid interface. Part 1. Slender body in a quiescent fluid. *J. Fluid Mech.* **136**, 393.

Figure Captions

Figure 1: Coordinate system with an interface in the $x_1 - x_2$ plane and description of decomposed problems. *A*: a sphere in the pure straining flow $\hat{\mathbf{U}}_1 = \mathbf{E} \cdot \mathbf{x}$; *B*: a uniform streaming flow $\hat{\mathbf{U}}_1 = \mathbf{E} \cdot \mathbf{x}_p$ past a stationary sphere at \mathbf{x}_p ; *C*: a sphere at the stagnation point \mathbf{x}_p of the pure straining flow $\hat{\mathbf{U}}_1 = \mathbf{E} \cdot (\mathbf{x} - \mathbf{x}_p)$; *D*: a sphere in the simple shear flow $\hat{\mathbf{U}}_1 = \mu_1/\mu_2 \Gamma \cdot \mathbf{x}$; *E*: a uniform streaming flow $\hat{\mathbf{U}}_1 = \Gamma \cdot \mathbf{x}_p$ past a stationary sphere; *F*: a sphere at the stagnation point \mathbf{x}_p of the simple shear flow $\hat{\mathbf{U}}_1 = \Gamma \cdot (\mu_1/\mu_2 \mathbf{x} - \mathbf{x}_p)$.

Figure 2: Drag ratio for axisymmetric extensional flow relative to Stokes' drag in an unbounded fluid as a function of the dimensionless distance, d , between the sphere center and the interface: $\hat{\mathbf{U}}_2 = \mathbf{E} \cdot \mathbf{x}$, — for $\lambda = \infty$, --- for $\lambda = 1$, - - - - for $\lambda = 0$. \circ 's are the corresponding exact solution results ($\lambda = 0$) of Dukhin and Rudev (1977).

Figure 3: Drag ratio relative to the drag in an unbounded fluid as a function of the dimensionless distance, d , between the sphere center and the interface: $\hat{\mathbf{U}}_2 = \Gamma_{13} x_3 \mathbf{e}_1$, — for $\lambda = \infty$, --- for $\lambda = 1$, - - - - for $\lambda = 0$, Δ 's are the corresponding exact solution results of Goren and O'Neill (1971). \circ 's are the data of Wakiya (1957) for two parallel plates.

Figure 4: Orientation of a slender body in a simple shearing flow with the origin at the body center. The $x_1 - x_2$ plane is parallel to the interface.

Figure 5: Dimensionless force, $F_1/\varepsilon^2 \mu_2 E l^2$ of Eq. (24a), as a function of the orientation angle θ : $\hat{\mathbf{U}}_2 = \mathbf{E} \cdot (\mathbf{x} - \mathbf{x}_p)$, $\varepsilon = 0.1887$, $S(x) = 1/2 \ln(1 - (x/l)^2)$, — for $d = 1.01$, --- for $d = 2.0$, - - - - for an unbounded

fluid case.

Figure 6: Dimensionless force, $F_3/\varepsilon^2\mu_2El^2$ of Eq. (24a), as a function of the orientation angle θ : $\hat{\mathbf{U}}_2 = \mathbf{E} \cdot (\mathbf{x} - \mathbf{x}_p)$, $\varepsilon = 0.1887$, $S(x) = 1/2 \ln [1 - (x/l)^2]$, — for $d = 1.01$, --- for $d = 2.0$.

Figure 7: Dimensionless torque, $T_2/\varepsilon\mu_2El^3$ of Eq. (24b), as a function of the orientation angle θ : $\hat{\mathbf{U}}_2 = \mathbf{E} \cdot (\mathbf{x} - \mathbf{x}_p)$, $\varepsilon = 0.1887$, $S(x) = 1/2 \ln [1 - (x/l)^2]$, $d = 1.01$, — for $\lambda = \infty$, - - - for $\lambda = 1$, --- for $\lambda = 0$, — - — for an unbounded fluid case.

Figure 8: Critical viscosity ratio, λ_{cr} , as a function of the separation distance d for aspect ratios $\kappa = 20, 50$ and 100 : $\hat{\mathbf{U}}_2 = \mathbf{E} \cdot (\mathbf{x} - \mathbf{x}_p)$, and $S(x) = 1/2 \ln [1 - (x/l)^2]$.

Figure 9: Dimensionless force, $F_1/\varepsilon^2\mu_2\Gamma_{13}l^2$ of Eq. (28a), as a function of the orientation angle θ : $\hat{\mathbf{U}}_2 = \Gamma_{13}(x_3 + d)\mathbf{e}_1$, $\varepsilon = 0.1887$, $S(x) = 1/2 \ln [1 - (x/l)^2]$, — for $d = 1.01$, --- for $d = 2.0$, — - — for an unbounded fluid case.

Figure 10: Dimensionless force, $F_3/\varepsilon^2\mu_2\Gamma_{13}l^2$ of Eq. (28b), as a function of the orientation angle θ : $\hat{\mathbf{U}}_2 = \Gamma_{13}(x_3 + d)\mathbf{e}_1$, $\varepsilon = 0.1887$, $S(x) = 1/2 \ln [1 - (x/l)^2]$, — for $d = 1.01$, --- for $d = 2.0$, — - — for an unbounded fluid case.

Figure 11: Dimensionless disturbed translational velocity, $(U_1 - \Gamma_{13}d)/\Gamma_{13}a$, as a function of the dimensionless distance d between the sphere center and the interface: $\hat{\mathbf{U}}_2 = \Gamma_{13}x_3\mathbf{e}_1$, — for $\lambda = \infty$, --- for $\lambda = 1$, - - - for $\lambda = 0$, — - — for an unbounded fluid case. O's are the corresponding exact solution results of Goldman, Cox and Brenner (1967b).

Figure 12: Dimensionless angular velocity, $-\Omega_2/\Gamma_{13}$, as a function of the dimensionless distance, d , between the sphere center and the interface: $\hat{\mathbf{U}}_2 = \Gamma_{13}x_3\mathbf{e}_1$, — for $\lambda = \infty$, --- for $\lambda = 1$, - - - for $\lambda = 0$. — - — for an unbounded fluid case, O's are the corresponding exact solution results of Goldman, Cox and Brenner (1967b). Δ 's are the experimental data of Darabaner and Mason (1967).

Figure 13: Trajectories for a neutrally buoyant slender body in a pure straining flow, $\hat{\mathbf{U}}_2 = \mathbf{E} \cdot \mathbf{x}$, in terms of the θ and d : $\varphi_o = 0^\circ$, $\theta_o = 0^\circ, 30^\circ, 60^\circ, 70^\circ, 75^\circ, 85^\circ$ and 90° , $\varepsilon = 0.1883$, $S(x) = 1/2 \ln [1 - (x/l)^2]$, — for $\lambda = \infty$, --- for $\lambda = 1$, - - - for $\lambda = 0$, — - — for an unbounded fluid case.

Figure 14: Trajectories for a neutrally buoyant slender body in a simple shear flow, $\hat{\mathbf{U}}_2 = \Gamma_{13}x_3\mathbf{e}_1$, in terms of the separation distance d and the orientation angle θ : $\varphi_o = 0^\circ$, $\theta_o = -30^\circ, 0^\circ, 10^\circ, 50^\circ$, $\kappa = 20$, $S(x) = 0$, $\mathbf{x}_p^o = (0,0,-1.2)$, — for $\lambda = \infty$, — - — for $\lambda = 1$, - - - for $\lambda = 0$, --- for an unbounded fluid case.

Figure 15: Orbital trajectories as obtained by the projection of the end of the particle onto the plane of the shear flow, $\hat{\mathbf{U}}_2 = \Gamma_{13}x_3\mathbf{e}_1$: $\varphi_o = 0^\circ, \pi/48, \pi/36, \pi/24$ and $\pi/12$, $\theta_o = 0^\circ$, $\kappa = 20$, $S(x) = 0$, $\mathbf{x}_p^o = (0,0,-1.2)$, — for $\lambda = \infty$, — - — for $\lambda = 1$, - - - for $\lambda = 0$, --- for an unbounded fluid case.

Figure 16: Trajectories for a neutrally buoyant slender body in a simple shear flow, $\hat{\mathbf{U}}_2 = \Gamma_{13}x_3\mathbf{e}_1$, in terms of the separation distance d and the orientation angle θ : $\varphi_o = 30^\circ$, $\theta_o = -30^\circ, 0^\circ, 10^\circ, 50^\circ$, $\kappa = 20$, $S(x) = 0$, $\mathbf{x}_p^o = (0,0,-1.2)$, — for $\lambda = \infty$, — - — for $\lambda = 1$, - - - for $\lambda = 0$, --- for an unbounded fluid case.

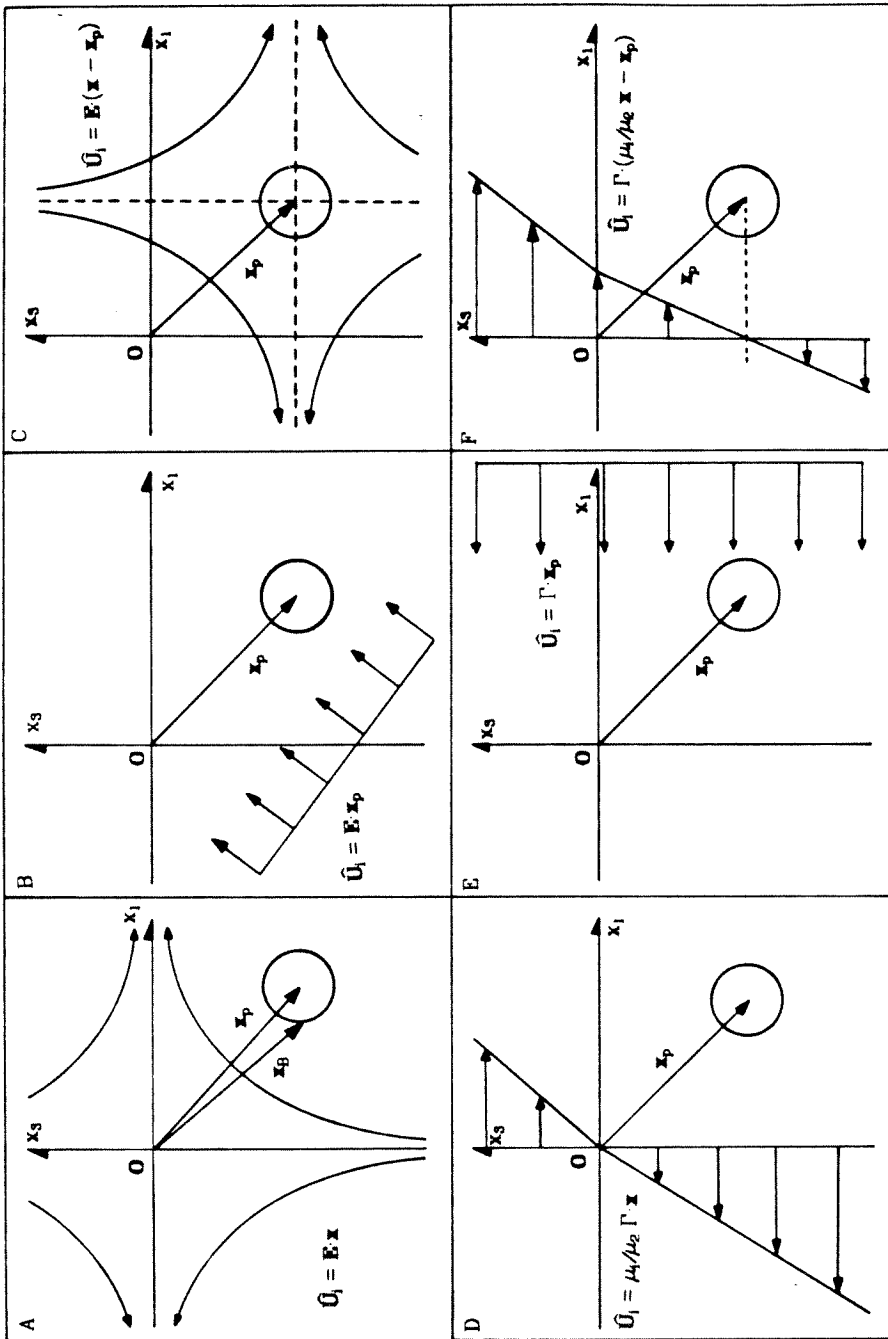


Figure 1

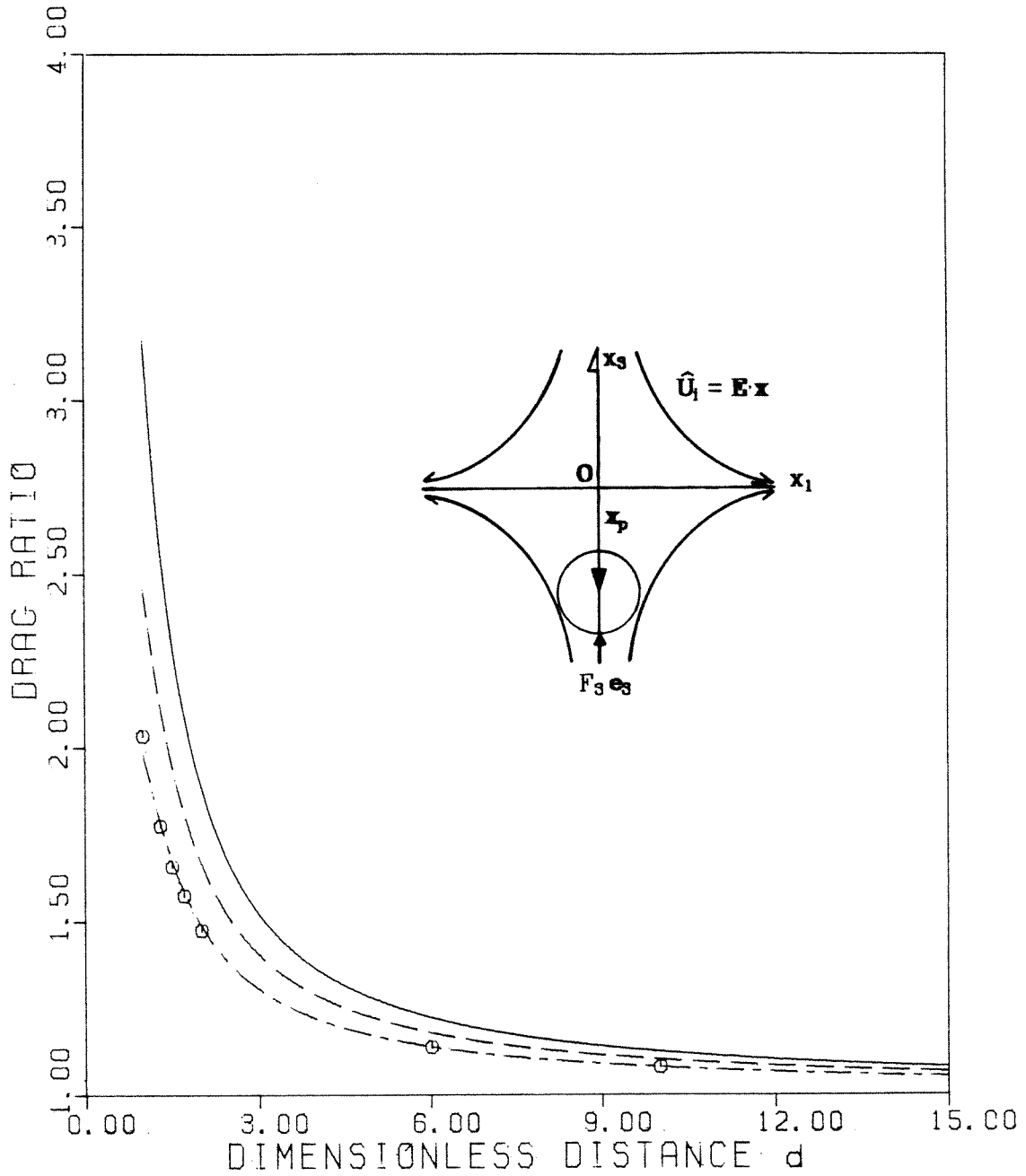


Figure 2

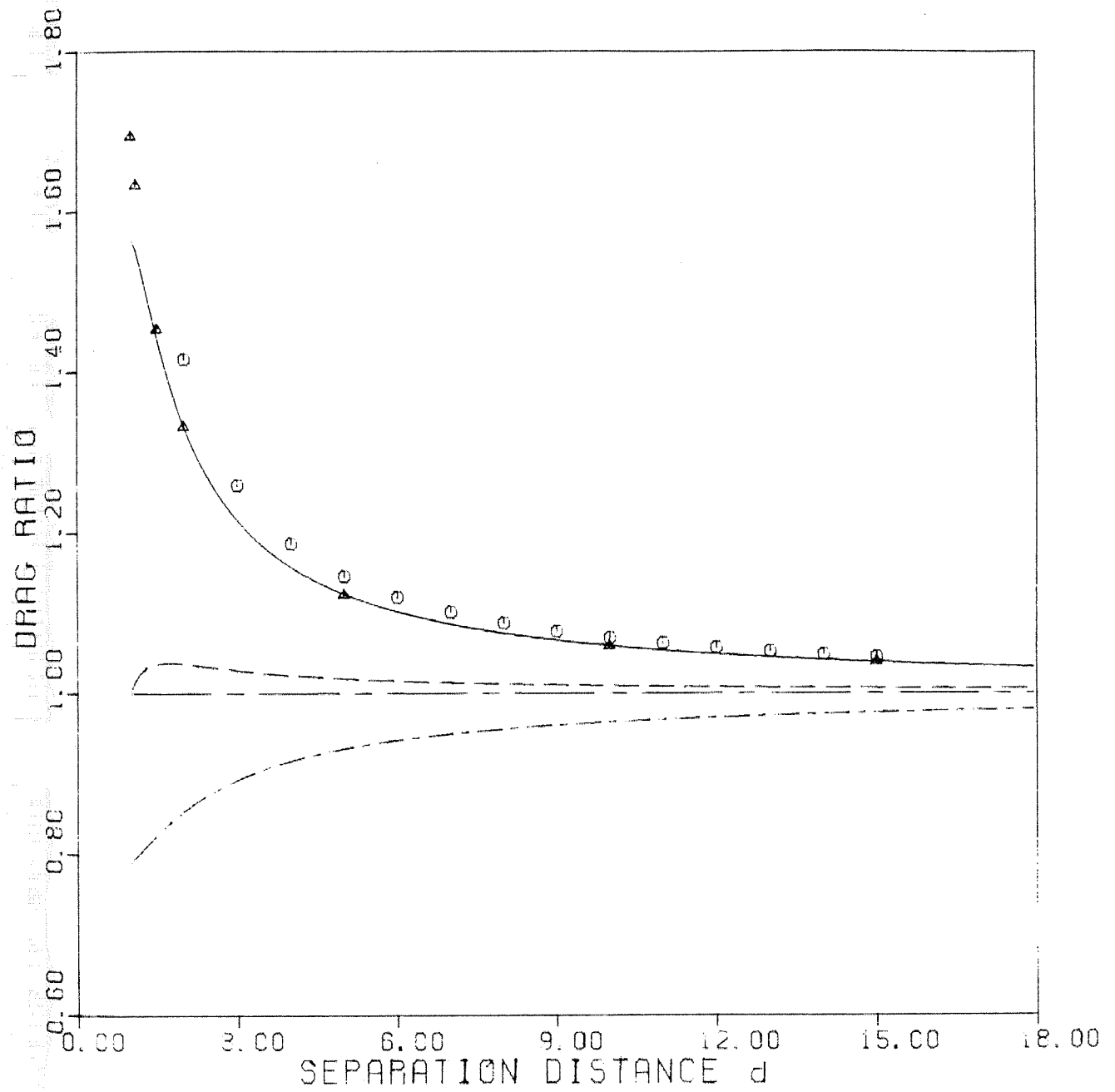


Figure 3

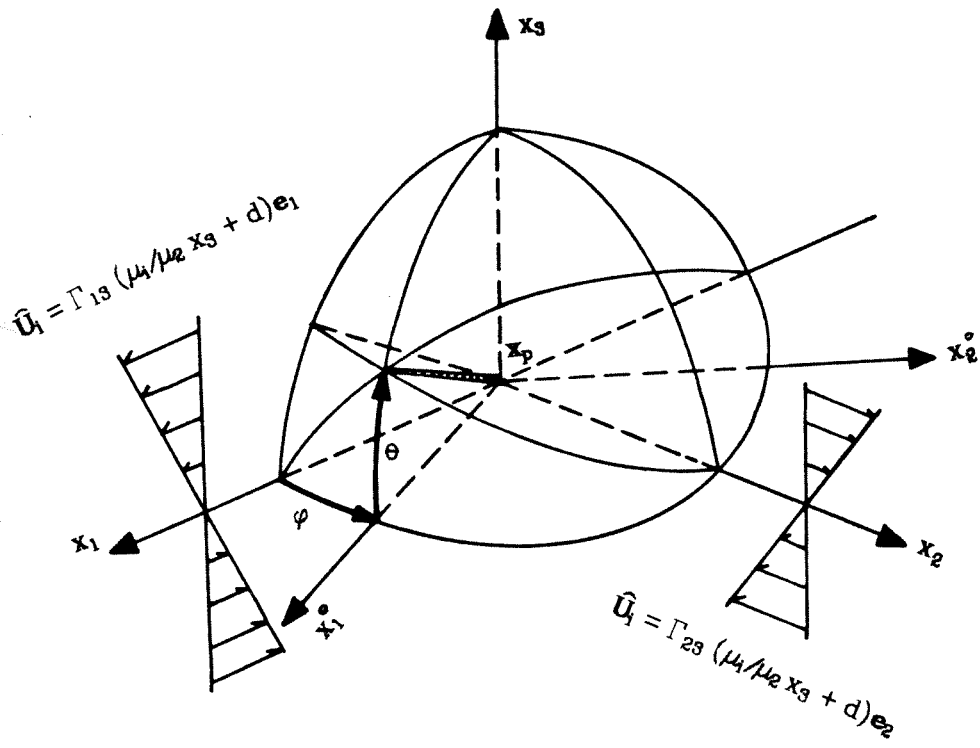


Figure 4

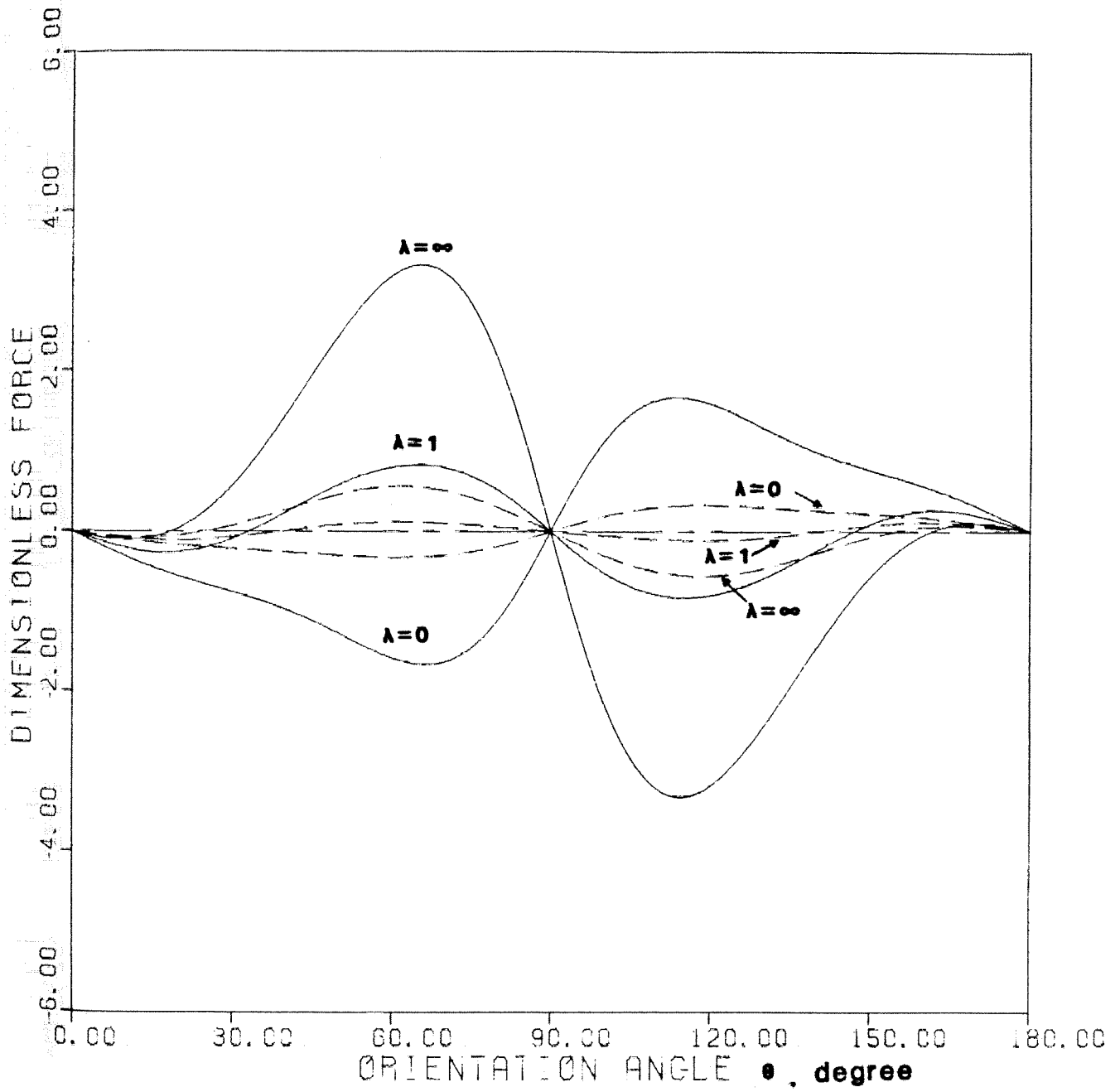


Figure 5

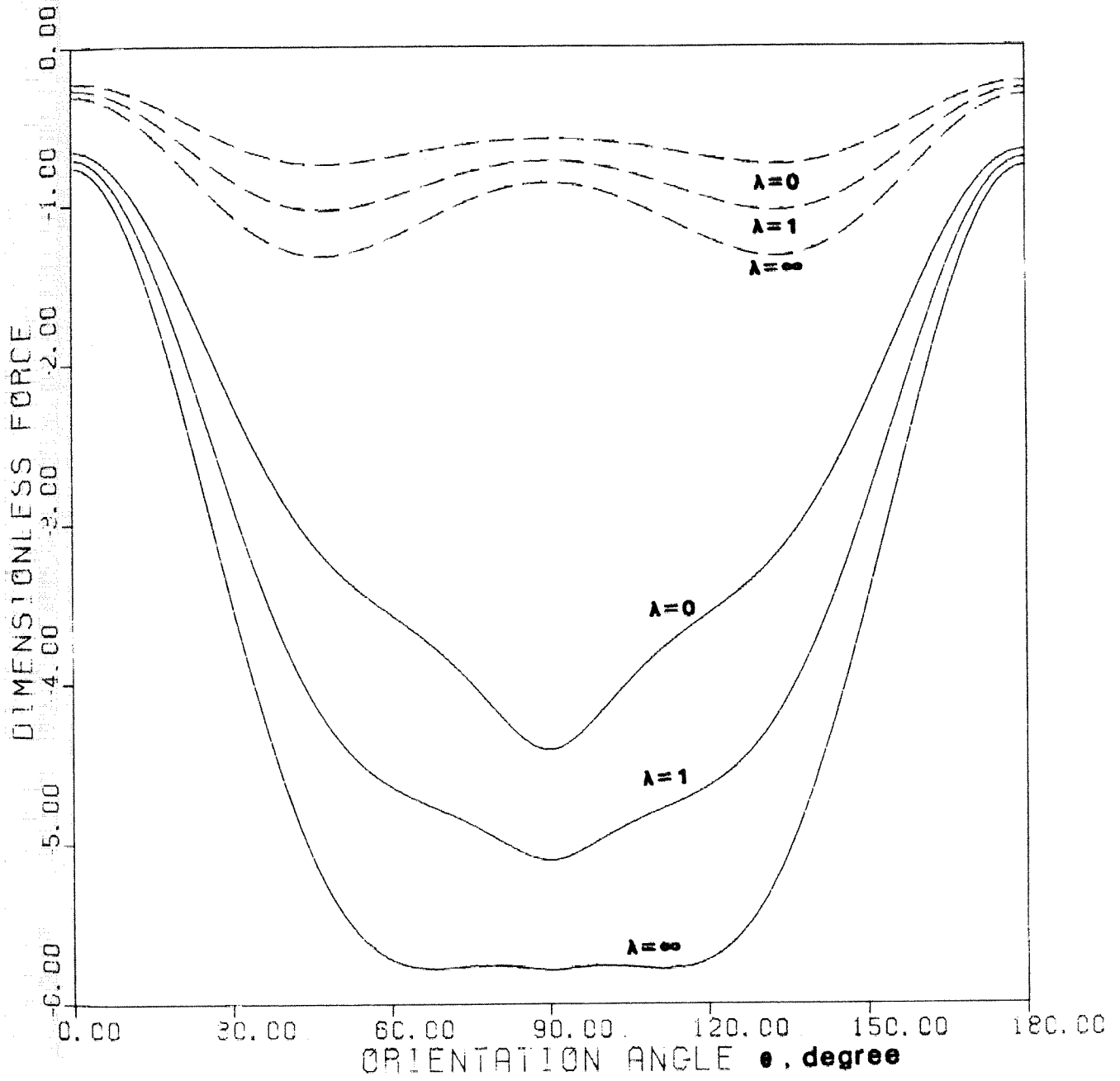


Figure 6

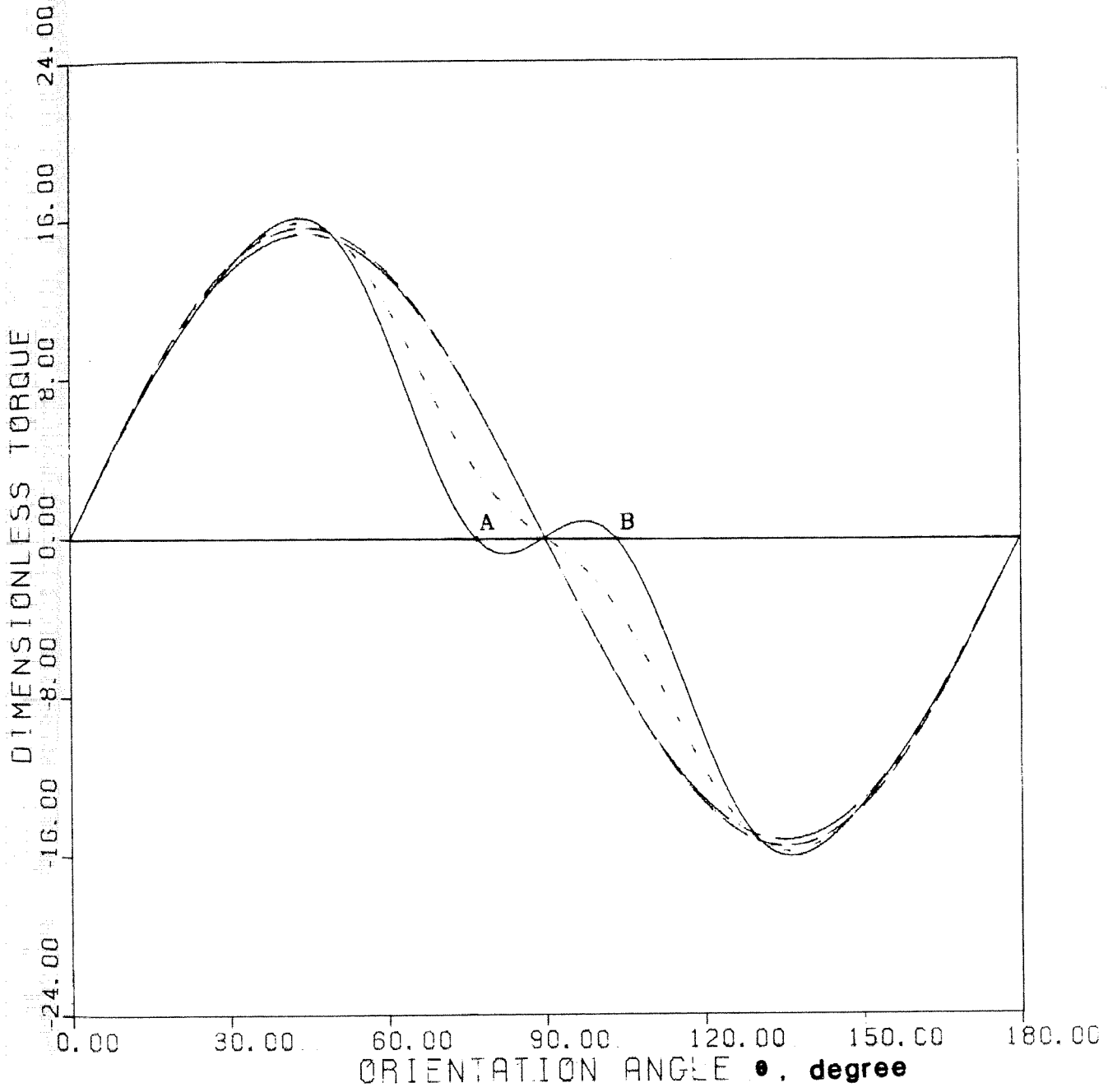


Figure 7

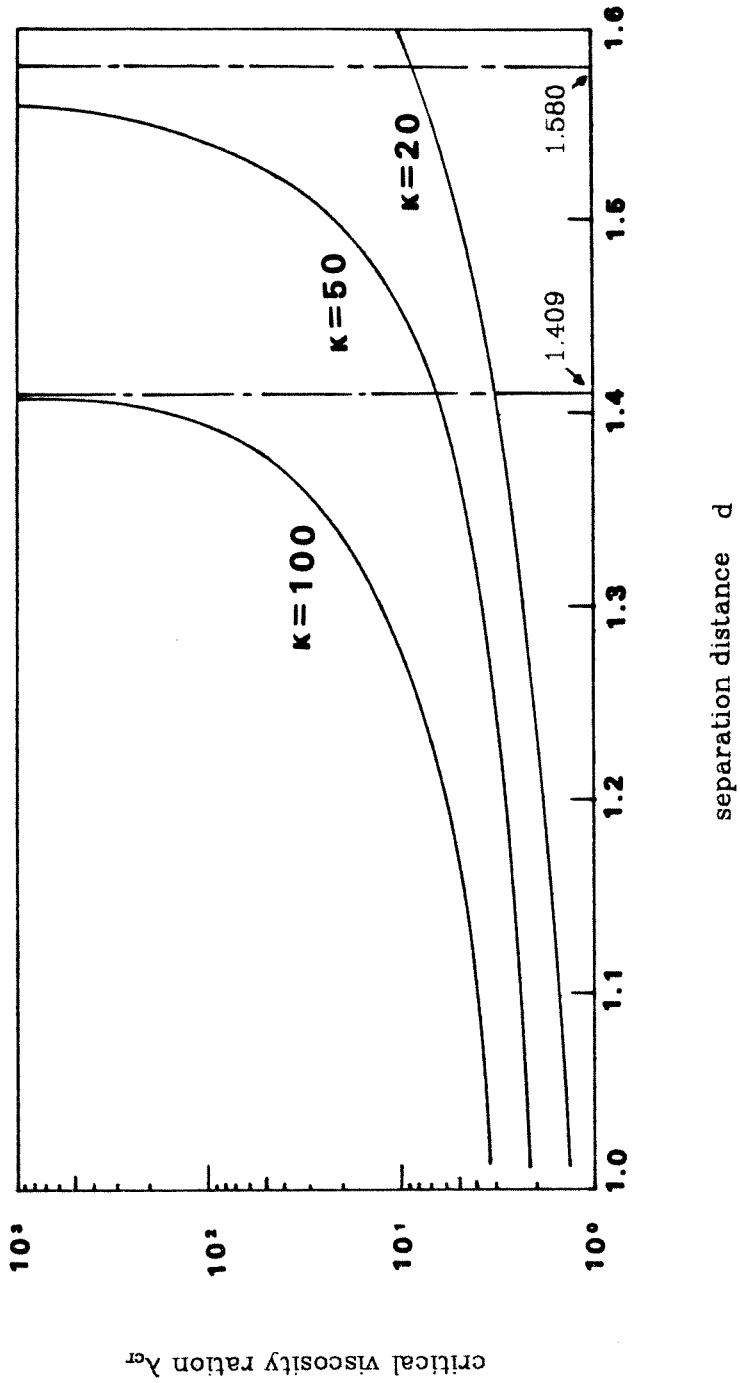


Figure 8

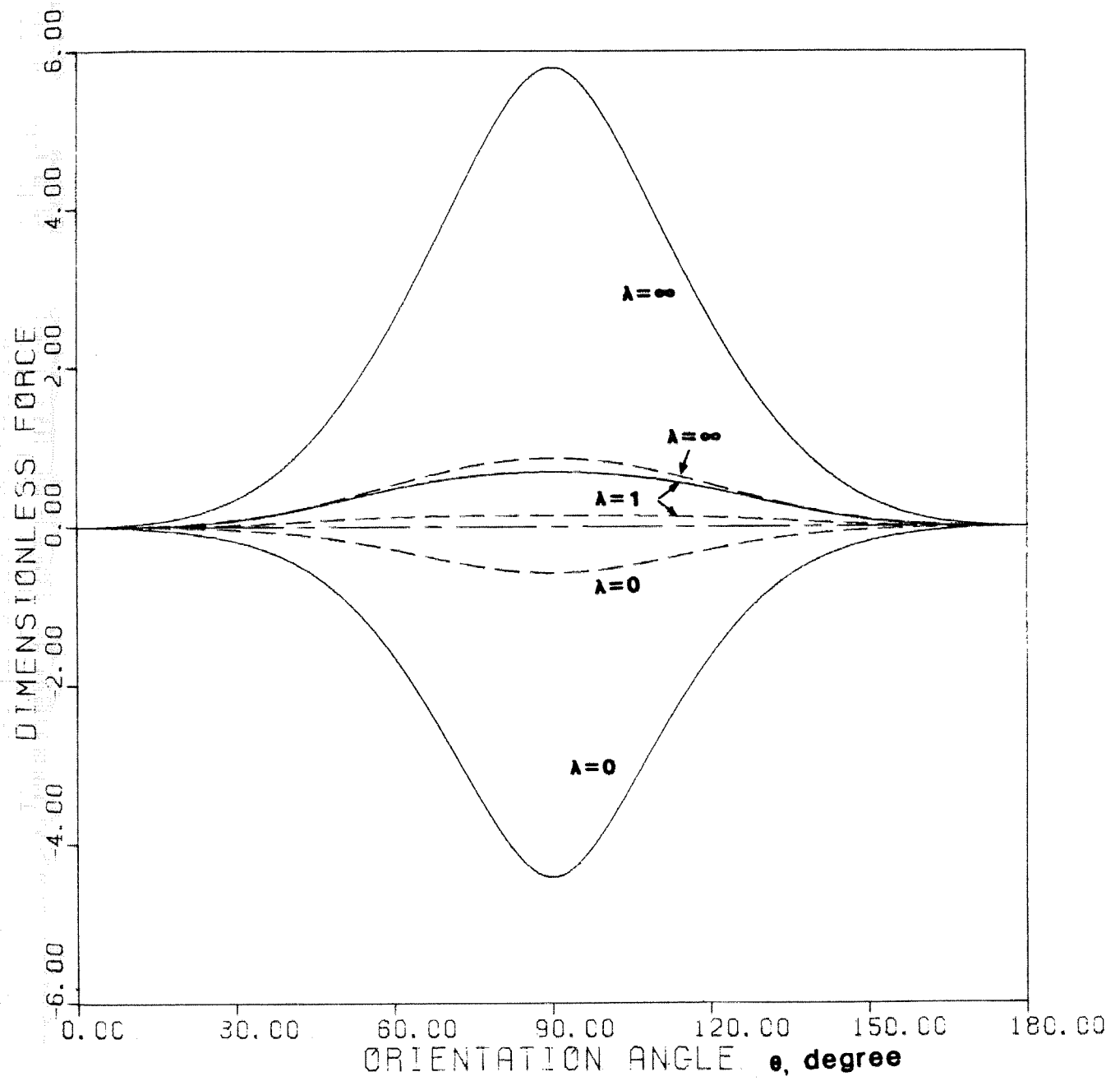


Figure 9

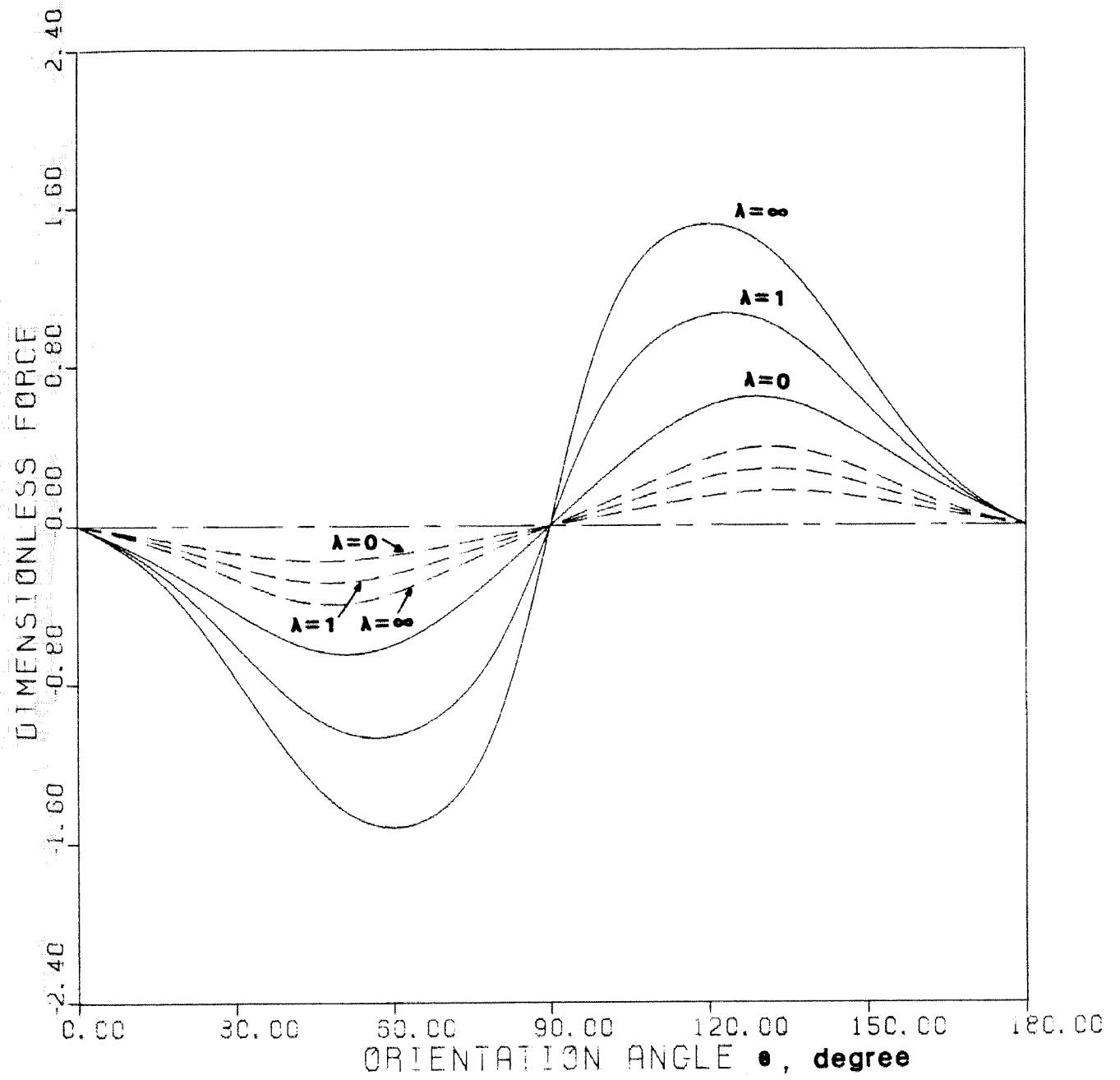


Figure 10

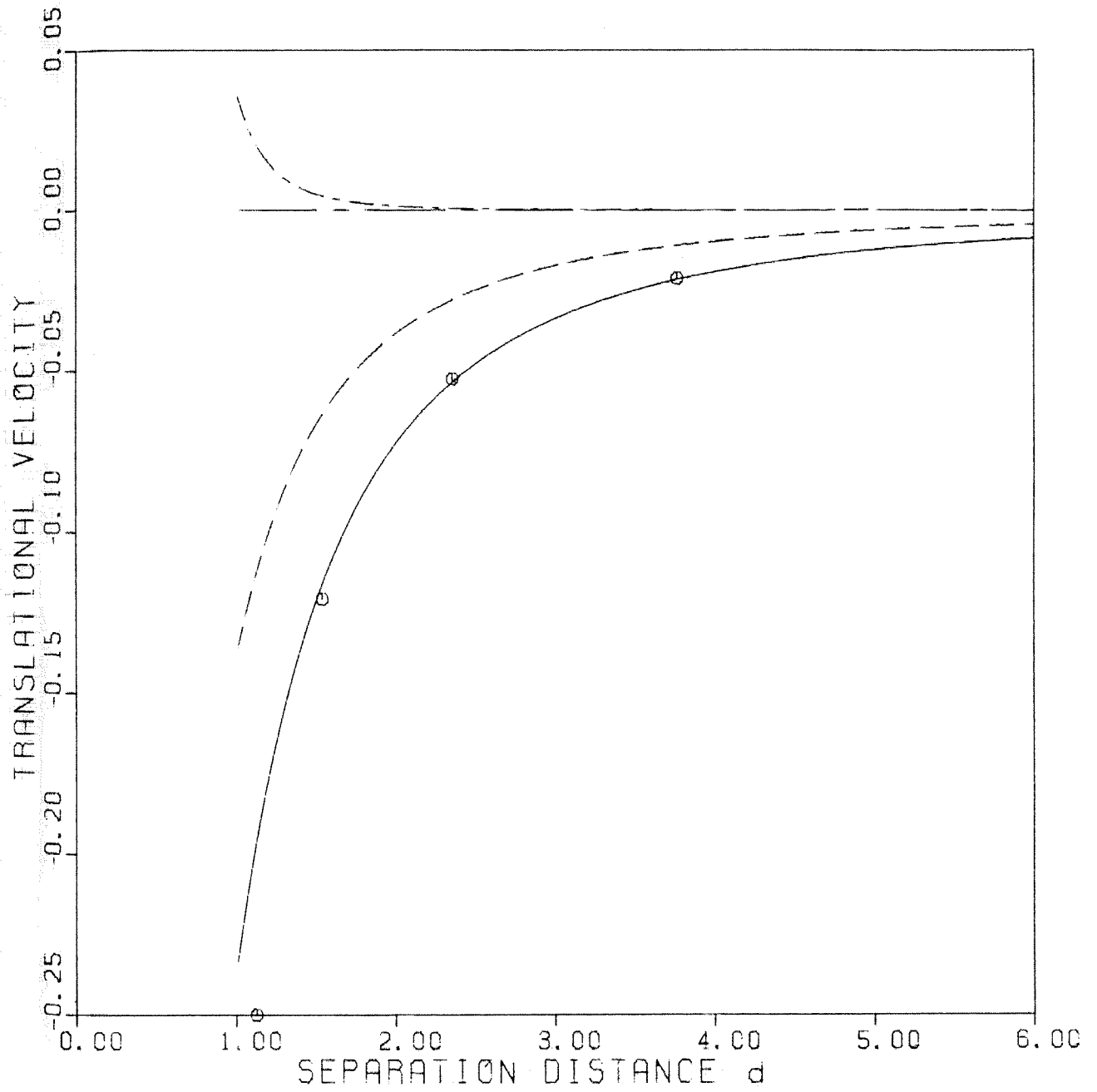


Figure 11

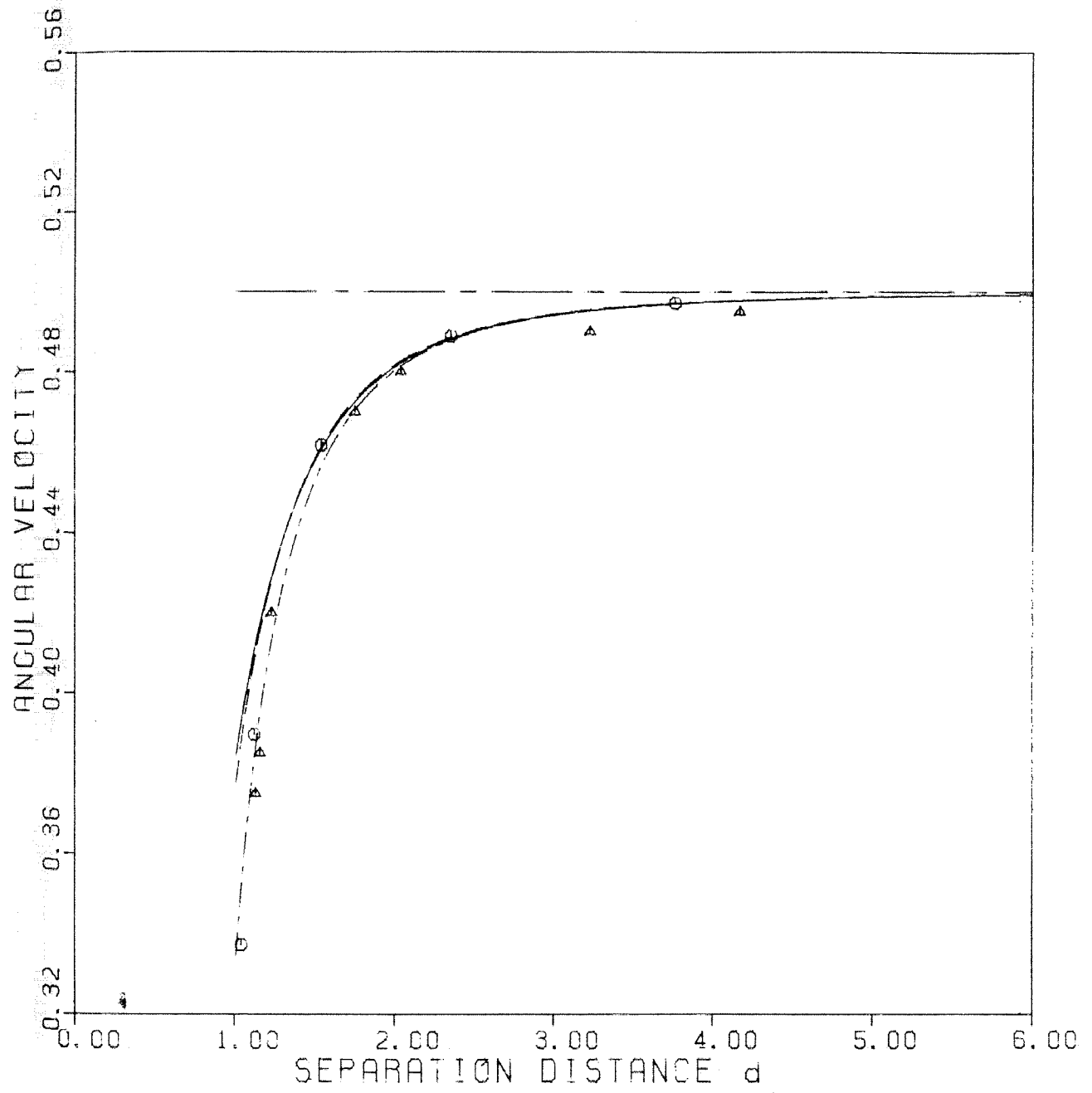


Figure 12

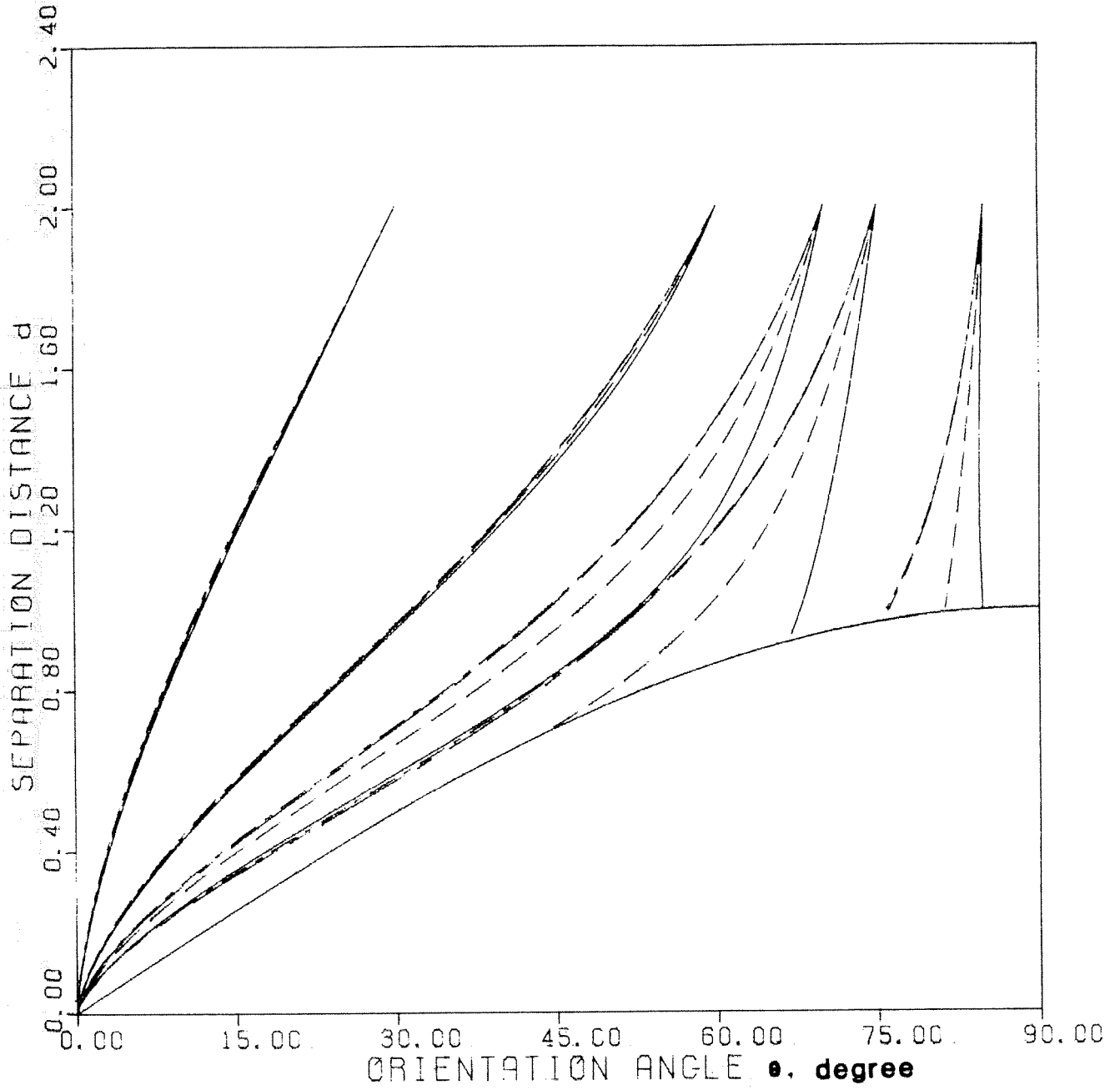


Figure 13

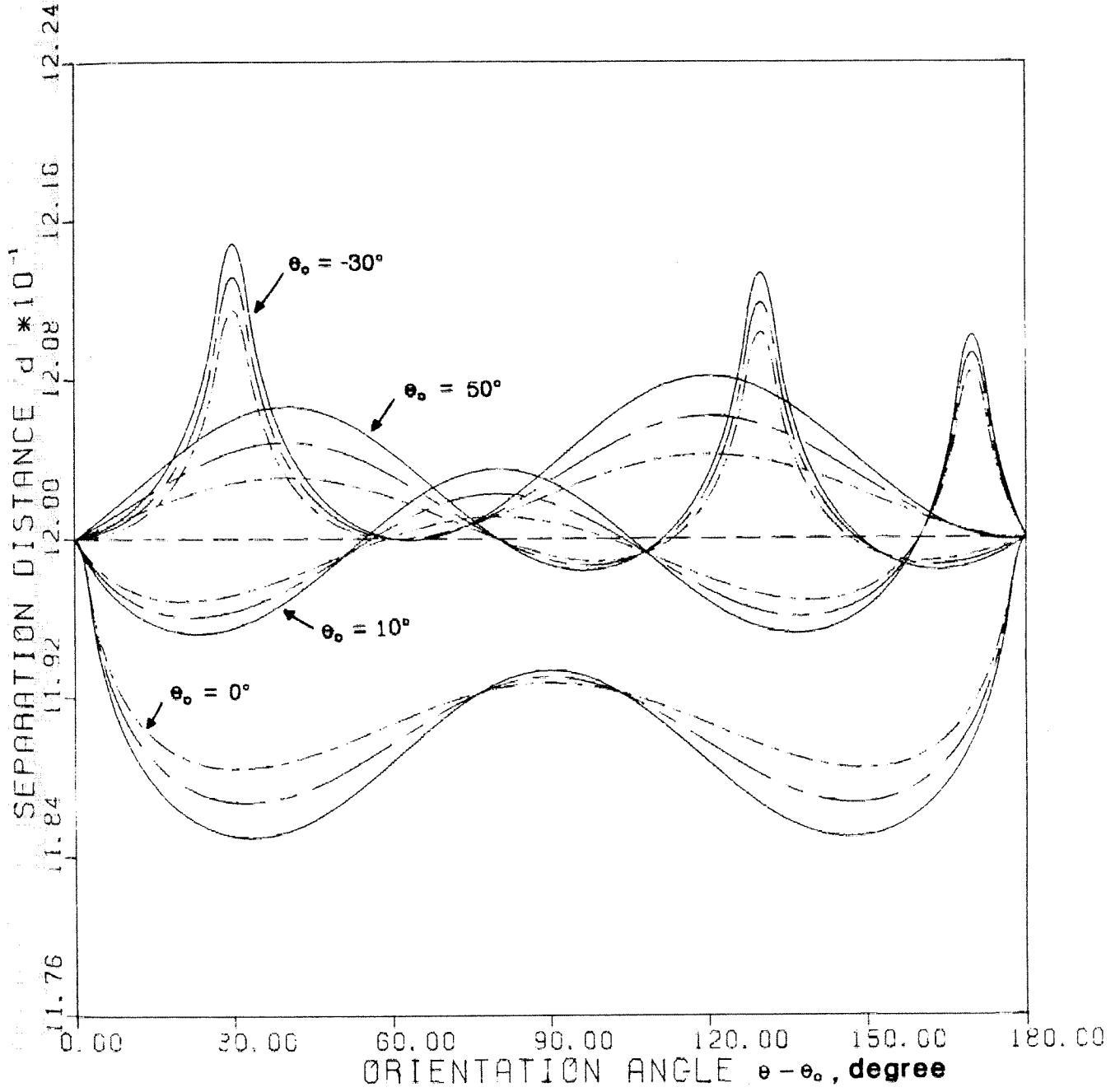


Figure 14

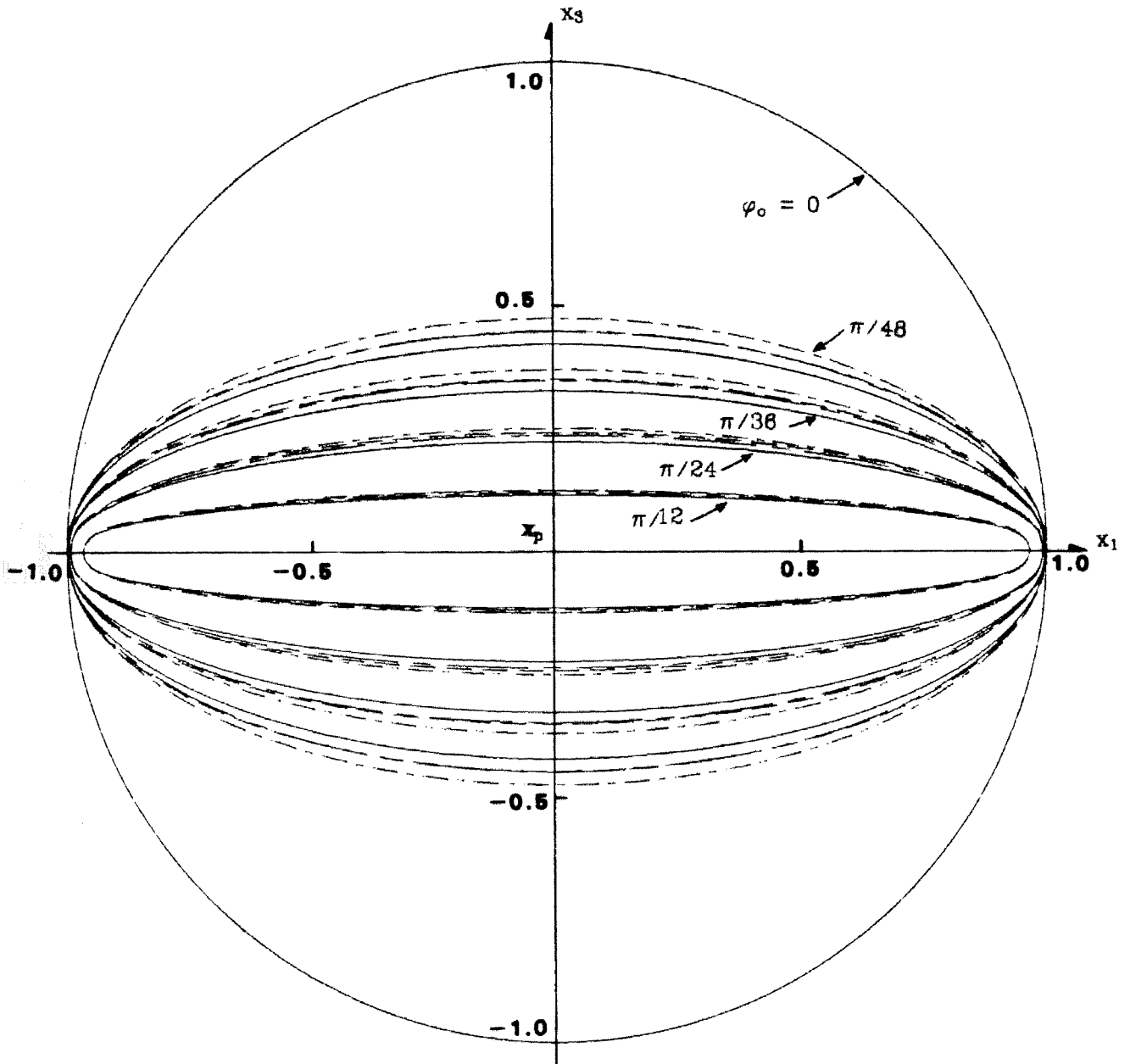


Figure 15

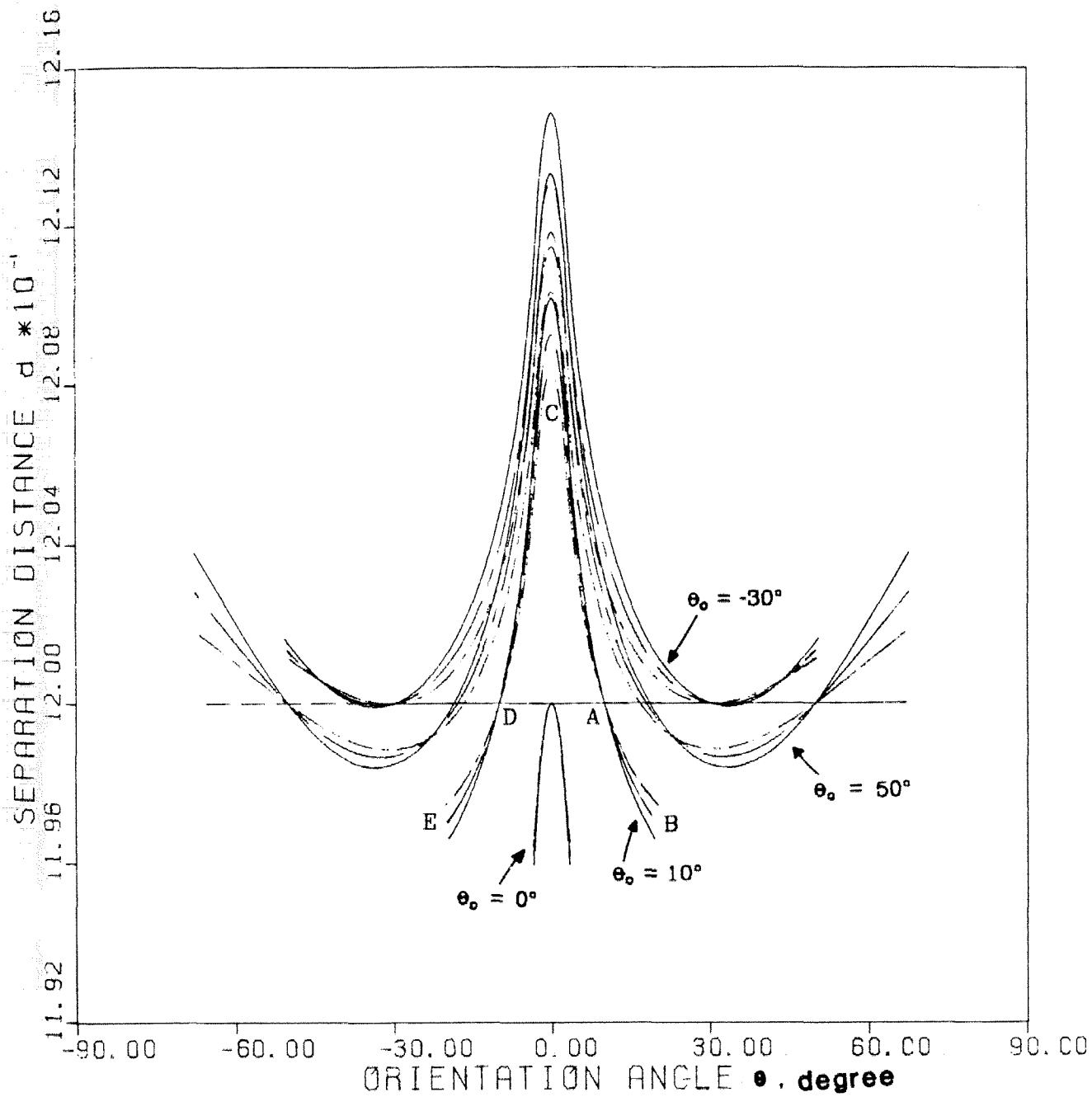


Figure 16

Chapter III.

**Motions of a Sphere in a Time-Dependent Stokes Flow —
A Generalization of Faxen's Law**

Abstract

A general solution of the unsteady Stokes' equation in spherical coordinates is derived for flows in both the exterior and interior of a sphere, and then applied to study the arbitrary unsteady motion of a rigid sphere in an unbounded single fluid domain which is undergoing a time-dependent mean flow. Calculation of the hydrodynamic force and torque on the sphere leads to a generalization of the Faxen's law to time-dependent flow fields which satisfy the unsteady Stokes' equation. For illustrative purposes, we consider the relative motion of gas bubbles which undergo very rapid oscillations so that the generalized Faxen's law derived for a solid sphere can be applied. We also demonstrate that our results reduce to those of Faxen for the steady flow limit.

I. Introduction

When a particle is immersed in a viscous fluid that is undergoing a time-dependent mean flow, the disturbance flow due to the presence of the particle has a number of characteristic properties. In this work we consider the motion of a spherical particle through a single unbounded fluid domain in the presence of an unsteady creeping motion at infinity. It is worthwhile to study the time-dependent motion of a sphere in a viscous fluid, not only because it is interesting in its own right, but also because the solution leads to a resolution of the initial value (or startup) problem for Stokes flow.

The motion of a single, small particle suspended in a Newtonian fluid which is undergoing a nonuniform undisturbed flow has been the subject of a large number of theoretical and experimental investigations. One main source of interest in this problem is its central role in theoretical determinations of the rheological properties of a dilute suspension. The majority of previous theoretical investigations were therefore restricted to *steady* creeping motion of particles in a linear flow, and solutions were obtained using eigenfunction expansions generated from the creeping flow equations by means of separation of variables in an appropriate coordinate system (cf. Brenner, 1963). Faxen (1921) considered the creeping motion of a sphere in an unbounded fluid subject to an *arbitrary* steady Stokes flow, in this case utilizing an eigenfunction expansion in spherical coordinates. The solution yields the so-called Faxen's law for the hydrodynamic force and torque on a rigid spherical particle in an arbitrary Stokes flow. The extension of the analyses to time-dependent flow has not yet received much attention in spite of its obvious importance. The earliest investigations were concerned with the motion of an oscillating sphere through a fluid *at rest* at infinity, due to Stokes (1851), Basset (1888) and Lamb (1932). Although this quiescent-fluid problem is of some intrinsic interest and provides

a resolution of the well-known *paradox* in the Langevin equation for motion of a Brownian particle (cf. Hauge and Martin-Löf, 1973), many problems of practical significance involve particle motions in a mean flow at infinity.

Recently, Mazur and Bedeaux (1974) and Hills (1975) independently obtained Faxen-like relations expressing the hydrodynamic force and torque exerted on a *rigid* sphere which is undergoing unsteady translation and rotation in a mean flow at infinity which may also be time-dependent. They adopted the singularity method, in which the sphere is replaced by a surface distribution of point forces, utilizing the fundamental "point force" solution of the Helmholtz equation.

In the present study, we derive a general solution of the time-dependent creeping flow equations for flow regions both interior and exterior to a sphere. The analysis is formally carried out as an eigenfunction expansion in terms of spherical harmonics, based on the creeping motion approximation but with the local inertia term retained in the equations to accommodate rapid accelerations. These general solutions can be, in principle, extended to the motions of spherical drops and bubbles, though this is not done here. The solution for a solid sphere that we do obtain yields a generalized Faxen's law which is identical to the results of Mazur and Bedeaux (1974) and Hills (1975), which were unfortunately not discovered until after the present work was completed.

The generalized Faxen-type law will be used in the analysis of Brownian motion of solid spherical particles in the next chapter of this thesis. In addition, in the present chapter we consider several additional applications, as well as demonstrating that the results reduce to those of Faxen for the steady flow limit. Current research in our group is presently completing the generalization to spherical drops in an unbounded fluid, and considering the related problem

of unsteady motion of a spherical particle or drop near a flat fluid interface.

II. Basic Equations and General Solutions

We begin by considering the governing differential equations and boundary conditions for time-dependent motion of a spherical body (fluid or solid) through an incompressible Newtonian fluid. The fluid is assumed to be undergoing a time-dependent undisturbed flow, which is defined by a velocity $\mathbf{U}^\infty(t, \mathbf{x})$ and pressure $p^\infty(t, \mathbf{x})$. The expression of Cauchy's first law appropriate to an incompressible Newtonian fluid with constant viscosity is the Navier-Stokes equation. By non-dimensionalizing, using appropriate characteristic length l_c , velocity u_c and time scales t_c , it can be seen that the solution of this equation, plus the continuity equation, will generally depend upon two basic dimensionless parameters. The first of these parameters is the Reynolds number defined by

$$Re = \frac{u_c l_c}{\nu}, \quad (1)$$

which we shall assume here to be sufficiently small that the creeping motion approximation is applicable. Here, $\nu (= \mu/\rho)$ is the kinematic viscosity of the fluid and l_c is a characteristic lengthscale of the particle (i.e., the sphere radius a). The second dimensionless parameter is the Strouhal number St , which is the ratio of the characteristic time scale t_c relative to the advection time scale, l_c/u_c ; i.e.,

$$St = \frac{t_c u_c}{l_c}. \quad (2)$$

When this parameter is sufficiently small, the local acceleration term in the equations of motion cannot be neglected, and this is the limit that we consider here. In this case, then, $Re \rightarrow 0$ but with $Re/St = O(1)$, and the governing equations reduce to the unsteady Stokes' equation plus the continuity equation for

the fluids both interior and exterior to the sphere.

For convenience, we consider the problem specified with respect to a disturbance flow field (\mathbf{u}, p) defined as the difference between actual flow (\mathbf{u}^*, p^*) in the presence of the sphere and the undisturbed flow; i.e.,

$$(\mathbf{u}, p) = (\mathbf{u}^*, p^*) - (\mathbf{U}^\infty, p^\infty) . \quad (3)$$

Here, the undisturbed velocity field $(\mathbf{U}^\infty, p^\infty)$ satisfies the unsteady Stokes' equation plus the continuity equation. In this formalism, the disturbance flow is at rest at infinity. The equation of motion for the disturbance velocity fields interior ($j=1$) and exterior ($j=2$) to the sphere is

$$\rho_j \frac{\partial \mathbf{u}_j}{\partial t} = -\nabla p_j + \mu_j \nabla^2 \mathbf{u}_j \quad (4)$$

and

$$\nabla \cdot \mathbf{u}_j = 0 . \quad (5)$$

The boundary conditions for (\mathbf{u}_j, p_j) in this disturbance-flow formulation are as follows:

$$(\mathbf{u}_2, p_2) \rightarrow \mathbf{0} \quad \text{as} \quad |\mathbf{x}| \rightarrow \infty , \quad (6)$$

$$(\mathbf{u}_1, p_1) \quad \text{bounded at the sphere center} \quad (7)$$

and at the interface of the sphere surface, $\mathbf{x} \equiv \mathbf{x}_B$,

$$\mathbf{t} \cdot \mathbf{u}_1 = \mathbf{t} \cdot \mathbf{u}_2 , \quad \mathbf{n} \cdot \mathbf{u}_1 = \mathbf{n} \cdot \mathbf{u}_2 = \frac{\partial a}{\partial t} \quad (8)$$

$$[|\mathbf{t} \cdot \mathbf{n} \cdot \boldsymbol{\sigma}|] = 0 \quad (9)$$

$$[|\mathbf{n} \cdot \mathbf{n} \cdot \boldsymbol{\sigma}|] = \frac{2\gamma}{a} . \quad (10)$$

The parameters appearing in (9) and (10) are the unit vectors, \mathbf{n} and \mathbf{t} , that are normal (outward) and tangential to the sphere surface, the stress tensor $\boldsymbol{\sigma}$ and

the interfacial tension γ between the two fluids. Equations (8) and (9) are the kinematic and continuity conditions for velocity and tangential stress, while the normal stress jump condition is represented by (10).

We now derive a *general* solution of the unsteady Stokes' equation (4) plus the continuity equation (5) in terms of the fundamental eigensolutions for a spherical coordinate system (r, θ, φ) . It is convenient, for this purpose, to represent the disturbance flow field $\{\mathbf{u}(t, \mathbf{x}), p(t, \mathbf{x})\}$ as a Fourier integral:

$$(\mathbf{u}, p) = \int (\hat{\mathbf{u}}, \hat{p}) e^{-i\omega t} d\omega . \quad (11)$$

Upon taking the divergence of the vector equation (4), expressed in terms of Fourier components $(\hat{\mathbf{u}}, \hat{p})$, and utilizing (5), it can be seen that the pressure field is harmonic, thus satisfying Laplace's equation; i.e.,

$$\nabla^2 \hat{p} = 0 . \quad (12)$$

The pressure can therefore be expressed as an infinite series in the general form:

$$\hat{p} = \sum_{n=-\infty}^{\infty} p_n(r, \theta, \varphi) \quad (13)$$

in which p_n is a solid (or volume) spherical harmonic of order n . Let us now consider a *general* solution for the velocity field $\hat{\mathbf{u}}$ with \hat{p} given by (13). The governing equation (4) in terms of Fourier components is given by

$$(\nabla^2 + h^2) \hat{\mathbf{u}} = \frac{1}{\mu} \nabla \hat{p} \quad (14)$$

where h is defined as

$$h = \left[\frac{i\omega}{\nu} \right]^{1/2} , \quad i = \sqrt{-1} . \quad (15)$$

Here h can be determined uniquely by taking a branch-cut along the positive real axis in the complex plane. We consider, for convenience, the velocity field $\hat{\mathbf{u}}$

as the sum of a homogeneous solution, $\hat{\mathbf{u}}_h$, satisfying the Helmholtz equation

$$(\nabla^2 + h^2)\hat{\mathbf{u}}_h = \mathbf{0} \tag{16}$$

and a particular solution, satisfying the Laplace's equation. The particular solution can be obtained by inspection,

$$\hat{\mathbf{u}}_p = \frac{1}{\mu h^2} \nabla \hat{p} = \frac{1}{\mu h^2} \sum_{n=-\infty}^{\infty} \nabla p_n. \tag{17}$$

The homogeneous solution $\hat{\mathbf{u}}_h$ can be represented as an expansion in terms of products of solid spherical harmonics χ_n , φ_n and Hankel functions of the second kind, $H_{n+\frac{1}{2}}^{(2)}$ of order $n + \frac{1}{2}$. Hence, a general solution of the unsteady Stokes' equation plus the continuity equation for a general velocity field, expressed in terms appropriate to a spherical coordinate system, is

$$\begin{aligned} \hat{\mathbf{u}} = \sum_{n=-\infty}^{\infty} \left[\frac{1}{h^2 \mu} \nabla p_n - f_n(hr) \nabla \times (\mathbf{r} \chi_n) \right. \\ \left. + \{(n+1)f_{n-1}(hr) - n f_{n+1}(hr) h^2 r^2\} \nabla \varphi_n + n(2n+1) f_{n+1}(hr) h^2 \varphi_n \mathbf{r} \right] \end{aligned} \tag{18}$$

in which

$$f_n(\zeta) = i \cdot \sqrt{\pi/2} \zeta^{-(n+\frac{1}{2})} H_{n+\frac{1}{2}}^{(2)}(\zeta) \tag{19}$$

and \mathbf{r} is the position vector. It should be emphasized that Eq. (18) is just the *general* solution form for the unsteady Stokes' equations, and does not yet satisfy any of the boundary conditions, (6)-(10), of the problem. We now specialize the general solution, (18), to determine the solution forms interior and exterior to a spherical body.

A. Flow Exterior to a Sphere

In the derivation of the general solution, (18), we defined the disturbance velocity field as in (3), thus reducing the problem to a vanishing velocity at

infinity. For the situation in which the velocity is required to vanish at infinity [i.e., boundary condition (6)], we must have

$$p_n = 0 \quad \text{for} \quad n \geq -1 \tag{20}$$

$$\varphi_n, \chi_n = 0 \quad \text{for} \quad n \leq 0 \tag{21}$$

and thus we are restricted to the harmonic functions φ_n, χ_n of positive order and p_n of order less than -1. We recall that variables exterior to the spherical body have been identified by the subscript "2", i.e., $(\hat{\mathbf{u}}_2, \hat{\mathbf{p}}_2)$. Taking into account conditions (20) and (21), we see that

$$\begin{aligned} \hat{\mathbf{u}}_2 = \sum_{n=1}^{\infty} \left[\frac{1}{\mu_2 h_2^2} \nabla p_{-(n+1)}^0 - f_n(h_2 r) \nabla \times (\mathbf{r} \chi_n^0) \right. \\ \left. + \{(n+1)f_{n-1}(h_2 r) - n f_{n+1}(h_2 r) h_2^2 r^2\} \nabla \varphi_n^0 + n(2n+1) f_{n+1}(h_2 r) h_2^2 \varphi_n^0 \mathbf{r} \right] \end{aligned} \tag{22}$$

and

$$\hat{\mathbf{p}}_2 = \sum_{n=1}^{\infty} p_{-(n+1)}^0 \tag{23}$$

The superscript "0" associated with the harmonic functions φ_n^0, χ_n^0 and $p_{-(n+1)}^0$ is inserted to stress that the solution (22) and (23) represents the flow exterior to the sphere, and $h_2 = (i\omega/\nu_2)^{1/2}$.

B. Flow Interior to a Spherical Body

When the fluid occupies the interior of a sphere, the condition of boundedness of the velocity at the sphere center limits us to positive harmonics in the general solution form (18); thus we must put

$$p_n = \varphi_n = \chi_n = 0 \quad \text{for} \quad n \leq 0 \tag{24}$$

and replace the function $f_n(\xi) = i \cdot \sqrt{\pi/2} \xi^{-(n+1/2)} H_{n+1/2}^{(2)}(\xi)$ by

$$\psi_n(\zeta) = \sqrt{\pi/2} \zeta^{-(n+\frac{1}{2})} J_{n+\frac{1}{2}}(\zeta) \quad (25)$$

where $J_{n+\frac{1}{2}}(\zeta)$ is the Bessel function of the first kind. The resulting flow field

$(\hat{\mathbf{u}}_1, \hat{\mathbf{p}}_1)$ is given by

$$\hat{\mathbf{u}}_1 = \sum_{n=1}^{\infty} \left[\frac{1}{h_1^2 \mu_1} \nabla p_n^i - \psi_n(h_1 r) \nabla \times (\mathbf{r} \chi_n^i) \right. \\ \left. + \{(n+1)\psi_{n-1}(h_1 r) - n\psi_{n+1}(h_1 r) h_1^2 r^2\} \nabla \varphi_n^i + n(2n+1)\psi_{n+1}(h_1 r) h_1^2 \varphi_n^i \mathbf{r} \right] \quad (26)$$

and

$$\hat{\mathbf{p}}_1 = \sum_{n=1}^{\infty} p_n^i \quad (27)$$

in which the harmonic functions p_n^i , χ_n^i and φ_n^i with superscript "i" denoting the corresponding functions for the interior flow field and $h_1 = (i\omega/\nu_1)^{1/2}$.

C. General Expression for Hydrodynamic Force and Torque

So far we have derived a general solution for the flow fields both exterior and interior to the sphere by satisfying the governing differential equations (4) and (5) plus the boundary condition (6) at infinity and the condition (7) of boundedness of the velocity and pressure at the sphere center. All that remains is to determine the unknown solid spherical harmonics p_n , χ_n and φ_n in each flow from the boundary conditions (8)-(10) at the interface of the sphere surface. However, if we wish only to calculate the hydrodynamic force and torque on a sphere (fluid or rigid), and not the velocity field itself, it is possible to do so by evaluating only a small number of spherical harmonics p_n , χ_n and φ_n as a consequence of the integral theorem for the spherical harmonics (see Happel and Brenner, 1983). To show this, we now derive a general expression for the Fourier component of the hydrodynamic force $\hat{\mathbf{F}}$ and torque $\hat{\mathbf{T}}$ on an arbitrary body by integrating over a circumscribed sphere in the fluid.

The Fourier components of the hydrodynamic force and torque exerted on the sphere can be obtained from the general solution for the *disturbance* flow field either interior or exterior to the sphere, using the basic definitions

$$\hat{\mathbf{F}} = \int \mathbf{n} \cdot \hat{\boldsymbol{\sigma}} ds \quad (28)$$

$$\hat{\mathbf{T}} = \int \mathbf{r}_0 \times (\mathbf{n} \cdot \hat{\boldsymbol{\sigma}}) ds \quad (29)$$

Here, $\hat{\boldsymbol{\sigma}}$ is the Fourier transform of the stress tensor associated with the *disturbance-flow* problem, and \mathbf{r}_0 is the position vector of a surface element ds ($=r^2 \sin\theta d\theta d\phi$) relative to the sphere center. Then, the Fourier component of the *total* hydrodynamic force $\hat{\mathbf{F}}^*$ and torque $\hat{\mathbf{T}}^*$ for the *actual* flow field (\mathbf{u}^*, p^*) can also be determined from the actual stress tensor $\boldsymbol{\sigma}^* = \boldsymbol{\sigma} + \boldsymbol{\sigma}^\infty$

$$\hat{\mathbf{F}}^* = \int \mathbf{n} \cdot (\hat{\boldsymbol{\sigma}} + \hat{\boldsymbol{\sigma}}^\infty) ds = \hat{\mathbf{F}} + \int \mathbf{n} \cdot \hat{\boldsymbol{\sigma}}^\infty ds \quad (30)$$

$$\hat{\mathbf{T}}^* = \int \mathbf{r}_0 \times \{\mathbf{n} \cdot (\hat{\boldsymbol{\sigma}} + \hat{\boldsymbol{\sigma}}^\infty)\} ds = \hat{\mathbf{T}} + \int \mathbf{r}_0 \times (\mathbf{n} \cdot \hat{\boldsymbol{\sigma}}^\infty) ds \quad (31)$$

in which the stress tensor $\hat{\boldsymbol{\sigma}}^\infty$ is associated with the undisturbed flow field ($\hat{\mathbf{U}}^\infty, \hat{p}^\infty$) and defined by

$$\hat{\boldsymbol{\sigma}}^\infty = -\hat{p}^\infty \mathbf{I} + \mu [\nabla \hat{\mathbf{U}}^\infty + (\nabla \hat{\mathbf{U}}^\infty)^T] \quad (32)$$

Here \mathbf{I} is the idemfactor and $(\nabla \hat{\mathbf{U}}^\infty)^T$ is the transpose of the velocity gradient tensor. Utilizing the unsteady Stokes' equation which is satisfied by the undisturbed flow ($\hat{\mathbf{U}}^\infty, \hat{p}^\infty$) and applying the divergence theorem to the surface integration of (30), we can easily show that

$$\int \mathbf{n} \cdot \hat{\boldsymbol{\sigma}}^\infty ds = -i\omega\rho \int \hat{\mathbf{U}}^\infty dv \quad (33)$$

Thus the Fourier component of the total hydrodynamic force is

$$\hat{\mathbf{F}}^* = \hat{\mathbf{F}} - i\omega\rho \int \hat{\mathbf{U}}^\infty dv \quad (34)$$

where $dv (=r^2 \sin\theta dr d\theta d\phi)$ is the volume element of the sphere. Here the addi-

tional term, $-i\omega\rho\int\hat{U}^\infty dv$ can be interpreted as an apparent (or 'fictitious') body-force that compensates for the acceleration of the external flow. Similarly, the total hydrodynamic torque relative to the sphere center is

$$\hat{\mathbf{T}} = \hat{\mathbf{T}} - i\omega\rho\int(\mathbf{r}_0 \times \hat{U}^\infty)dv. \quad (35)$$

We now evaluate the Fourier component of the stress vector $\hat{\sigma}_N (= \mathbf{n} \cdot \hat{\sigma})$ acting on the surface of a sphere associated with the *disturbance* flow in order to determine the total hydrodynamic force and torque on the sphere. The stress vector $\hat{\sigma}_N$ on the sphere surface of radius a , in general, can be expressed as

$$\hat{\sigma}_N = -\frac{\mathbf{r}}{r}\hat{p} + \mu\left[\frac{\partial\hat{\mathbf{u}}}{\partial r} - \frac{\hat{\mathbf{u}}}{r}\right] + \frac{\mu}{r}\nabla(\mathbf{r}\cdot\hat{\mathbf{u}}) \quad (36)$$

for an incompressible Newtonian fluid (cf. Happel and Brenner, 1983). By means of the general solution (13) and (18), Eq. (36) can ultimately be expressed in the form

$$\begin{aligned} \hat{\sigma}_N = \frac{1}{r} \sum_{n=-\infty}^{\infty} \left[-Q_n(hr)\nabla \times (\mathbf{r}\chi_n) + \frac{2}{h^2}(n-1)\nabla p_n - p_n\mathbf{r} \right. \\ \left. + R_n(hr)\nabla\varphi_n - \frac{(2n+1)}{r^2}S_n(hr)\varphi_n\mathbf{r} \right] \quad (37) \end{aligned}$$

where

$$Q_n(\zeta) = \mu\{\zeta f_n'(\zeta) + (n-1)f_n(\zeta)\}$$

$$R_n(\zeta) = \mu(n+1)\{\zeta f_{(n-1)}'(\zeta) + 2(n-1)f_{n-1}(\zeta)\} - \mu n\zeta^2\{\zeta f_{(n+1)}'(\zeta) - f_{n+1}(\zeta)\}$$

and

$$S_n(\zeta) = -\mu n\zeta^2\{\zeta f_{(n+1)}'(\zeta) - f_{n+1}(\zeta)\}.$$

The Fourier components of the hydrodynamic force and torque exerted on the sphere can be obtained from (28), (29) and (37) by integrating the stress over the sphere surface. This general expression can be evaluated by resorting

to the surface integral theorem for spherical harmonics outlined by Brenner (1963). The result is

$$\hat{\mathbf{F}} = -\frac{4\pi}{3} [r^3 \nabla p_1 + \nabla (r^3 p_{-2})]_{r=a} + 4\pi a \{R_1(ha) - S_1(ha)\} [\nabla \varphi_1]_{r=a} + \frac{4\pi}{a^2} S_{-2}(ha) [\nabla (r^3 \varphi_{-2})]_{r=a} \quad (38)$$

$$\hat{\mathbf{T}} = -\frac{8\pi}{3} \left\{ a^3 Q_1(ha) [\nabla \chi_1]_{r=a} - Q_{-2}(ha) [\nabla (r^3 \chi_{-2})]_{r=a} \right\}. \quad (39)$$

It should be noted that the general expressions, (38) and (39), have been derived for an arbitrary motion satisfying the unsteady Stokes' equation plus the continuity equation without application of any boundary condition.

Now, however, we determine the general form for the *total* hydrodynamic force and torque on the sphere from (34) and (35), evaluating the hydrodynamic force and torque associated with the disturbance flow *exterior* to the sphere by applying the conditions (20) and (21), corresponding to a vanishing velocity at infinity, to the general expressions (38) and (39). The result is

$$\hat{\mathbf{F}}^* = -\frac{4\pi}{3} [\nabla (r^3 p_{-2}^0)]_{r=a} + 4\pi a \{R_1(h_2 a) - S_1(h_2 a)\} [\nabla \varphi_1^0]_{r=a} - i\omega \rho_2 \int \hat{\mathbf{U}}^* dv \quad (40)$$

$$\hat{\mathbf{T}}^* = -\frac{8\pi}{3} a^3 Q_1(h_2 a) [\nabla \chi_1^0]_{r=a} - i\omega \rho_2 \int \mathbf{r}_0 \times \hat{\mathbf{U}}^* dv. \quad (41)$$

Thus, in order to evaluate the total hydrodynamic force and torque, it is sufficient to determine the unknown spherical harmonics p_{-2}^0 , φ_1^0 and χ_1^0 by applying the boundary conditions, (8)-(10), at the sphere surface using the solution, (26) and (27), for the flow field *interior* to the sphere.

Similarly, starting with the general expressions, (38) and (39), we can also readily derive a general expression for the total force and torque in terms of the disturbance flow *interior* to the sphere

$$\hat{\mathbf{F}} = -\frac{4\pi}{3} a^3 [\nabla p_1^i]_{r=a} + 4\pi a \{R_1(h_1 a) - S_1(h_1 a)\} [\nabla \varphi_1^i]_{r=a} - i\omega\rho_2 \int \hat{\mathbf{U}}^\infty dv \quad (42)$$

$$\hat{\mathbf{T}} = -\frac{8\pi}{3} a^3 Q_1(h_1 a) [\nabla \chi_1^i]_{r=a} - i\omega\rho_2 \int \mathbf{r}_0 \times \hat{\mathbf{U}}^\infty dv. \quad (43)$$

Here, the functions $R_1(\zeta)$, $S_1(\zeta)$ and $Q_1(\zeta)$ are defined in terms of function $\psi_n(\zeta)$, (25), instead of $f_n(\zeta)$ using the previous definitions following Eq. (37).

This completes our derivation of the general solution forms for the flow fields both exterior and interior to a sphere. If we are interested in evaluating the hydrodynamic force and torque on the sphere, it is possible to do so by determining the spherical harmonics, *either* p_{-2}^0 , φ_1^0 and χ_1^0 for the exterior flow *or* p_1^i , φ_1^i and χ_1^i for the interior flow, by applying the boundary conditions, (8)-(10), at the sphere surface to the general solution forms, (22), (23), (26) and (27). In the next section, for illustrative purposes, we shall consider motion of a *solid* sphere in an arbitrary unsteady creeping flow. In this case of a solid sphere, the boundary conditions, (8)-(10), at the sphere surface together with the boundedness condition (7) of the velocity at the sphere center can be simply replaced by the "no-slip" condition; i.e.,

$$\mathbf{u} = \mathbf{U} + \boldsymbol{\Omega} \times \mathbf{r}_0 - \mathbf{U}^\infty \quad \text{at the body surface} \quad (44)$$

which enables us to determine the unknown spherical harmonics, p_{-2}^0 , φ_1^0 , and χ_1^0 . Here, \mathbf{U} and $\boldsymbol{\Omega}$ are the time-dependent translational and angular velocities of the rigid sphere, respectively.

III. Flow Exterior to a Rigid Sphere

Let us now consider the specific problem of a *rigid* sphere which moves with translational velocity $\mathbf{U}(t)$ and angular velocity $\boldsymbol{\Omega}(t)$ in an undisturbed flow field $\{\mathbf{U}^\infty(t, \mathbf{x}), p^\infty(t, \mathbf{x})\}$ which itself satisfies the unsteady Stokes' equation and the continuity equation. As we shall see shortly, this problem may be solved

directly, for an arbitrary time-dependent translation and rotation, using the general solution obtained in Section II. All that is required is a specification of the unknown functions of $p_{(n+1)}^0$, φ_n^0 , and χ_n^0 from the boundary conditions at the sphere surface, i.e., the no-slip condition, (44), with $\hat{\mathbf{u}}(\omega, \mathbf{x}_B) = \hat{\mathbf{U}}(\omega) + \hat{\mathbf{\Omega}}(\omega) \times \mathbf{r}_0$. In the present section, we shall use the general method of Brenner (1963) for obtaining these solid spherical harmonic functions when the velocity field is prescribed on a spherical surface.

Utilizing Euler's theorem for the homogeneous polynomial of any solid spherical harmonics ξ_n of order n (i.e. $r \frac{\partial \xi_n}{\partial r} = n \xi_n$), we now represent the radial component of velocity $\hat{\mathbf{u}}_r^0 (= \hat{\mathbf{u}}^0 \cdot \mathbf{n})$ from (22).

$$\hat{\mathbf{u}}_r^0 = \sum_{n=1}^{\infty} \left[\frac{(n+1)}{r h^2 \mu} p_{(n+1)}^0 + n \left\{ \frac{(n+1)}{r} f_{n-1}(hr) + (n+1) f_{n+1}(hr) h^2 r \right\} \varphi_n^0 \right] \quad (45)$$

Differentiation of (43) with respect to r and again applying Euler's theorem yields

$$r \frac{\partial \hat{\mathbf{u}}_r^0}{\partial r} = \sum_{n=1}^{\infty} \left[\frac{(n+1)(n+2)}{r h^2 \mu} p_{(n+1)}^0 + n \left\{ \frac{(n^2-1)}{r} f_{n-1}(hr) + (n+1)^2 h^2 r f_{n+1}(hr) + (n+1) h f_{n-1}'(hr) + (n+1) h^3 r^2 f_{n+1}'(hr) \right\} \varphi_n^0 \right] \quad (46)$$

Similarly, we have another relationship from (22)

$$\mathbf{r} \cdot \nabla \times \hat{\mathbf{u}}^0 = - \sum_{n=1}^{\infty} n(n+1) f_n(hr) \chi_n^0 \quad (47)$$

Thus, at the surface of a sphere ($r=a$) we can obtain the quantities of $\hat{\mathbf{u}}_r^0(r=a)$, $\left[r \frac{\partial \hat{\mathbf{u}}_r^0}{\partial r} \right]_{r=a}$ and $[\mathbf{r} \cdot \nabla \times \hat{\mathbf{u}}^0]_{r=a}$ from (45)-(47), which are necessarily equal to those given by the boundary condition (44). Let us now suppose that the boundary condition (44) has been expressed as a uniformly convergent series expanded in

terms of *surface* spherical harmonics X_n , Y_n and Z_n . Then

$$\hat{u}_r^0(r=a) = \mathbf{n} \cdot \{\hat{\mathbf{U}} - [\hat{\mathbf{U}}^\infty]_{r=a}\} = \sum_{n=1}^{\infty} X_n \quad (48)$$

$$\left[r \frac{\partial \hat{u}_r^0}{\partial r} \right]_{r=a} = a \nabla \cdot [\hat{\mathbf{U}}^\infty]_{r=a} = \sum_{n=1}^{\infty} Y_n \quad (49)$$

and

$$[\mathbf{r} \nabla \times \hat{\mathbf{u}}^0]_{r=a} = \{\mathbf{r}_0 \cdot [2\hat{\Omega} - \nabla \times [\hat{\mathbf{U}}^\infty]_{r=a}]\} = \sum_{n=1}^{\infty} Z_n \quad (50)$$

Since the functions X_n , Y_n and Z_n are known in principle from the prescribed velocity field at the sphere surface, any boundary value problem may therefore be considered to be solved in principle, with the unknown functions $p_{-(n+1)}^0$, φ_n^0 , and χ_n^0 determined from (45)-(47) combined with (48)-(50). If we wish only to calculate the hydrodynamic force and torque on a rigid spherical particle, but not the velocity field itself, it should be possible in view of (40) and (41) to do so by determining only p_{-2}^0 , φ_1^0 , and χ_1^0 . Indeed, it can be shown, by solving the tedious algebraic Eqs. (45)-(50) for $n=1$, that

$$[\varphi_1^0]_{r=a} = \frac{ha^2[3X_1 + Y_1]}{6} e^{iha} \quad (51)$$

$$[p_{-2}^0]_{r=a} = \frac{\mu[(3 + 3iha - h^2a^2)X_1 + (1 + iha)Y_1]}{2a} \quad (52)$$

and

$$[\chi_1^0]_{r=a} = - \frac{h^3a^3e^{iha}Z_1}{2(1 + iha)} \quad (53)$$

in which we have used the special property of the function $f_n(\zeta)$:

$$\zeta f_{n+1}(\zeta) = -f_n'(\zeta) \quad \text{with} \quad f_0(\zeta) = \frac{e^{-iha}}{\zeta}$$

Finally, recalling the relationship between an arbitrary solid spherical harmonic

ξ_n and the corresponding surface spherical harmonic $[\xi_n]_{r=a}$, i.e. $\xi_n = (\frac{r}{a})^n [\xi_n]_{r=a}$, we can obtain the unknown functions p_0^0 , φ_1^0 , and χ_1^0 and thus derive the general formulae for the hydrodynamic force and torque as follows:

$$\hat{\mathbf{F}}^* = -6\pi\mu a(1 + ahi)[\nabla(rX_1)]_{r=a} + \frac{2\pi\mu}{3} a^3 h^2 [\nabla(rX_1)]_{r=a} - 2\pi\mu a(1 + ahi)[\nabla(rY_1)]_{r=a} - i\omega\rho \int \hat{\mathbf{U}}^* dv \quad (54)$$

$$\hat{\mathbf{T}}^* = -\frac{4\pi\mu a^3}{3} \left[\frac{3 + 3ahi - a^2 h^2}{1 + ahi} \right] [\nabla(rZ_1)]_{r=a} - i\omega\rho \int \mathbf{r}_0 \times \hat{\mathbf{U}}^* dv. \quad (55)$$

All that remains is to determine the unknown surface harmonics X_1 , Y_1 and Z_1 from the boundary condition (48)-(50) utilizing the orthogonality properties of the spherical harmonics. For example,

$$X_1 = \sum_{m=-1}^1 f_{m,1} \xi_1^m(\theta, \varphi) \quad (56)$$

where ξ_1^m is the normalized surface harmonic of order 1 and degree m ; i.e., $\xi_1^0 = \cos\theta$, $\xi_1^1 = \sin\theta(\cos\varphi + i\sin\varphi)$ and $\xi_1^{-1} = \sin\theta(\cos\varphi - i\sin\varphi)$, and $f_{m,1}$ is the corresponding coefficient defined by

$$f_{m,1} = \frac{1}{N_{m,1}} \int_0^{2\pi} \int_0^\pi \mathbf{n} \cdot \{\hat{\mathbf{U}} - [\hat{\mathbf{U}}^*]_{r=a}\} \xi_1^m \sin\theta d\theta d\varphi \quad (57)$$

with the normalizing factor $N_{m,n} = \frac{4\pi}{2n+1} \cdot \frac{(n+|m|)!}{(n-|m|)!}$. Similarly, the surface harmonics Y_1 and Z_1 can also be determined, and the resulting general solution for the total force and torque including the fictitious body force and couple terms is given by

$$\hat{\mathbf{F}}^* = 6\pi\mu a \left\{ 1 + ahi - \frac{a^2 h^2}{9} \right\} \cdot \{[\hat{\mathbf{U}}^*]_0 - \hat{\mathbf{U}}\} + \pi\mu a^3 \left\{ 6(1 + ahi) \frac{(ah - \sin ah)}{a^3 h^3} + 2 \left[\frac{\sin ah - ah \cdot \cos ah}{h^3 a^3} - \frac{1}{3} \right] \right\} [\nabla^2 \hat{\mathbf{U}}^*]_0 - i\omega\rho \int \hat{\mathbf{U}}^* dv$$

(58)

$$\hat{\mathbf{T}}^* = \frac{4\pi\mu a^3}{3} \left\{ \frac{3 + 3ahi - a^2h^2}{1 + ahi} \right\} \left\{ \frac{\sinh ah}{ah} [\nabla \times \hat{\mathbf{U}}^\infty]_0 - 2\hat{\mathbf{\Omega}} \right\} - i\omega\rho \int (\mathbf{r}_0 \times \hat{\mathbf{U}}^\infty) dv \quad (59)$$

with $h = -\sqrt{\omega/2\nu}(1 + i)$.

Here, $\nu(=\mu/\rho)$ is the kinematic viscosity of the fluid and the symbol $[]_0$ implies that the quantity in the bracket is to be evaluated at the location of the sphere center. The solution (58) and (59) is identical to the results of Mazur and Bedeaux (1974) and Hills (1975), which were derived using the singularity method in the Helmholtz equation (16).

As we noted earlier, the undisturbed velocity field $\hat{\mathbf{U}}^\infty$ which satisfies the unsteady creeping-motion equation can be divided into two parts ($\hat{\mathbf{U}}^\infty = \hat{\mathbf{U}}_p^\infty + \hat{\mathbf{U}}_h^\infty$): one is the irrotational part $\hat{\mathbf{U}}_p^\infty$ governed by Laplace's equation $\nabla^2 \hat{\mathbf{U}}_p^\infty = \mathbf{0}$ and the other is the rotational part $\hat{\mathbf{U}}_h^\infty$ satisfying Helmholtz equation $(\nabla^2 + h^2)\hat{\mathbf{U}}_h^\infty = \mathbf{0}$. For the purpose of evaluating the integrals (58) and (59), it is convenient to utilize the mean value theorems for the Laplace's and Helmholtz equations, respectively; i.e.,

$$\int \hat{\mathbf{U}}^\infty dv = \frac{4\pi a^3}{3} \{ [\hat{\mathbf{U}}_p^\infty]_0 + W(h)[\hat{\mathbf{U}}_h^\infty]_0 \} \quad (60)$$

where $W(h)$ is a weighting function defined as

$$W(h) = 3 \left[\frac{\sinh ah}{a^3 h^3} - \frac{\cosh ah}{a^2 h^2} \right] \quad (61)$$

So far we have determined the Fourier components $\hat{\mathbf{F}}^*$ and $\hat{\mathbf{T}}^*$ of the hydrodynamic force and torque on a sphere which moves with arbitrary translational and rotational velocities through an unbounded fluid that undergoes an undisturbed flow $(\hat{\mathbf{U}}^\infty, \hat{\mathbf{\rho}}^\infty)$ that is governed by the unsteady Stokes' equation. In the next section, we shall briefly consider the application of the fundamental results

determined above.

II. Discussion

Let us now begin with the creeping motion of a *solid* sphere in an undisturbed steady Stokes' flow, thus providing a basis to check the present results against Faxen's (1921) law. It is a simple matter to reproduce Faxen's law by taking limit $h \rightarrow 0$, in the solution (58) and (59):

$$\mathbf{F} = 6\pi\mu a\{[\mathbf{U}^\infty]_0 - \mathbf{U}\} + \pi\mu a^3[\nabla^2 \mathbf{U}^\infty]_0 \quad (62)$$

and

$$\mathbf{T} = \frac{8\pi\mu a^3}{3} \left\{ \frac{1}{2} [\nabla \times \mathbf{U}^\infty]_0 - \boldsymbol{\Omega} \right\}. \quad (63)$$

According to this well-known result, we can evaluate the hydrodynamic force and torque on a sphere with an arbitrary motion \mathbf{U} and $\boldsymbol{\Omega}$ in an unbounded fluid that is itself undergoing a steady creeping (but otherwise arbitrary) flow at infinity ($\mathbf{U}^\infty, p^\infty$), in terms solely of the values of \mathbf{U}^∞ , $\nabla \times \mathbf{U}^\infty$ and $\nabla^2 \mathbf{U}^\infty$ at the position occupied by the center of the sphere.

As another simple illustration of the application of (58) and (59), we consider the problem of a rigid sphere moving with an arbitrary time-dependent velocity $\mathbf{U}(t)$ through a fluid which is *at rest* at infinity (i.e. $\mathbf{U}^\infty = \mathbf{0}$). We can readily calculate the hydrodynamic force on the sphere by taking an inverse Fourier-transform of expression (58). The result is

$$\mathbf{F} = -6\pi\mu a\mathbf{U} - \frac{2\pi\rho a^3}{3} \cdot \frac{\partial \mathbf{U}}{\partial t} - 6\pi\rho a^2 \sqrt{\nu/\pi} \int_{-\infty}^t \frac{d\mathbf{U}}{d\tau} \cdot \frac{d\tau}{\sqrt{t-\tau}}. \quad (64)$$

The solution (64) was originally developed by Stokes (1851) and Basset (1888). The first term is the so-called Stokes drag; the second is known as the added mass contribution and accounts for the change of fluid inertia in incompressible flow past an accelerating sphere; the last term is called the Basset term and

expresses the effect of the previous history of the particle velocity on the hydrodynamic force. It may be noted that the added mass contribution is independent of the viscosity of the fluid, and would thus be expected even in an inviscid potential flow.

Closely related to the problem of an accelerating sphere in a stationary fluid is the complementary problem of an accelerating uniform streaming flow $\mathbf{U}^\infty(t)$ past a *stationary* sphere. It is tempting to suppose that the hydrodynamic force in this case is simply the force evaluated from (64) with $\mathbf{U} = -\mathbf{U}^\infty(t)$. In this case, however, we must take into account the fictitious body force $\frac{4\pi a^3 \rho}{3} \frac{d\mathbf{U}^\infty}{dt}$, owing to the acceleration of the external flow. Then

$$\mathbf{F} = 6\pi\mu a\mathbf{U}^\infty + 2\pi\rho a^3 \frac{d\mathbf{U}^\infty}{dt} + 6\pi\rho a^2 \sqrt{\nu/\pi} \int_{-\infty}^t \frac{d\mathbf{U}^\infty}{d\tau} \cdot \frac{d\tau}{\sqrt{t-\tau}}. \quad (65)$$

When a freely suspended, spherical particle is immersed in an oscillating fluid, the particle motion has a number of important properties. In order to study these, it is convenient to begin with a simple but typical example that was considered previously by Batchelor (1967). We now consider the problem in detail, demonstrating that the present result, (58), reduces to that of Batchelor (1967). Let us suppose that an unbounded, incompressible fluid executes a simple harmonic oscillation corresponding to the passage of a sound wave; i.e.,

$$\mathbf{U}^\infty = \mathbf{c}e^{-i\omega t + \mathbf{k}\cdot\mathbf{x}}, \quad k = |\mathbf{k}| = \frac{2\pi}{\lambda} \quad (66)$$

and that the magnitude of this undisturbed velocity, $c = |\mathbf{c}|$ is small enough for the convective inertia associated with the sound wave to be negligible. Then, since the undisturbed flow (i.e., the sound wave) will be governed by the unsteady Stokes' equation, we can apply the general expressions (58) and (59) to determine the hydrodynamic force and torque on a solid sphere for any arbitrary

trary frequency ω and wave number k . For purposes of the present discussion, however, we make the further simplifying assumption that the frequency is large enough that the vorticity boundary layer is vanishingly thin compared to both the sphere radius a and the wave length λ (i.e. $\frac{\omega a^2}{\nu} \gg 1$ and $\frac{\omega \lambda^2}{\nu} \gg 1$). In this case, by non-dimensionalizing the unsteady Stokes' equation, using the characteristic length a , velocity c and time ω^{-1} , we can easily show that the viscous stress contribution in the equation of motion is negligible relative to the local acceleration $\partial \mathbf{u} / \partial t$. The flow exterior to the sphere is therefore irrotational except for the very thin vorticity boundary-layer around the sphere surface, and the hydrodynamic force can be determined easily by taking a limit $\frac{\omega a^2}{\nu} \gg 1$ and $\frac{\omega \lambda^2}{\nu} \gg 1$ to the general expression (58) to be

$$\mathbf{F}^* = \frac{2\pi\rho a^3}{3} \left\{ \left[\frac{d\mathbf{U}^*}{dt} \right]_0 - \frac{d\mathbf{U}}{dt} \right\} + \rho \int \frac{d\hat{\mathbf{U}}^*}{dt} dv. \quad (67)$$

It should be noted that the hydrodynamic force, (67), is valid for any spherical body (*solid or fluid*) and is actually independent of the fluid viscosity — indeed, in this limit the fluid motion exterior to the sphere can be regarded as an irrotational-potential flow. This hydrodynamic force is balanced in the equation of motion for a spherical body (solid or fluid) by the particle inertia contribution, $\frac{4\pi a^3 \rho_p}{3} \cdot \frac{\partial \mathbf{U}}{\partial t}$. Evaluating the fictitious body force term, $\rho \int \frac{\partial \mathbf{U}^*}{\partial t} dv$ in (67), by means of the mean value theorem for Laplace's equation, we can use the equation of motion for the particle to obtain its velocity as a function of the instantaneous velocity of the external undisturbed flow

$$\mathbf{U} = \frac{3\rho}{2\rho_p + \rho} [\mathbf{U}^*]_0. \quad (68)$$

Here ρ_p denotes the particle density. For a neutrally buoyant particle, it can be

seen that the amplitude of the oscillation of the sphere velocity is exactly the same as that of the undisturbed motion of the surrounding fluid. If the sphere is lighter, however, its velocity oscillates with greater amplitude than the undisturbed velocity of the fluid. Indeed, for a gas bubble (i.e., $\rho_p \rightarrow 0$) immersed in a fluid, the instantaneous velocity is approximately three times larger than the local undisturbed velocity of the fluid evaluated at the location of the bubble center, a result which can be observed in flow-visualization experiments as Batchelor (1967) has pointed out.

Finally, let us turn to a further application of the general result, (58), to investigate the 'relative motion' of two gas bubbles which undergo very rapid and small amplitude oscillations in volume in the same phase. As we mentioned in the foregoing problem, the existence of high frequency (i.e., $\omega a^2/\nu \gg 1$ and $\omega \lambda^2/\nu \gg 1$) and small amplitude bubble oscillations ensures that the viscous boundary layer is very thin and thus the general solution (58), which is initially derived for a *solid* sphere, can be applied to the *fluid* sphere problem in this asymptotic limit. Conditions for validity of the high-frequency approximation can be derived by expressing the oscillation amplitude in terms of the physical properties of the system. For a spherically expanding bubble, the velocity field exterior to the sphere is given by $\mathbf{u} = \left(\frac{a}{r}\right)^2 \frac{da}{dt} \mathbf{n}$, and this is an irrotational velocity distribution (i.e., $\nabla \times \mathbf{u} = \mathbf{0}$). The corresponding Navier-Stokes equation, in this case, reduces to the Rayleigh-Plesset equation for the instantaneous bubble radius $a(t)$

$$a \frac{d^2 a}{dt^2} + \frac{3}{2} \left(\frac{da}{dt} \right)^2 - \frac{4\mu}{a} \frac{da}{dt} = \frac{1}{\rho} \left[p - p^\infty - \frac{2\gamma}{a} \right]. \quad (69)$$

Here p is the pressure inside the bubble which is related to $a(t)$ by the thermodynamic equation

$$\frac{p}{p_0} = \left(\frac{a_0}{a} \right)^3 \quad (70)$$

provided the gas inside the bubble is ideal and remains at a constant temperature. In (70), p_0 and a_0 denote the equilibrium pressure and radius, respectively. We seek a solution of (69) combined with (70) in the form:

$$a(t) = a_0(1 + \varepsilon_0 e^{-i\omega_0 t}), \quad \varepsilon_0 \ll 1 \quad (71)$$

Substituting (70) and (71) into (69) and then expanding the resultant equation in terms of small ε_0 , we can determine a_0 and ω_0 :

$$a_0 = \frac{2\gamma}{p_0 - p^\infty} \quad (72)$$

$$\omega_0 = \left(\frac{2p_0 + p^\infty}{\rho a_0^2} \right)^{1/2} \quad (73)$$

Thus, the conditions for validity of the high-frequency approximation are

$$\frac{4\gamma[2p_0 + p^\infty]}{\rho \nu^2 (p_0 - p^\infty)^2} \gg 1 \quad (74)$$

$$\frac{\lambda^4 (2p_0 + p^\infty)(p_0 - p^\infty)^2}{4\rho\gamma^2 \nu^2} \gg 1. \quad (75)$$

When these conditions are satisfied, the viscous terms in (58) will be negligible. We now consider two adjacent gas bubbles 1 and 2, each executing rapid but small-amplitude oscillations in volume such that (74) and (75) are satisfied. In view of (71), the volume v of each gas bubble is approximately $v = v_0(1 + \varepsilon e^{-i\omega_0 t})$ with $\varepsilon = 3\varepsilon_0$ ($\ll 1$). Each oscillating bubble will then induce an accelerating velocity field in the surrounding fluid and thus influence the other's motion. The velocity field generated by the second bubble in the direction of the first bubble, say \mathbf{e}_1 , is simply

$$\mathbf{U}^{\infty} = - \frac{i\omega_0 \varepsilon V_0 e^{-i\omega_0 t}}{4\pi r^2} \mathbf{e}_1 \quad (76)$$

in which r is the distance from the center of the second bubble. But, the equation of motion for the first bubble in the flow field \mathbf{U}^{∞} , under the limiting conditions, (74) and (75), can be derived by balancing the particle inertia,

$\frac{4\pi\rho_p a^3}{3} \frac{d\mathbf{U}_1}{dt}$, with the hydrodynamic force evaluated from (58) in the limit of $\omega a^2 \nu \gg 1$, i.e.

$$\frac{\rho_p}{\rho} \cdot \frac{d\mathbf{U}_1}{dt} = \frac{1}{2a^3} \frac{d}{dt} [a^3 \{[\mathbf{U}^{\infty}]_0 - \mathbf{U}_1\}] + \left[\frac{d\mathbf{U}^{\infty}}{dt} \right]_0 \quad (77)$$

Upon substituting the expression for a , (71) combined with (72) and (73), into (77) and expanding \mathbf{U}_1 asymptotically in powers of ε_0 ,

$$\mathbf{U}_1 = \varepsilon_0 \mathbf{U}_1^{(0)} + \varepsilon_0^2 \mathbf{U}_1^{(1)} + \varepsilon_0^3 \mathbf{U}_1^{(2)} + \dots \quad (78)$$

we can readily evaluate the acceleration of the first bubble with the additional condition $\rho_p/\rho \rightarrow 0$:

$$\frac{d\mathbf{U}_1}{dt} = 3 \left[\frac{d\mathbf{U}^{\infty}}{dt} \right]_0 + 6i\omega_0 \varepsilon_0 [\mathbf{U}^{\infty}]_0 e^{-i\omega_0 t} + O(\varepsilon_0^3) \quad (79)$$

The average acceleration of the first bubble over one cycle of oscillation can also be determined by combining (76) with (79),

$$\left\langle \frac{d\mathbf{U}_1}{dt} \right\rangle = - \frac{6\varepsilon_0^2 \gamma \{2p_0 + p^{\infty}\}}{(p_0 - p^{\infty}) \rho d^2} \mathbf{e}_1 + O(\varepsilon_0^3) \quad (80)$$

in which d is the separation distance between the centers of the two gas bubbles. It is obvious, from the definition of the vector \mathbf{e}_1 and the expression (80), that the first bubble undergoes a mean displacement over each cycle of oscillation in the direction of the second bubble. Thus, it appears as though there were an interaction force, between the two gas bubbles, that is attractive and results in a tendency for gas bubbles to approach one another and ultimately coalesce.

The "attractive force" is normally small, but ultrasonic vibrations of a liquid can be used to clear it of gas bubbles as noted by Batchelor (1967).

This completes our illustrative applications of interest using the general solutions that were developed in Sections II and III. In the next chapter of this thesis, the present results of Faxen-type law will be used in the analysis of Brownian motion of spherical particles. A generalization of the present analysis is currently under way in this research group to an arbitrary motion of a spherical drop through a time-dependent Stokes flow in either an unbounded fluid or in the presence of a plane fluid interface.

References

1. Basset, A. B. 1888 *A Treatise on Hydrodynamics*, Vol. II. Dover, New York.
2. Batchelor, G. K. 1967 *An Introduction to Fluid Dynamics*. Cambridge University Press, Cambridge.
3. Brenner, H. 1963 *Chem. Eng. Sci.* **18**, 1.
4. Faxen, H. 1921 Dissertation, Uppsala University.
5. Happel, J. and Brenner, H. 1983 *Low Reynolds Number Hydrodynamics*. Martinus Nijhoff Publishers.
6. Hauge, E. H. and Martin-Löf, A. 1973 *J. Stat. Phys.* **7**, 259.
7. Hills, B. P. 1975 *Physica* **80A**, 360.
8. Lamb, H. 1932 *Hydrodynamics*. Dover, New York.
9. Lighthill, J. 1978 *Waves in Fluids*. Cambridge University Press, Cambridge.
10. Mazur, P. and Bedeaux, D. 1974 *Physica* **76**, 235.
11. Stokes, G. G. 1851 *Trans. Camb. Phil. Soc.* **9**, 29.

Chapter IV.

Brownian Motion of Spherical Particles near a Deformable Interface

Abstract

The motion of a Brownian sphere in the presence of a deformable fluid interface is studied by considering both the random distortions of interface shape due to spontaneous thermal impulses from the surrounding fluid, and interface deformations that are caused by impulsive motions of the Brownian particle. First, the fluctuation-dissipation theorem is derived for the spontaneous fluctuations of interface shape using the method of normal modes in conjunction with a Langevin type equation of motion for a Brownian sphere, in which the fluctuating force arises from the continuum motions induced near the sphere by the fluctuations of interface shape. This analysis results in the prediction of autocorrelation functions for the location of the dividing surface, for the random force acting on the sphere, and for the particle velocity. The particle velocity correlation, in turn, yields the effective diffusion coefficient due to random fluctuations of the interface shape. The effect of the interface on the impulsive motion of a Brownian sphere is also investigated. In this case, we consider both the spatial modification of the hydrodynamic mobility due to hydrodynamic interaction effects, and the interface relaxation back toward a flat configuration from the deformed shape that is initially caused by the impulsive particle motion.

I. Introduction

The irregular random motion of small particles suspended in liquids, known as "Brownian motion", was first described by the English botanist, Robert Brown in 1828. Controversy concerning the origin of the Brownian motion persisted for many decades and it was not until 1905 that Albert Einstein first advanced a satisfactory theory, and eventually confirmed the molecular nature of matter by relating the Brownian motion to the thermal fluctuations of molecules in the suspending fluid.

In his pioneering paper, Einstein (1905) showed that the irregular motions of uncharged noninteracting particles can be modeled as a *diffusion* and thus the probability distribution function $P(\mathbf{x})$ of Brownian particles in the configuration space \mathbf{x} must be governed by the so-called Einstein-Smoluchowski diffusion equation

$$\frac{\partial P}{\partial t} = \nabla \cdot [\mathbf{D} \nabla P(\mathbf{x})] \quad (1)$$

in which \mathbf{D} denotes the diffusion coefficient tensor, and t is the time variable. In deriving Eq. (1), Einstein assumed that the movements of a Brownian particle could be idealized as a Markoff process, in the sense that the course which a Brownian particle will take depends only on the instantaneous values of its physical parameters and is entirely independent of its whole previous history. Utilizing the solution of the diffusion Eq. (1) with an appropriate initial condition, Einstein (1905) also derived the relationship between the diffusion coefficient D and the mean square displacement $\langle |\Delta \mathbf{x}|^2 \rangle$ of a Brownian sphere:

$$\langle |\Delta \mathbf{x}|^2 \rangle = 6D\Delta t \quad (2)$$

The mean square displacement is therefore proportional to the time interval Δt . This general relationship, (2), in conjunction with the velocity correlation func-

tion plays an important role in determining the diffusion coefficient, as we will see in Section IV.

The diffusion coefficient in (1) and (2), according to Einstein's theory, can be determined from the molecular-kinetic theory of heat, employing only thermodynamic concepts and the properties of systems in dynamic equilibrium. For a suspension of uncharged, noninteracting particles with spatial number-density gradient, the translational diffusion flux at equilibrium is evidently the same as the convective flux resulting from the application to each particle of a steady thermodynamic force which is due solely to the existence of osmotic pressure. As far as osmotic pressure is concerned, solute molecules and suspending Brownian particles are identical in their behavior at great dilution. According to van't Hoff's law, the osmotic pressure in dilute solution obeys the relationship, $p^{os} = c\kappa_B T$, in which c denotes the number density of solute particles that may be regarded as the probability density $P(\mathbf{x})$ in the configuration space of a dilute suspension. Then, the thermodynamic force, as a consequence of the concentration gradient of Brownian particles, can be derived from the osmotic pressure and is given by

$$\mathbf{F}^{os} = -\kappa_B T \nabla \ln\{P(\mathbf{x})\}. \quad (3)$$

Thus, the corresponding convective flux is equal to

$$-P(\mathbf{x})\mathbf{M}[\kappa_B T \nabla \ln\{P(\mathbf{x})\}].$$

This convection flux is balanced by the diffusion flux

$$\mathbf{j}_D = -\mathbf{D} \cdot \nabla P(\mathbf{x}) \quad (4)$$

with the diffusivity tensor \mathbf{D} related to the hydrodynamic mobility tensor \mathbf{M} for a particle by the Nernst-Planck-Einstein relation:

$$\mathbf{D} = \kappa_B T \mathbf{M} . \tag{5}$$

Here, κ_B is the Boltzmann constant and T is the absolute temperature. This classical expression for diffusivity of uncharged particles has been verified experimentally in many types of diffusion. It is noteworthy that Einstein's approach employs only the concept of a *thermodynamic* driving force on the particle as representation of the diffusive effect of Brownian motion, without taking into account the dynamics of the particle motion in the suspending fluid.

Brownian movements of individual particles in a single unbounded fluid domain can also be modeled as a diffusion process in a dilute suspension by a "rigorous" generalization of the Liouville equation (cf. Kreuzer, 1981) of classical dynamics to include Brownian motion. This approach to Brownian motion begins with a consideration of the equation of motion for a suspended particle, i.e., the Langevin (1908) equation

$$\frac{d\mathbf{U}}{dt} = -\beta \cdot \mathbf{U} + \mathbf{A}(t) \tag{6}$$

where \mathbf{U} denotes the particle velocity. According to the Langevin equation, the influence of the surrounding medium on the motion of the Brownian particle can be split up into two parts: first, a very *rapidly* fluctuating part $\mathbf{A}(t)$ with a molecular motion time scale, τ_f ($\sim 10^{-13}$ sec for water); and, second, a systematic hydrodynamic friction part $-\beta \cdot \mathbf{U}$ associated with the much *slower* response of the fluid to motion of the particle with a characteristic time scale $\tau_{vp} \equiv \beta^{-1}$ ($\sim 10^{-9}$ sec for a free sphere in water). Assuming that $\tau_f \ll \tau_{vp} \ll 0(1)$, as is characteristic of Brownian motion, we can introduce time intervals Δt in which the physical parameters such as position, orientation and velocity of the Brownian particle change by *infinitesimal* amounts, while the number of fluctuations arising from collisions with surrounding fluid molecules remains extremely large:

$$\tau_f \ll \tau_{vp} \ll \Delta t \ll O(1). \quad (7)$$

That a transformation of Liouville equation into the famous Fokker-Planck equation should be possible under these circumstances is apparent when we recall that the Brownian movements in a time interval Δt satisfying (7) can be regarded as a Markoff process so that the probability distribution $P(\mathbf{U} + \Delta\mathbf{U}, \mathbf{x} + \Delta\mathbf{x}, t + \Delta t)$ in the phase space governing the probability of occurrence of $\mathbf{U} + \Delta\mathbf{U}$ at time $t + \Delta t$ can be derived from the distribution $P(\mathbf{U}, \mathbf{x}, t)$ at the present time t and a knowledge of the transition probability $\Gamma(\mathbf{U}, \Delta\mathbf{U})$ that \mathbf{U} suffers an increment $\Delta\mathbf{U}$ in the time interval Δt . According to the Langevin equation (6)

$$\Delta\mathbf{U} = -\beta \cdot \mathbf{U} \Delta t + \int_t^{t+\Delta t} \mathbf{A}(s) ds, \quad \Delta\mathbf{x} = \mathbf{U} \Delta t \quad (8)$$

in which the integral denotes the net acceleration arising from fluctuations that a Brownian particle suffers in the time interval Δt . From the molecular-kinetic theory, the probability distribution of the integral must be Maxwellian and thus it follows at once that the transition probability has the Maxwellian distribution in terms of $\Delta\mathbf{U} + \beta \cdot \mathbf{U} \Delta t$. With condition (7), it can also be expected that a Maxwell-Boltzmann distribution of the velocity will be established at all points after time intervals Δt as the result of superposition of large number of random accelerations caused by collisions with the individual surrounding molecules (cf. Chandrasekhar, 1943, and Batchelor, 1976). Thus, the Fokker-Planck equation in the phase space (\mathbf{U}, \mathbf{x}) can be applied to the configuration space, \mathbf{x} , independently of the velocity space, \mathbf{U} , provided that we are interested only in the time intervals Δt . Then, integration of the Fokker-Planck equation over the velocity space \mathbf{U} provides us the Einstein-Smoluchowski equation (1), i.e., differential equation for the probability distribution function, $P(\mathbf{x})$, of Brownian particles in the configuration space, \mathbf{x} , and yields the same diffusivity coefficient matrix of

(5) as Einstein's thermodynamic approach.

It will be evident, however, that the Langevin equation (6) with the instantaneous friction law determined from the steady Stokes' equation gives only a partial picture of the effect of thermal fluctuations in the system and predicts a rapid exponential decay on the time scale β^{-1} in the velocity correlation function. The first indication of a deficiency in the Langevin equation came in numerical simulations of the molecular motions in liquids which produced velocity correlations of spherical particles with a long tail decaying as $t^{-3/2}$ rather than exponentially as predicted by (6) (cf. Rahman, 1964, and Alder and Wainwright, 1967). Recently, several separate analyses, e.g., Hauge and Martin-Löf (1973) and Hinch (1975), which allow for the distribution of thermal fluctuation throughout the fluid, have predicted correctly the full velocity correlation as well as the diffusion coefficient matrix of (5). Linearity is, however, preserved in the governing differential equations for fluid motion, because the velocities remain small enough to render the convective terms negligible. It is important to realize that both the classical Langevin method with β determined from the *steady* Stokes' equation and the above corrected approaches lead to exactly the Einstein-Smoluchowski diffusion equation (1) with the same diffusion coefficient matrix (5), provided the condition (7) is satisfied.

Recent years have witnessed an increasing amount of interest in the description of Brownian diffusion near a rigid wall or a fluid-fluid interface (cf. Brenner and Leal, 1977 and 1982, and Larson, 1982, and Gotoh and Kaneda, 1982). Treatments of this kind are designed to provide a theoretical basis in terms of molecular properties, for understanding and predicting the various transport coefficients that enter into the description of the same processes from a macroscopic point of view. Of considerable importance is prediction and interpretation of interphase mass-transfer rates in liquid-liquid systems, which

are usual in many industrial operations, liquid extraction being a primary example. However, little is known about the effects of a *fluid interface* on the motion of Brownian particles. Indeed, our objective in the present study is to investigate the effect of the presence of an interface on the motion of Brownian particles by employing the general methods of statistical physics in combination with fundamental fluid mechanics. It is, of course, obvious from the point of view of nonequilibrium thermodynamics that the interface will fluctuate around equilibrium due to the thermal agitations of the surrounding fluid molecules, and these random changes in the interface shape produce random motions of Brownian particles in the vicinity of the interface. Further, due to the impulsive motion of a Brownian particle the interface exhibits also a continuously changing shape which depends on the prior history of the particle motion and the interface shape at earlier times. Although the interface deformation is small, resulting from infinitesimal displacement of the Brownian particle on the time interval τ_{vp} , the displacement of the particle induced by interface relaxation back toward equilibrium may be of the same order of magnitude as that initially caused by the random impulse.

In the present study, first we derive the fluctuation-dissipation theorem for the random fluctuations of interface shape that are caused by spontaneous thermal impulses from the surrounding fluids. This analysis is carried out using the method of normal modes in conjunction with a Langevin-type stochastic equation for the Brownian particles, and determines the autocorrelation functions for the location of the interface, for the random force on the particle, and for the particle velocity. The velocity correlation function will produce the effective diffusion coefficient due to spontaneous random fluctuations of the interface shape. Finally, we also investigate the effects of interface deformation that are induced by the impulsive motion of a sphere which is undergoing

Brownian motion, by considering the effects on the velocity correlation (or Brownian diffusivity) of the interface relaxation back towards the flat equilibrium configuration after an initial deformation that is caused by the particle motion. However, we begin by considering a relatively simple model system in which the interface remains *flat*, nondeforming in spite of the arbitrary motion of particle in order to explore the validity of the diffusion equation (1) for Brownian particles near an interface.

II. Brownian Motion near a Nondeforming Flat Interface

Let us begin by considering a model system consisting of Brownian particles dispersed in a viscous incompressible Newtonian fluid in the semi-infinite domain $-\infty < x_3 < 0$, bounded by a plane fluid interface at $x_3 = 0$ (cf. Figure 1). In the region $x_3 > 0$, we suppose that there is a second unbounded fluid. The viscosity ratio λ between the two fluids is assumed to be arbitrary. In the present section we assume that the interface remains flat. Later in this chapter, we consider the effects associated with interface deformation.

The difference between the problem discussed in this section and the classical problem of Brownian motion in an unbounded domain is the possible existence of a short-range force of interaction (attractive or repulsive), $\mathbf{F}_{\text{ex}}(\mathbf{x})$, which we assume acts between the particles and interface (Brenner and Leal, 1977), and the dependence of the hydrodynamic mobility \mathbf{M} [i.e., $(m\beta)^{-1}$; m is the particle mass] on the configuration of the particle relative to the interface (i.e., its position, and if the particle is nonspherical, its orientation), as a consequence of hydrodynamic interactions. For a freely rotating torque-free particle in creeping flow, the hydrodynamic mobility is given by

$$\mathbf{M} = (m\beta)^{-1} = [\mathbf{K}_T - \mathbf{K}_C^t \mathbf{K}_R^{-1} \mathbf{K}_C]^{-1} \quad (9)$$

where \mathbf{K}_T , \mathbf{K}_C and \mathbf{K}_R are the so-called translation, coupling and rotation tensors

(cf. Lee, Chadwick and Leal, 1979, and Yang and Leal, 1983). These so-called resistance tensors provide a complete description of the effect of hydrodynamic interactions with the interface on the relationships between the translational and angular velocities of a particle in steady creeping flow and the force and torque that act on the particle.

Application of the so-called "thermodynamic approach" that was outlined in the preceding section shows that the same relationship holds between the mobility and diffusion tensors as in (5) even in the presence of a *nondeforming* flat interface in the *absence* of a physicochemical interaction force. Further, this approach shows that the relevant hydrodynamic mobility is still that for steady creeping motions. For spherical particles, each component of the mobility tensor \mathbf{M} can thus be determined either from the exact solution results of Lee and Leal (1980) or the asymptotic solutions of Lee et al. (1979) and Yang and Leal (1984), and the diffusion tensor is given by

$$\mathbf{D} = \begin{bmatrix} D_{11} & 0 & 0 \\ 0 & D_{22} & 0 \\ 0 & 0 & D_{33} \end{bmatrix}, \quad D_{11} = D_{22} \quad (10)$$

in which the components D_{ij} are functions of the particle position relative to the interface as a consequence of spatially modified mobility. In order to illustrate the qualitative nature of these effects, the components D_{11} and D_{33} based on the approximate singularity-method solution of Yang and Leal (1984) are plotted in Figure 2 as a function of the distance between the sphere center and interface for $\lambda = 0, 1$ and ∞ . The magnitudes of the diffusion coefficients, D_{11} and D_{33} is either increased or decreased owing to the presence of an interface, and the effect is a strong function of the particle position relative to the interface arising from the spatial modification of hydrodynamic mobility.

For nonspherical particles (e.g., elongated slender particles), the mobility is,

in general, dependent on the particle orientation relative to the interface in addition to the separation distance d between the particle center and interface. In Figure 3, as an example of this orientation dependence, the diffusivity coefficient D_{11} of a slender rod-like particle with the length of axis $2l$, is illustrated as a function of the oblique angle θ between the body axis and the interface for two values of particle position $d/l = 1.01$ and 2 . For each value of d/l , we include three values of the viscosity ratio, $\lambda = 0, 1$ and ∞ . Also shown is the corresponding result for diffusion in an unbounded single fluid domain. The quantitative dependence of the diffusivity on the particle configuration (i.e., d and θ) relative to the interface is a consequence of the spatially modified and orientation-dependent hydrodynamic mobility due to the *direct* hydrodynamic interactions between the particles and the interface.

The presence of a short-range physicochemical attraction (or repulsion) between the particles and the interface will generate steep spatial gradients in the particle number density, $P(\mathbf{x})$ (cf. Leal and Brenner, 1982). The resulting nonuniform hydrodynamic interactions between particles will also lead to nonisotropic and spatially dependent mobility. These *indirect* interface effects owing to particle-particle hydrodynamic interactions will contribute to nonisotropy and spatial dependence of the diffusivity. Furthermore, although successful in determining the relevant diffusion coefficient of Brownian particles near an interface in the absence of a physicochemical interaction, the thermodynamic approach cannot provide any conditions for the validity of the normal diffusion theory in the presence of the physicochemical attraction (or repulsion).

Let us thus turn to the fundamental statistical approach in which the governing differential equation for the probability density in the phase space (\mathbf{U}, \mathbf{x}) is the Liouville equation, in order to explore the conditions for validity of the

diffusion process defined by (4) and (5) in the presence of a nondeforming flat fluid-fluid interface. Compared to the case of a single unbounded fluid domain, the Langevin equation is modified by the interface in that the hydrodynamic mobility is dependent upon proximity to the interface (and is anisotropic even for spherical particles) due to the direct and indirect hydrodynamic interaction effects that were described above, and by the existence in some cases of an interface-induced physicochemical force field $\mathbf{F}_{\text{ex}}(\mathbf{x})$:

$$\frac{d\mathbf{U}}{dt} = -\boldsymbol{\beta}(\mathbf{x}) \cdot \mathbf{U} + \mathbf{F}_{\text{ex}}(\mathbf{x}) + \mathbf{A}(t) . \quad (11)$$

When one observes the process of Brownian motion in the averaging time intervals Δt satisfying the condition of (7), the stochastic movements of a Brownian particle can be regarded as a Markoff process. Further, if the length scales characteristic of variations in $\boldsymbol{\beta}(\mathbf{x})$ and $\mathbf{F}_{\text{ex}}(\mathbf{x})$ are *sufficiently* large relative to the mean-square displacements $\langle |\Delta \mathbf{x}|^2 \rangle$ of a Brownian particle in the time interval Δt , the physical parameters $\boldsymbol{\beta}(\mathbf{x})$ and $\mathbf{F}_{\text{ex}}(\mathbf{x})$ can be approximated as constant during Δt . In effect, this is the condition of a fixed "configuration" over the averaging period, Δt , in which the increments $\Delta \mathbf{x}$ and $\Delta \mathbf{U}$ in position and velocity of a typical particle are given by

$$\Delta \mathbf{U} = -[\boldsymbol{\beta}(\mathbf{x}) \cdot \mathbf{U} - \mathbf{F}_{\text{ex}}(\mathbf{x})] \Delta t + \int_t^{t+\Delta t} \mathbf{A}(s) ds \quad (12)$$

with $\Delta \mathbf{x} = \mathbf{U} \Delta t$. The integral in (12) represents the net acceleration that a Brownian particle may suffer during Δt due to the thermal fluctuations of surrounding molecules. We now assert that the invariance of the Maxwell-Boltzmann distribution requires that the probability of occurrence of different values for the net acceleration be governed by the Maxwellian distribution function, and it follows that the transition-probability distribution $\Gamma(\mathbf{U}, \Delta \mathbf{U})$ is Maxwellian in terms of $\Delta \mathbf{U} + [\boldsymbol{\beta}(\mathbf{x}) \cdot \mathbf{U} - \mathbf{F}_{\text{ex}}(\mathbf{x})] \Delta t$.

A conservative estimate of the length scales of variations in $\mathbf{F}_{\text{ex}}(\mathbf{x})$ and $\beta(\mathbf{x})$, i.e., l_f and l_β , respectively, which are allowable for (11) and (12) to be valid, can be obtained by using the Stokes resistance for a particle at large distances from the interface, β (cf. Leal and Brenner, 1977, and Larson, 1982). The resulting condition for the fixed configuration is

$$l_\beta, l_f \gg \frac{(\kappa_B T / m)^{1/2}}{\beta} \approx 0(\langle |\Delta \mathbf{x}|^2 \rangle). \quad (13)$$

For the extremely short-range interaction force $\mathbf{F}_{\text{ex}}(\mathbf{x})$, the condition (13) may not always be satisfied for the very small Brownian particles (i.e., large solute molecules), for which the mean-square displacements in the average time intervals Δt can be quite large (cf. Larson, 1982, for the case in which the condition (13) is not satisfied). If we adopt (12) and (13), a generalized Einstein-Smoluchowski equation governing the time evolution of the local number density $P(\mathbf{x})$ in the configuration space \mathbf{x} can be derived from the Liouville equation via the Fokker-Planck equation by averaging the probability distribution $P(\mathbf{U}, \mathbf{x})$ in the phase space over the time interval Δt satisfying the condition (7):

$$\frac{\partial P(\mathbf{x})}{\partial t} = \nabla \cdot [\mathbf{D}(\mathbf{x}) \cdot \nabla P(\mathbf{x}) - \mathbf{M}(\mathbf{x}) \cdot \mathbf{F}_{\text{ex}}(\mathbf{x}) \cdot P(\mathbf{x})] \quad (14)$$

in which the mobility and diffusivity tensors $\mathbf{M}(\mathbf{x})$ and $\mathbf{D}(\mathbf{x})$ refer to a torque-free particle and are related by (5). Thus, the simple Fickian form of the diffusion equation is obtained in the presence of a flat fluid-fluid interface under the conditions (7) and (13), and the diffusivity tensor can be calculated from a knowledge of the mobility tensors for steady motion of a freely rotating particle in the vicinity of a plane interface.

All of the preceding results discussed in this section so far pertain to the case in which the interface remains precisely *flat*, in spite of the motions induced in the two fluids by the motions of the Brownian particles. It is, of course, obvious

that a real interface cannot remain precisely flat except for the limiting case of $\lambda \rightarrow \infty$ (i.e., a "solid" wall case). In particular, the motions induced in the two fluids by the motions of a Brownian particle will generally lead to a normal stress difference across the interface which can only be balanced by capillary forces if the interface deforms. In general, then, the interface will exhibit a continuously changing shape which depends on its shape at earlier times, and thus, on the prior history of the particle motion (cf. Lee and Leal, 1982). Although the magnitude of interface deformations will be small compared to the particle size, corresponding to infinitesimal displacements of the Brownian particle on the inertial time scale β^{-1} , the *displacement* induced in the particle by interface relaxation back toward equilibrium (i.e., the flat configuration) may be of the same order of magnitude as that caused initially by the random impulse $\mathbf{A}(t)$ and this "rebound" effect may have an appreciable affect on the mean-square displacements (or the Brownian diffusivity) of the particle.

In addition, the interface will fluctuate around the equilibrium flat configuration due to thermal agitation of the surrounding fluids, even in the absence of Brownian particles, and these random changes in the interface shape will produce fluctuating velocity fields and so induce random motions of the Brownian particles in the vicinity of the interface. These induced random motions are in addition to the random motions caused by *direct* interactions between the Brownian particles and the molecules of the suspending fluid. Thus, the interface effects on the motion of Brownian particles are of two distinct types: first, *mechanical* effects due to the spatially modified hydrodynamic mobility and the interface relaxation back toward a flat configuration from the deformed shapes caused by the particle motion and second, nonequilibrium *thermodynamic* effects due to the fluctuating velocity fields caused by the random changes in the interface shape. In the next section, we first examine the

interface fluctuations due to random thermal impulses, and evaluate the corresponding velocity fields in order to determine the induced particle motions. This is done by employing nonequilibrium thermodynamics in combination with a capillary-wave model to describe the interface dynamics. Following that, we consider the second effect of interface deformation: namely, the modification in mean-square displacement due to the "elastic rebound" associated with the motion that is induced in the particle as the interface relaxes back toward equilibrium. We begin with the theory of nonequilibrium thermodynamics for the interface fluctuations.

III. Theory of Nonequilibrium Thermodynamics for Interface Fluctuations

Whilst considerable progress has been made over the last decade in understanding the equilibrium properties of the liquid-vapor interface (cf. Evans, 1981 and Buff, Lovett and Strillingger, 1965, and references therein), the macroscopic structure and thermodynamical properties of an interface between two immiscible fluids are relatively less well understood. One approach, in principle, to understanding the structure of the fluid-fluid interface would be to use the same type of detailed *microscopic* molecular theory that has been used widely in the study of liquid-vapor interface (cf. Teletzke, Scriven and Davis, 1982). In this present study, however, we approach the problem from a *macroscopic* statistical framework in order to develop physically appealing and mathematically tractable theory for systems of this type. Philosophically similar macroscopic statistical methods have been very successful in determining macroscopic properties of gases (e.g., the relationship between pressure and temperature in the system) that are identical to the results from the molecular kinetic theory. Further, essentially the same macroscopic method that we describe here has been the cornerstone of theoretical descriptions of the relevant dynamics of

Brownian motion. In particular, we adopt the conceptual idea of separating the phenomenon into two parts: one associated with rapid fluctuations with time scales characteristic of molecular motion, and the other associated with a much slower response time characteristic of viscous relaxation of the system. The objective of our study in this section is to determine the statistical properties of near equilibrium fluctuations of an interface between two immiscible fluids based on macroscopic statistical mechanics coupled with the concept of a fluctuation-dissipation principle as developed by Landau and Lifshitz (1959). According to the fluctuation-dissipation principle, the statistical properties of *nonequilibrium* fluctuations, linear in the external forces from a macroscopic point of view, can be related to equilibrium self-correlations. We thus begin our analysis by determining the *equilibrium* self-correlations of interface fluctuations.

A. Equilibrium Fluctuations

Before turning to the details of calculation referred to in Section I, we believe that it may be helpful to the reader to review briefly the fundamental foundations of classical statistical physics, that are relevant to the remainder of this chapter.

Nonequilibrium thermodynamics, which is a phenomenological macroscopic field theory concerned with states and processes in systems that are not in equilibrium, examines relaxation phenomena during the approach to equilibrium. The physical quantities describing a macroscopic body in equilibrium are, almost always, very nearly equal to their mean values. Nevertheless, deviations from the mean values (i.e., *fluctuations* around equilibrium), though small, are induced by opening a system to an external supply of energy or matter (Landau and Lifshitz, 1980). The relaxation processes, whether they are stationary

or time dependent, will always evolve with a positive entropy production, and the problem arises of determining the probability distribution of the deviations from equilibrium based upon a knowledge of the entropy change in the system.

Let us consider the equilibrium state of a thermodynamic system with a set $\{\Theta_n\}$ of linearly independent extensive variables. If the system is in contact with appropriate reservoirs, these extensive variables will not be constant but will fluctuate randomly around their equilibrium values owing to transfers to and from the reservoirs. These random variables denoted by $\{\tilde{\Theta}_n\}$ constantly fluctuate around the equilibrium state, $\{\Theta_n\}$. According to the postulational approach to thermodynamics (cf. Callen, 1960), there exists a function of the instantaneous extensive parameters of the system, $S(\tilde{\Theta}_n)$, called the instantaneous entropy, such that the probability distribution for the occurrence of fluctuations $\{\xi_n\}$ characterized by $\xi_n = \tilde{\Theta}_n - \Theta_n$ is given by

$$W(\xi) = \Omega \exp[\{\Delta S(\xi)/k_B\}] \quad (15)$$

where Ω is a normalization factor and ΔS denotes the entropy deviation, $S(\tilde{\Theta}_n) - S(\Theta_n)$, from the equilibrium value, which is a function of $\xi = (\xi_1, \xi_2, \dots, \xi_N)$. The relationship (15) is commonly known as the Einstein fluctuation formula (Einstein, 1910).

Before proceeding to examine the consequences of equation (15), let us consider its range of applicability. All the arguments leading to (15) tacitly assume that the quantity ξ behaves classically so that quantum effects are negligible. Landau and Lifshitz (1980) developed a condition which ensures that the formula (15) is applicable

$$T \gg \frac{h}{2\pi k_B \tau_\xi} \quad \text{or} \quad \tau_\xi \gg \frac{h}{2\pi k_B T} \approx (10^{-14} \text{ sec at } T = 300^\circ\text{K}) \quad (16)$$

in which h is the Planck constant and τ_ξ denotes a time scale that is charac-

teristic of the rate of change of the fluctuating quantity ξ . When the temperature T is too low or when the quantity ξ varies too rapidly (i.e., τ_ξ is too small), the fluctuations cannot be treated thermodynamically, and purely quantum fluctuations become of major significance.

Let us then turn to a thermodynamic system which is not at equilibrium (i.e., the state at which $\xi = \mathbf{0}$), and satisfies the conditions (16) so that the formula (15) is applicable. For sufficiently small fluctuations $\xi = (\xi_1, \xi_2, \dots, \xi_N)$ of the thermodynamic variables around the equilibrium state, the assumption of local equilibrium (cf. Kreuzer, 1981) can be used to expand the entropy $S(\tilde{\Theta}_n)$ of the system as a Taylor series about its equilibrium value $S(\Theta_n)$:

$$S(\tilde{\Theta}_n) = S(\Theta_n) + S_k(\Theta_n) \cdot \xi_k - \frac{1}{2} S_{km}(\Theta_n) \xi_k \xi_m + \dots \quad (17)$$

with

$$S_k(\Theta_n) = \left. \frac{\partial S}{\partial \tilde{\Theta}_k} \right|_{\tilde{\Theta} = \Theta_n} = \left. \frac{\partial S}{\partial \xi_k} \right|_{\xi = \mathbf{0}} = \left. \frac{\partial \Delta S}{\partial \xi_k} \right|_{\xi = \mathbf{0}}$$

and

$$S_{km}(\Theta_n) = - \left. \frac{\partial^2 S}{\partial \tilde{\Theta}_k \partial \tilde{\Theta}_m} \right|_{\tilde{\Theta} = \Theta_n} = - \left. \frac{\partial^2 S}{\partial \xi_k \partial \xi_m} \right|_{\xi = \mathbf{0}} = - \left. \frac{\partial^2 \Delta S}{\partial \xi_k \partial \xi_m} \right|_{\xi = \mathbf{0}}$$

Since the entropy has a maximum for $\xi = \mathbf{0}$, it follows that $S_k = 0$ and $S_{km} > 0$ near equilibrium. Neglecting all higher order expansion terms in (17), we can thus write

$$\Delta S(\xi) = S(\tilde{\Theta}_n) - S(\Theta_n) = - \frac{1}{2} S_{km} \xi_k \xi_m < 0. \quad (18)$$

The probability distribution for the fluctuation ξ is then given by (15) and (18), and its form can be seen to be Gaussian. Using (15), the expectation values of the near equilibrium variables can be shown to be

$$\langle \xi_k \rangle = 0 \tag{19}$$

and

$$\langle \xi_k \xi_m \rangle = \kappa_B S_{km}^{-1}. \tag{20}$$

Let us now apply these results to a system which consists of two immiscible Newtonian fluids 1 and 2 that are separated by an interface, as depicted in Figure 4. The surface of the interface is denoted as Π_s , defined by

$$\Pi_s \equiv x_3 - \eta(\mathbf{x}_s, t) = 0$$

where \mathbf{x}_s is a position vector representing points lying in a plane parallel to the undeformed, flat interface. In our model system, the shape function $\eta(\mathbf{x}_s, t)$ is envisioned as fluctuating around equilibrium, i.e., $\eta(\mathbf{x}_s, t) = 0$, due to the spontaneous random impulses from the surrounding fluids. Indeed, our objective in this section is to evaluate the autocorrelation function $\langle \eta^2(\mathbf{x}_s, t) \rangle$ of the interface fluctuation by determining the probability distribution of interface distortion, $\eta(\mathbf{x}_s, t)$, and utilizing the preceding general results, (19) and (20). The autocorrelation function $\langle \eta^2(\mathbf{x}_s, t) \rangle$ will in turn provide the statistical properties of the system at equilibrium necessary to calculate the random velocity field induced by the spontaneous fluctuations in interface shape. In order to determine the probability distribution of $\eta(\mathbf{x}_s, t)$, we thus need to be able to evaluate the entropy change due to the interface fluctuations.

The entropy change $\Delta S\{\eta(\mathbf{x}_s, t)\}$ associated with the interface distortion can be related to the free energy functional $A\{\eta(\mathbf{x}_s, t)\}$ corresponding to the distortion $\eta(\mathbf{x}_s, t)$ as:

$$\Delta S\{\eta(\mathbf{x}_s, t)\} = - \frac{A\{\eta(\mathbf{x}_s, t)\}}{T} \tag{21}$$

and thus the derivative of the entropy change with respect to the free energy is just $-1/T$, where T is the temperature of the system; the temperatures of fluids 1

and 2 are the same, since the system is assumed to be in equilibrium. The free energy functional $A\{\eta(\mathbf{x}_s, t)\}$ associated with the distortion $\eta(\mathbf{x}_s, t)$ is defined to be the isothermal reversible work necessary at equilibrium to impose the disturbance, i.e.,

$$A\{\eta(\mathbf{x}_s, t)\} = \frac{1}{2} \int_{\mathbf{x}_s} [(\Delta\rho)g\{\eta(\mathbf{x}_s, t)\}^2 + \gamma|\nabla_s\eta(\mathbf{x}_s, t)|^2] d\mathbf{x}_s. \quad (22)$$

Here, $\Delta\rho (= \rho_2 - \rho_1)$ is the density difference between fluids 1 and 2, ∇_s denotes the two-dimensional gradient operator on the plane defined by \mathbf{x}_s and γ is the surface tension between the two fluids. The first term in the integrand represents the free energy associated with the external acceleration due to gravity g and the second is associated with an increase in surface area. The required probability distribution for $\eta(\mathbf{x}_s, t)$ is thus

$$W\{\eta(\mathbf{x}_s, t)\} = \Omega \cdot \exp\left[-\frac{1}{2k_B T} \int_{\mathbf{x}_s} [(\Delta\rho)\{\eta(\mathbf{x}_s, t)\}^2 + \gamma|\nabla_s\eta(\mathbf{x}_s, t)|^2] d\mathbf{x}_s\right]. \quad (23)$$

The distribution (23) is a Gibbs (or canonical) distribution for the interface distortion (cf. Landau and Lifshitz, 1980, and Buff, Lovett and Stillinger, 1965). We now determine the autocorrelation function $\langle \eta^2(\mathbf{x}_s, t) \rangle$ using the probability distribution, (23), and the general results, (19) and (20). Since the integrand of (23) contains $|\nabla_s\eta(\mathbf{x}_s, t)|^2$, however, we cannot apply the results of (19) and (20) to evaluate the autocorrelation function $\langle \eta^2(\mathbf{x}_s, t) \rangle$ of the interface fluctuation $\eta(\mathbf{x}_s, t)$ directly from (23). We now proceed via an alternative approach of Landau and Lifshitz (1959) by resolving the arbitrary fluctuation $\eta(\mathbf{x}_s, t)$ into *independent* modes of a two-dimensional Fourier-transform

$$\eta(\mathbf{x}_s, t) = \int_{\mathbf{k}} \hat{\eta}(\mathbf{k}, t) \exp(i\mathbf{k} \cdot \mathbf{x}_s) d\mathbf{k}. \quad (24)$$

In this formulation, the disturbed surface is represented as a *collective coordinate* of decoupled surface harmonic waves, and the entropy change can also be

expressed in terms of the Fourier-transform variables,

$$\Delta S\{\hat{\eta}(\mathbf{k},t)\} = \frac{(2\pi)^{-2}}{2\kappa_B T} \int_{\mathbf{k}} \{\hat{\eta}(\mathbf{k},t)\}^2 \{(\Delta\rho)g + \gamma k^2\} d\mathbf{k}. \quad (25)$$

Here \mathbf{k} is the wave vector (i.e., the wave number $k = |\mathbf{k}|$), and $\hat{\eta}(\mathbf{k},t)$ is a Fourier component of $\eta(\mathbf{x}_s,t)$. Let us now replace the integral in (25) by a discrete sum for a large number of surface elements $\Delta\Pi_{\mathbf{k}}$ ($= \Delta k_1 \Delta k_2$) in the \mathbf{k} -plane:

$$\Delta S\{\hat{\eta}(\mathbf{k},t)\} = \frac{(2\pi)^{-2}}{2\kappa_B T} \sum_{\mathbf{k}} \{\hat{\eta}(\mathbf{k},t)\}^2 \{(\Delta\rho)g + \gamma k^2\} \Delta\Pi_{\mathbf{k}}. \quad (26)$$

Since each term in the sum depends only on the specific wave vector \mathbf{k} around which the surface element $\Delta\Pi_{\mathbf{k}}$ is taken, the fluctuations for two different wave vectors \mathbf{k} and \mathbf{k}' are statistically independent. Thus, the correlation of the fluctuations $\hat{\eta}(\mathbf{k},t)$ and $\hat{\eta}(\mathbf{k}',t)$ between two wave vectors \mathbf{k} and \mathbf{k}' is zero, i.e.,

$$\langle \hat{\eta}(\mathbf{k},t) \hat{\eta}(\mathbf{k}',t) \rangle = 0 \quad (27)$$

if the two quantities are taken in different surface elements $\Delta\Pi_{\mathbf{k}}$ and

$$\langle \hat{\eta}(\mathbf{k},t) \hat{\eta}(\mathbf{k},t) \rangle = (2\pi)^{-2} \frac{\kappa_B T}{\Delta\Pi_{\mathbf{k}}} \{(\Delta\rho)g + \gamma k^2\} \quad (28)$$

if the same surface is involved. The autocorrelation function, $\langle \{\hat{\eta}(\mathbf{k},t)\}^2 \rangle$ of (28), can be determined simply from the result of (20) combined with the summed form of (26). Passing now to the limit $\Delta\Pi_{\mathbf{k}} \rightarrow 0$, one can evidently write both these formulae together as

$$\langle \hat{\eta}(\mathbf{k},t) \hat{\eta}(\mathbf{k}',t) \rangle = (2\pi)^{-2} \kappa_B T \{(\Delta\rho)g - \gamma \mathbf{k} \cdot \mathbf{k}'\} \delta(\mathbf{k} + \mathbf{k}') \quad (29)$$

where $\delta(\mathbf{k} + \mathbf{k}')$ is the two-dimensional Dirac-delta function. The correlation function in terms of the position vector \mathbf{x}_s can then be evaluated by Fourier transformation of (29). The result is

$$\langle \eta(\mathbf{x}_s, t) \eta(\mathbf{x}_s', t) \rangle = \kappa_B T \int_{k_{\min}}^{k_{\max}} \frac{k J_0(rk)}{(\Delta\rho)g + \gamma k^2} dk \quad (30)$$

in which $r = |\mathbf{x}_s - \mathbf{x}_s'|$ and J_0 is the Bessel function of the first kind of order 0. The lower limit, k_{\min} , of possible wave numbers is inversely proportional to the largest length scale of the system and thus $k_{\min} \rightarrow 0$ if the interface is unbounded. The choice for an upper cutoff on wave number, k_{\max} , is somewhat arbitrary, and the present continuum treatment cannot make a rigorous identification of this quantity. However, in a theoretical treatment of a liquid-vapor interface, Buff et al. (1965) selected k_{\max} as being inversely proportional to the interface width, L_p , across which a sharp discontinuity in density may occur. In addition, thermodynamic perturbation theories have been developed for the study of a planar interface which show that the order of magnitude of L_p is approximately the same as the intermolecular length scale σ of surrounding molecules (cf. Evans, 1981), and in fact $L_p \approx 1.5\sigma \sim 3.0\sigma$.

The mean-square fluctuation, which provides a measure of the magnitude of interface distortion via spontaneous fluctuations, can be obtained readily from (30) with $r = 0$ and $k_{\min} = 0$:

$$\langle \{\eta(\mathbf{x}_s, t)\}^2 \rangle = \frac{\kappa_B T}{4\pi\gamma} \ln \left[1 + \frac{\gamma}{(\Delta\rho)g} k_{\max}^2 \right]. \quad (31)$$

It can be noted from (31) that the mean-square fluctuation $\langle \{\eta(\mathbf{x}_s, t)\}^2 \rangle$ becomes *magnified* as either the density difference or the surface tension between the two fluids becomes smaller. In fact, in the limit $\Delta\rho \rightarrow 0$, the auto-correlation function of $\eta(\mathbf{x}_s, t)$ diverges logarithmically. This *weak* divergence is related to the fact that $\eta(\mathbf{x}_s, t)$ characteristic of distortions of the interface is a symmetry breaking collective coordinate in terms of decoupled harmonic surface waves (i.e., the Fourier decomposition, (24), breaks down in this particular case of $\Delta\rho = 0$), which was also noted by Jhon, Desai and Dahler (1978). Jhon et

al. (1978) have developed the so-called memory function approach for interface dynamics and found that, associated with the symmetry breaking variable, $\eta(\mathbf{x}_s, t)$ is a propagating mode whose long-wave length dispersion relation is identical to the classical hydrodynamic result for capillary waves, i.e., $\omega(\mathbf{k}) = \{\gamma k^3 / \Delta\rho\}^{1/2}$ in which ω is the frequency of capillary waves. It then follows that capillary waves must always exist if a nonuniform density distribution exists (i.e., $\Delta\rho \neq 0$), even if $\gamma = 0$. It is noteworthy, in this context, that the mean-square fluctuation $\langle \eta^2(\mathbf{x}_s, t) \rangle$ approaches a finite limiting value, $\frac{\kappa_B T k_{\max}^2}{4\pi(\Delta\rho)g}$, as the surface tension between the two fluids vanishes (i.e., $\gamma \rightarrow 0$).

So far we have dealt only with fluctuations around the equilibrium state of the system using Gibbs *ensembles*, i.e., we have derived the equilibrium correlation functions for the interface distortion in terms of ensemble averages. According to the ergodic hypothesis (Landau and Lifshitz, 1980), however, ensemble averages yield the same results as *long-time* averages over the history of a single system providing the system is statistically stationary. Thus, we can regard the correlation functions in (29)-(31) as limiting time-average values with $t \rightarrow \infty$.

In the Section III.B, the time-dependent interface fluctuations and the corresponding velocity fields will be considered explicitly. The time-averages from these detailed time-dependent fluctuating fields must have the same long-time values (or forms) as calculated in the present section using the concept of an ensemble of near-equilibrium fluctuations (cf. Landau and Lifshitz, 1980, and Kreuzer, 1981).

B. Time Correlations and the Velocity Field Induced by Spontaneous Fluctuations in Interface Shape

The impulsive motion of a body surrounded by a "viscous" fluid is accom-

panied by frictional processes, which ultimately bring the motion to a stop. The kinetic energy of a Brownian particle, contributed by thermal *fluctuations* of the surrounding medium, is thereby converted into heat and is said to be *dissipated*. This is the basic concept of the fluctuation-dissipation theorem developed by Landau and Lifshitz (1959). A rigorous, purely mechanical treatment of such a motion is clearly impossible. Since the energy of macroscopic motion is converted to thermal energy of the molecules of the suspending fluid, such a treatment would require a solution of the equations of motion for all of these molecules. The problem of setting up an equivalent description, with a macroscopic scale of resolution proportional to the Brownian particle dimensions, is therefore a problem of statistical physics.

In our present system, it is the interface which fluctuates around the equilibrium flat configuration, and thereby generates velocity fields in fluids 1 and 2. In the presence of fluctuations, however, there are also spontaneous local stresses in the bulk fluids 1 and 2, which are not related to the velocity gradient; Landau and Lifshitz (1959) determined the statistical properties of these *random* stresses, including formulae for the correlation between the components of the stress tensor. Recently, Hauge and Martin-Löf (1973) and Hinch (1975) showed that the macroscopic framework with fluctuating stresses could provide a self-consistent theoretical description of Brownian motion. In their theories, the fluctuating stress acts on the particle through its divergence, which drives fluctuations in the *bulk* fluid and thence fluctuations in the viscous stress on the particle and relates the white noise $\mathbf{A}(t)$ in the bulk fluid, see equation (6), to the fluctuating stress in the surrounding fluid. It is the white noise contribution to the motion of Brownian particles, i.e., $\mathbf{A}(t)$, that will continue to be present even when the particle is far removed from the interface. The random force contribution on a Brownian particle due to interface fluctuations is in *addition*

to the white noise $\mathbf{A}(t)$ that derives from the fluctuating stresses in the bulk fluids. In the present section we thus determine the statistical properties of the fluctuating velocity fields in fluids 1 and 2 caused solely by spontaneous random changes in the interface shape. In our analysis, we introduce a fluctuating forcing function $y(\mathbf{x}_s, t)$ in the normal stress balance for the interface as the "energy source" for interface shape fluctuations.

The energy of the interface imparted by thermal impulses decays via viscous dissipation in the surrounding fluids, and this process is governed by a fluctuation-dissipation theorem (cf. Landau and Lifshitz, 1959). The construction of this fluctuation-dissipation theorem begins from a purely macroscopic description of the system, based upon the equations of motion for the fluctuating quantities, e.g., the interface position $\eta(\mathbf{x}_s, t)$, and the velocity and pressure fields ($\mathbf{u}^{(j)}, p^{(j)}$) in fluids j ($= 1$ and 2). The equations describing the fluid motions are simply the Navier-Stokes equations with appropriate boundary conditions. Provided the order of magnitude of the fluctuating velocity $\mathbf{u}^{(j)}$ is sufficiently small, as we shall assume here, we can neglect the convective inertia terms in these equations (see Section II of Chapter III), and we thus find that the fluid motion is described by the unsteady Stokes' equation plus the equation of continuity for each fluid j ($= 1$ and 2)

$$\rho_j \frac{\partial \mathbf{u}^{(j)}}{\partial t} = -\nabla p^{(j)} + \mu_j \nabla^2 \mathbf{u}^{(j)} \quad (32)$$

$$\nabla \cdot \mathbf{u}^{(j)} = 0, \quad (33)$$

The boundary conditions to be satisfied in dimensional form are the following:

$$\mathbf{u}^{(1)} \text{ and } \mathbf{u}^{(2)} \rightarrow \mathbf{0} \text{ as } |\mathbf{x}| \rightarrow \infty. \quad (34a)$$

At the surface of the interface, defined by $\Pi_s \equiv x_3 - \eta(\mathbf{x}_s, t) = 0$

$$\mathbf{u}^{(1)} = \mathbf{u}^{(2)} \quad (34b)$$

$$\mathbf{n} \cdot \mathbf{u}^{(1)} = \mathbf{n} \cdot \mathbf{u}^{(2)} = \frac{1}{|\nabla \Pi_s|} \frac{\partial \eta(\mathbf{x}_s, t)}{\partial t} \quad (34c)$$

$$[|\mathbf{t} \cdot \mathbf{n} \cdot \mathbf{T}|] = 0 \quad (34d)$$

and

$$[|\mathbf{n} \cdot \mathbf{n} \cdot \mathbf{T}|] = \gamma(\nabla \cdot \mathbf{n}) + (\Delta \rho) g \eta(\mathbf{x}_s, t) + y(\mathbf{x}_s, t). \quad (34e)$$

The parameters appearing in (34c)-(34e) are the unit outward pointing normal vector \mathbf{n} from fluid 2 (i.e., $\mathbf{n} = \nabla \Pi_s / |\nabla \Pi_s|$), the unit tangential vector, \mathbf{t} in the interface and a fluctuating forcing function $y(\mathbf{x}_s, t)$ which is introduced in this 'macroscopic theory' as the source of the interface fluctuations. The statistical properties of this *white noise* function $y(\mathbf{x}_s, t)$ will be discussed in detail shortly. Equations (34b) and (34d) are the conditions of continuity of velocity and tangential stress, respectively, while (34c) is the kinematic condition which relates the rate of change of the random displacement, $\eta(\mathbf{x}_s, t)$, to the normal velocities at the interface. The objective of the present analysis is to derive from equation (32)-(34e) a Langevin-type *stochastic* equation for the unknown fluctuation function $\eta(\mathbf{x}_s, t)$ which is driven by random forcing function $y(\mathbf{x}_s, t)$. A correct formulation of the stochastic equations ultimately requires that this forcing function (i.e., white noise) $y(\mathbf{x}_s, t)$ be chosen so that the interface fluctuations exhibit the correct equilibrium correlations (i.e., those from the equilibrium fluctuation theory of the preceding section) on taking the limit $t \rightarrow \infty$. The procedure for determining $y(\mathbf{x}_s, t)$ is very similar to the method used to specify the statistical properties of the white noise function $\mathbf{A}(t)$ in the Langevin equation (6) from the assumption of equipartition of energy at equilibrium (cf. Batchelor, 1976).

The problem represented by (32)-(34e) is, of course, both time-dependent and

highly nonlinear due to the fact that $\eta(\mathbf{x}_s, t)$ is unknown. As noted from (31), however, the magnitude of $\eta(\mathbf{x}_s, t)$ is very small and we can therefore linearize the terms in (34c) and (34e) to proceed analytically. The most effective approach to solving the resulting linearized problem is to apply the method of *normal modes*, whereby the small fluctuations $\eta(\mathbf{x}_s, t)$ are resolved into a complete set of normal modes. In particular, we resolve the arbitrary fluctuation $\eta(\mathbf{x}_s, t)$ into independent modes of the form:

$$\eta(\mathbf{x}_s, t) = \int_{\mathbf{k}} \int_{\omega} \hat{\eta}(\mathbf{k}, \omega) e^{i(\mathbf{k}\mathbf{x}_s - \omega t)} d\omega d\mathbf{k} \quad (35)$$

and it follows from this and equations (32)-(34e) that

$$(\mathbf{u}^{(i)}, p^{(i)}) = \int_{\mathbf{k}} \int_{\omega} \{\hat{\mathbf{u}}^{(i)}(\mathbf{x}_s; \mathbf{k}, \omega), \hat{p}^{(i)}(\mathbf{x}_s; \mathbf{k}, \omega)\} e^{i(\mathbf{k}\mathbf{x}_s - \omega t)} d\omega d\mathbf{k}. \quad (36)$$

In this formulation, the fluctuating variables $\eta(\mathbf{x}_s, t)$ and $(\mathbf{u}^{(i)}, p^{(i)})$ in the problem are being expanded in terms of the same Fourier-transform normal modes, $\hat{\eta}(\mathbf{k}, \omega)$ and $(\hat{\mathbf{u}}^{(i)}, \hat{p}^{(i)})$, that are usually employed in theories of linear dispersive wave motion and hydrodynamic stability. It can be seen that the normal mode, as usual, has an exponential dependence on time with a complex exponent.

On substituting the expressions (35) and (36) into equations (32) and (33) [i.e., applying the Fourier-transform directly to equations (32) and (33)], we obtain a system of ordinary differential equations for $\{\hat{\mathbf{u}}^{(i)}(\mathbf{x}_s; \mathbf{k}, \omega), \hat{p}^{(i)}(\mathbf{x}_s; \mathbf{k}, \omega)\}$ and $\hat{\eta}(\mathbf{k}, \omega)$. We adopt here the Squire (1933) transformation in order to reduce the three-dimensional fluctuation problem, i.e., $\hat{\mathbf{u}} = (\hat{u}^0, \hat{v}^0, \hat{w}^0)$ to an *equivalent* two-dimensional problem $\hat{\mathbf{u}} = (\hat{u}, 0, \hat{w})$. For this purpose, we transform the coordinate system by rotating the $x_1 - x_2$ plane about the x_3 -axis so that the new x_1 -axis has the same direction as the wave vector \mathbf{k} . Then the velocity field in the equivalent two-dimensional problem is given by $\hat{u} = \frac{k_1 \hat{u}^0 + k_2 \hat{v}^0}{k}$, $\hat{v} = 0$ and $\hat{w} = \hat{w}^0$ with the unit vector in the x_1 -direction defined by $\mathbf{e}^1 = \mathbf{k}/k$. The resulting

governing equations for $\hat{\mathbf{u}}^{(j)} = (\hat{u}^{(j)}, 0, \hat{w}^{(j)})$ and $\hat{\mathbf{p}}^{(j)}$ are as follows:

$$ik\hat{u}^{(j)} = -D\hat{w}^{(j)} \tag{37}$$

$$(D^2 - k^2)[i\omega\rho_j + \mu_j(D^2 - k^2)]\hat{w}^{(j)} = 0 \tag{38}$$

and

$$ik\hat{\mathbf{p}}^{(j)} = i\omega\rho_j\hat{\mathbf{u}}^{(j)} + \mu_j(D^2 - k^2)\hat{\mathbf{u}}^{(j)} \tag{39}$$

with D representing the differential operator $D = d/dx_3$. The general solution of equation (38) is a linear combination of the solutions $e^{\pm kx_3}$ and $e^{\pm \alpha_j x_3}$ [with $\alpha_j = (k^2 - 1\omega/\nu_j)^{1/2}$ and $\nu_j = \mu_j/\rho_j$]. Recalling the boundary condition (34a) which requires that $w^{(j)}$ must vanish both when $x_3 \rightarrow -\infty$ ($j = 2$, in the lower fluid) and $x_3 \rightarrow +\infty$ ($j = 1$, in the upper fluid), we can write

$$\hat{w}^{(1)}(x_3; \mathbf{k}, \omega) = A_1(\mathbf{k}, \omega)e^{-kx_3} + B_1(\mathbf{k}, \omega)e^{-\alpha_1 x_3}, \quad (x_3 > 0) \tag{40}$$

and

$$\hat{w}^{(2)}(x_3; \mathbf{k}, \omega) = A_2(\mathbf{k}, \omega)e^{kx_3} + B_2(\mathbf{k}, \omega)e^{\alpha_2 x_3}, \quad (x_3 < 0). \tag{41}$$

The velocity component $\hat{u}^{(j)}$ can also be evaluated by combining (37), (40) and (41). All that remains is to determine the coefficient functions $A_j(\mathbf{k}, \omega)$ and $B_j(\mathbf{k}, \omega)$ from the boundary conditions at the interface. Substituting the general solutions, $\hat{u}^{(j)}$ and $\hat{w}^{(j)}$, into the conditions of continuity of velocity, (34b), and tangential stress, (34d), we obtain a set of four simultaneous algebraic equations for the unknown functions A_j and B_j ($j = 1, 2$). The resulting solution is

$$A_j(\mathbf{k}, \omega) = \Phi_j(\mathbf{k}, \omega)\hat{\eta}(\mathbf{k}, \omega) \tag{42}$$

and

$$B_j(\mathbf{k}, \omega) = \Psi_j(\mathbf{k}, \omega)\hat{\eta}(\mathbf{k}, \omega) \tag{43}$$

in which

$$\Phi_j(\mathbf{k}, \omega) = \frac{i\omega\lambda^{j-1}\nu_j(\mathbf{k} + \alpha_j) + \nu_q(\alpha_q - \mathbf{k})\{2k^2\nu_j(\lambda - 1)(-1)^j + i\omega\lambda^{2-j}\}}{\nu_1(\mathbf{k} - \alpha_1) + \lambda\nu_2(\mathbf{k} - \alpha_2)} \quad (44)$$

and

$$\Psi_j(\mathbf{k}, \omega) = \frac{2i\omega k\lambda^{j-1}\nu_j - 2\nu_1\nu_2k^2(\lambda - 1)(-1)^j(\alpha_q - \mathbf{k})}{\lambda\nu_2(\alpha_2 - \mathbf{k}) + \nu_1(\alpha_1 - \mathbf{k})} \quad (45)$$

Here $\lambda (= \mu_1/\mu_2)$ is the viscosity ratio of the two fluids and the subscript q is defined by $q = j - (-1)^j$.

So far we have determined the Fourier components of the velocity and pressure field $(\hat{\mathbf{u}}^{(j)}, \hat{p}^{(j)})$ in each fluid in terms of the stochastic function $\hat{\eta}(\mathbf{k}, \omega)$ representing normal modes of the interface shape, which is related to the random forcing function $\hat{y}(\mathbf{k}, \omega)$ through the normal-stress balance across the interface according to equation (34e). To obtain the stochastic Langevin-type equation for $\hat{\eta}(\mathbf{k}, \omega)$, in terms of the random forcing function $\hat{y}(\mathbf{k}, \omega)$, we therefore substitute expressions for the stress components calculated from $(\hat{\mathbf{u}}^{(j)}, \hat{p}^{(j)})$ into (34e). The result is

$$[\hat{H}_1(\mathbf{k}, \omega)] \cdot \hat{\eta}(\mathbf{k}, \omega) = \hat{y}(\mathbf{k}, \omega) \quad (46)$$

If the function $\hat{H}_1(\mathbf{k}, \omega)$ is specified, the response $\hat{\eta}(\mathbf{k}, \omega)$ of the interface to the random force $\hat{y}(\mathbf{k}, \omega)$ is completely determined. The functional quantity $\hat{H}_1(\mathbf{k}, \omega)$, which is known as the *generalized susceptibility* (or system function), plays a fundamental part in the theory described below and is given by

$$\begin{aligned} \hat{H}_1(\mathbf{k}, \omega) = & \frac{i\omega}{k} \{ \rho_2 \Phi_2(\mathbf{k}, \omega) + \rho_1 \Phi_1(\mathbf{k}, \omega) \} \\ & - 2(\mu_2 - \mu_1) \{ k\Phi_2(\mathbf{k}, \omega) + \alpha_2\Psi_2(\mathbf{k}, \omega) \} - \{ (\Delta\rho)g + \gamma k^2 \}. \end{aligned} \quad (47)$$

The statistical properties of the fluctuating forcing function $\hat{y}(\mathbf{k}, \omega)$ must now be specified so that the statistical properties of the interface normal modes, $\hat{\eta}(\mathbf{k}, \omega)$, at equilibrium are the same as those derived in the preceding section via

equilibrium fluctuation theory, i.e., equations (28)-(30). Thus, for the fluctuating random force $\hat{y}(\mathbf{k},\omega)$, the following principal assumptions are made:

i. $\hat{y}(\mathbf{k},\omega)$ is independent of $\hat{\eta}(\mathbf{k},\omega)$,

ii. $\hat{y}(\mathbf{k},\omega)$ varies extremely rapidly compared to the variations of $\hat{\eta}(\mathbf{k},\omega)$.

The second assumption implies that time intervals of duration Δt_1 exist such that the expected variations in $\hat{\eta}(\mathbf{k},\omega)$ in period Δt_1 are very small while the number of fluctuations in $\hat{y}(\mathbf{k},\omega)$ is still very large. Thus, the fluctuating force $\hat{y}(\mathbf{k},\omega)$ appears as white noise (i.e., random and uncorrelated) on the time scale characteristic of variations of $\hat{\eta}(\mathbf{k},\omega)$:

$$\langle \hat{y}(\mathbf{k},\omega) \rangle = 0. \quad (48)$$

However, it is evident from (46) and (28) that the self-correlation of $\hat{y}(\mathbf{k},\omega)$ cannot be zero but must take the general form:

$$\langle y(\mathbf{x}_s,t)y(\mathbf{x}_s',t') \rangle = R_y(\mathbf{x}_s,\mathbf{x}_s')\delta(t-t') \quad (49a)$$

or

$$\langle \hat{y}(\mathbf{k},\omega)\hat{y}(\mathbf{k}',\omega') \rangle = \hat{R}_y(\mathbf{k},\mathbf{k}')\delta(\omega+\omega'). \quad (49b)$$

The unknown function R_y (or \hat{R}_y), which specifies the intensity of fluctuations in $y(\mathbf{x}_s,t)$ [or $\hat{y}(\mathbf{k},\omega)$], must be chosen so that we obtain the correct equilibrium correlation results. The very drastic nature of the *ad hoc* assumptions implicit in (48) and (49) lies in the presumption that the forces that the surrounding fluid molecules exert on the interface can be divided into two parts; one associated with *rapid* fluctuations $y(\mathbf{x}_s,t)$ with time scales characteristic of molecular motion, and the other associated with a much *slower* response time characteristic of viscous relaxation of the system. They are, however, made with reliance on physical intuition and an *a posteriori* justification based on the success of the hypothesis, which will be shown shortly.

In order to determine the functions R_y and \hat{R}_y by comparison with the equilibrium correlation function, (29), from the preceding section, we must solve (46) together with (47). Using white noise $\hat{y}(\mathbf{k}, \omega)$ with properties (48) and (49) as input into (46), we can evaluate the correlation function $\langle \hat{\eta}(\mathbf{k}, \omega) \hat{\eta}(\mathbf{k}', \omega') \rangle$ in terms of $\hat{R}_y(\mathbf{k}, \mathbf{k}')$ and $\hat{H}_I(\mathbf{k}, \omega)$. Then, from the Fourier inversion formula, it follows that $\langle \hat{\eta}(\mathbf{k}, t) \hat{\eta}(\mathbf{k}', t + t^0) \rangle$ can be expressed in the form:

$$\langle \hat{\eta}(\mathbf{k}, t) \hat{\eta}(\mathbf{k}', t + t^0) \rangle = \hat{R}_y(\mathbf{k}, \mathbf{k}') \int_{-\infty}^{\infty} \frac{e^{i\omega t^0} d\omega}{\hat{H}_I(\mathbf{k}, \omega) \hat{H}_I(\mathbf{k}', -\omega)} \quad (50)$$

It can be seen from (50) that the correlation function for $\hat{\eta}(\mathbf{k}, t)$ is independent of the present time t but depends only on the time difference t^0 , and thus satisfies the *invariance* of the equilibrium state under a time translation $t \rightarrow t'$ which is expected as a consequence of the hypothesis of microscopic reversibility in statistical physics. The unknown function $\hat{R}_y(\mathbf{k}, \mathbf{k}')$ can now be determined from (50) by setting $t^0 = 0$ and comparing the result with the equilibrium self-correlation function given by (29). From this, we see

$$\hat{R}_y(\mathbf{k}, \mathbf{k}') = \frac{\kappa_B T \delta(\mathbf{k} + \mathbf{k}') \{(\Delta\rho)g - \gamma \mathbf{k} \cdot \mathbf{k}'\}^{-1}}{(2\pi)^2 \left[\int_{-\infty}^{\infty} \frac{d\omega}{\hat{H}_I(\mathbf{k}, \omega) \hat{H}_I(\mathbf{k}', -\omega)} \right]} \quad (51)$$

The central importance of the fluctuation-dissipation theorem can now be grasped from equation (51). The left-hand side of (51) involves a correlation function which results from and is a measure of the magnitude of *spontaneous fluctuations* about the equilibrium state, i.e., of the ever-present thermal noise $y(\mathbf{x}_s, t)$. The response function on the right-hand side incorporates the macroscopic mechanical (i.e., dynamical) response when the system has been removed from equilibrium by the imposition of external forces or constraints. The fluctuation-dissipation theorem then says that the time-correlations of the *nonequilibrium* fluctuations, linear in the external forces, are related to and

can, indeed, be calculated from equilibrium self-correlations. Finally, with \hat{R}_y determined, we have all the statistical properties that are necessary to specify the system from a macroscopic point of view. In particular,

$$\langle \hat{y}(\mathbf{k}, \omega) \hat{y}(\mathbf{k}', \omega') \rangle = \frac{\kappa_B T \{ (\Delta \rho) g - \gamma \mathbf{k} \cdot \mathbf{k}' \}^{-1} \delta(\mathbf{k} + \mathbf{k}') \delta(\omega + \omega')}{(2\pi)^2 \left[\int_{-\infty}^{\infty} \frac{ds}{\hat{H}_I(\mathbf{k}, s) \hat{H}_I(\mathbf{k}', -s)} \right]} \quad (52)$$

and, thus

$$\langle \hat{\eta}(\mathbf{k}, \omega) \hat{\eta}(\mathbf{k}', \omega') \rangle = \frac{\kappa_B T \{ (\Delta \rho) g - \gamma \mathbf{k} \cdot \mathbf{k}' \}^{-1} \delta(\mathbf{k} + \mathbf{k}') \delta(\omega + \omega')}{(2\pi)^2 \left[\int_{-\infty}^{\infty} \frac{ds}{\hat{H}_I(\mathbf{k}, s) \hat{H}_I(\mathbf{k}', -s)} \right] \hat{H}_I(\mathbf{k}, \omega) \hat{H}_I(\mathbf{k}', \omega')} \quad (53)$$

The statistical properties of the random velocity fields $\hat{\mathbf{u}}^{(j)} = (\hat{\mathbf{u}}^{(j)}, 0, \hat{\mathbf{w}}^{(j)})$ associated with the interface disturbances can be evaluated readily from (37) and (40)-(45), i.e.,

$$\hat{\mathbf{u}}^{(j)} = (-1)^{j-1} \{ i \Phi_j(\mathbf{k}, \omega) e^{(-1)^j k x_3} + i \frac{\alpha_j}{k} \Psi_j(\mathbf{k}, \omega) e^{(-1)^j \alpha_j x_3} \} \hat{\eta}(\mathbf{k}, \omega) \quad (54)$$

and

$$\hat{\mathbf{w}}^{(j)} = \{ \Phi_j(\mathbf{k}, \omega) e^{(-1)^j k x_3} + \Psi_j(\mathbf{k}, \omega) e^{(-1)^j \alpha_j x_3} \} \hat{\eta}(\mathbf{k}, \omega) \quad (55)$$

along with the correlation function (53) for $\hat{\eta}(\mathbf{k}, \omega)$.

So far we have developed a general theory for the spontaneous "thermal" fluctuations of shape which occur in a real fluid interface, and determined the statistical properties of the fluctuating flow field $(\hat{\mathbf{u}}^{(j)}, \hat{\mathbf{p}}^{(j)})$ driven by the random boundary fluctuations, $\hat{\eta}(\mathbf{k}, \omega)$. Before concluding this section, we turn, for illustrative purposes, to a detailed evaluation of the correlation function, given by (53). It can be seen from (54) and (55) that the vorticity generated by the interface disturbances diffuses towards the interior of each fluid and the depth of penetration of the vorticity is of order $(\nu_j/\omega)^{1/2}$. Two important limiting cases

are thus possible; the length scale for vorticity penetration may be either large or small compared to the wave length $2\pi/k$. We consider only the case of $k^2 \gg \omega/\nu_j$, in which viscous effects on the interface relaxation cannot be neglected. In this asymptotic limit ($\omega/(\nu_j k^2) \ll 1$), we can expand the functions Φ_j and Ψ_j defined by (43) and (44) in the forms:

$$\Phi_j(\mathbf{k}, \omega) = k^2 \nu_j \left\{ 2 - i \frac{\omega}{k^2 \nu_j} + 0 \left[\left(\frac{\omega}{k^2 \nu_j} \right)^2 \right] \right\} \quad (56)$$

and

$$\Psi_j(\mathbf{k}, \omega) = k^2 \nu_j \left\{ -2 + 0 \left[\left(\frac{\omega}{k^2 \nu_j} \right)^2 \right] \right\} \quad (57)$$

and thus the susceptibility $\hat{H}_I(\mathbf{k}, \omega)$ of the system becomes

$$\hat{H}_I(\mathbf{k}, \omega) = (\Delta\rho)g + \gamma k^2 + i\omega k \left[\mu_2 \left\{ 2 - i \frac{\omega}{k^2 \nu_2} \right\} + \mu_1 \left\{ 2 - i \frac{\omega}{k^2 \nu_1} \right\} + 0 \left[\left(\frac{\omega}{k^2 \nu_j} \right)^2 \right] \right]. \quad (58)$$

It can be noted that the dynamical response of the system to an impulse, in this limit, contains an inertial contribution, $(\rho_1 + \rho_2)/k$, a viscous damping, contribution $2k(\mu_1 + \mu_2)$ and an elastic contribution, $(\Delta\rho)g + \gamma k^2$. Utilizing the general formula (51) together with $\hat{H}_I(\mathbf{k}, \omega)$ given by (58), we have

$$\hat{R}_y(\mathbf{k}, \mathbf{k}') = \pi^{-2} \kappa_B \Gamma(\mu_1 + \mu_2) \delta(\mathbf{k} + \mathbf{k}') \left\{ k + 0 \left[\frac{\omega}{\nu_j k^2} \right]^2 \right\} \quad (59)$$

comprising a fluctuation-dissipation theorem, for the particular limiting case $\omega/(\nu_j k^2) \ll 1$, relating the strengths of the random fluctuations $y(\mathbf{x}_s, t)$ to the macroscopic viscous forces, thereby reflecting their common origin in the interactions between the interface and the surrounding fluid molecules. Taking the inverse Fourier-transform of (53) combined with (58), we can also evaluate the correlation function

$$\langle \hat{\eta}(\mathbf{k}, t) \hat{\eta}(\mathbf{k}', t') \rangle = \frac{\kappa_B T \delta(\mathbf{k} + \mathbf{k}')}{(2\pi)^2 [(\Delta\rho)g - \gamma \mathbf{k} \cdot \mathbf{k}']} e^{-\zeta |\tau|} \left\{ \cos \sqrt{1 - \zeta^2} \tau + \frac{\zeta}{\sqrt{1 - \zeta^2}} \sin \sqrt{1 - \zeta^2} |\tau| + 0 \left[\frac{\omega}{k^2 \nu_j} \right]^2 \right\} \quad (60)$$

in which $\tau = (t' - t)/\tau_{I0}$ and $\zeta = \tau_{I0}/\tau_{IR}$. The time scales τ_{I0} and τ_{IR} are defined by

$$\tau_{I0}^{-1} = \omega_0 = \left\{ \frac{(\Delta\rho)gk + \gamma k^3}{\rho_1 + \rho_2} \right\}^{1/2} \quad (61)$$

and

$$\tau_{IR} = \frac{\rho_1 + \rho_2}{k^2(\mu_1 + \mu_2)} \quad (62)$$

Here, ω_0 is the *natural* frequency for interface oscillation in the absence of viscous friction, while τ_{IR} denotes the viscous relaxation time scale for the interface displacement on which the initial amplitude due to the impulse decays exponentially. It is noteworthy that, although the results (60)-(62) pertain to the limiting case in which $\omega/(\nu_j k^2) \ll 1$, the physics inherent in the description via ζ , τ_{I0} and τ_{IR} is preserved in the general case. The same exponential attenuation of capillary waves at the free surface of a body of liquid (i.e., $\mu_1 = 0$ and $\rho_1 = 0$) was predicted by Lamb (1932) from the fact that the loss of total energy (kinetic plus potential) of the liquid over one cycle is necessarily equal to the rate of viscous dissipation of energy per cycle, provided the net flux of energy into the volume of liquid concerned is zero. In Figure 5, the correlation function given by equation (60) is illustrated as a function of the dimensionless time difference τ for $\zeta = 0.2, 0.6, 1.0$ and 1.4 . It can be seen that the restoring process which drives the system back to a flat configuration exhibits three particular modes depending on the ratio ζ , of viscous forces to capillary elastic-response forces: an oscillatory damping ($\zeta < 1$), a critical damping ($\zeta = 1$) and underdamping ($\zeta > 1$).

This completes our study of the spontaneous fluctuations of interface shape that are caused by the thermal agitation in the surrounding fluids. In the next section, we shall consider motions of spherical Brownian particles due to the random flow field that is induced by these interface fluctuations.

IV. Brownian Motion near a Spontaneously Fluctuating Interface

In the previous section we studied and derived a fluctuation-dissipation theorem for spontaneous fluctuations of a fluid interface around its equilibrium configuration. In this section we will consider the motions of a nearby Brownian particle which occur as a consequence of the velocity field, (54) and (55), that is generated by these fluctuations.

In general, a Brownian particle near an interface will undergo random motions due to random fluctuating forces of two types: the first, which we shall denote as $\mathbf{F}_R(\mathbf{x};t)$, is caused by the boundary-driven random velocity field associated with spontaneous interface fluctuations, and the second, which we shall denote as $\mathbf{A}(t)$, is caused by random fluctuations in the molecular environment immediately adjacent to the particle. It is this latter contribution which will continue to be present even when the particle is far removed from the interface. In this section, we consider the motion of a spherical Brownian particle of radius a that is near a fluid interface. The usual supposition is that, for sufficiently small fluctuations, the independent random forces and the macroscopic time-evolution of particle momentum have to obey a linear law or a macroscopic rate equation of the Langevin type, i.e.,

$$\frac{d\mathbf{U}}{dt} + \mathbf{B}(t) \cdot \mathbf{U} = \mathbf{F}_R(\mathbf{x};t) + \mathbf{A}(t) \quad (63)$$

in which \mathbf{B} is a linear operator (called the Boussinesq operator) determined from the unsteady Stokes' equation such that $\mathbf{B} \cdot \mathbf{U}$ represents the time depen-

dent viscous forces including the virtual mass and Basset memory contributions, as well as, in principle, the hydrodynamic "wall" effects due to the presence of a nearby interface.

In the present section, we consider the motion which results from the random force $\mathbf{F}_R(\mathbf{x};t)$ that results from the fluctuating velocity field (54) and (55). In so doing, however, we consider only a first approximation in which we imagine the particle to be moving in the absence of direct hydrodynamic interactions with the interface. That is, we suppose that the particle moves as though it experienced the velocity field (54) and (55) in an infinite fluid domain. The analysis which follows therefore pertains to the case in which the random velocity field due to interface fluctuations is longer range than hydrodynamic interactions between the particle and the interface. It can be noted from (54) and (55) that the velocity field corresponding to a particular Fourier mode of the interface deformation decays exponentially on the scale of the wave length, k^{-1} . Thus, the range of significant induced particle motion by the random velocity field is $d \sim O(k^{-1})$. On the other hand, hydrodynamic "wall" effects owing to particle-interface interactions, are significant within the range of $d \sim O(a)$. Thus the conditions, in which we can neglect the hydrodynamic wall effects but still have significant induced motion of the Brownian sphere, are simply $ka \ll 1$ and $a/d \ll 1$. In this case, we can evaluate the random force $\mathbf{F}_R(\mathbf{x};t)$ corresponding to the velocity field (54) and (55) using the generalization of Faxen's (1921) law to an arbitrary time-dependent unbounded flow that was derived in Chapter III.

We begin by taking the Fourier-transform of the Langevin equation (63) to obtain

$$[\hat{H}_U(\omega)]\hat{U}(d;\mathbf{k},\omega) = \hat{F}_R(d;\mathbf{k},\omega) + \hat{A}(\omega) \quad (64)$$

in which the susceptibility for the particle motion is given by

$$\hat{H}_U(\omega) = -\omega i + \frac{6\pi\mu_2 a}{m} \left\{ 1 + a\sqrt{\omega\lambda(2\nu_2)} (1-i) \right\} - \frac{2\pi\rho_2 a^3 \omega}{3m} i. \quad (65)$$

The Fourier component of the random force $\hat{F}_R(\mathbf{k},\omega)$ determined from the generalized Faxen's law, (58) of Chapter III, is given by

$$\hat{F}_R(d;\mathbf{k},\omega) = \frac{6\pi\mu_2 a}{m} \left\{ 1 + a\sqrt{\omega\lambda(2\nu_2)} (1-i) \right\} [\hat{U}^\infty(\mathbf{k},\omega)]_0^s - \frac{2\pi a^3 \rho_2 \omega}{m} i [\hat{U}^\infty(\mathbf{k},\omega)]_0^v. \quad (66)$$

Here, $[\]_0^s$ and $[\]_0^v$ denote the average values of the quantity in the bracket over the sphere surface and volume, respectively, and each component of the undisturbed velocity $\hat{U}^\infty = (\hat{u}^{(2)}(\mathbf{k},\omega), 0, \hat{w}^{(2)}(\mathbf{k},\omega))$ is defined by (54) and (55). Since the velocity field $\hat{U}^\infty(\mathbf{k},\omega)$ can be divided into two parts, i.e., $\hat{U}^\infty = \hat{U}_p^\infty + \hat{U}_h^\infty$, an irrotational part \hat{U}_p^∞ which satisfies the Laplace's equation and a rotational part \hat{U}_h^∞ which is governed by the Helmholtz equation, it is convenient to utilize the mean value theorems associated with these differential equations in order to evaluate the average values in (66). Indeed, by defining the weighting factors for the Helmholtz equation as follows:

$$W_s(\omega) = \frac{\sin a\sqrt{\omega i \nu_2}}{a\sqrt{\omega i \nu_2}} \quad (67)$$

$$W_v(\omega) = \frac{\sin a\sqrt{\omega i \nu_2} - a\sqrt{\omega i \nu_2} \cos a\sqrt{\omega i \nu_2}}{a^3(\omega i \nu_2)^{3/2}}, \quad (68)$$

We see that the average velocities in (66) can actually be evaluated completely in terms of the local undisturbed velocities at the location of the sphere center, i.e., $[\hat{U}_p^\infty]_0$ and $[\hat{U}_h^\infty]_0$

$$[\hat{U}^\infty]_0^s = [\hat{U}_p^\infty]_0 + W_s(\omega)[\hat{U}_h^\infty]_0 \quad (69)$$

and

$$[\hat{U}^{\infty}]_0 = [\hat{U}_p^{\infty}]_0 + W_v(\omega)[\hat{U}_R^{\infty}]_0 \quad (70)$$

Since the random fluctuating forces \hat{F}_R and \hat{A} are not correlated (i.e., $\langle \hat{F}_R \hat{A} \rangle = 0$) and the problem is linear, we can consider the contribution of the random force \hat{F}_R in (64) independently of the white noise \hat{A} . We thus examine the net effect of random fluctuations of the interface configuration on the motions of a spherical Brownian particle by determining the velocity correlation of a Brownian sphere that is freely immersed in the fluctuating velocity field driven by the spontaneous interface distortions. Then, the particle velocity correlation function will, in turn, determine the net diffusion coefficient of the Brownian particle associated with the random force F_R . First, we now evaluate the particle velocity correlation function $\hat{R}_U(d; \mathbf{k}, \mathbf{k}', \omega, \omega') = \langle \hat{U}(d; \mathbf{k}, \omega) \hat{U}(d; \mathbf{k}', \omega') \rangle$ by solving the Langevin equation (64) for each mode of random force $\hat{F}_R(d; \mathbf{k}, \omega)$

$$\hat{R}_U(d; \mathbf{k}, \mathbf{k}', \omega, \omega') = \frac{\hat{F}_F(d; \mathbf{k}, \mathbf{k}', \omega, \omega')}{\hat{H}_U(\omega) \cdot \hat{H}_U(\omega')} \quad (71)$$

and then relating the required statistics of the random force (i.e., the correlation function \hat{R}_F for the random force \hat{F}_R) to the statistical properties, (52) and (53), of the interface fluctuations. The correlation function for the random force \hat{F}_R can be determined from the generalized Faxen's law of (66) together with the random velocity field (54) and (55) which is related to the random stochastic fluctuations $\hat{\eta}(\mathbf{k}, \omega)$ by (53). The resulting expression in terms of the correlation function for $\hat{\eta}(\mathbf{k}, \omega)$ is simply

$$\hat{R}_F(d; \mathbf{k}, \mathbf{k}', \omega, \omega') = \langle \hat{F}_R(d; \mathbf{k}, \omega) \hat{F}_R(d; \mathbf{k}', \omega') \rangle = \hat{G}(d; \mathbf{k}, \omega) \langle \hat{\eta}(\mathbf{k}, \omega) \hat{\eta}(\mathbf{k}', \omega') \rangle \quad (72)$$

in which each component of the tensor \hat{G} can be obtained from (53)-(55) combined with (66). Taking the inverse Fourier transform of (72) with respect to \mathbf{k} and \mathbf{k}' , and utilizing the properties of the Dirac δ -function, we get

$$\hat{R}_F(d; \omega, \omega') = \frac{\kappa_B T}{2\pi} \int_{\mathbf{k}} \frac{\hat{G}(d; \mathbf{k}, -\mathbf{k}, \omega, -\omega) \{(\Delta\rho)g + \gamma k^2\} \delta(\omega + \omega') k d k}{\left[\int_{-\infty}^{\infty} \frac{ds}{|\hat{H}_I(\mathbf{k}, s)|^2} \right] \cdot |\hat{H}_I(\mathbf{k}, \omega)|^2} \quad (73)$$

Thus, the particle velocity correlation function $\langle U(d; t)U(d; t + t^0) \rangle$, which relates the present particle velocity to its velocities at other times, can be determine from (71) and (73), i.e.,

$$R_U(d; t^0) = \langle U(d; t)U(d; t + t^0) \rangle = \int_{-\infty}^{\infty} \frac{\hat{R}_F(d; \omega, -\omega) e^{i\omega t^0}}{|\hat{H}_U(\omega)|^2} d\omega \quad (74)$$

It can be seen from (74) that the velocity correlation function $R_U(d; t^0)$ is independent of the present time t and depends only on the time difference t^0 between the present time and other times as a consequence of the time-translational invariance of the equilibrium state (cf. Kreuzer, 1981). Equations (71) and (74) are two versions of the famous fluctuation-dissipation theorem; the correlation function \hat{R}_F is defined with reference to the equilibrium state of the system and contains statistical information about the spontaneous random force fluctuating at equilibrium. The fact that the velocity correlation $R_U(t^0)$ has to do with energy dissipation in a fluctuating system was already proved in the theory of Brownian motion in an unbounded single fluid domain (Hauge and Martin-Löf, 1973, and Hinch, 1975). In order to show the fluctuation-dissipation theorem and the statistical properties of the motions of the Brownian sphere in the presence of the random velocity field due to interface fluctuations, we now calculate one component $\langle U_3(d; t)U_3(d; t + t^0) \rangle$ of the velocity correlation function R_U . From (53)-(54) together with (66), we can determine the corresponding component \hat{G}_{33} of \mathbf{G} in (73)

$$\hat{G}_{33}(d; \mathbf{k}, \omega) = \frac{1}{m^2} \left[6\pi\mu_2 a \left\{ 1 + a\sqrt{\omega/(2\nu_2)} (1 - i) \right\} - 2\pi\rho_2 a^3 i \omega \right] \Phi_2(\mathbf{k}, \omega) e^{-kd}$$

$$+ [6\pi\mu_2a \left\{ 1 + a\sqrt{\omega/(2\nu_2)} (1-i) \right\} W_s(\omega) - 2\pi\rho_2a^3i\omega W_v(\omega)] \Psi_2(\mathbf{k},\omega) e^{-\alpha_2 d} \Big|^2. \quad (75)$$

Since equation (75) contains the terms $e^{-\alpha_j d}$, $\Phi_j(\mathbf{k},\omega)$ and $\Psi_j(\mathbf{k},\omega)$, which are defined by (44) and (45) and functions of the complex variables $\alpha_j = \left[k^2 - \frac{i\omega}{\nu_j} \right]_{j=1,2}$, it is not possible to derive analytically an *explicit* expression for the particle velocity correlation from the general formula (74). In order to proceed analytically, there are two possible asymptotic limits corresponding to the relative importance of viscous damping forces on the interface relaxation compared to the capillary forces (i.e., $k^2 \gg \frac{\omega}{\nu_j}$ or $k^2 \ll \frac{\omega}{\nu_j}$). In the weak dissipation limit (i.e., $k^2 \ll \frac{\omega}{\nu_j}$), however, the amplitude of interface fluctuations caused by an initial impulse sustains and does not decay since the viscous damping effects are negligible. We thus consider the asymptotic limit ($k^2 \gg \frac{\omega}{\nu_j}$) in which the length scale characteristic of the vorticity diffusion from the interface is very large compared to the wave length of the interface fluctuation so that the viscous effects are important. In this asymptotic limit, $k^2 \gg \frac{\omega}{\nu_j}$, there exist two limiting cases depending upon the relative magnitude of the particle radius a compared to the length scale of vorticity penetration generated by the particle motions, i.e. $\nu_2/(\omega a^2) \gg 1$ (or $\ll 1$).

(i). Velocity Correlation Function for the Limiting Case of $\nu_2/(\omega a^2) \gg 1$

Let us first consider the limiting case, $\nu_2/(\omega a^2) \gg 1$ and $\nu_2 k^2/\omega \gg 1$, in which viscous effects have a significant influence on both the particle motion and the interface fluctuation. Taking the limit of $\nu_2/(\omega a^2) \gg 1$ in (67) and (68), we can easily show that

$$\lim_{\substack{\omega a^2 \\ \nu_2} \rightarrow 0} W_s(\omega), W_v(\omega) \rightarrow 1 \quad (76)$$

and thus from (65) and (75) we have

$$\hat{G}_{33}(d; \mathbf{k}, \omega) = 36\pi^2 m^{-2} \mu_2^2 a^2 \omega^2 e^{-2dk} \quad (77)$$

and

$$\hat{H}_U(\omega) = i\omega + \beta \quad \text{with} \quad \beta = \frac{6\pi\mu_2 a}{m} \quad (78)$$

We now utilize the result of (53) for the correlation function of the interface displacement function $\hat{\eta}(\mathbf{k}, \omega)$, which in combination with (77) and (78), will determine the correlation functions for the random force \hat{F}_R and the velocity \hat{U}

$$\langle \hat{F}_{R_3}(d; \mathbf{k}, \omega) \hat{F}_{R_3}(d; \mathbf{k}', \omega') \rangle = \frac{36\kappa_B T \mu_2^2 (\mu_1 + \mu_2) k^3 a^2 \omega^2 \delta(\mathbf{k} + \mathbf{k}') e^{-2dk}}{m^2 (\rho_1 + \rho_2) \left[(\omega^2 - \omega_0^2)^2 + \left(\frac{\omega}{2\tau_{IR}} \right)^2 \right]} \quad (79)$$

and

$$\langle \hat{U}_3(d; \mathbf{k}, \omega) \hat{U}_3(d; \mathbf{k}', \omega') \rangle = \frac{\langle \hat{F}_{R_3}(d; \mathbf{k}, \omega) \hat{F}_{R_3}(d; \mathbf{k}, \omega) \rangle}{(\omega^2 + \beta^2)} \quad (80)$$

Let us now take the inverse Fourier transform with respect to ω and ω' in order to calculate the time correlations

$$\begin{aligned} \langle \hat{F}_{R_3}(d; \mathbf{k}, t) \hat{F}_{R_3}(d; \mathbf{k}', t + \tau) \rangle &= \frac{9\kappa_B T \mu_2^2 a^2 k \delta(\mathbf{k} + \mathbf{k}') e^{-2dk}}{m^2 (\rho_1 + \rho_2)} \\ &\cdot e^{-\zeta|\tau|} \left[\cos\sqrt{1 - \zeta^2} \tau - \frac{\zeta}{\sqrt{1 - \zeta^2}} \sin\sqrt{1 - \zeta^2} |\tau| \right] \end{aligned} \quad (81)$$

$$\langle \hat{U}_3(d; \mathbf{k}, t) \hat{U}_3(d; \mathbf{k}', t + \tau) \rangle = \frac{9\kappa_B T \mu_2^2 a^2 \delta(\mathbf{k} + \mathbf{k}') e^{-2dk}}{m^2 [(\Delta\rho)g + \gamma k^2] [4\lambda_{a\omega}^2 \zeta^2 - (\lambda_{a\omega}^2 + 1)^2]}$$

$$\cdot \left[2\zeta\lambda_{a\omega} e^{-\lambda_{a\omega}|\tau|} - (1 + \lambda_{a\omega}^2) e^{-\zeta|\tau|} \left[\cos\sqrt{1 - \zeta^2} \tau + \frac{1 - \lambda_{a\omega}^2}{1 + \lambda_{a\omega}^2} \cdot \frac{\zeta}{\sqrt{1 - \zeta^2}} \sin\sqrt{1 - \zeta^2} |\tau| \right] \right] \quad (82)$$

in which $\lambda_{a\omega} \left(= \frac{\tau_{I0}}{\tau_{vp}} \right)$ is the ratio of the time scale for the interface fluctuation

(i.e., ω_0^{-1}) to that of the viscous relaxation of the particle velocity, τ is the dimensionless time difference, i.e., $\tau = (t' - t)/\tau_{10}$ and $\zeta = \tau_{10}/\tau_{1R}$ [cf. (61) and (62)]. The nature of the response, in this limiting case in which $\nu_2/(\omega a^2) \gg 1$ and $\nu_2 k^2/\omega \gg 1$, can be understood most clearly by plotting (81) and (82) as shown in Figures 6 and 7, where the correlation functions for \hat{F}_{R_3} and \hat{U}_3 are given as a function of τ for the same values of the parameter ζ as in the previous Figure 4. It can be seen from Figure 6 that the force on the sphere that is generated by the random impulse of the interface decays exponentially on the same viscous dissipation time scale, $\tau_{1R}(= (\rho_1 + \rho_2) / (k^2(\mu_1 + \mu_2)))$, as the amplitude $\hat{\eta}(\mathbf{k}, t)$ of the interface distortion. The viscous damping of the force on the particle can be characterized by three typical modes depending on ζ (i.e., the ratio of viscous forces to elastic-response forces) as can be expected from the result of (60), and the *frequency* of the oscillatory damping case ($\zeta < 1$) is exactly the same as the frequency of the interface oscillation. The force correlation lags behind the interface fluctuation. The phase lag φ_F is always negative

$$\varphi_F = -2 \tan^{-1} \left(\frac{\zeta}{\sqrt{1 - \zeta^2}} \right) \quad (83)$$

and dependent on the ratio of the two intrinsic forces of the system [i.e., $\varphi_F(\zeta \rightarrow 0) = 0$ and $\varphi_F(\zeta \rightarrow 1) = -\pi$]. The velocity correlation function indicates that the energy imparted to a particle by each thermal impulse on the interface decays exponentially on the two independent time scales, τ_{1R} on which the amplitude η and the induced force \hat{F}_{R_3} decay, and $\tau_{VP}(= m/(6\pi\mu_2 a))$ characteristic of the viscous relaxation time for motions of Brownian particles in an unbounded fluid. Thus the correlation functions of (80) and (81) constitute the fluctuation-dissipation theorem for the motion of a Brownian sphere due to the spontaneous fluctuations of a nearby fluid interface. They relate the spontaneous fluctuations in interface shape caused by the thermal white noise to the viscous

dissipation due to the corresponding motions of the surrounding fluids. From (82) we can evaluate the phase lag φ_U for the velocity response of the particle to the interface oscillations

$$\varphi_U = -\tan^{-1} \left(\frac{\xi}{\sqrt{1-\xi^2}} \right) + \tan^{-1} \left(\frac{1-\lambda_{a\omega}^2}{1+\lambda_{a\omega}^2} \cdot \frac{\xi}{\sqrt{1-\xi^2}} \right). \quad (84)$$

However, the velocity oscillates with the same frequency as the force and interface fluctuations. Recently, Chaplin (1984) experimentally measured forces acting on a horizontal cylinder with radius a which is located at a distance $d = 2a \sim 5a$ from the undeformed plane of a free surface which is executing wave motions with the range of the dimensionless wave number, $ka = 0.146 \sim 0.824$. The existence of phase lags in the fluctuating force and the particle velocity with respect to the phase of the incident waves, which has been predicted in the present analysis, was demonstrated by the experimental data of Chaplin. It should be noted, however, that the present analysis is based on the condition, $ka \ll 1$ and $a/d \ll 1$, in order to neglect the hydrodynamic wall effect due to the particle-interface interactions.

(ii). Velocity Correlation Function for the Limiting Case of $\nu_2/(\omega a^2) \ll 1$

Now, consider the other limiting case, $\nu_2/\omega a^2 \ll 1$ and $\nu_2 k^2/\omega \gg 1$. In this case viscous effects on the particle can be neglected since the frequency ω is large enough to make the vorticity boundary layer very small. By taking the limit $\nu_2/(\omega a^2) \ll 1$ in (85), we find the susceptibility $\hat{H}_U(\omega)$ for the particle motion

$$\hat{H}_U(\omega) = -\omega i - \frac{2\pi\rho_2 a^3 \omega i}{3m} \quad (85)$$

and, with the vanishing weighting functions (i.e., $W_s(\omega), W_v(\omega) \rightarrow 0$),

$$\hat{G}_{33}(d; \mathbf{k}, \omega) = 16\pi^2 m^{-2} \mu_2^2 a^2 \omega^2 \left\{ (ka)^4 + \left(\frac{a^2 \omega}{2\nu_2} \right)^2 \right\} e^{-2dk}. \quad (86)$$

Utilizing (73) and (74), we can determine the correlation functions for the *induced* force on the particle caused by the interface fluctuations and for the particle velocity

$$\begin{aligned} \langle \hat{F}_{R_3}(d; \mathbf{k}, t) \hat{F}_{R_3}(d; \mathbf{k}', t + \tau) \rangle &= \frac{\kappa_B T \mu_2^2 a^2 k \delta(\mathbf{k} + \mathbf{k}') e^{-2dk}}{m^2(\rho_1 + \rho_2)} \\ &\cdot \left[\frac{4\xi \delta(\tau)}{\lambda_{\nu_2}^2} + \left\{ 4(ak)^4 + \frac{1 - 4\xi^2}{\lambda_{\nu_2}^2} \right\} e^{-\xi|\tau|} \right. \\ &\cdot \left. \left[\cos\sqrt{1 - \xi^2} \tau - \left\{ \frac{4(ak)^4 \lambda_{\nu_2}^2 + 3 - 4\xi^2}{4(ak)^4 \lambda_{\nu_2}^2 + 1 - 4\xi^2} \right\} \frac{\xi}{\sqrt{1 - \xi^2}} \sin\sqrt{1 - \xi^2} |\tau| \right] \right] \end{aligned} \quad (87)$$

and

$$\begin{aligned} \langle \hat{U}_3(d; \mathbf{k}, t) \hat{U}_3(d; \mathbf{k}', t + \tau) \rangle &= \frac{\kappa_B T \mu_2^2 a^2 \delta(\mathbf{k} + \mathbf{k}') e^{-2dk}}{(m + m')^2 [(\Delta\rho)g + \gamma k^2]} \\ &\cdot \left\{ \frac{1 + 4(ka)^4 \lambda_{\nu_2}^2}{\lambda_{\nu_2}^2} \right\} e^{-\xi|\tau|} \left[\cos\sqrt{1 - \xi^2} \tau + \left\{ \frac{4(ka)^4 \lambda_{\nu_2}^2 - 1}{4(ka)^4 \lambda_{\nu_2}^2 + 1} \right\} \right. \\ &\cdot \left. \frac{\xi}{\sqrt{1 - \xi^2}} \sin\sqrt{1 - \xi^2} |\tau| \right] \end{aligned} \quad (88)$$

in which m' is the virtual mass of the Brownian sphere (i.e., $m' = \frac{2\pi a^3 \rho_2}{3}$). It can be seen from (87) that the force acting on the particle, induced by the thermal impulse on the interface, exhibits a delta function $\delta(\tau)$ -response at the initial instant, and then decays exponentially on the time scale $\tau_{R} (= (\rho_1 + \rho_2) \lambda (\mu_2 + \mu_1) k^2)$. The exponential decay on the time scale τ_{R} is a consequence of the fact that the amplitude of interface displacement due to the thermal impulse decays exponentially on τ_{R} in the limiting case of $\nu_2 k^2 / \omega \gg 1$, which has been considered in detail in Section III.B [cf. (60)]. The initial $\delta(\tau)$ -response in (87) is due to the virtual mass contribution to the force on the

particle which exhibits a δ -function response to the sudden change in the flow velocity, i.e., when a sphere is brought instantaneously into uniform motion $\mathbf{U} = U\mathbf{e}_1$, the impulsive drag on the sphere at $\tau = 0$ is $\frac{2\pi}{3}\rho a^3 U \delta(\tau)\mathbf{e}_1$ due to the virtual mass effect. In the previous case of $\nu_2/(\omega a^2) \gg 1$ and $\nu_2 k^2/\omega \gg 1$, the parameter λ_{ω}^{-1} ($= a^2 \omega_0/\nu_2$) characteristic of the virtual mass contribution to the total force is sufficiently small that the impulsive response did not appear in the final result (81). The correlation function (88) shows that the particle velocity will decay exponentially on the same time scale τ_{IR} as the fluctuating force and the interface displacement η . In this limiting case, $\nu_2/(\omega a^2) \ll 1$ and $\nu_2 k^2/\omega \gg 1$, the velocity correlation of (88) does not exhibit the viscous relaxation of the particle velocity [i.e., $e^{-\lambda_{\omega}\tau}$ decay in (82)], since the viscous friction force is very small compared with the virtual mass and fictitious body force contributions to the total force on the particle.

So far we have determined the *general* formulae of the correlation functions, (73) and (74), for the fluctuating force induced on the particle and for the particle velocity, respectively. We have also derived explicitly, in the asymptotic cases of $\nu_2/(\omega a^2) \gg 1$ and $\nu_2 k^2/\omega \gg 1$ and of $\nu_2/(\omega a^2) \ll 1$ and $\nu_2 k^2/\omega \gg 1$, the fluctuation-dissipation theorem for the interface fluctuations and the particle motion.

Let us now turn to the *general* expression for the velocity correlation function, equation (74), in order to consider the effect of interface fluctuations caused by the thermal noise of surrounding molecules on the Brownian diffusion of particles in the vicinity of the interface. As we mentioned earlier, the relaxation of the interface distortion, η , back toward the equilibrium configuration is very rapid and the displacement η after receiving a thermal impulse decays exponentially on the time scale τ_{IR} ($\sim 10^{-8}$ sec in water). Further, the correla-

tion functions of (82) and (88) show that the relaxation of the particle velocity is exponentially rapid on the time scales τ_{vp} and τ_{IR} characteristic of the viscous relaxation of particle motion and of the interface relaxation. In a time interval Δt which is very large compared to the relaxation time scales τ_{IR} and τ_{vp} (i.e., $\Delta t \gg \tau_{IR}, \tau_{vp}$), the motion of a particle can therefore be viewed as random and the mean square displacement $\langle |\mathbf{x}(t)|^2 \rangle$ and the Brownian diffusivity \mathbf{D} are related at equilibrium (i.e., $t \rightarrow \infty$) according to

$$\mathbf{D} = \lim_{t \rightarrow \infty} \frac{1}{2} \frac{d}{dt} \langle |\mathbf{x}(t)|^2 \rangle \quad (89)$$

Recalling the fact that the time differential is commuted with the ensemble averaging and the displacements written as integrals of the velocity from the initial zero conditions (i.e., $\mathbf{x}(0) = \mathbf{0}$), it follows that

$$\mathbf{D}(d) = \int_0^\infty \langle \mathbf{U}(d;t) \mathbf{U}(d;t+t^0) \rangle dt^0 \quad (90)$$

in which the integrand is the velocity correlation function $\mathbf{R}_U(d;t^0)$ given by (74). The diffusivity, being the time integral of $\mathbf{R}_U(d;t^0)$, is immediately recognized as $\lim_{\omega \rightarrow 0} \hat{\mathbf{R}}_U(d;\omega)$ which is the Fourier transform of the velocity correlation, that is, the spectral density function at frequency $\omega = 0$. Utilizing (74), we thus have

$$\mathbf{D}(d) = \lim_{\omega \rightarrow 0} \pi \left[\frac{\hat{\mathbf{R}}_F(d;\omega, -\omega)}{|\hat{\mathbf{H}}_U(\omega)|^2} \right] \quad (91)$$

In this low frequency limit, the functions $\Phi_j(\mathbf{k}, \omega) = 2k^2 \nu_j$, $\Psi_j(\mathbf{k}, \omega) = -2k^2 \nu_j$, and the susceptibility for the interface fluctuations $\hat{\mathbf{H}}_I(\mathbf{k}, \omega) = -[(\Delta\rho)g + k^2\gamma]$. Thus we can readily evaluate the diffusion coefficient by substituting the various functions into (73) and (74). The result is

$$\mathbf{D} = \mathbf{0} \quad (92)$$

The fact that the diffusion coefficient turns out to be identically equal to *zero*

implies that the fluctuating velocity field caused by the random distortion of an interface does not produce any *net* rate of change of mean-square particle displacement. Thus, the Brownian diffusion coefficient for spherical particles near a fluid interface can be determined from the Langevin equation (63) without considering the induced force term $\mathbf{F}_R(\mathbf{x};t)$, in spite of the fact that the velocity correlation function is altered by the presence of the fluctuating force. One possible explanation of the present result, (92), stems from the linear theory of plane progressive waves which predicts that at any fixed point the fluid speed remains constant, while the direction of fluid motion rotates with angular velocity ω . Thus, a particle of fluid displaced by the waves moves through a circular orbit and the time average of *net* displacement is identically zero in the linear theory, since the second order [in the wave amplitude, $O(\eta^2)$] mean Stokes' drift in the direction of the wave propagation can be neglected in the low frequency limit, $\omega \rightarrow 0$. In the low frequency limit, which represents almost steady motion, the trajectories of a Brownian sphere are exactly the same as those of the fluid particle, provided the effects of hydrodynamic interaction with the interface are neglected. It is noteworthy that the present result for the diffusivity, i.e., equation (92) is based on the fluctuating force field determined from the generalization of Faxen's law to include the effects of time-dependent local inertia of the flow on the fluctuating force, but without taking into account the hydrodynamic interaction effect associated with the presence of an interface. The force covariance $\hat{\mathbf{R}}_F$ in (91) therefore pertains to the case in which $ka \ll 1$ and $a/d \ll 1$ so that we can neglect the hydrodynamic "wall" effect due to the particle-interface interactions while still having significant induced motion of the particle by the random change in interface configuration. In order to extend the present results to include the hydrodynamic wall effects, it would be necessary to generalize Faxen's law to take into account the hydrodynamic interactions

between the particle and the interface. However, this is not done here.

Up to now, we have considered the motions of Brownian particles in the fluctuating velocity field induced by the random spontaneous changes in interface shape owing to thermal impulses from the surrounding fluid. We have, in addition, determined the various covariance functions and the corresponding effect on the diffusion coefficient. A second effect, noted earlier in Section II, of interface deformability, is that the interface will also deform as a consequence of the impulsive motion of the Brownian particles that occur due to direct random forces of the type that would exist even if the fluid interface were absent. Although the deformation will be small, corresponding to the small displacements on the inertial time scale τ_{vp} of a Brownian particle caused by the thermal impulses, the displacement induced in the particle by the relaxation of the interface back towards equilibrium may be of the same order of magnitude as that initially caused by the impulse. In Section V, we will examine the effect of this relaxation process on the Brownian diffusion of the particle, applying the general solution obtained in Section III to describe the relaxation of deformed interface.

V. Brownian Motion near a Deformable Interface

The motion of particles in the presence of a fluid interface is, in general, nonlinear and depends on the prior history of the particle motion and of the interface deformation. This nonlinear interface deformation problem cannot be solved exactly (except by numerical methods) but can be solved approximately by linearizing the boundary conditions at the interface in the case of sufficiently small deformations. It is obvious that the difficulty arising from the time-dependence of the interface shape can be resolved by considering limiting cases corresponding to either very slow or very rapid particle motion. In particular, if

the process of interface deformation is very slow relative to the time scale characteristic of particle motion, then the interface will not be able to deform significantly and remains arbitrarily close to flat at all times. At the other end of the spectrum, if the time scale for particle motion is very long compared to an intrinsic time scale for interface deformation, the interface shape at any instant will be the steady equilibrium form, in which $\mathbf{u} \cdot \mathbf{n} = 0$ at the interface. In the analysis which follows the two bulk phase fluids are assumed to occupy the domain $x_3 > 0$ (fluid 1) and $x_3 < 0$ (fluid 2) as depicted in Figure 8. A uniform bulk concentration (i.e., number density) gradient is presumed to be maintained at the constant value parallel to the bounding interface and to be characterized by a macroscopic length scale $L \gg a$. This gives rise to a steady flux of Brownian particles in a direction normal to the interface; one-dimensional description is therefore appropriate. Analysis of this normal mode of diffusion transport has been motivated both by potential important applications in the fields of aerosol and hydrosol deposition, and also as models for transient, nonequilibrium adsorption processes.

Let us consider the consequences of small deformations caused by *rapid* random motions of Brownian sphere *normal* to the interface, since the random Brownian displacement, $\sqrt{\langle |\Delta \mathbf{x}|^2 \rangle}$, of a sphere is only about $10^{-2} a \sim 10^{-3} a$ in the very short fluctuation time τ_{vp} of the particle velocities. In view of the infinitesimal displacement corresponding to an impulse on the inertial time scale τ_{vp} characteristic of the motions of a Brownian particle, we can assume that the relevant hydrodynamic mobility is that associated with a flat, but deforming interface. In this limiting case, the equations governing the motion in each fluid are then the quasi-steady creeping motion equation and the equation of continuity. Since the deformation is sufficiently small, the boundary conditions at the interface can be linearized as:

$$\mathbf{n} \cdot \mathbf{u}^{(1)} = \mathbf{n} \cdot \mathbf{u}^{(2)} = \frac{\partial \eta(\mathbf{x}_s, t)}{\partial t} \quad (93)$$

$$[|\mathbf{n} \cdot \mathbf{T}|] = \mathbf{0} \quad (94)$$

plus the continuity condition of tangential velocities.

Recently, O'Neill and Ranger (1983) derived a solution to the problem posed when a rigid sphere normally approaches an interface between two immiscible viscous fluids by utilizing a general solution of Stokes' equation, plus the continuity equation in terms of the fundamental eigensolutions for bipolar coordinates (ξ, θ, σ) which can be related to the cylindrical coordinates (r, θ, x_3) by

$$x_3 = \frac{c \sinh \xi}{\cosh \sigma - \cos \xi} \quad \text{and} \quad r = \frac{c \sin \xi}{\cosh \sigma - \cos \xi} \quad (95)$$

Each coefficient of the eigenfunction has been determined by satisfying the boundary condition at the sphere surface [i.e., $\sigma = \sigma_0 = -\cosh^{-1}(d/a)$], the condition of vanishing velocity at infinity, together with the conditions (93) and (94) at the interface which we can identify with the coordinate surface $\xi = 0$. Thus, the solution pertains to the limiting case, in which the interface remains arbitrarily close to flat at all times albeit with $\mathbf{u} \cdot \mathbf{n} \neq 0$ due to the particle motion, and can be applied to the present study. According to O'Neill and Ranger's solution, the stream function ψ in fluid II is given by

$$\psi_2 = c^2 (\cosh \sigma - \cos \xi)^{-3/2} \sum_{n=1}^{\infty} W_n(\sigma) Q_{n+1}(\cos \xi) \quad (96)$$

where $Q_{n+1}(\cos \xi)$ is the Gegenbauer polynomial of order $(n+1)$ and degree $-\frac{1}{2}$ and $W_n(\sigma)$ is determined from the boundary conditions. From this solution (96), the normal component of velocity at the surface of interface can be found which is the first approximation to the rate at which the surface is *deforming*. It follows that the first approximation to the nonzero deformation can then be obtained by integrating the kinematic condition (93).

We now consider the first order approximation for the interface shape by calculating the velocity at the interface from the solution of (96). The velocity

component $w = \frac{U}{r} \frac{\partial \psi_2}{\partial r}$ can be evaluated readily, and utilizing

$$c \frac{\partial}{\partial r} = - \left\{ \sin \xi \cdot \sinh \sigma \frac{\partial}{\partial \sigma} + (1 - \cos \xi \cdot \cosh \sigma) \frac{\partial}{\partial \xi} \right\} \quad (97)$$

$$c \frac{\partial}{\partial x_3} = \left\{ (1 - \cosh \sigma \cdot \cos \xi) \frac{\partial}{\partial \sigma} - \sin \xi \cdot \sinh \sigma \frac{\partial}{\partial \xi} \right\}, \quad (98)$$

we have the maximum velocity component w_{\max} corresponding to the largest displacement η_{\max} of the interface, as shown in Figure 8:

$$w_{\max} = \frac{\partial \eta_{\max}}{\partial t} = -2\sqrt{2} U \sum_{n=1}^{\infty} (-1)^n H_n(d). \quad (99)$$

Here U is the magnitude of the particle velocity and H_n is defined by

$$H_n(\sigma_0) =$$

$$\frac{\sqrt{2} n(n+1) [(1 + \lambda) \{ (2n+1)^2 \sinh^2 \sigma_0 - (2n+1) \sinh 2\sigma_0 + 2 \} + 2(1 - \lambda) e^{-(2n+1)\sigma_0}]}{(2n-1)(2n+3) [4 \{ \cosh(n + \frac{1}{2})\sigma_0 - \lambda \sinh(n + \frac{1}{2})\sigma_0 \}^2 + (1 - \lambda^2)(2n+1)^2 \sinh^2 \sigma_0]} \quad (100)$$

The effects of hydrodynamic interaction between the particle and the interface are contained in the complicated function $H_n(d)$ (i.e., $H_n \rightarrow 0$ as $d \rightarrow \infty$) in (99).

Thus, in order to proceed analytically to illustrate the qualitative nature of these effects, we will expand H_n in terms of the small ε ($= a/d \ll 1$) assuming that the particle is not closer than a few radii from the interface. The result is

$$w_{\max} = \frac{\partial \eta_{\max}}{\partial t} = \frac{3}{1 + \lambda} U \varepsilon \left\{ 1 - \frac{9}{8} \cdot \frac{1 - \lambda}{1 + \lambda} \cdot \varepsilon - \frac{1}{3} \varepsilon^2 + \left[\frac{9}{8} \cdot \frac{1 - \lambda}{1 + \lambda} \cdot \varepsilon \right]^2 + O(\varepsilon^3) \right\}. \quad (101)$$

The kinematic condition (101) provides a relationship between the particle velocity and the maximum deformation rate, w_{\max} , of the interface. The maximum displacement η_{\max} caused by a thermal impulse can then be obtained by

integrating (101).

$$\eta_{\max} = \frac{3}{1+\lambda} \sqrt{\kappa_B \Gamma / \pi} \tau_{vp} \cdot \varepsilon \left\{ 1 - \frac{9}{8} \cdot \frac{1-\lambda}{1+\lambda} \cdot \varepsilon - \frac{1}{3} \varepsilon^2 + \left(\frac{9}{8} \cdot \frac{1-\lambda}{1+\lambda} \cdot \varepsilon \right)^2 + O(\varepsilon^3) \right\}. \quad (102)$$

In (102), the viscous relaxation time τ_{vp} ($= 1/\beta = m/C_D$) is a function of the distance d between the sphere center and the interface, and the drag coefficient C_D in this case is given by

$$C_D = \frac{\sqrt{2}}{3} (1+\lambda) \sinh \sigma_0 \sum_{n=1}^{\infty} H_n. \quad (103)$$

Again, utilizing an asymptotic expansion for H_n in terms of small ε and

$\sinh \sigma_0 = -\frac{1}{\varepsilon} + \frac{1}{2} \varepsilon + O(\varepsilon^2)$, we can show that

$$C_D = 6\pi\mu_2 a \left[1 - \frac{9}{8} \cdot \frac{1-\lambda}{1+\lambda} \cdot \varepsilon + \left(\frac{9}{8} \cdot \frac{1-\lambda}{1+\lambda} \cdot \varepsilon \right)^2 \right] + O(\varepsilon^3). \quad (104)$$

The effect of the viscosity ratio, λ , on the drag coefficient in the presence of a deforming interface is clearly evident in (104) for the limiting case in which the interface is instantaneously flat. In particular, for $\lambda = 1$ the instantaneous values of $\mathbf{u} \cdot \mathbf{n}$ along the interface are identical to the values which would exist along the same plane for sphere motion in a single unbounded fluid domain. As a consequence, the instantaneous fluid motion is unaffected by the interface and the drag coefficient is identically equal to Stokes' drag coefficient $6\pi\mu_2 a$. For values of $\lambda < 1$, on the other hand, the drag for a sphere near a flat, deforming interface is decreased as the sphere moves closer to the interface, while for $\lambda > 1$ the drag is increased under the same conditions. These results are all a consequence of the fact that the normal velocity given by (101) at the interface is smaller for $\lambda > 1$ and larger for $\lambda < 1$ than it would be on the same plane if the sphere were moving through single unbounded fluid. Thus, the drag for a flat, but deforming interface is highly sensitive to the viscosity ratio λ between

two fluids.

Since the energy imparted by the thermal noise is dissipated very rapidly with respect to the averaging time scale Δt , the particle motion due to thermal agitation can be regarded as an impulsive fluctuation source for interface displacements. In Section III, we developed a general solution for the attenuation of capillary waves on an interface. From this solution, the time variation of wave amplitude can be written as

$$\eta(\tau) = \eta_{\max} e^{-\zeta\tau} \left[\cos\sqrt{1-\zeta^2}\tau + \frac{\zeta}{\sqrt{1-\zeta^2}} \sin\sqrt{1-\zeta^2}\tau \right]. \quad (105)$$

From (72) and (75) combined with (105), the force acting on the sphere can be evaluated as

$$\mathbf{F} = -6\pi\mu_2 a \omega_0 \eta_{\max} e^{-kd} \frac{e^{-\zeta\tau}}{\sqrt{1-\zeta^2}} \sin\sqrt{1-\zeta^2}\tau \mathbf{e}_3. \quad (106)$$

It can be seen from (105) and (106) that the interface displacement and the associated force decays exponentially on the same time scale $\tau_{\text{IR}} \left[= \frac{\rho_1 + \rho_2}{k^2(\mu_1 + \mu_2)} \right]$ characteristic of the interface relaxation back toward the equilibrium flat configuration which has been studied in detail in Section III. Solving the Langevin equation for motion of the particle under the action of fluctuating force \mathbf{F} given by (106), we can readily evaluate the velocity correlation function of the particle as

$$R_U(d;\tau) = \langle U(t)U(t+\tau) \rangle = - \frac{\beta\eta_{\max}\omega_0^2 e^{-kd} \sqrt{\kappa_B T / \pi n}}{(\zeta\omega_0 - \beta)^2 + (1 - \zeta^2)\omega_0^2} \left[e^{-\lambda_{\text{av}}|\tau|} - e^{-\zeta|\tau|} \left\{ \cos\sqrt{1-\zeta^2}\tau + \frac{\zeta\omega_0 - \beta}{\sqrt{1-\zeta^2}\omega_0} \sin\sqrt{1-\zeta^2}\tau \right\} \right]. \quad (107)$$

Thus, the energy of the Brownian particle will be dissipated by the irreversible frictional processes of both the exponential viscous relaxation of the particle

velocity on the time scale $\tau_{vp}(=m/C_D)$ which would be $m/(6\pi\mu_2a)$ in an unbounded single fluid and of the interface relaxation on the time scale τ_{IR} . In Figure 9, the velocity correlation function $R_V(d;\tau)$ is plotted as a function of the dimensionless time difference τ for $\zeta = 0.2, 0.6, 1.0$ and 1.4 , $\lambda = 1$ and $d/a = 3$. As we can anticipate from the previous results in Section III, the viscous relaxation of the particle velocity exhibits the three typical modes depending on the values of ζ (i.e., oscillatory damping for $\zeta < 1$, critical damping for $\zeta = 1$, and underdamping for $\zeta > 1$). It is obvious from (101) that the interface displacement due to the impulsive motion of a Brownian particle is decreased as the viscosity ratio λ becomes higher since the normal velocity at the interface is smaller. As a consequence, the magnitude of the particle velocity induced by the interface relaxation back to the flat configuration is decreased for the higher viscosity ratio λ , which is illustrated in Figure 10 for $\zeta = 0.2$ and $d/a = 3.0$. But, the particle mobility is also decreased so that the initial impulsive displacement will also be smaller. Perhaps the *relative* importance of the relaxation process is not so highly decreased in the limit of high viscosity ratio.

It is important to realize that the solution of (107) contains the Einstein-Smoluchowski theory [i.e., (1) and (2)] for the Brownian diffusion process as a limiting case when $\Delta t \gg \tau_{vp}$ and τ_{IR} , so that the non-Markovian effects can be negligible in the averaging time Δt (cf. Hauge and Martin-Löf, 1973). Under these circumstances, we can simply evaluate the Einstein-Smoluchowski diffusion coefficient from (90) combined with (107)

$$D = \frac{\kappa_B T}{C_D} \left[1 - \frac{3}{1+\lambda} e^{-kd} \left\{ 1 - \frac{9}{8} \cdot \frac{1-\lambda}{1+\lambda} \cdot \varepsilon + \left[\frac{9}{8} \cdot \frac{1-\lambda}{1+\lambda} \cdot \varepsilon \right]^2 - \frac{1}{3} \varepsilon^2 \right\} \right] + O(\varepsilon^4) \quad (108)$$

where the drag coefficient C_D is given by (104). We now consider, in detail, the condition $\Delta t \gg \tau_{vp}$ and τ_{IR} for validity of the Einstein-Smoluchowski equation (1) with the diffusion coefficient D of (108). The time scales τ_{vp} and τ_{IR} , on which

the particle velocity and the interface displacement relax exponentially, are approximately determined as

$$\tau_{vp} \approx 0 \left(\frac{2\rho_p a^2}{9\mu_2} \right) \quad (109)$$

$$\tau_{IR} \approx 0 \left(\frac{(\rho_1 + \rho_2)}{(\mu_1 + \mu_2)} a^2 \right) \quad (110)$$

Thus, we can certainly choose an averaging time scale Δt which is much smaller than the observation time interval [$\approx 0(1 \text{ sec})$] but still very large compared to τ_{vp} and τ_{IR} which are $0(\sim 10^{-8} \text{ sec})$ in usual systems of Brownian particles in water.

In Figure 11, the diffusion coefficient D given in (108) is illustrated as a function of the separation distance d between the interface and the sphere center for viscosity ratios $\lambda = 0.0, 0.5, 1.0, 5.0$ and 10.0 . As is obvious from (108), the diffusion coefficient is either increased or decreased by the presence of an interface depending on the viscosity ratio λ and the particle position relative to the interface. For $\lambda = 1$, although drag coefficient C_D is unchanged by the nearly flat, deforming interface, the *displacement* induced in the particle by the interface relaxation back toward equilibrium is increased as the particle moves closer to the interface. As a consequence, the diffusion coefficient, which approaches $\kappa_B T / (6\pi\mu_2 a)$ as $d \rightarrow \infty$, is decreased as the separation distance becomes smaller. For values of $\lambda < 1$, on the other hand, the diffusion coefficient is greater than it would be in a single unbounded fluid for larger separation distances due to the spatially modified drag coefficient. However, for smaller separation distances, the dominant effect of the interface relaxation again causes the diffusivity to decrease. When the viscosity ratio is greater than one, the presence of an interface yields very low mobility (i.e., higher drag) for the particle motion and thus the diffusion coefficient is always less than

$\kappa_B T / (6\pi\mu_2 a)$.

This completes our illustrative calculations of the diffusion coefficient using the solutions of particle motion near a deforming interface in combination with the fundamental solutions developed in Sections III and IV. Before concluding this work, it is worth commenting that the scope of the analysis can be extended readily to study the Brownian motion of a drop or any deformable body (cf. Zotovskiy and Lisy', 1983). It is expected from the present results that the relaxation of shape fluctuations could contribute an effective impulse to the particle so that the rate of change of the mean-square displacement is either increased or decreased by the shape fluctuations. In general, the surface of a drop can be expressed in terms of the spherical coordinates (r, θ, φ) so that the instantaneous shape is given by an eigenfunction expansion of the radial distance r from the origin in the form

$$r = a \left\{ 1 + \varepsilon \sum_{l,n} \alpha_{ln} Y_{ln}(\theta, \varphi) e^{-i\omega t} \right\}. \quad (111)$$

Here Y_{ln} is the normalized spherical surface harmonic of order l, n which is defined in terms of the Legendre polynomial $P_l(\cos\theta)$ of order l as

$$Y_{ln}(\theta, \varphi) = (1 - \cos^2\theta)^{n/2} \frac{d^n P_l(\cos\theta)}{d(\cos\theta)^n} e^{in\varphi} \quad (112)$$

with

$$l = 0, 1, 2, 3, \dots \quad \text{and} \quad n = 0, \pm 1, \pm 2, \dots, \pm l.$$

Thus, for each choice of l , there exist $(2l+1)$ modes of the shape fluctuations. The fluctuations for the values $l = 0$ and 1 , however, are impossible for an incompressible drop and the smallest possible mode of drop surface oscillations is a quadrupole (or ellipsoidal) deformation corresponding to the $l = 2$ mode. Now, for convenience, we consider the simplest case in which the drop surface

executes oblate (or prolate) spherical fluctuations. Utilizing the incompressible condition, we can readily evaluate the coefficient matrix α_{ln} in the general expression (111) for $l = 2$. Further, the free energy functional $A(\varepsilon)$ for the shape fluctuations can also be evaluated from the reversible work against surface tension that is necessary to impose the disturbances ε at equilibrium

$$A(\varepsilon) = \frac{7\pi}{3} \gamma a^2 \varepsilon^2 . \quad (113)$$

Following the general procedures described in Section III, we have the average values of ε and ε^2 as follows:

$$\langle \varepsilon \rangle = 0 \quad (114)$$

$$\langle \varepsilon^2 \rangle = \frac{3\kappa_B \Gamma}{14\pi\gamma a^2} . \quad (115)$$

In order to derive the time-correlation function $\langle \varepsilon(t)\varepsilon(t + \tau) \rangle$, which will in turn provide the solution of the shape relaxation problem, we must develop an appropriate fluctuation-dissipation formula by following the general procedures presented in this work, thus solving the hydrodynamic flow problems of both the interior and exterior to the drop.

References

1. Alder, B. J. and Wainwright, T. E. 1967 *Phys. Rev. Lett.* **18**, 988.
2. Batchelor, G. K. 1976 Developments in microhydrodynamics. In *Theoretical and Applied Mechanics*, ed. W. Koiter, North Holland.
3. Brenner, H. and Leal, L. G. 1977 *J. Colloid Interface Sci.* **62**, 238.
4. Brenner, H. and Leal, L. G. 1982 *J. Colloid Interface Sci.* **88**, 136.
5. Buff, F. P., Lovett, R. A. and Stillinger, F. H. 1965 *Phys. Rev. Lett.* **15**, 621.
6. Callen, H. B. 1960 *Thermodynamics*. Wiley, New York.
7. Chandrasekhar, S. 1943 *Rev. Modern Phys.* **15**, 1.
8. Chaplin, J. R. 1984 *J. Fluid Mech.* **147**, 449.
9. Einstein, A. 1905 *Ann. Phys.* **17**, 549.
10. Einstein, A. 1910 *Ann. Phys.* **33**, 1275.
11. Evans, R. 1981 *Mol. Phys* **42**, 1169.
12. Faxen, H. 1921 Dissertation, Uppsala University.
13. Gotoh, T. and Kaneda, Y. 1982 *J. Chem. Phys.* **76**, 3193.
14. Hauge, E. H. and Martin-Löf, A. 1973 *J. Stat. Phys.* **7**, 259.
15. Hinch, E. J. 1975 *J. Fluid Mech.* **72**, 499.
16. Jhon, M. S., Desai, R. C. and Dahler, J. S. 1978 *J. Chem. Phys.* **68**, 5615.
17. Kreuzer, H. J. 1981 *Nonequilibrium Thermodynamics and its Statistical Foundations*. Oxford University Press, Oxford.
18. Lamb, H. 1932 *Hydrodynamics*. Dover, New York.
19. Landau, L. D. and Lifshitz, E. M. 1959 *Fluid Mechanics*, Pergamon Press, New

York.

20. Landau, L. D. and Lifshitz, E. M. 1980 *Statistical Physics - Part I*. Pergamon Press, New York.
21. Langevin, P. 1908 *C. R. Acad. Sci.* **146**, 530.
22. Larson, R. S. 1982 *J. Colloid Int. Sci.* **88**, 487.
23. Lee, S. H., Chadwick, R. S. and Leal, L. G. 1979 *J. Fluid Mec.* **93**, 705.
24. Lee, S. H. and Leal, L. G. 1980 *J. Fluid Mec.* **98**, 193.
25. Lee, S. H. and Leal, L. G. 1982 *J. Colloid Interface Sci.* **87**, 81.
26. O'Neill, M. E. and Ranger, K. B. 1983 *Phys. Fluid* **26**, 2035.
27. Rahman, A. 1964 *Phys. Rev. A* **136**, 405.
28. Squire, H. B. 1933 *Proc. Roy. Soc. London Ser. A* **142**, 621.
29. Teletzke, G. F., Scriven, L. E. and Davis, H. T. 1982 *J. Colloid Interface Sci.* **87**, 550.
30. Whitham, G. B. 1974 *Linear and Nonlinear Waves*. Wiley-Interscience, New York.
31. Yang, S.-M. and Leal, L.G. 1983 *J. Fluid Mech.* **136**, 393.
32. Yang, S.-M. and Leal, L.G. 1984 *J. Fluid Mech.* **149**, 275.
33. Zatovsky, A. V. and Lisy, V. 1983 *Physica* **119A**, 369.

Figure Captions

Figure 1. Definition sketch for a planar interface. The instantaneous coordinates of the center of the Brownian sphere are $\mathbf{x} \equiv (x_1, x_2, x_3)$ and the points lying in a plane parallel to the interface are conveniently represented by the planar position vector $\mathbf{x}_s = x_1 \mathbf{e}_1 + x_2 \mathbf{e}_2$.

Figure 2. Dimensionless diffusion coefficients, $\frac{D_{11}}{\kappa_B T / (6\pi\mu_2 a)}$ (or $\frac{D_{22}}{\kappa_B T / (6\pi\mu_2 a)}$) and $\frac{D_{33}}{\kappa_B T / (6\pi\mu_2 a)}$, as a function of the separation distance d/a ; ---, for D_{11} (or D_{22}); —, for D_{33} .

Figure 3. Dimensionless diffusion coefficients, $\frac{D_{11}}{\kappa_B T / (4\pi\mu_2 l \varepsilon)}$, as a function of the orientation angle θ ; the aspect ratio of the circular cylindrical slender body $\kappa = 100$ (i.e., $\varepsilon = 0.1887$); —, for $d/l = 1.01$; ----, for $d/l = 2.0$; - - - -, for an unbounded single fluid case.

Figure 4. Schematic sketch of the fluctuating interface and a Brownian sphere.

Figure 5. Dimensionless correlation function $\frac{\langle \hat{\eta}(\mathbf{k}, t) \hat{\eta}(\mathbf{k}', t) \rangle}{\kappa_B T \delta(\mathbf{k} + \mathbf{k}') / [(2\pi)^2 \{(\Delta\rho)g + \gamma k^2\}]}$, as a function of the dimensionless time difference τ .

Figure 6. Dimensionless correlation function $\frac{\langle \hat{F}_{R_3}(d; \mathbf{k}, t) \hat{F}_{R_3}(d; \mathbf{k}', t + \tau) \rangle}{9\kappa_B T \mu_2^2 a^2 \kappa \delta(\mathbf{k} + \mathbf{k}') e^{-2d\kappa} / [m^2(\rho_1 + \rho_2)]}$, as a function of the dimensionless time difference τ .

Figure 7. Dimensionless correlation function $\frac{\langle \hat{U}_3(d; \mathbf{k}, t) \hat{U}_3(d; \mathbf{k}', t + \tau) \rangle}{9\kappa_B T \mu_2^2 a^2 \delta(\mathbf{k} + \mathbf{k}') e^{-2d\kappa} / [m^2 \{(\Delta\rho)g + \gamma k^2\} (2\lambda_{\alpha\omega} \zeta + \lambda_{\alpha\omega}^2 + 1)]}$, as a function of the dimensionless time difference τ for $\lambda_{\alpha\omega} = 2.0$.

Figure 8. Schematic sketch of the geometry of the problem when a sphere approaches a deforming interface.

Figure 9. Dimensionless correlation function

$$\frac{\langle U(t)U(t + \tau) \rangle}{\beta \eta_{\max} \omega_0^2 e^{-2dk} \sqrt{\kappa_B T / m} / \{(\zeta \omega_0 - \beta)^2 + (1 - \zeta^2) \omega_0^2\}},$$

as a function of the dimensionless time difference τ for $\lambda_{\alpha\omega} = 2.0$.

Figure 10. Dimensionless correlation function

$$\frac{\langle U(t)U(t + \tau) \rangle}{\beta \eta_{\max} \omega_0^2 e^{-2dk} \sqrt{\kappa_B T / m} / \{(\zeta \omega_0 - \beta)^2 + (1 - \zeta^2) \omega_0^2\}},$$

as a function of the dimensionless time difference τ for $\lambda_{\alpha\omega} = 2.0$.

Figure 11. Dimensionless diffusion coefficient, $\frac{D}{\kappa_B T / (6\pi\mu_2 a)}$, as a function of the separation distance for $ka = 1.0$.

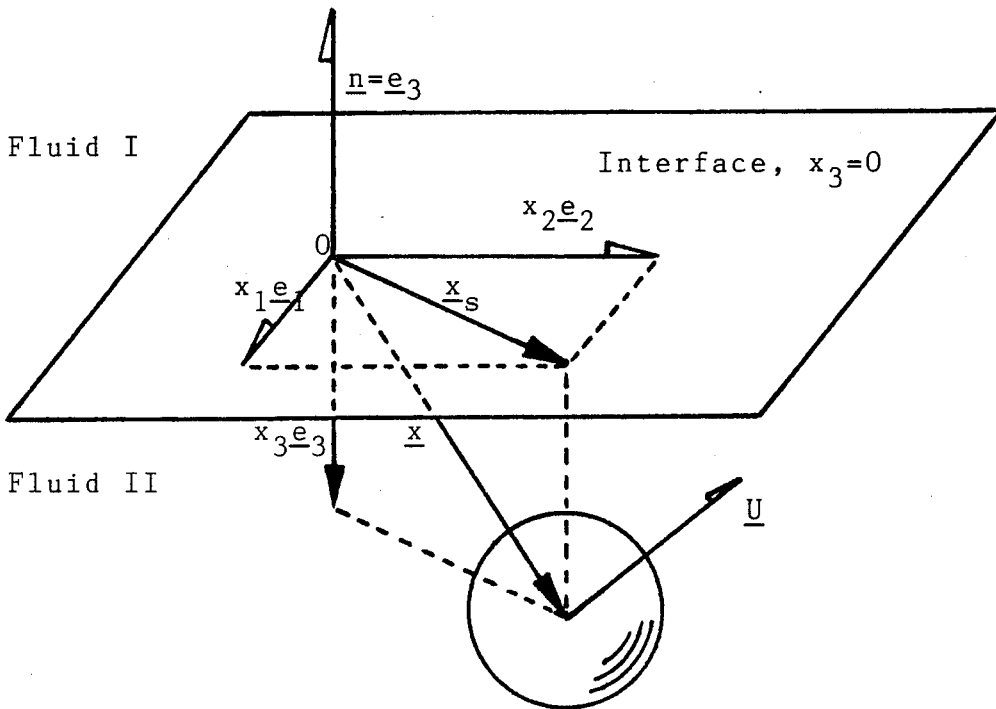


Figure 1

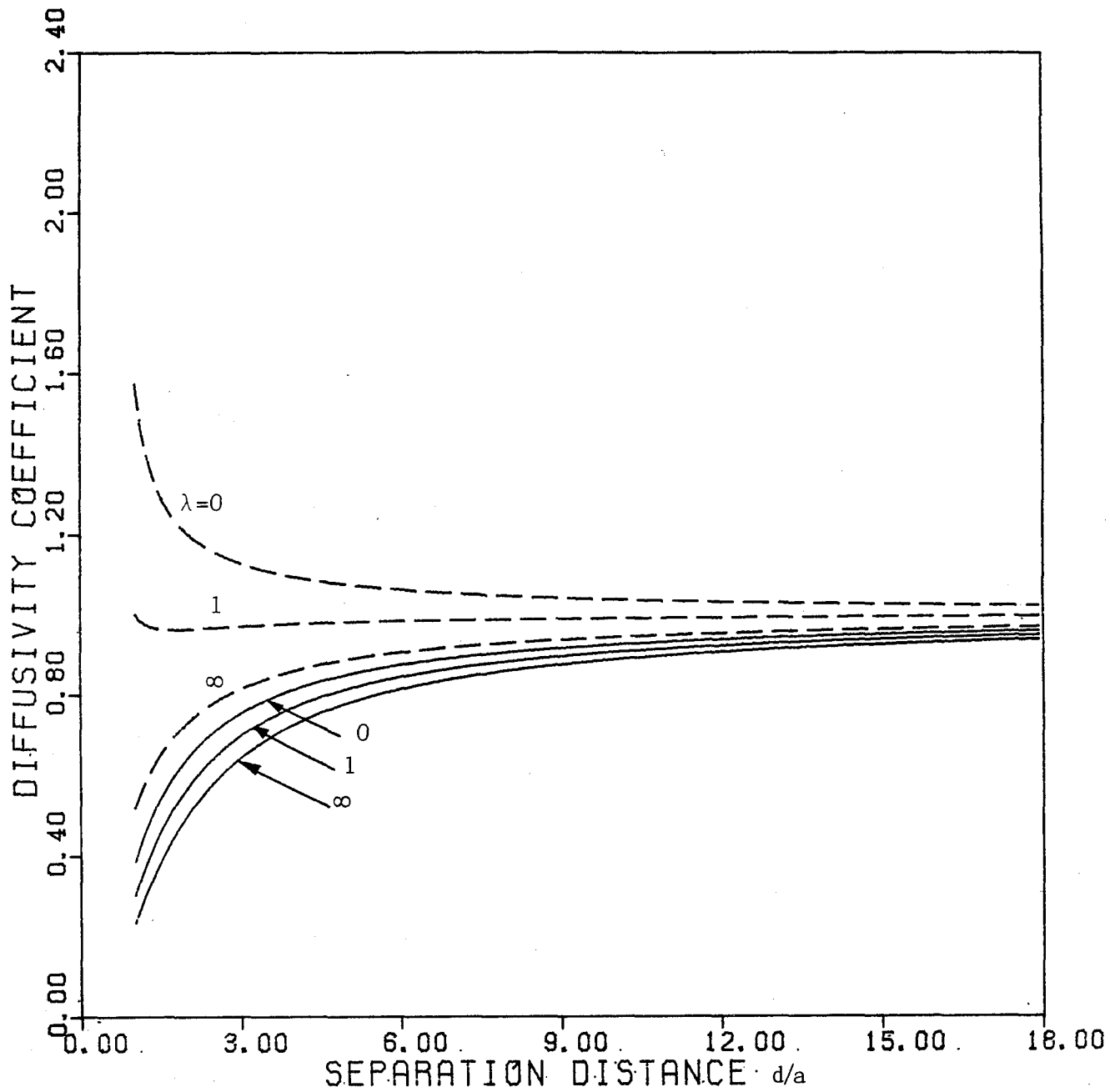


Figure 2

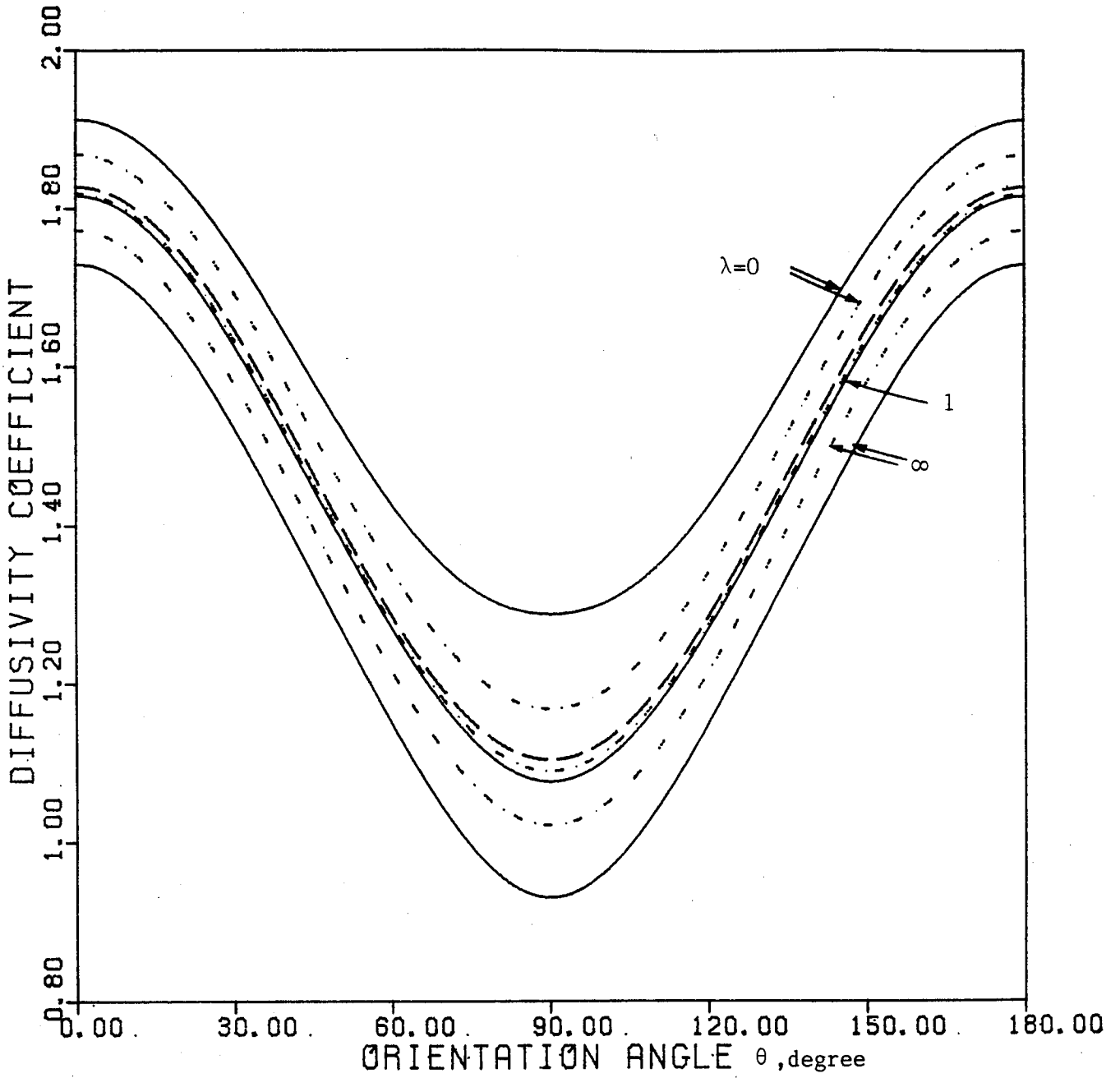


Figure 3

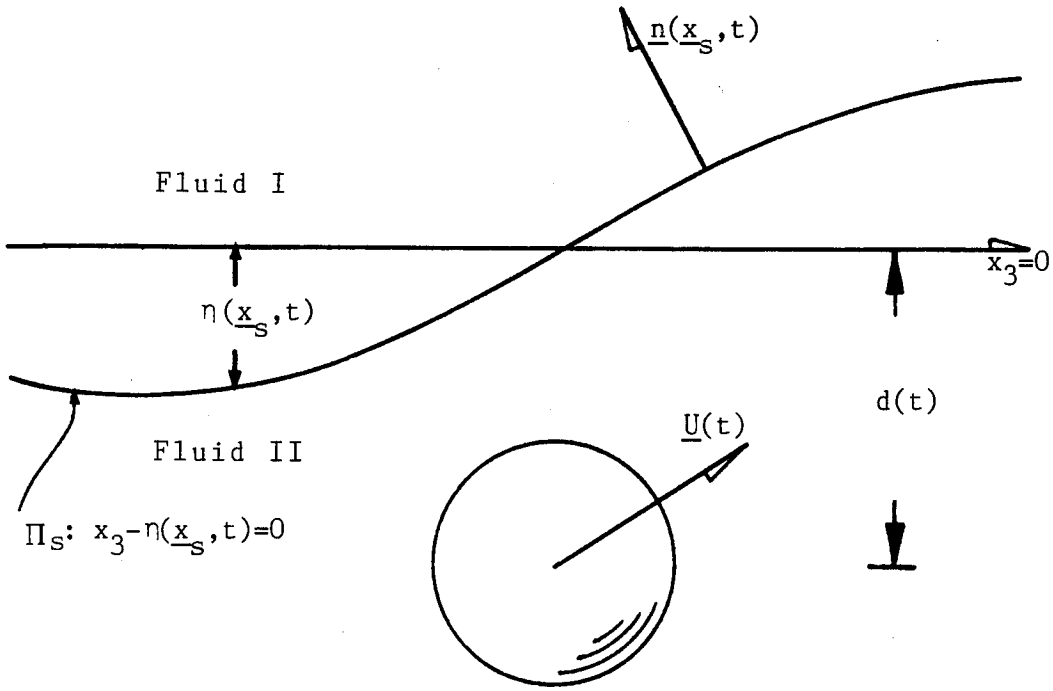


Figure 4

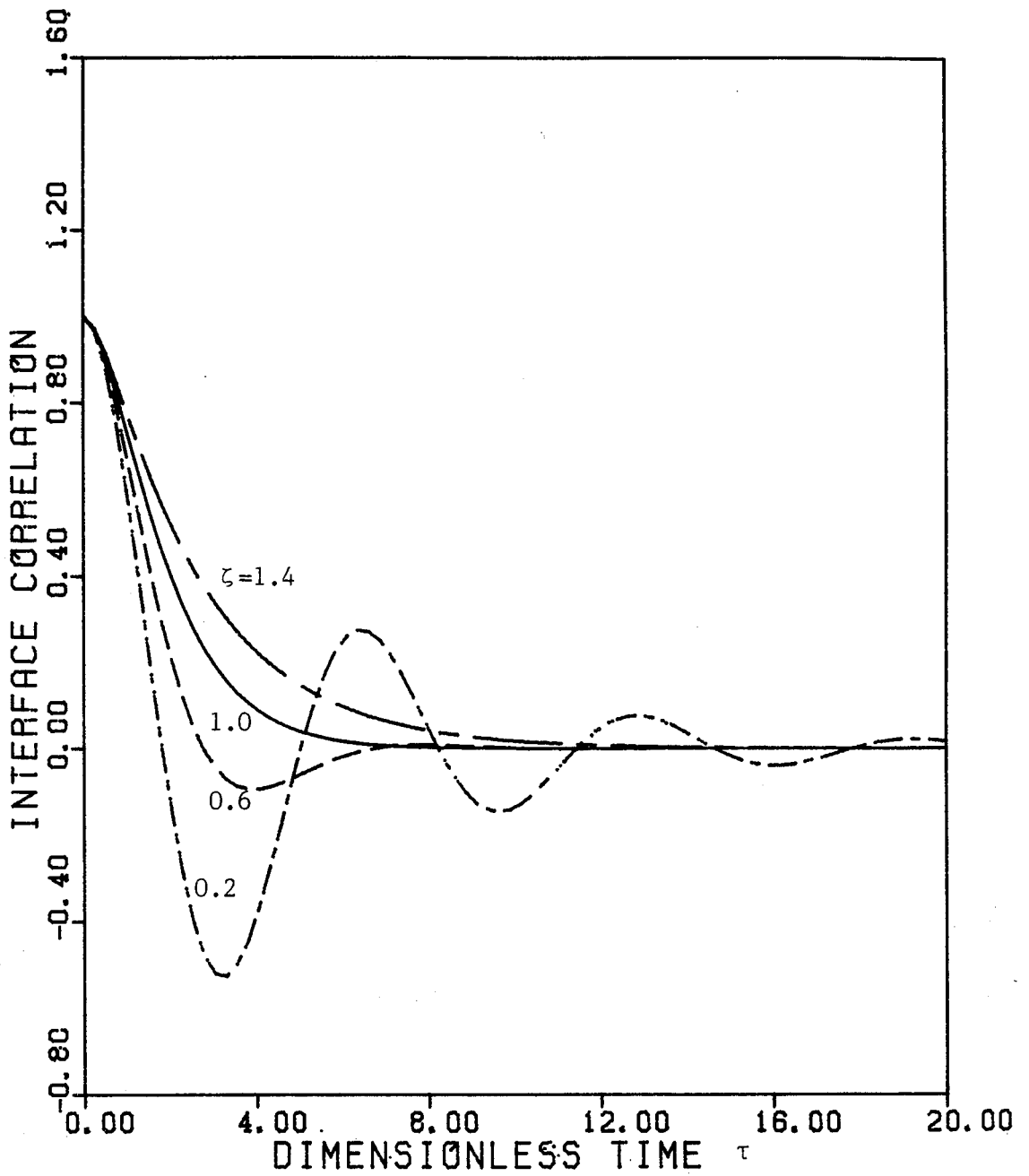


Figure 5

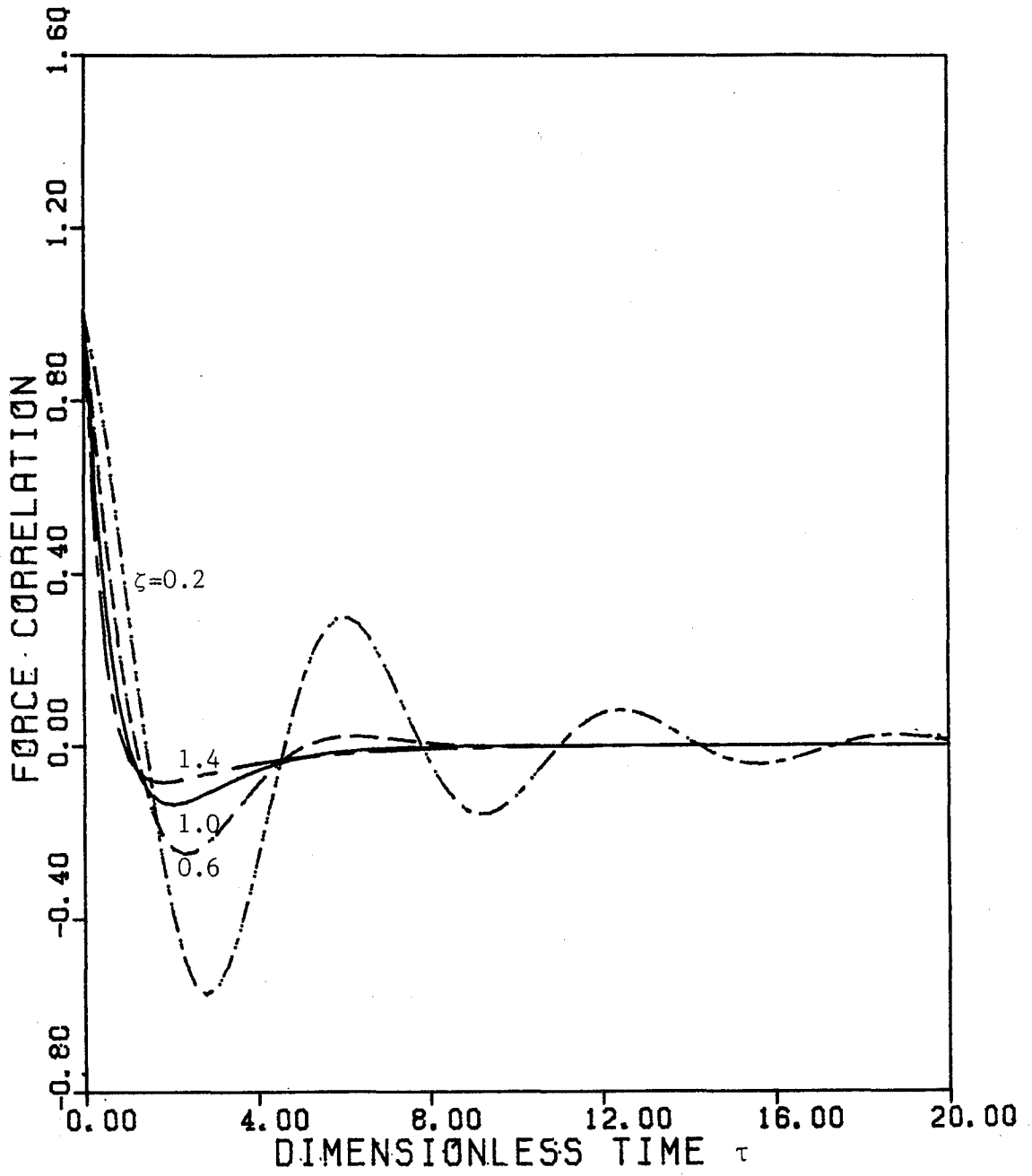


Figure 6

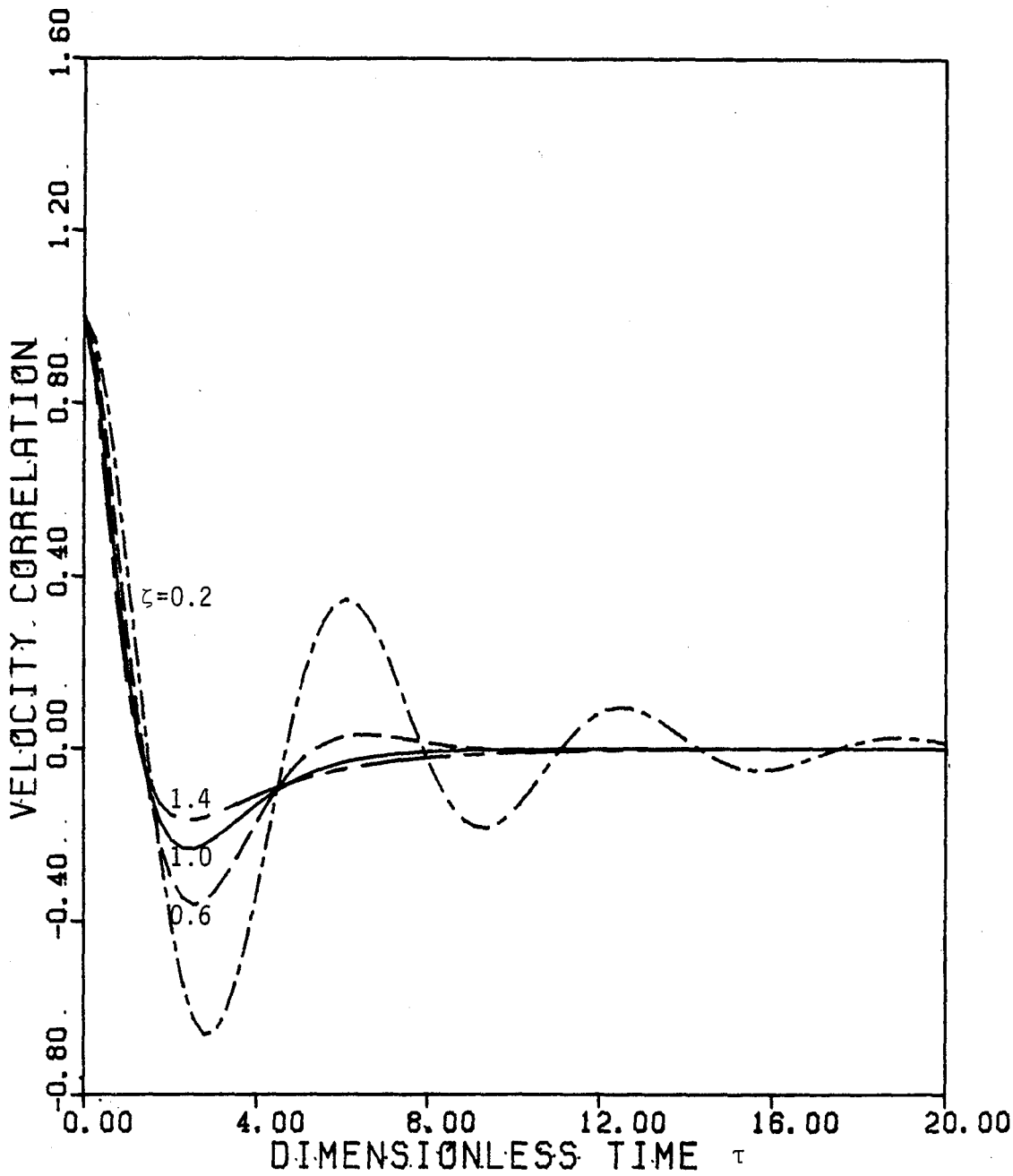


Figure 7

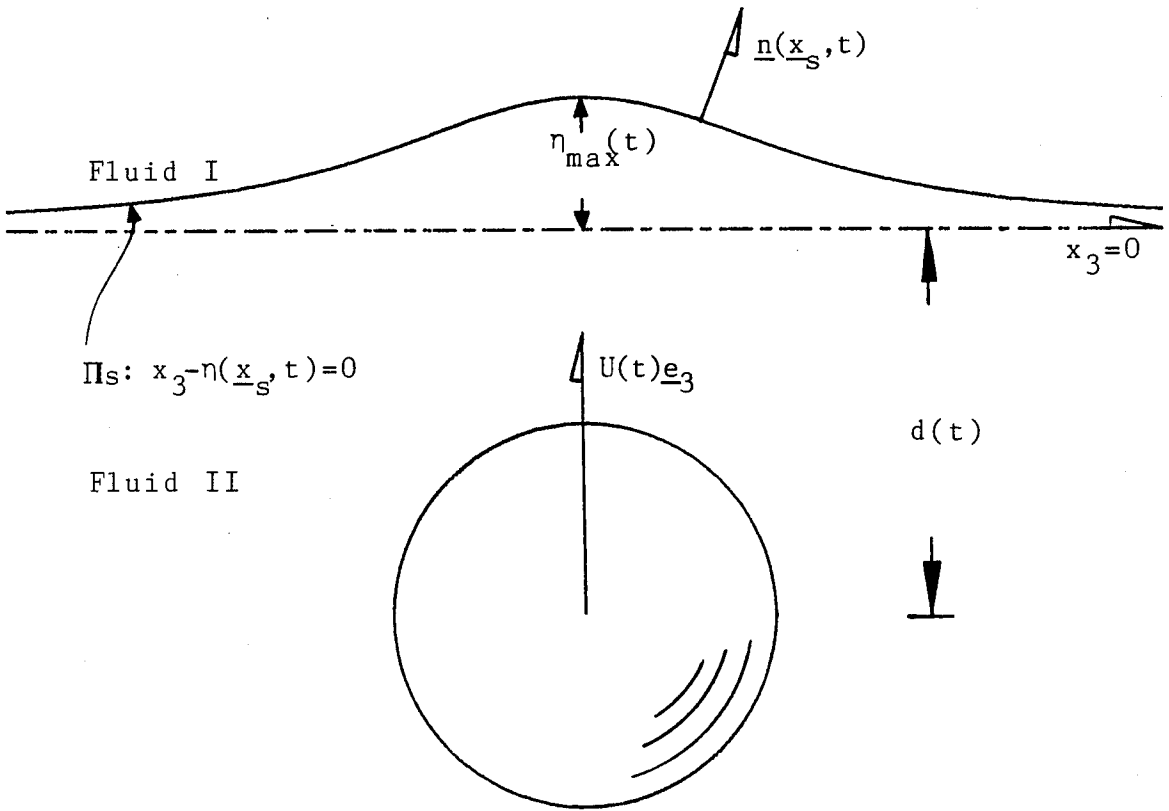


Figure 8

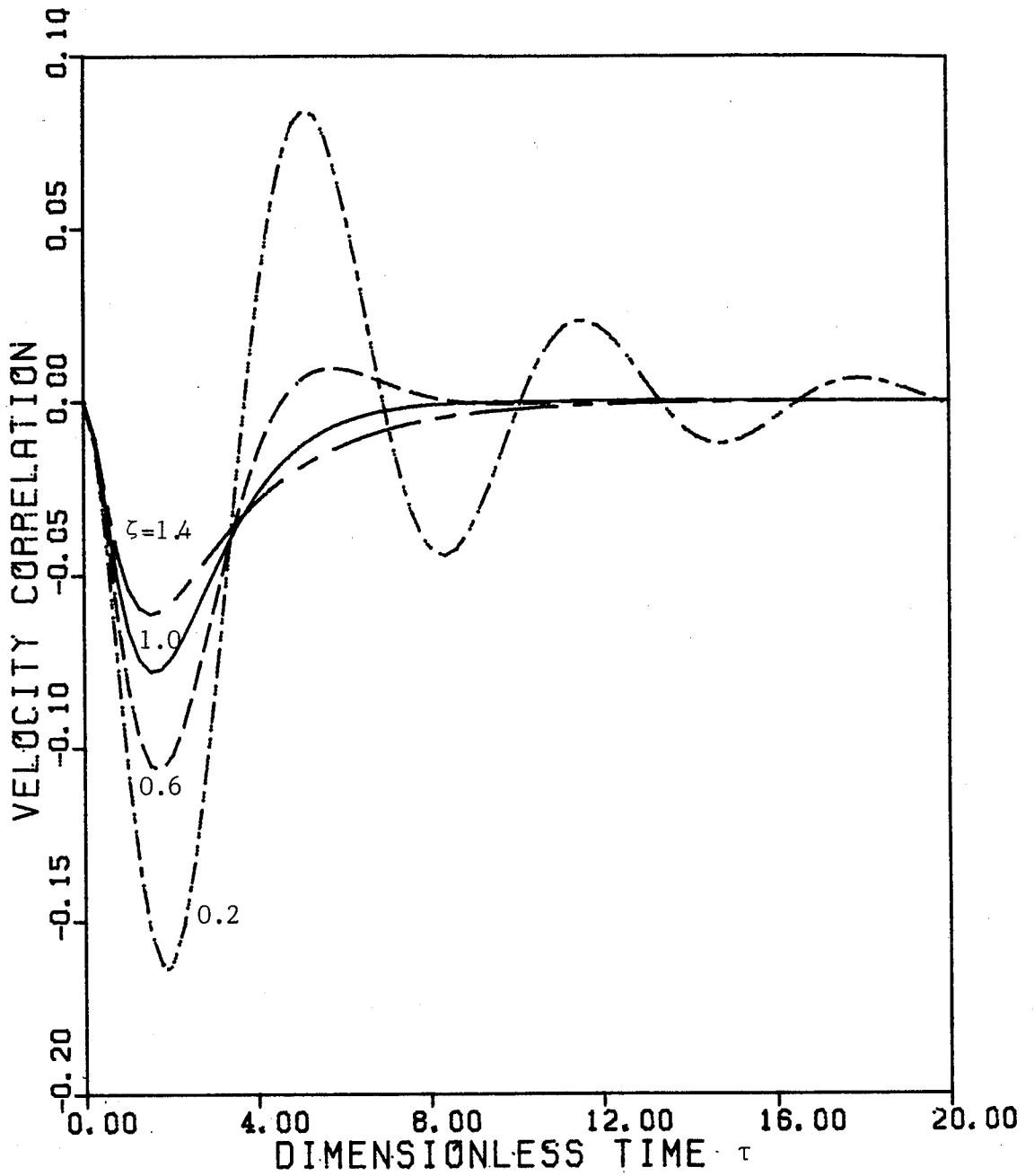


Figure 9

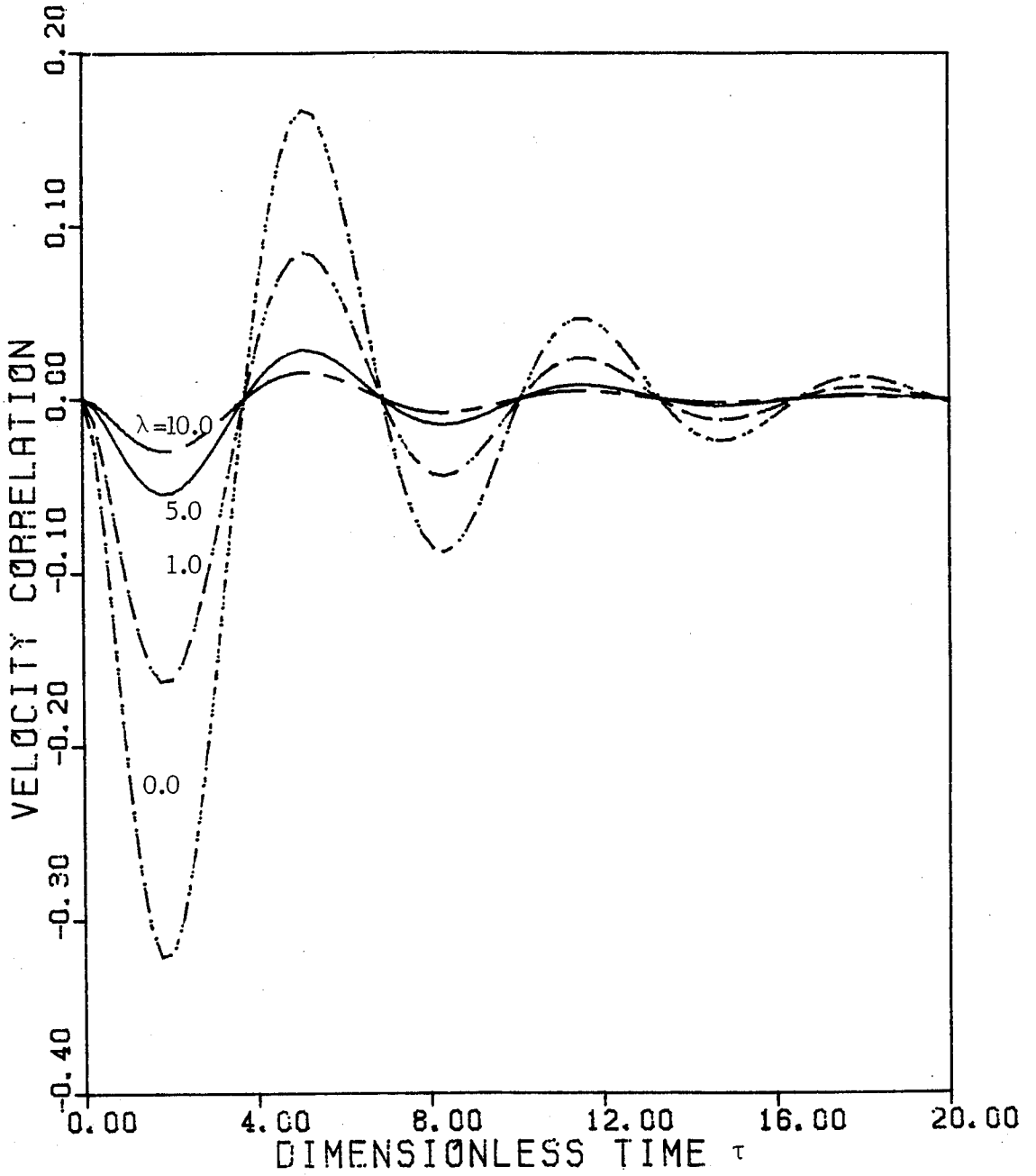


Figure 10

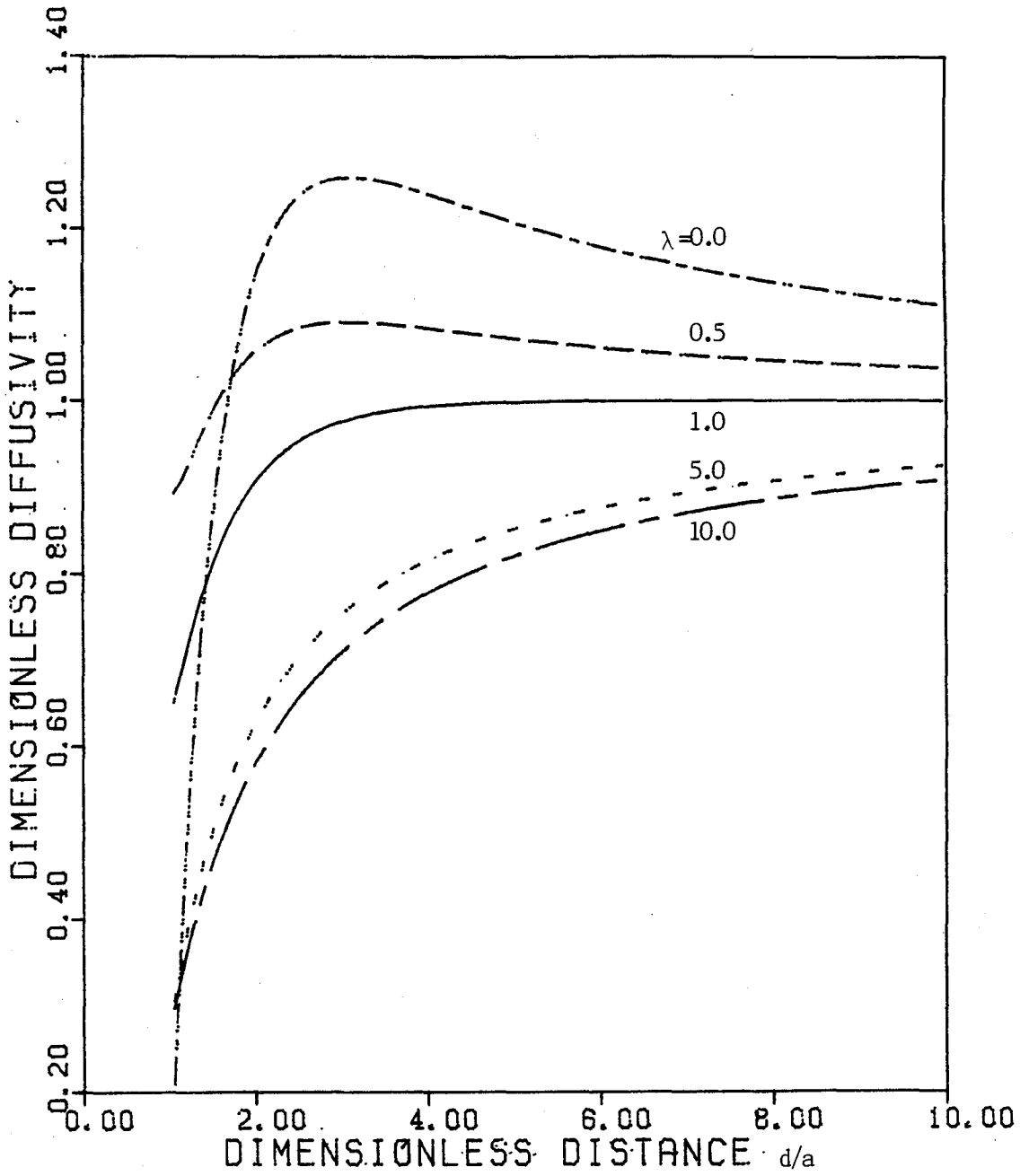


Figure 11